Identification of molecular-genetic determinants of quality traits of tomato fruit

Megan Jayne Morgan

Linacre College

Thesis submitted for the degree of

Doctor of Philosophy at the University of Oxford

Trinity Term 2011

Abstract

Identification of molecular-genetic determinants of quality traits of tomato fruit

Megan Jayne Morgan, Linacre College, University of Oxford.

D. Phil. Thesis, Trinity Term 2011

Tomato is an important food crop and a model for fleshy fruit development. The process of fruit ripening involves changes in chemical composition and in particular the accumulation of sugars, organic, amino acids and carotenes. The research described in this thesis aimed to identify key regulatory aspects associated with the accumulation of the major acids in tomato fruit by analysis of introgression lines resulting from a cross between a cultivated variety, *Solanum lycopersicum*, and a wild progenitor species, *Solanum pennellii*. Line 2-5 showed increases in citrate, malate, aspartate and glutamate in fruit grown under greenhouse conditions.

The genetic differences between line 2-5, its overlapping lines, sub-introgression lines and the recurrent parent were used to link the metabolite phenotypes to smaller chromosomal regions. This analysis suggested multiple epistatic loci control fruit metabolite accumulation. Investigation of the biochemical differences between line 2-5 and the recurrent parent revealed that organic and amino acid accumulation did not dependent upon increased TCA cycle capacity. Regulation at the metabolic level was identified for citrate accumulation with changes in cytosolic aconitase in line 2-5. As these metabolites accumulate in the vacuole, tonoplast transport was investigated. Correlation of ATPase-dependent malate influx with altered malate content suggested malate tonoplast transport plays a role in malate accumulation and highlights the importance of vacuolar storage and transport in the regulation of organic and amino acid accumulation.

Acknowledgements

I would like to thank Lee Sweetlove, my supervisor, for providing me with this opportunity, for his ongoing support, guidance and time throughout this DPhil. and for having the faith that I could do it in the first place. Also, to Nick Kruger, my second supervisor, for help with the isotope feeding assays and George Ratcliffe for help with the NMR experiments. I would like to thank the members of the Sweetlove Lab (Andy Howden, Miriam Laxa, Kate Beard, Markus Schwarzlander and Tom Williams) who all contributed but especially Laurent Miguet for his invaluable help with the HPLC, Iris Finkemeier for help with the expression analysis and Chris Snowden for the extraction of gene annotation data. A huge thank you to Jack Dumenil for the optimisation experiments of the tonoplast isolation, transport and ATPase assays and Andrew Smith who, in combination with Jack, helped with the transport work. A special thank you goes to Christine Surman, Jake Hodson, and Timothy Wroe for their help with the tomatoes and John Baker for his photography.

I would also like to thank Ian Puddephat and Charles Baxter who provided direction, Liz Reynolds, Rosie Woodruff and the greenhouse support team at Syngenta in the UK, Laurent Grivet at Syngenta in France for the genotyping analysis and Syngenta in the USA.

I would also like to thank Alisdair Fernie for giving me the opportunity to visit and work in his laboratory, Adriano Nunes-Nesi and Johannes Rohrmann at the Max Planck Institute of Molecular Plant Physiology in Golm. Also, to Paul Fraser at the Plant Molecular Sciences, Royal Holloway University of London for the carotenoid analysis and Antony Willis at the Department of Biochemistry, University of Oxford for the initial HPLC analysis. I would also like to acknowledge and thank the BBSRC and Syngenta for funding.

Special thanks to my husband, family and friends for their invaluable support.

Abbreviations

2OGDH	2-oxoglutarate dehydrogenase
AAT	aspartate amino transferase
acetyl CoA	acetyl coenzyme A
ADP	adenosine triphosphate
AOX	alternative oxidase
APAD	3-acetylpyridine adenine dinucleotide
ATP	adenosine triphosphate
ATPase	adensosine triphosphatase
BTP	BIS-TRIS propane (1,3-bis[tris(hydroxymethyl)methylamino]propane
Brij-58	polyethylene glycol hexadecyl ether
BSA	bovine serum albumin
cDNA	complementary deoxyribonucleic acid
cM	centimorgan
COX	cytochrome c oxidase or Complex IV
CTAB	hexadecyltrimethylammonium bromide
DAA	days after anthesis
DEPC	diethyl pyrocarbonate
DHs	double haploids
DNase	deoxyribonuclease
DMSO	dimethyl sulfoxide
DNA	deoxyribonucleic acid
dNTP	deoxynucleotide triphosphate
DPA	days post anthesis
DTT	dithiothreitol
EDTA	ethylenediaminetetraacetic acid
EGTA	ethylene glycol-bis(2-aminoethylether)-*N,N,N′,N′*-tetraacetic acid
EST	expressed sequence tag
$FADH_2$	flavin adenine dinucleotide
GABA	γ-aminobutyric acid
GAD	glutamate decarboxylase
GDC	glutamate decarboxylase
GS	glutamine synthetase
GC-MS	gas chromatography-mass spectrometry
HEPES	4-(2-hydroxyethyl)piperazine-1-ethanesulfonic acid
HPLC	high performance liquid chromatography
IBDC	*N*-isobutyryl-D-cysteine
ICDH	isocitrate dehydrogenase
IL	introgression line
INT	iodonitrotetrazolium chloride
K_m	Michaelis-Menten constant
MDH	malate dehydrogenase
ME	malic enzyme
MES	2-(N-morpholino)ethanesulfonic acid
MIP	major intrinsic protein

mMDH	mitochondrial malate dehydrogenase
mRNA	messenger ribonucleic acid
NAD^+	nicotinamide adenine dinucleotide (oxidized)
NADH	nicotinamide adenine dinucleotide (reduced)
$NADP^+$	nicotinamide adenine dinucleotide phosphate (oxidised)
NADPH	nicotinamide adenine dinucleotide phosphate (reduced)
NMR	nuclear magnetic resonance
OPA	*o*-phthaldialdehyde
P5CR	pyrroline-5-carboxylate reductase
PEP	phosph*enol*pyruvate
PEPC	phosph*enol*pyruvate carboxylase
PEPCK	phosph*enol*pyruvate carboxykinase
PMSF	phenymethylsulphonyl fluoride
PVP-40	polyvinylpyrrolidone
QTL	quantitative trait loci
quinacrine	6-chloro-9-(4-diethylamino-1-methylbutylamino)-2-methoxyacridine dihydrochloride
RILs	recombinant inbred lines
RFLP	restriction fragment length polymorphism
RNA	ribonucleic acid
RNase	ribonuclease
RT	room temperature
RT-PCR	reverse transcription - polymerase chain reaction
SDH	succinate dehydrogenase
SDS	sodium dodecyl sulphate
TAE	Tris-acetate-EDTA buffer
TAIR	The Arabidopsis Information Resource
TCA	tricarboxylic acid
TES	N-[tris(hydroxymethyl)methyl]-2-aminoethanesulfonic acid
TRAMP	tomato ripening-associated membrane protein
Tris	tris(hydroxymethyl)aminomethane
TPP	thiamine pyrophosphate
UDP-glucose	uridinediphosphate glucose
UGPase	uridine diphosphate glucose pyrophosphorylase
V-ATPase	vacuolar type H^+-adensosine triphosphatase
V-PP_iase	vacuolar type H^+-inorganic pyrophsphotase

Contents

Chapter 1

General Introduction

1.1 Statement of aims

The aim of the work presented in this thesis was to identify the genetic and biochemical factors that regulate organic and amino acid accumulation during tomato fruit ripening. An introgression line (2-5) that had increased glutamate, aspartate and isocitrate was chosen from an introgression line population (Schauer *et al.*, 2006). The genetic and metabolic differences in line 2-5 compared to the parent allowed the research to be approached using two different strategies. Firstly, using a genetic strategy, the following questions were addressed: can the phenotypic trait of increased organic and amino acids in line 2-5 be linked to specific smaller chromosomal regions within the introgressed segment by analysis of overlapping introgression lines? If so, can potential candidate genes be identified that could be responsible for this phenotypic trait? Secondly, applying a biochemical strategy: are there any metabolic differences in line 2-5 that could explain the increased organic and amino acid content?

1.2 The importance of this work

Crop improvement has been a continual process since the domestication of wild species began approximately 10,000 years ago and is necessary for the development and improvement of desired characteristics in agricultural crops, especially for food production. The improvement of crop characteristics has relied heavily on classic genetics and breeding and was mainly focussed on characteristics that were agriculturally important (i.e. yield, pest and disease resistance). This process, although successful, is slow and has limitations due to the dependence on the narrow genetic variability found in modern crop plants (Eshed and Zamir, 1994; Zamir, 2001; Giovannoni, 2006). More recently the breeding focus has shifted to select characteristics for the improvement of crop composition (i.e. colour, flavour, nutrition) which relies on altering the metabolism in the plant. This requires identifying the genes or genetic region associated with the desired trait and altering the metabolic pathway to enhance that trait. In the last few decades new plant breeding techniques have been developed and incorporated into classic breeding programs (Paszkowski *et al.*, 1984; Tanksley *et al.*, 1989; Kameswara Rao *et al.*, 2002). The use of DNA-marker assisted breeding and direct gene transfer in plant breeding has allowed incorporation of genes from wider genetic sources and more direct manipulation of metabolic pathways. The success of these techniques involves using existing knowledge of the target pathway, which is not always available. Therefore, the manipulation of metabolic pathways does not always result in expected changes unless there is an understanding of the regulation of that pathway. Understanding the regulation and control of a pathway will lead to more efficient and effective breeding strategies. Currently there is very little known about the regulation of organic and amino acid accumulation during tomato fruit ripening.

Identifying the molecular factors involved in the regulation of organic and amino acid accumulation will aid improvement to the quality of tomato fruit in the future.

1.3 Crop improvement

1.3.1 Importance of tomato as a fruit crop

Tomato is a major food crop of high economic value. In 2004, over 120,000,000 tonnes were produced worldwide of which 88% was used in food production (FAO Statistical database, http://faostat.fao.org). The tomato is consumed as a fresh fruit and as a processed product (e.g. ketchup, pastes, sauces) and is widely cultivated. Fruits constitute a large part of the human diet and have a high nutritional value (Coombe, 1976).

1.3.2 Fruit crop improvement

During the process of crop breeding, the focus has typically been on improvements that benefit the grower such as yield, storage characteristics and field performance (Schuch, 1994; Giovannoni, 2006; Tieman *et al.*, 2006b). As a result there has been an unintentional loss of consumer quality traits such as flavour, texture and nutritional value (Causse *et al.*, 2002; Giovannoni, 2006).

There are 13 recognised species of wild tomatoes (Peralta *et al.*, 2006). One of these species, *Solanum lycopersicum*, was brought to Europe during exploration of South America and is the ancestor from which the European cultivars were domesticated (Yilmaz, 2001; Giovannoni, 2006; Peralta *et al.*, 2006; Bai and Lindhout, 2007). From this small genetic pool all modern-high yielding varieties have been developed (Giovannoni, 2006). Advances made

in the area of genetic modification/manipulation (GM) have led to an efficient way of improving crop plants. However, lack of consumer acceptance of GM crops, combined with problems with safety testing and patent filing, means that length of time to market can be longer than with conventional breeding (Zamir, 2001; Levin *et al.*, 2004; Bai and Lindhout, 2007). Consequently, alternative strategies to improve crop qualities are being investigated. For example, it is possible to use the wild ancestors of crop plants and exploit them as a source of genetic variation (Zamir, 2001). However, crossing these varieties with an elite crop can introduce agriculturally undesirable traits (Bai and Lindhout, 2007). Through the use of marker-assisted breeding, improvements can be introduced (i.e. taste, texture and appearance) to commercial cultivars without compromising the qualities (i.e. yield and field performance) of the elite crop variety (Giovannoni, 2006; Bai and Lindhout, 2007).

1.3.3 Flavour

Although taste and flavour are interchangeable in everyday use, in sensory fruit evaluation they have different meanings. Flavour is the sensory perception of a food or other substance and consists of a number of components. Taste is one component of the flavour perception and is detected by the sensory organs in the mouth. The organoleptic qualities that make up the perception of flavour include taste, texture, aroma and appearance (Goff and Klee, 2006). The perception of flavour is complex and involves the integration of information in the brain from different sensory organs. For example, the taste component of flavour from non-volatile compounds is detected by taste receptors on the tongue and the aroma component from volatile compounds is detected in the olfactory cells in the nasal cavity.

In tomato over 400 volatile components have been identified (Grierson and Kader, 1986; Petro-Turza, 1986; Goff and Klee, 2006) although only 30 of them are known to contribute to aroma and can therefore impact on the flavour of tomatoes (Tieman *et al.*, 2006b). Some of these volatile components are derived from amino acids (Petro-Turza, 1986; Tieman *et al.*, 2006b). For example, the volatile compound 2-phenylethanol is derived from the amino acid phenylalanine (Tieman *et al.*, 2006a). Structural studies and pathway comparisons to yeast have also predicted that the volatiles 2-methylbutanal and 2-methoxybutanol, 3-methylbutanal and 3-methoxybutanol may be derived from isoleucine and leucine respectively (Mathieu *et al.*, 2009). Although volatiles must play a part in the perception of flavour, the contribution they make to fruit flavour is not fully understood (Tieman *et al.*, 2006b). For this reason only the non-volatile components of tomato will be discussed.

In tomato fruit, the main components contributing to taste arise principally from the interaction between sugars (e.g. fructose and glucose), organic acids (e.g. citrate and malate) and free amino acids (e.g. glutamate and aspartate) (Jones and Scott, 1983; Petro-Turza, 1986; Yilmaz, 2001). The quantity of each taste component varies according to variety, stage of ripeness and conditions of cultivation but generally sugars constitute about 50%, organic acids 13-15% and free amino acids 2-3% of the dry matter content of fresh tomato fruit (Davies and Hobson, 1981; Grierson and Kader, 1986; Ho and Hewitt, 1986; Petro-Turza, 1986; Yilmaz, 2001).

Consumer complaints about poor tomato flavour have been widely reported in the literature, motivating research in the area (Schuch, 1994; Ratanachinakorn *et al.*, 1997; Saliba-Colombani *et al.*, 2001; Yilmaz, 2001; Causse *et al.*, 2002; Fulton *et al.*, 2002). This

research includes looking at the effects of adding sugars or acids directly to tomato tissue and assessing the impact on flavour. For example, the effects of adding differing amounts of reducing sugars or citrate to diced tomato tissue was investigated (Malundo *et al.*, 1995). Infused fruit tissue was assessed by a small number of trained panellists for three different descriptors of flavour (sweet, sour and 'fresh tomato impact') and by chemical analysis. 'Fresh tomato impact' is a descriptor used by the sensory panellists in this research. However, there is no explanation to what it exactly describes other than the sensory panellists were trained to identify this flavour in the samples. It was found that increasing the total sugar and acid levels did not affect the 'fresh tomato impact' but did significantly alter flavour acceptability. In earlier research, citrate and/or sucrose was added to tomato juice (Gould, 1978). The ratio of soluble solids to total acidity less than 10:1 or greater than 18:1 was found to be unacceptable by a taste panel. Also, if the percentage of total acidity was greater than 0.6 then sucrose was required for acceptable flavour. Although in both these investigations the flavour was altered in an artificial way, changing the ratio of sugars to acid did impact on flavour acceptability by the taste panellists.

Further research involved creating a cocktail of synthetic chemicals to simulate the main components contributing to taste from a compositional analysis of tomato fruit with a focus on amino acids (Fuke and Konosu, 1991). The chemical cocktail contained citrate, glucose, potassium dihydrogen phosphate, magnesium sulphate and calcium chloride. The cocktail had glutamate and aspartate added in differing ratios and a taste panel evaluated the flavour. It was found that when the weight ratio of glutamate to aspartate was 4, the cocktail was found to taste similar to tomato fruit. Also, that both glutamate and aspartate were needed to reproduce the tomato flavour. Citrate was found to give the perception of

thickness to the cocktail compared to other organic acids and glucose could be substituted for other sugars without affecting the overall flavour considerably. This research is quite interesting in that it removes the perception of aroma, some texture aspects and appearance from the assessment, leaving taste as the only sensory input. However, as fresh tomato fruit flavour is a whole sensory experience, whether their findings can actually be used to enhance flavour in a whole fruit for the consumer is debatable and the findings may be of more significance for artificial food flavourings in the processing industry.

The effect of changing the sugar to acid ratio on flavour by less artificial means has been assessed using lines or varieties that differed in their sugar to acid ratio. Flavour was investigated using high sugar and acid breeding lines of tomato (Jones and Scott, 1983). In these lines the composition was determined and flavour was evaluated using a sensory panel and compared to standard cultivars (Cal Ace or T_3). It was found that the high sugar breeding lines had higher reducing sugars, pH and soluble solid content compared to the control lines. The panellists rated these high sugar lines as having greater sweetness, more tomato-like flavour and overall flavour intensity. Correlation analysis between flavour characteristics and chemical composition showed positive correlations between sweetness and reducing sugars, soluble solids, 'tomato-like' flavour and overall flavour intensity. In other research to identify non-volatile markers for flavour, 36 tomato samples from different varieties of *Solanum lycopersicum* grown in different locations (Spain and the United States) were used (Bucheli *et al.*, 1999). Samples of the different varieties were assessed by taste panellists for 'fruitiness intensity' and the composition of glucose, reducing sugars, citrate, malate and glutamate was determined. A significant correlation was found between perceived fruitiness intensity and both glucose and reducing sugar

content. Also, there was a high correlation between fruitiness and a high ratio of reducing sugars to glutamate content and it was suggested that the sugar to acid ratio was affected. Although glutamate is found in quite high quantities in tomato fruit, the amount of glutamate relative to the main acid components (malate and citrate) is relatively low. It seems unlikely that glutamate could significantly alter the acidity of the fruit but may have instead altered the flavour which was perceived as having more fruitiness, rather than a change in acidity, in the taste test. It was also found that the Spanish varieties that had increased sugar to acid ratios were also associated with increased fruitiness intensity. Multiple regression analysis was then used to examine the more complex combination of parameters. The best model, found from the regression analysis, combined reducing sugars, glutamate and malate. This was surprising as the authors had previously found that malate was not correlated to fruitiness and glutamate was negatively correlated to fruitiness. The discrepancy, at first appears unusual, but can be explained by looking at the other data where they also found a high correlation between fruitiness and the ratio of reducing sugars/glutamate. Individually, the malate and glutamate do not correlate well with fruitiness, but in the regression analysis, the combined effect with reducing sugars gives a good correlation. This suggests that it is the sugars to acid ratio that is important to fruitiness intensity rather than the single contribution of the individual components.

Much of this research is based on correlation analysis and the ability of trained panellists to detect changes in the taste of tomato fruit and score these changes, a process which is highly subjective. Whether these changes in the taste of tomato fruit, as detected by panellists, is also able to be identified and accepted by the average consumer remains to be discovered. In these studies the threshold for flavour acceptability or unacceptability was

defined but identification of individual flavour-enhancing compounds was not. This research has highlighted that flavour and its perception is complex due to the number of sensory inputs involved in detecting flavour and the number of compounds in the fruit contributing to it. To help analyse the complex interactions a more recent study has used a biological network analysis approach (Carli *et al.*, 2009). Eight tomato varieties (six traditional landrace tomato varieties, a fresh market and a processing variety) had 37 characteristic organoleptic quality traits measured (four agronomic, 14 biochemical (consisting of four organic acids, 10 amino acids), nine physicochemical and 10 sensory traits). Network analysis was performed by statistical analysis of the data to identify significant trait variation among the genotypes followed by correlation analysis. A network was constructed and visualised graphically where each trait is represented by a node and links are represented by significant correlations. Three main nodes and two minor nodes interconnected between themselves and with other traits. The first module contained most amino acids and two colour components (green-to-red and lightness) with strong intercorrelations between the amino acids. The second module contained glutamate and asparagine; citrate and fumarate; acidity, ash, chloride ions and Brix; tomato smell, juiciness and overall aroma. In this module tomato smell was affected by Brix, acidity and citrate. Juiciness was positively correlated with glutamate and flavour was negatively correlated with acidity and chloride ion content. The three sensory parameters (tomato smell, juiciness and flavour) were interconnected with few links to other nodes while the biochemical traits were linked with nodes in other modules particularly the third nodule. The third module contained three of the four agronomic traits, ascorbate, the remaining colour component (blue-to-yellow), pH, dry matter, granulosity and hardness. The agronomic traits did not influence any sensory

parameters apart from skin resistance. Two smaller modules grouped malate, skin resistance and redness together and sweetness, saltiness and sourness. This research has found some interesting and expected connections (e.g. between amino acids in the same pathways, dry matter with links to Brix and citrate) but it has also uncovered some unexpected connections (e.g. sweetness, sourness and saltiness sensory traits grouped together with few links to other traits). One interesting finding is that some metabolic traits were found to have a direct influence on sensory traits, such as citrate on tomato smell and glutamate on juiciness, confirming that there is an association between organic and amino acids and aspects of fruit quality. However, further research will be required to confirm a biological basis to these interactions.

The research described above has used a variety of different approaches to assess and identify the components contributing to tomato fruit flavour. Although this research is correlative and reliant upon taste panellists scoring there is a consistent pattern emerging of an association between the ratio of sugars to acid in the fruit, certain amino acids (e.g. glutamate and aspartate) and improved fruit flavour. Although the biosynthetic pathways of these molecules are well known the regulation of these pathways (and therefore the rate of accumulation) is still not fully understood. As sugars are the main taste component of tomato fruit much of the research to date has been on sugar accumulation and its regulation (some of which has been described in Section 1.5.1). However, very little research has explored the regulation of organic and amino acid synthesis even though the studies described above show that these metabolites have an impact on tomato fruit flavour. For this reason the regulation of organic and amino acid accumulation has been the focus of the research in this thesis.

1.4 Fruit ripening

Metabolites, such as organic and amino acids, alter throughout ripening. The ripening process can influence the levels of organic and amino acids affecting the final flavour of the fruit.

Fruit ripening can be defined as the summation of physiological and biochemical changes in tissue metabolism rendering the fleshy (non-dehiscent) fruit attractive and palatable for consumption by organisms that assist in seed dispersal (Coombe, 1976; Gray *et al.*, 1992; Giovannoni, 2001; Adams-Phillips *et al.*, 2004). The process of fruit ripening consists of an ordered and highly regulated sequence of events. Ripening can be characterised by alterations in pigmentation, carbohydrate metabolism, cell wall structure and texture, production of aromatic volatiles and flavour and increased susceptibility to opportunistic pathogens (Grierson and Kader, 1986; Giovannoni *et al.*, 1999; Adams-Phillips *et al.*, 2004; Carrari and Fernie, 2006).

Due to the extensive research in these areas only the processes that can have an impact of the levels of organic and amino acid accumulation will be discussed here (e.g. organic acid, amino acid and carbohydrate metabolism). Other physiological processes, such cell wall structure and texture, and susceptibility to pathogens have not been found to affect organic and amino acid accumulation and therefore will not be discussed.

1.4.1 Developmental stages of tomato fruit ripening

During fruit development and ripening a number of specific physiological and biochemical changes occur during distinct growth phases (Table 1.1 and Figure 1.1). The

initial phase is characterised by ovary development, fertilization and fruit set. During development of the ovary, the decision is made whether to abort the developing fruit or continue to the next phase. The decision to set fruit is dependent upon one or more positive growth signals generated during pollination up until and including fertilization (e.g. positive growth stimuli, possibly gibberellins and/or auxin, produced by pollen during germination and pollen tube growth) (Gillaspy *et al.*, 1993). The second phase is characterised by active cell division of the tissue, seed formation, slow growth but high metabolic activity (Coombe, 1976; Thimann, 1980; Gillaspy *et al.*, 1993). During the third phase with seed maturation complete, there is cell expansion involving major increases of fresh and dry weight of the fruit due to the accumulation of water and hexoses (Coombe, 1976; Thimann, 1980; Faurobert *et al.*, 2007). Cell volumes can increase more than 10-fold during this phase (Gillaspy *et al.*, 1993). There are some alterations to organic and amino acids (Baxter *et al.*, 2005a). In the final phase, when ripening begins, there is differentiation of functional chloroplasts into chromoplasts and subsequent pigment changes, increased rate of respiration and production of ethylene and further alterations to organic and amino acid levels that continue throughout ripening (Thimann, 1980; Piechulla *et al.*, 1987; Baxter *et al.*, 2005a).

	Phase 1	**Phase 2**	**Phase 3**	**Phase 4**
	Fruit set	Cell division 7-14 days	Cell expansion 6-7 weeks	Ripening 3-4 weeks
Fruit stage	Fruit set	Green	Mature green	Mature green/Breaker /Ripe
Developmental	Fertilisation Abort or set fruit? Development of ovary	Active cell division Seed formation Slow growth High metabolic activity	Increase in cell volume Seed development and maturation	Increase in respiration (climacteric) Cell wall degradation
Pigments	Chlorophyll	Chlorophyll	Chlorophyll	Lycopene β-carotene
Plastids	Chloroplasts	Chloroplasts	Chloroplasts	Chromoplasts
Hormones	Gibberellins Auxin	Gibberellins Cytokinins	Gibberellins Auxin	Ethylene

Table. 1.1. Physiological changes that occur during different growth phases through tomato fruit development. Growth phases as described by Gillaspy *et al.* (1993).

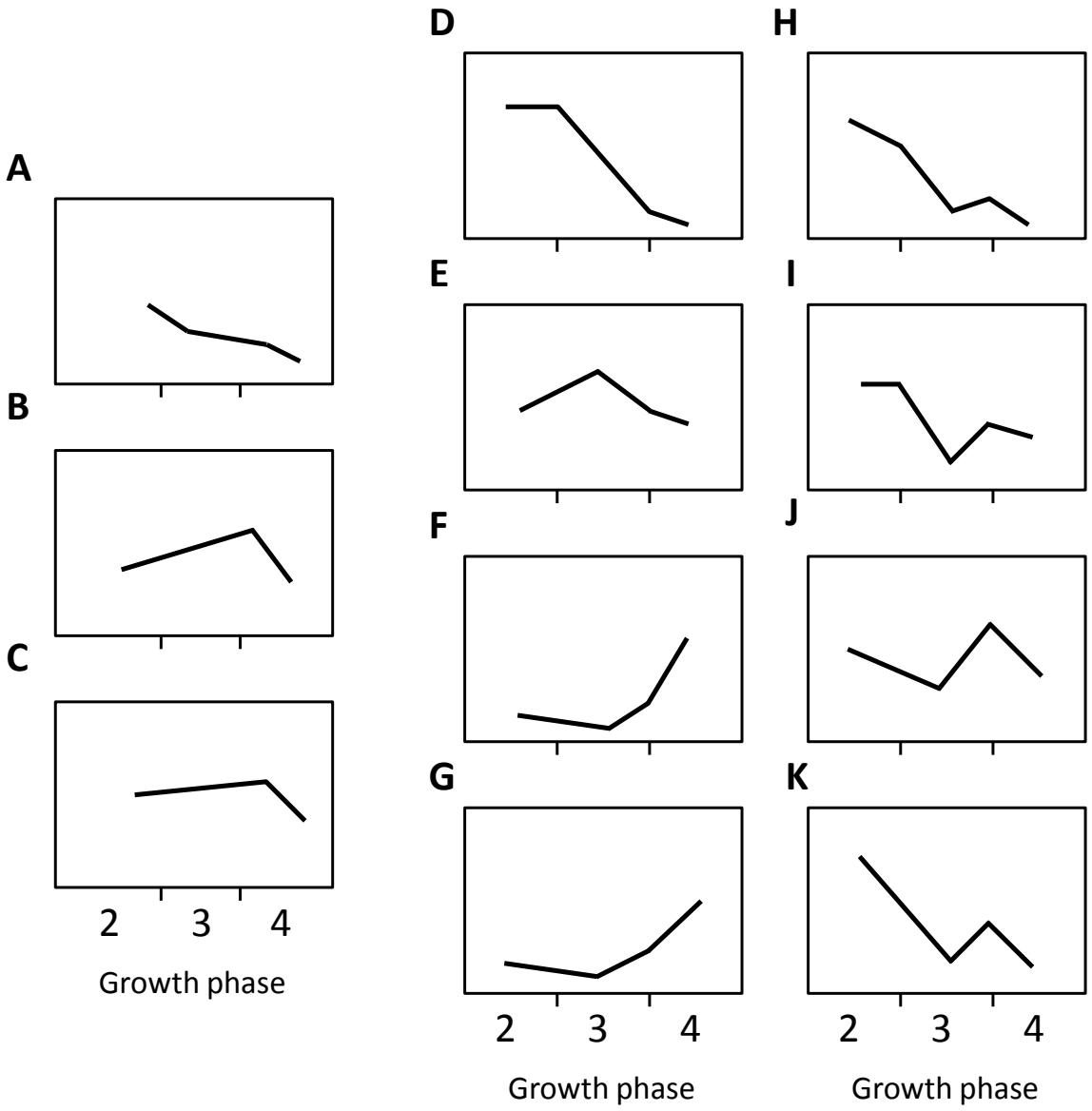

Fig. 1.1. Schematics showing metabolite changes in pericarp tissue from Lycopersicum esculentum fruit during different growth phases through development. Metabolites shown are the sugars sucrose (A), glucose (B), and fructose (C); the amino acids valine (D), phenylalanine (E), glutamate (F), aspartate (G), 2-oxoglutarate (H); and the organic acids fumarate (I), citrate (J) and malate (K). Growth phases as described by Gillaspy *et al.* (1993). Data redrawn from Baxter *et al.* (2005a).

1.4.2 Biochemical changes that may influence metabolite accumulation

1.4.2.1 Ethylene biosynthesis

Ethylene is a gaseous phytohormone that plays a critical role in coordinating and regulating fruit ripening (Theologis, 1992). The ethylene synthesis pathway is a well known pathway in plants. Ethylene is synthesised from methionine via *S*-adenosyl-L-methionine (SAM) and 1-aminocyclopropane-1-carboxylic acid (ACC) (Figure 1.2). ACC is formed from SAM by ACC synthase and the conversion of ACC to ethylene is carried out by ACC oxidase. The reaction of SAM to ACC by ACC synthase also produces 5'-methylthioadenosine which is utilized for the re-synthesis of new methionine via the methionine cycle. This recycling of the methylthio group ensures methionine availability and continued ethylene biosynthesis. Conversion of ACC to *N*-malonyl-ACC instead of ethylene allows depletion of the ACC pool thereby reducing the rate of ethylene production.

Although this pathway was elucidated over 25 years ago by Yang and Hoffman, there is still some uncertainty surrounding the regulation of ethylene synthesis. Research in this area has focussed on the activities of 1-aminocyclopropane-1-carboxylic acid (ACC) synthase and oxidase. Initially it was thought that induction of ACC synthase was the key step in regulating ethylene production (Buchanan *et al.*, 2000). However, more recent research suggests that the first step in ethylene synthesis may be the production of ACC oxidase. The subsequent ethylene then induces ACC synthase gene expression leading to the production of more ACC (Alexander and Grierson, 2002). Although the regulation of ethylene biosynthesis is still unresolved, expression of antisense RNA to ACC oxidase or synthase in transgenic plants resulted in a reduction in the amount of these enzymes (Hamilton *et al.*,

1990; Oeller *et al.*, 1991). This inhibited ethylene biosynthesis and consequently ripening, thus demonstrating the critical role of ethylene in fruit ripening.

As the research has been primarily focussed on ethylene biosynthesis, little was known about the regulation of ripening upstream of ethylene induction or of the regulatory mechanisms shared by climacteric and non-climacteric fruits until more recently. Research using previously characterised ripening mutants and genomic approaches has allowed insights into ripening regulation upstream of ethylene and down-stream ripening-related signal transduction components (Figure 1.3). The tomato ripening-inhibitor (*rin*) mutant is a recessive mutation (Giovannoni, 2007). The *rin* loci encodes a MADS-box transcription factor and is necessary to induce ripening-associated increases in respiration and ethylene (Vrebalov *et al.*, 2002). The fruit, as result of this mutation, exhibits inhibition of the respiratory climacteric, ripening-related ethylene biosynthesis, provitamin A carotenoid accumulation, fruit softening and production of flavour compounds (Vrebalov *et al.*, 2002). The *rin* mutant is responsive to exogenously applied ethylene (ethylene-responsive genes are induced) but does not ripen and therefore lies upstream of ethylene production (Lincoln and Fischer, 1988; Giovannoni, 2007). The tomato non-ripening (*nor*) mutant also encodes a transcription factor and has the same phenotypic traits as exhibited by the *rin* mutant (Giovannoni *et al.*, 1995; Giovannoni, 2001). Despite having similar traits the mutations for both *rin* and *nor* are in two different unlinked loci but the molecular mechanism of the *nor* mutant is still unknown (Giovannoni *et al.*, 1995). A colourless non-ripening (*Cnr*) dominant mutant encodes a transcription factor. The mutation occurred as a result of a spontaneous epigenetic change that altered the promoter methylation of a SQUAMOSA promoter binding (SPB) protein in a commercial population (Thompson *et al.*, 1999; Manning *et al.*, 2006;

Giovannoni, 2007). The *Cnr* mutant also exhibits an inhibition of ethylene production and softening but has a non-pigmented pericarp and yellow skin due to inhibition of caroteniod biosynthesis and shows excessive loss of cell-to-cell adhesion (Thompson *et al.*, 1999). Like the *rin* mutant, the *Cnr* mutant is necessary to induce ripening-associated increases in respiration and ethylene, inhibits the ripening process, does not respond to exogenously applied ethylene but does induce ethylene-responsive genes and therefore must lie upstream of ethylene production. However, it is still unclear as to whether these two mutants operate independently or are part of the same pathway. The mutants never-ripe 2 (*Nr-2*) and green-ripe (*Gr*) are dominant spontaneous mutants that show a reduction in the rate of ripening due to a decreased ethylene sensitivity (Barry *et al.*, 2005). The *Nr* mutation was shown to be an ethylene receptor gene whereas the *Gr* mutant encodes a component of ethylene signalling that might be involved in fruit specific receptor-copper homeostasis both of which act downstream of ethylene induction (Giovannoni, 2007).

This research has helped in our understanding in the role of ethylene in and the regulation of the ripening process. Whether ethylene has a direct influence on organic and amino acid content is not clear. Links between suppression of ethylene biosynthesis and tomato flavour metabolites have been investigated recently (Gao *et al.*, 2007). No valid conclusions could be drawn from the study given the scope of the experimental work, lack of statistical analysis and poor interpretation of the data. However, Carrari *et al.* (2006) have found that there are correlations between transcripts of the ethylene biosynthesis pathway and levels of organic acids.

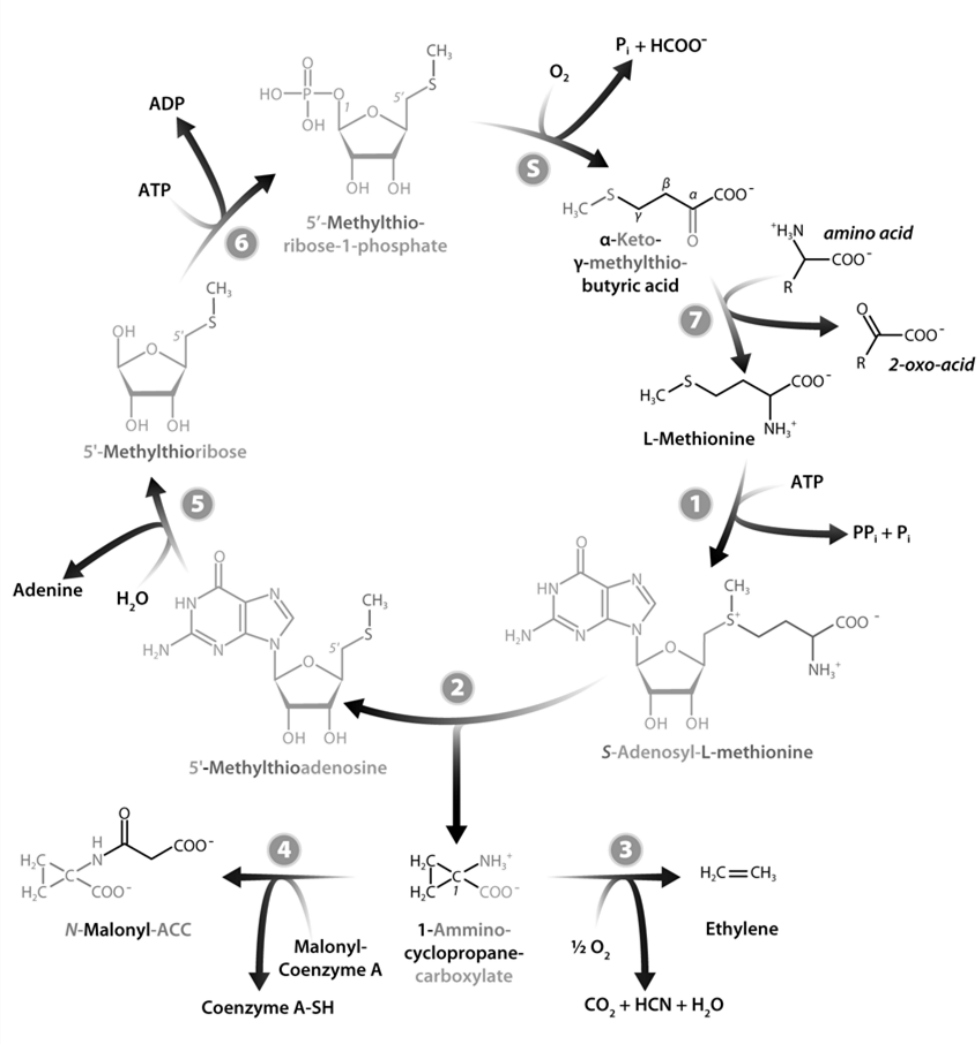

Fig. 1.2. The methionine cycle and ethylene biosynthesis. (1) SAM synthetase, (2) ACC synthase, (3) ACC oxidase, (4) ACC *N*-malonyl-transferase, (5) MTA nucleosidase, (6) MTR kinase, (7) transaminase, (S) spontaneous reaction. ATP: adenosine triphosphate, ADP: adenosine diphosphate, ACC: 1-aminocyclopropane-1-carboxylic acid, HCN: hydrocyanide acid, MTA: 5'-methylthioadensoin, MTR: 5'-methylthioribose, PP_i: pyrophosphate, P_i: phosphate, SAM: *S*-adenosyl-L-methionine. Modified from Wikipedia Community Member Crenim http://commons.wikimedia.org/wiki/File:Yang_cycle.png.

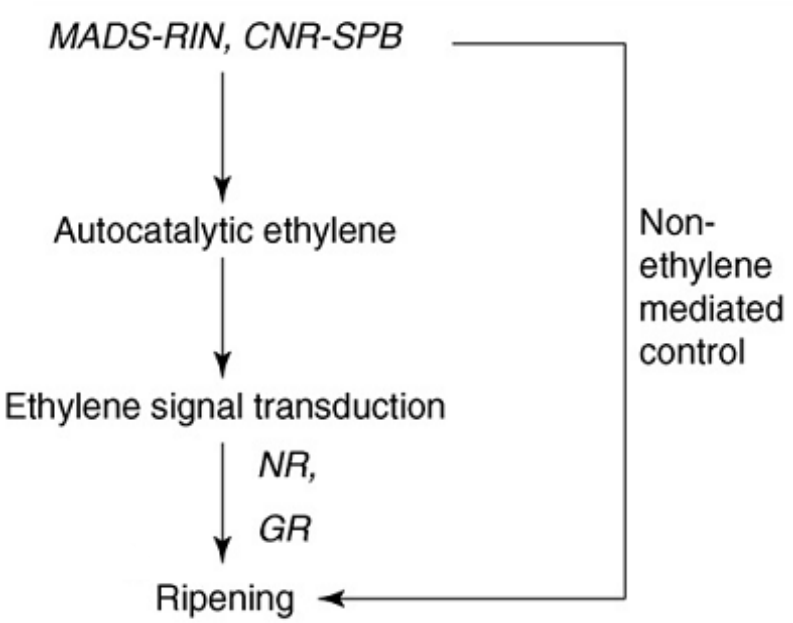

Fig. 1.3. Summary of ripening regulation. Current understanding of the regulation of the ripening process in tomato fruit. The transcription factors MADS-RIN (identified from a mutation in the MADS-box promoter of the ripening-inhibitor mutant) and CNR-SPB (identified from an alteration in the SQUAMOSA promoter binding protein in the colourless non-ripening mutant) are necessary for the induction of ethylene and non-ethylene mediated ripening. The ethylene receptors NR and GR proteins (identified from mutations in the never-ripe and green-ripe mutants) transfer the ethylene signal to downstream ripening components. Taken from Giovannoni (2007).

1.4.2.2 Respiration

Fruits can be physiologically classified as 'climacteric' or 'non-climacteric'. This classification is based on their respiratory behaviour during fruit ripening. In climacteric fruit, at the onset of ripening, respiration in the fruit rapidly increases to a maximum (the 'climacteric peak' or 'respiratory climacteric') and subsequently declines, a process associated with increased ethylene biosynthesis rates (Giovannoni, 2001). The respiratory climacteric tends to take approximately ten days from start to finish (Grierson and Kader, 1986). It should be noted that the increase in respiration is not essential in order for ripening to take place as all non-climacteric fruit ripen without a respiratory peak.

Ethylene has been shown to stimulate and control the increase in respiration (Grierson and Kader, 1986; Oeller *et al.*, 1991; Gray *et al.*, 1992; Lelievre *et al.*, 1997) nevertheless, there is lack of understanding as to the function of the respiratory climacteric. It has been suggested that this burst of respiration may be used to provide energy for the other biosynthetic changes that occur during ripening (Gray *et al.*, 1992). However, it seems unlikely that a single burst of respiration would provide the energy required to fuel the fruit through the entire ripening process. Also, the metabolic demands on the fruit seem to be higher during the early stages of fruit development (i.e. rapid cell division and high metabolic activity) before the climacteric occurs. Another suggestion is that the respiratory rise is purely a response to ethylene and not a demand for energy (Brady, 1987). This was proposed after the observation that when non-climacteric fruit and climacteric fruit that lack maturity to ripen are exposed to ethylene, the respiration rate in these fruit increases. When ethylene is withdrawn, the respiration rate subsequently decreases again. This observation has also been seen in ethylene treated fruits of the *rin* ripening mutants

(Herner and Sink, 1973). In these mutants the tomato fruit ripens incompletely, does not synthesize ethylene and has no respiratory climacteric. Exogenously applied ethylene to *rin* fruits induced CO_2 production for as long as the exogenous ethylene was present. In further experiments, repeated short consecutive applications of exogenous ethylene were applied. Again, peaks in CO_2 production corresponded to the peaks in ethylene. Also, in the non-climacteric lemon fruit, exogenously applied ethylene stimulates CO_2 production and subsequent withdrawal of the ethylene leads to a decrease in CO_2 (Denny, 1924).

This research shows that the reason for the respiratory peak in climacteric fruit is most likely just a response to the increased ethylene biosynthesis. However, further research is still needed to uncover the function of the respiratory climacteric.

1.5 Photoassimilation and photoassimilate partitioning

The green tomato fruit contains functional chloroplasts and is able to photosynthesise (Smillie *et al.*, 1999). However, the contribution made by the chloroplasts is not sufficient to meet the total photosynthate requirements of a developing and ripening fruit (Piechulla *et al.*, 1987; Gillaspy *et al.*, 1993; Smillie *et al.*, 1999). Therefore, tomato fruit are sink organs and are dependent upon the translocation and importation of photosynthates (e.g. sugars, amino acids, organic acids) (Ho, 1988; Valle *et al.*, 1998; Boggio *et al.*, 2000). Moreover, the sink strength, as defined by the ability of the fruit to attract and import assimilate, changes throughout tomato fruit development. The sink strength of a fruit is genetically determined (e.g. by sink size or metabolic activity) but is affected by the availability of assimilate supply, proximity to the source and stage of development (Ho, 1988; Gillaspy *et al.*, 1993). During the early stages of development the fruit is a utilization

sink and will compete with expanding leaves for assimilate (Ho, 1984; 1988; Gillaspy *et al.*, 1993). In the later stages of development the fruit is a storage sink and is a stronger sink than young leaves and roots (Ho, 1988).

Identifying if organic and amino acids are translocated and imported, or synthesised from photoassimilates within the fruit is an important factor in understanding the regulation of organic and amino acid accumulation in the fruit. However, little is known about the translocation and uptake of organic and amino acids during tomato fruit development. Research in tomato has identified that a number of organic and amino acids are translocated and imported into the fruit whilst the remainder are synthesised from imported photoassimilates (e.g. sugars). In research investigating carbon translocation, tomato leaves were fed with $^{14}CO_2$ (Walker and Ho, 1977). The photosynthates exported from the source leaf to the sink fruit were identified by measuring the ^{14}C-compounds at different places within the translocation pathway from the source leaf to a young fruit. Ten percent of the total translocates imported into the fruit comprised of organic and amino acids. Malate was the only organic acid found to be exported from the leaf. However, both malate and citrate were found in the translocation pathway and the fruit with malate being the most abundant. Aspartate and glutamate were the only amino acids found in detectable quantities to be exported from the source leaf. Other amino acids were increasingly found from samples taken further along the translocation pathway (e.g. glycine, proline, valine, threonine, alanine and leucine) suggesting that they were synthesised either in the phloem or imported from neighbouring cells. Although enzymes of the antioxidant defence system for plant defence (Walz *et al.*, 2002) and sugar metabolism (Hu *et al.*, 2009) have been found in plant phloem it is unlikely that enzymes of the amino acid synthesis pathway would

be present. Therefore, it is more likely that the amino acids detected further along the translocation pathway were synthesised in the neighbouring cells and imported into the phloem.

Further research has investigated the composition of free amino acids in phloem sap of tomato fruit using aphid stylectomy and EDTA-enhanced phloem exudate (Valle *et al.*, 1998). Glutamate and glutamine were the predominant amino acids in the translocation pathway with aspartate, serine and threonine found at high levels. Differences in the amino acids translocated between the two research projects may be due to differences in the tomato variety used and the sensitivity of the methods of amino acid detection.

The mechanism by which amino acids are taken up in tomato fruit from the phloem is unknown. Valle *et al.* (1998) suggested that uptake of amino acids (i.e. phloem unloading) is coupled to the mass flow of sucrose. This was the mechanism proposed in a study of phloem transport of amino acids in barley leaves (Winter *et al.*, 1992). Given that 90% of the photosynthates imported into the tomato fruit is sucrose (Walker and Ho, 1977) this suggestion may at first seem plausible. However, the study by Winter *et al.* (1992) investigated the unloading of amino acids from the source leaf into the phloem (i.e. phloem loading). There is no evidence to suggest that the mechanism for phloem loading from the leaves in barley should be the same as phloem unloading in tomato fruit and so more research is needed to identify the mechanism for uptake of amino acids.

Grierson and Kader (1986) observed that mature-green fruits detached from the plant and allowed to ripen contained many of the same compositional changes as found in fruit that remain attached. Therefore, some aspects of ripening must be dependent on the metabolism of compounds within the fruit and not on the import of photoassimilates

directly. However, they also noted that fruit quality was affected in detached fruit relative to fruit ripened 'on the vine'. Due to the formation of an abscission layer between the calyx and the fruit 10 days after the breaker stage, assimilate importation was shown to cease (Ho and Hewitt, 1986) indicating that compositional changes after this point cannot be dependent upon photoassimilate importation. From this research, to maximise fruit flavour harvest time should be at the ripe stage (10 days after the breaker stage) to ensure maximum uptake of photoassimilates (e.g. sugars) and harvest time after this point should not significantly alter fruit flavour.

Although some organic and amino acids are imported into the fruit the majority are metabolised from imported assimilates and/or their products (e.g. sugars, starch) within the fruit. Therefore, the regulation of organic and amino acid accumulation is most likely to be dependent upon fruit metabolism and carbon uptake than on direct importation.

1.5.1 Regulation of carbon uptake in fruit during ripening

Assimilates imported into sinks, such as tomato fruit, must be partitioned either between different compartments and/or to different compounds. The focus of the literature has been on invertases and the key role they play in the accumulation and partitioning of sugars in storage organs.

Sucrose, glucose and fructose, are the major sugars found in tomato fruits in varying ratios according to variety. For example, *Solanum lycopersicum* mainly accumulates sugars as hexoses whereas *Solanum pennellii* tends to accumulate mainly sucrose (Yelle *et al.*, 1988). Invertases catalyse the irreversible hydrolysis of sucrose to form the hexoses glucose and fructose. In plants there are different isoforms of invertases that are found in discrete

subcellular locations and are characterized by their subcellular location and pH optima. There are two intracellular (vacuolar and cytoplasmic) invertases and one extracellular (cell wall) invertase. The vacuolar and cell wall invertases are acid invertases as they have an acidic pH optima (Sturm and Tang, 1999; Buchanan *et al.*, 2000). The cytoplasmic invertase is a neutral or alkaline invertase (Sturm, 1999; Sturm and Tang, 1999; Buchanan *et al.*, 2000). Cell wall invertases are insoluble invertases involved in sucrose partitioning between sink and source organs but could be involved in the response to wounding/infection and in the control of cell differentiation and plant development (Sturm and Tang, 1999). Cell wall invertases were found to increase in activity at wound and infection sites in carrot tap roots (Sturm and Chrispeels, 1990). The increase in invertase activity was accompanied by a rapid accumulation of hexoses at the site (Sturm and Tang, 1999). It is thought that the increased metabolic activity associated with the plants response to stresses (e.g. increased respiration, production of defence compounds and strengthening of the cell wall) is provided by sucrose accumulation at the sites of wounding or infection where the invertases are hydrolysed to hexoses for a source of energy and carbon. In seeds of developing fava beans a decrease in invertase activity was found in the seed coat during the transition of the embryo in the cell division phase to the storage phase. The decreased invertase activity was accompanied by an increase in the sucrose-to-hexose ratio and an increase in biomass. It is thought that alterations to the sucrose-to-hexose ratio by invertase can control cell fate and seed development by maintaining cell division or triggering cell differentiation (Sturm and Tang, 1999). Vacuolar invertases are soluble invertases involved in osmoregulation and cell enlargement. These invertases are also involved in the control of sugar composition in fruits and storage organs and in their response to cold (cold sweetening) by conversion of the

resynthesised sucrose (from starch degradation) to glucose and fructose for storage (Sturm and Tang, 1999). Cytosolic invertases are less well characterised. These invertases are probably involved in channelling sucrose into metabolism as they are sucrose specific, unlike the cell wall and vacuolar invertases, which also hydrolyze other β-fructose-containing oligosaccharides, such as raffinose (Sturm, 1999; Sturm and Tang, 1999).

Invertases play a part in controlling the uptake capacity of sugar in tomato fruit. For example, a decreased hexose/sucrose ratio was observed in transgenic fruit of *S. lycopersicum* expressing an antisense invertase (*TIV1*) (Klann *et al.*, 1996). This has been further demonstrated through a genetic study using an introgression line (IL9-2-5) that produced tomato fruit with increased soluble solids (Brix). The introgression line contains a single homozygous restriction fragment length polymorphism (RFLP)-defined chromosome segment of the *S. pennellii* wild species in the cultivated *S. lycopersicum* background. A quantitative trait loci (Brix9-2-5) relating to the increased phenotypic fruit sugar trait found in this introgression line was subsequently delimited to a region of the apoplastic fruit-specific invertase (*LIN5*) (Fridman *et al.*, 2000). In a further study, sequencing analysis of the Brix9-2-5 region of *LIN5* showed that an aspartate residue (Asp^{348}) was uniquely associated with *S. pennellii*. Multiple alignments with other plant invertases showed this apartate as a conserved residue at this position suggesting a non-neutral role near the catalytic site. Growth analysis of the yeast invertase-deficient strain overexpressing a *LIN5* mutated allele from *S. lycopersicum* showed that the expressed invertase complemented the invertase deficient yeast strain more closely than the control when grown on sucrose. Kinetic analysis of the expressed invertase showed that the Michaelis-Menten constant (Km) for sucrose was much lower than for the control indicating that the enzymes rate of catalysis at a lower

sucrose concentration is more rapid than the *S. lycopersicum* allele (Fridman *et al.*, 2004). The invertase cleaves sucrose in the apoplast which maintains sucrose unloading from the phloem and also allows use of both the sucrose and monosaccharide transporters increasing the capacity of sugar uptake (Bush, 1993; Roitsch, 1999; Sturm and Tang, 1999). Therefore, enhancing the activity of *LIN5* would increase sucrose cleavage and, through the utilisation of the transporters for both sucrose and hexoses, would increase the rate at which sucrose is unloaded from the phloem and taken up by the fruit. Subsequent biochemical analysis of IL9-2-5 showed that this introgression line had an increased capacity to take up sucrose (Baxter *et al.*, 2005b).

This research has shown that sucrose metabolising enzymes can affect the final composition of the fruit. It also highlights the important role of transporters in hexose accumulation within the fruit. Although invertase was shown to have a greater activity in the IL9-2-5 introgression line, this would not have increased the uptake capacity of the sugars into the fruit without the presence and activity of the appropriate transporters. To investigate this, research characterising three tomato hexose transporter genes (*LeHT1*,*2* and *3*) showed that *LeHT* expression was highest at 10 DAA which preceded the peak in hexose concentration (Dibley *et al.*, 2005). *In situ* hybridisation showed *LeHT3* transcripts were localised to storage parenchyma cells in the outer pericarp, but not in vascular bundles or nearby storage parenchyma cells where the site of phloem unloading takes place. Protein levels throughout fruit development of *LeHT* were found to correlate well with hexose concentration suggesting post-transcriptional regulation. Although this research is based on correlative evidence, the activity of these hexose transporters, especially *LeHT3*, could contribute to the control of hexose accumulation in tomato fruit. As organic and amino acid

accumulation in the vacuole requires transport across the tonoplast, it is possible that their accumulation may be similarly regulated in part by tonoplast transport.

1.6 Organic and amino acid accumulation during fruit ripening

Amino acids are synthesised from the carbon skeletons of organic acids produced in glycolysis, the TCA cycle and the Calvin cycle (Figure 1.4) (Buchanan *et al.*, 2000). Glutamate, and subsequently glutamine, are synthesised from 2-oxoglutarate which is in turn derived from citrate. Aspartate, and subsequently asparagine, are synthesised from oxaloacetate which is derived from malate. Glutamate is the primary amino acid product of nitrogen assimilation.

1.6.1 Organic acid accumulation

Organic acids (especially citrate and malate) can accumulate to very high levels in plant cells due to their storage in the vacuole (Farre *et al.*, 2001; Martinoia *et al.*, 2007). For example, in leaves of CAM plants (Martinoia and Rentsch, 1994) and in the juice cells of *Citrus aurantifolia* (Brune *et al.*, 1998) malate and citrate, respectively, can accumulate to concentrations up to 350 mM.

There are a number of reasons why organic acids are transported into the vacuole:

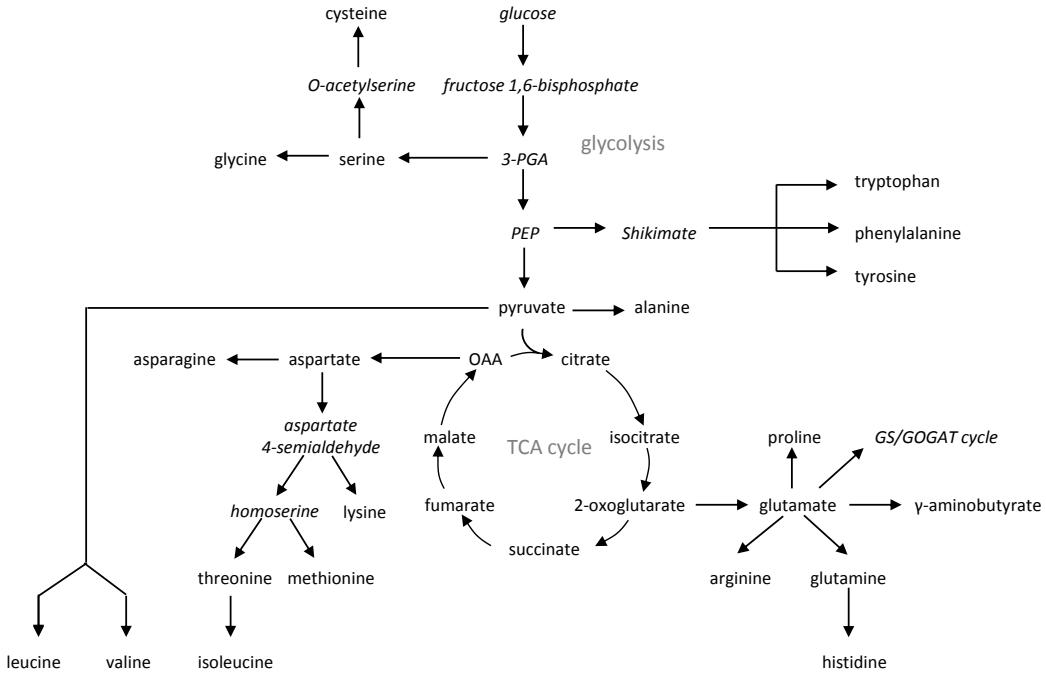

Fig. 1.4. Organic and amino acid biosynthesis pathways. GS/GOGAT: glutamine synthetase/glutamate synthase, OAA: oxaloacetic acid, PEP: phospho*enol*pyruvate, PGA: phosphoglycerate.

1.6.1.1 Organic acids act as counter ions in the vacuole

The vacuole carries out a number of varied functions within the cell. One of these functions is to store important cations such as calcium or cations that have been taken up from the soil such as potassium. For these cations to be stored in the vacuole without altering the charge there is a need for balancing anions (or counter ions). Organic acids are often used as counter ions as they are readily available or can be synthesised easily. The organic acid malate is utilized as a counter ion and as a solute in the vacuole. In *Arabidopsis thaliana*, leaf malate levels increased significantly in plants grown in high salt (50 mM) for two weeks. This suggests that under salt stress malate may be used as a counter ion to compensate for charge differences from sodium and chloride uptake (Emmerlich *et al.*, 2003). Malate, as a counter ion, is also involved in regulating stomatal aperture. In stomatal guard cells accumulation of K^+ ions is important for stomatal opening. However, accumulation of K^+ ions can only occur if counterbalanced by anions. Newly synthesised malate or malate from the vacuole is often used for this purpose along with other anions. In *Tulipa* spp. and in *Vicia faba* malate is the most important counter ion for this purpose (Martinoia and Rentsch, 1994).

1.6.1.2 Organic acids help to generate turgor for growth by cell expansion

During cell growth, the least expensive way metabolically for a plant to increase cell size is to enlarge the vacuole (Buchanan *et al.*, 2000). In order for the cell to uptake water for cell expansion and to maintain turgor pressure, the vacuole must accumulate solutes. Organic acids, such as malate and citrate, can fulfil this role. This has been investigated in the fruit of *Solanum lycopersicum* Mill. (Guillet *et al.*, 2002). A phospho*enol*pyruvate

carboxylase (PEPC), which is involved in malate synthesis, isolated from these fruit (LYCes;Ppc2) was shown to increase in expression at the same time as malate and citrate accumulation during early fruit development. These two events also coincided with the main period of cell expansion in developing fruit. This suggests that PEPC could be involved in the synthesis of malate and citrate to maintain turgor pressure necessary for cell expansion in early fruit development.

1.6.1.3 Regulation of accumulation of organic acids

The crucial factors in regulating accumulation of organic acids are therefore likely to be:

1.6.1.3.1 Rate of organic acid production

Organic acids such as malate and citrate are synthesised (via the TCA cycle) in the mitochondrion. Citrate and malate are required to maintain turnover of the TCA cycle and are exported to the cytosol to be used as metabolic intermediates. Although the structure and components of the TCA cycle are well known, the regulation of this pathway is still largely unknown (Fernie *et al.*, 2004). Recently, research into the role of the TCA cycle has being investigated in tomato where the activities of individual enzymes of the TCA cycle were reduced. A description of this research follows and a summary will be provided at the end.

An aconitase mutant (*Aco1*) was characterised in plants of *Solanum pennellii* (Carrari *et al.*, 2003a). Plants of the aconitase mutant (*Aco1*) exhibited large increases in fruit weight and an increased rate of CO_2 assimilation. There was a decreased flux through the TCA cycle and decreased levels of TCA cycle intermediates (fumarate, succinate and 2-oxoglutarate)

but an increased rate of CO_2 assimilation. An increased rate in photosynthetic sucrose synthesis taken together with the increased fruit weight suggests that carbon partitioning was redirected through the sucrose synthesis pathway.

The activity of mitochondrial malate dehydrogenase (mMDH) was reduced using antisense inhibition in *Solanum lycopersicum* plants (Nunes-Nesi *et al.*, 2005). These plants also had increased fruit weight and enhanced photosynthetic activity as well as increased accumulation of starch and sugars. As with the aconitase mutant there was a decreased flux through the TCA cycle and reduced respiration rates. There were no consistent changes to the levels of TCA cycle intermediates except for an increase in succinate.

Fumarase was antisense inhibited in plants of *Solanum lycopersicum* (Nunes-Nesi *et al.*, 2007). These plants also exhibited a decrease in flux through the TCA cycle, decreased dark respiration and reduced CO_2 assimilation. However, there was no impact on the maximal catalytic activities of the enzymes in the TCA cycle and only minor changes to the levels of organic acids.

The enzyme succinyl-coenzyme A ligase was antisense inhibited in *Solanum lycopersicum* (Studart-Guimaraes et al., 2007). These antisense plants exhibited decreased fruit weight, had no alterations in CO_2 assimilation and only slightly reduced rates of dark respiration. There were increases in TCA cycle intermediates upstream from succinate (isocitrate, citrate and 2-oxoglutarate) in the strongly repressed lines but no observable differences in the other intermediates. Analysis of the amino acids showed increases in glutamate, γ-aminobutyric acid (GABA) and alanine in the strongly repressed lines. The GABA shunt was shown to be an alternative pathway for the production of succinate with an increase in transcript levels of glutamate decarboxylase (GAD) and increased activities of

GAD and glutamate dehydrogenase. Further experiments to evaluate flux through the GABA shunt showed increased incorporation of label to intermediates of the GABA shunt in leaves of the antisense lines supplied with ^{13}C-glucose and increased release of labelled CO_2 with leaf discs supplied with [1-^{14}C]-glucose.

Mitochondrial citrate synthase was antisense inhibited in plants of *Solanum lycopersicum* (Sienkiewicz-Porzucek *et al.*, 2008). There were no differences in the rate of photosynthetic carbon assimilation and partitioning in feeding assays with $^{14}CO_2$. There was a slight increase in electron transport rate for the strongest antisense line and an increase (3-3.5-fold) in dark respiration. There was a slight decrease in total protein content but no change in total nitrogen in these plants. Some decreases in the levels of organic acids of the TCA cycle and carotenoids but increases in several amino acids were found.

The activity of mitochondrial NAD^+-dependent isocitrate dehydrogenase was reduced by antisense inhibition in *Solanum lycopersicum* plants (Sienkiewicz-Porzucek *et al.*, 2010). There was a reduction in the diameter of the fruits and total fresh fruit weight. There were no major differences in assimilation or chloroplastic electron transport but a reduction in the maximal efficiency of photosystem II (Fv/Fm). There was a reduction in some pigments including chlorophyll a and b and reductions in NADH and NADPH. The total insoluble protein and nitrate content increased but there were no changes to the total amino acid content and decreased starch accumulation in leaves. However, the content of β-alanine, glycine, proline, γ-aminobutyrate, malate, succinate and pyruvate was decreased and asparagine content increased. There were no alterations to TCA cycle enzymes except for a strong reduction in fumarase and an increase in glutamate dehydrogenase. Transcript expression comparisons between the antisense lines and the wild type revealed Calvin cycle

genes slightly down-regulated in the antisense line and genes associated with protein degradation, redox regulation-associated and G-protein-associated were increased. Flux analysis, by feeding leaves with positionally labelled ^{14}C-glucose and monitoring $^{14}CO_2$ evolution, revealed a lower proportion of carbohydrate oxidation is carried out by the TCA cycle. In a second feeding experiment using ^{13}C-labelled pyruvate the rate of label redistribution was unaltered to citrate but was significantly reduced to isocitrate, 2-oxoglutarate, malate, fumarate and glutamate. This suggests that there was a reduced flux through the TCA cycle.

Collectively, this research has shown that reducing one component of the TCA cycle is not overly detrimental to the plants, despite the TCA cycle being a central metabolic pathway, which is quite unexpected. Generally there were few alterations in measures of growth and/or yield in these plants. However, this result can be explained as there were quite significant changes to the metabolism of these plants. Changes in the carbon partitioning from the TCA cycle into alternative pathways (i.e. GABA shunt, photosynthetic and nitrogen assimilation pathways) were found. This resulted in bypassing the enzyme with reduced activity to maintain the functioning of the TCA cycle, therefore compensating for the reductions in enzyme activity to some extent. However, there were instances where this was not an effective mechanism (i.e. in reductions of aconitase, malate dehydrogenase, and fumarase) and decreases in flux through the TCA cycle occurred leading to alterations in organic and amino acids. This shows that alterations to the enzymes in TCA cycle can have an impact on organic and amino acid biosynthesis. There are other pathways where alterations in the activities of enzymes in tomato fruit that have been linked to changes in organic and amino acid content. One such enzyme is phospho*enol*pyruvate carboxykinase

(PEPCK). This enzyme could be involved in malate dissimilation via conversion to phospho*enol*pyruvate and subsequently utilized in gluconeogenesis (Figure 1.5) (Bahrami *et al.*, 2001). PEPCK activity was found to increase during fruit ripening and was consistent with the large decrease in organic acid content. Organic acid content was not measured in this study, but compared with other published data. PEPCK abundance has also been correlated with citrate and malate content throughout development in a variety of fruits (Famiani *et al.*, 2005). PEPCK abundance coincided with the decrease of malate and/or citrate in blueberry, redcurrant and raspberry fruits, in agreement with Bahrami *et al.* (2001). However, this research also showed PEPCK was present in the fruit of blueberries, raspberries and redcurrants when there was no dissimilation of malate or citrate occurring. Furthermore, in strawberry fruit, where there is no dissimilation of malate or citrate, PEPCK could not be detected. Further research is required to establish the role of this enzyme in tomato fruit and in organic acid partitioning.

From these studies it can be seen that manipulation of the enzymes of these pathways can have an impact on the levels of organic and amino acids, but more importantly on the pathways which utilize them. Changes to the metabolism and partitioning within these plants indicate that the enzymes of the TCA cycle and pathways that share substrates of the TCA cycle are crucial factors in regulating the production, and therefore the accumulation, of organic and amino acids.

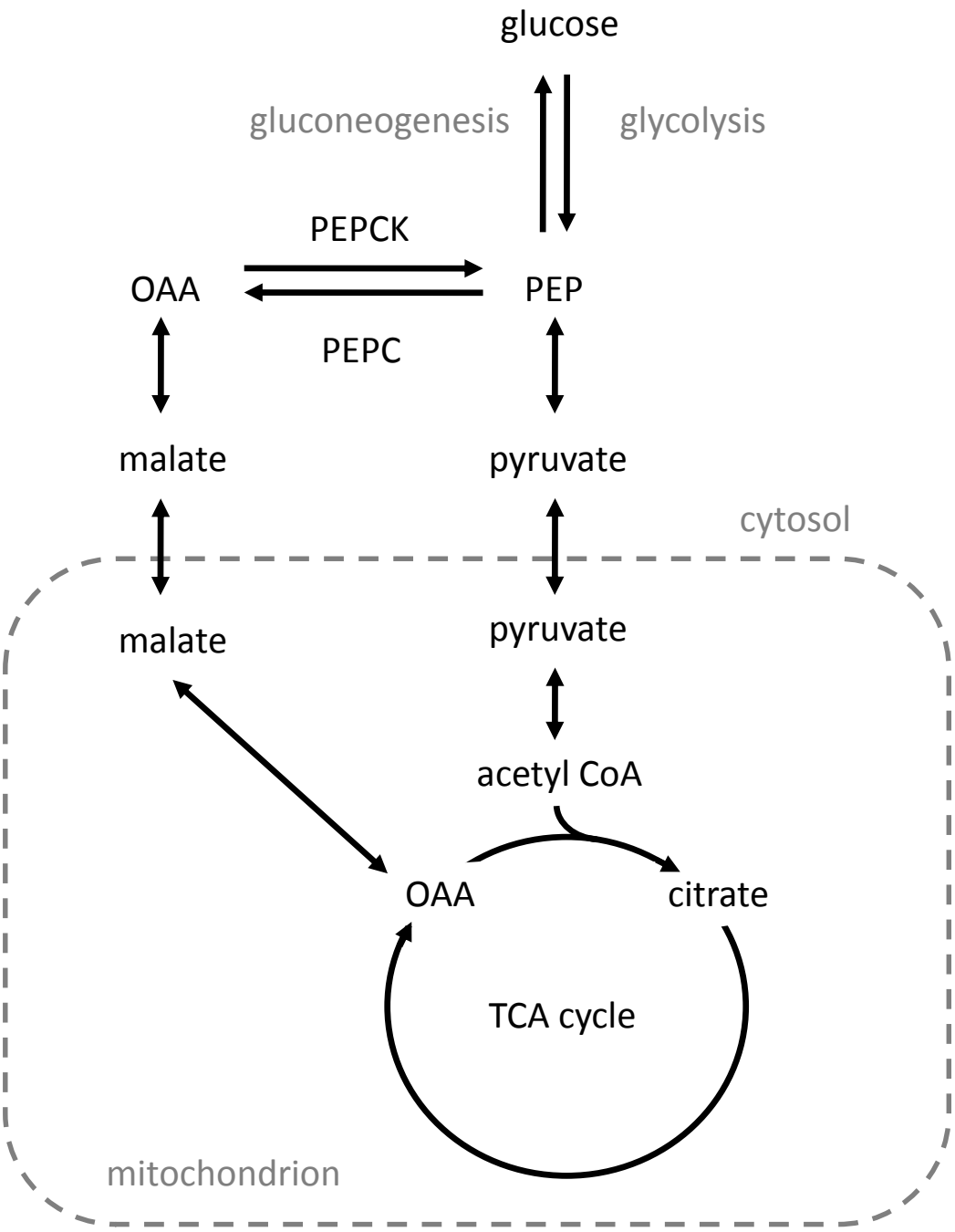

Fig. 1.5. Alternative pathway for malate utilization. Acetyl CoA: acetyl coenzyme A, OAA: oxaloacetic acid, PEP: phosphenolpyruvate, PEPC: phosph*enol*pyruvate carboxylase, PEPCK: phosho*enol*pyruvate carboxykinase, TCA: tricarboxylic acid.

1.6.1.3.2 Tonoplast organic acid transporters

To accumulate in the vacuole the organic acids must cross the vacuolar membrane or tonoplast. Therefore, tonoplast transporters can be a mechanism for the regulation for the accumulation of organic acids in the vacuole.

Malate transport across the tonoplast has been intensively researched due to the important role of malate in plant metabolism (Martinoia and Rentsch, 1994). In *Arabidopsis thaliana* there is a well characterised malate tonoplast transporter (A*tt*DT) (Emmerlich *et al.*, 2003; Hurth *et al.*, 2005) and malate channel (Kovermann *et al.*, 2007) but the molecular details of tonoplast anion transport in tomato are less clear. It has been suggested that transgenic tomatoes with reduced expression of tomato ripening-associated membrane protein (TRAMP) plays a role in tonoplast transport of organic acids (Chen *et al.*, 2001). TRAMP is a channel protein and member of the major intrinsic protein (MIP) family, which are mainly represented by aquaporins. Levels of organic acids were higher and the levels of sugar were lower in the fruit-specific TRAMP antisense plants. The authors proposed that TRAMP is involved in the movement of organic acids and/or sugars between the vacuole and cytosol. Although this research indicates that TRAMP affected the levels of organic acids and sugars, further investigation is required as to what role it may have with regards to tonoplast transporters.

Further tonoplast transport research into the regulation of fruit acidity has been investigated using two peach cultivars, normal acid (Fantasia) and low acid (Jalousia) varieties (Etienne *et al.*, 2002). This research involved expression analysis by northern blotting using probes from genes implicated in organic acid metabolism (NAD^+-malate dehydrogenase, mitochondrial citrate synthase and $NADP^+$-isocitrate dehydrogenase) and

storage (V-ATPase subunit A and two V-PP_iases, with low and high expression in fruit) from mesocarp/epidermis RNA throughout ripening in both varieties. There was no correlation found between the expressions of these genes with changes in organic acids. However, the V-PP_iase (high expression in fruit) showed a biphasic expression pattern that correlated with the accumulation of malate and citrate. This suggests that tonoplast pyrophosphatase proton pumps may play a role in fruit acidity. Other research in the relative expression of tomato V-ATPase cDNAs supports this suggestion (Coker *et al.*, 2003). The relative expression of 23 V-ATPase genes in tomato plants throughout development showed that mRNA levels decrease during development of green fruit then increase during ripening. This suggests that V-ATPases may be responsible for the proton accumulation necessary to drive the transport of citrate and malate across the vacuolar membrane.

There is evidence of an H^+-ATPase transporter and an anion carrier or channel present in tomato tonoplasts (Oleski *et al.*, 1987a; Oleski *et al.*, 1987b) that may be involved in anion tonoplast transport. In mature green tomatoes of *Solanum lycopersicum* fruit an anion-sensitive H^+-translocation ATPase was identified in tonoplasts isolated from pericarp tissue and found to be similar to other plant cell tonoplast H^+-ATPases (Oleski *et al.*, 1987b). This research was continued to investigate if H^+-ATPase activity was active in citrate uptake assays in tonoplasts isolated from mature green tomatoes of *Solanum lycopersicum* fruit (Oleski *et al.*, 1987a). Although H^+-ATPase was found to be active, the activity of H^+-ATPase did not affect the rate of citrate uptake suggesting that citrate accumulation is not energy dependent. It was suggested that citrate transport may occur by facilitated diffusion by an anion channel or carrier and is not specific for citrate and may be used for other anions.

Although a number of transport mechanisms have been identified in tomato, much research is still needed to identify and fully characterise the mechanisms that transport citrate and malate across the vacuolar membrane.

1.6.1.3.3 Role of organic acid accumulation in fruit

Organic acid accumulation tends to be greatest during the early stages of fruit development. With the onset of fruit ripening there is a subsequent decline in organic acids (Bahrami *et al.*, 2001; Carrari *et al.*, 2006) with the exception of citrate and isocitrate (Carrari *et al.*, 2006). This pattern of organic acid accumulation may be for two complementary reasons. The first reason may be for protection and dispersal. During the early stages of fruit development the role of fruit is to provide protection to the developing seeds from predators (Fray and Grierson, 1993). Having high levels of acid at this stage may make the fruit unpalatable to predators, protecting the developing seeds. Then, once the seeds have developed, the onset of ripening occurs and the role of the fruit changes from protection to seed dispersal (Fray and Grierson, 1993). Organic acid levels decline, the sugar to acid ratio increases, and amino acids increase making the fruit desirable and palatable to the seed dispersers. The second reason may be metabolic. Organic acids that accumulated in the early stages of development may provide a source of carbon skeletons for subsequent amino acid synthesis. Gallardo *et al.* (1995) have found that $NADP^+$-isocitrate dehydrogenase (NADP-ICDH) activity is higher is ripe fruit. High activity of NADP-ICDH coupled with the high levels of citrate and isocitrate could provide a supply of 2-oxoglutarate for amino acid biosynthesis (Carrari *et al.*, 2006).

1.6.2 Amino acid accumulation

Free amino acids contribute to the overall taste in many foods (Fuke and Konosu, 1991; Kisaka and Kida, 2003). The four most abundant free amino acids in tomatoes are glutamate, aspartate, asparagine and glutamine (Roessner-Tunali *et al.*, 2003; Pratta *et al.*, 2004). Of these, glutamate and aspartate have been shown to be the main contributors to flavour (Fuke and Konosu, 1991).

Little is known about the metabolism of amino acids during tomato fruit ripening. Free amino acid content of tomato fruits during ripening has been determined by Baxter *et al.* (2005a), Boggio *et al.* (2000) and Valle *et al.* (1998). Glutamine and glutamate were found to be the most abundant amino acids in tomato phloem and ripe fruit (Valle *et al.*, 1998; Boggio *et al.*, 2000). Both glutamate and aspartate increase during fruit ripening whereas glutamine and asparagine levels can be variable and are dependent upon fruit variety (Boggio *et al.*, 2000; Roessner-Tunali *et al.*, 2003; Baxter *et al.*, 2005a).

There has been some research into the enzymes involved in the biosynthesis of amino acids during tomato fruit ripening. Increases in cytosolic NADP-ICDH in *Solanum lycopersicum* Mill. fruit from the green to red developmental stage indicate the use of an alternative pathway for providing carbon skeletons for glutamate synthesis rather than from the mitochondrial NAD^+-isocitrate dehydrogenase (NAD-ICDH) in the TCA cycle (Gallardo *et al.*, 1995).

Changes to the activities of enzymes in the GABA shunt have altered amino acid content in tomato fruit. The total amount of free amino acids were significantly increased in fruit of tomato plants overexpressing an $NADP^+$-glutamate dehydrogenase from *Aspergillus nidulans* (Kisaka and Kida, 2003). Specifically, the fruit were significantly increased in

glutamate, aspartate, asparagine, alanine and GABA content. In later research by the same authors, tomato plants were transformed by antisense inhibition with glutamate decarboxylase (Kisaka *et al.*, 2006). These fruit contained significantly more total free amino acids and the content of a number of amino acids, including glutamate and aspartate, were also significantly increased indicating that these enzymes can strongly influence the rate of glutamate synthesis. In other research, glutamate content correlated with the activities of nitrogen-assimilating enzymes in three varieties (Platense, Vollendung and Cherry) of *Solanum esculentum* Mill. tomato fruit (Boggio *et al.*, 2000). Increases in the relative content of glutamate correlated with increased levels of glutamate dehydrogenase, aspartate aminotransferase and NAD^+-malate dehydrogenase and decreased glutamine synthetase in ripe fruit relative to green fruit suggesting a reciprocal expression pattern of induction.

Despite these efforts, the understanding of amino acid metabolism is still somewhat incomplete.

1.6.2.1 Tonoplast amino acid transporters

Very little is known about the intracellular compartmentation and storage of amino acids in tomato fruit. Studies of sub-cellullar compartmentation in potato has shown that a high proportion of amino acids are associated with the vacuole (Farre *et al.*, 2001) with the exceptions of aspartate and glutamate, which were mainly located in the cytosol and plastid. Due to the genetic similarity between tomato and potato it could be suggested that amino acid also accumulate in the vacuole in tomato fruit. However as the potato tuber is physiologically a different organ to the tomato fruit and performs an entirely different

function, care must be taken in assuming that sub-cellular compartmentation is the same in tomato.

Research in barley mesophyll vacuoles indicate that there are different mechanisms for the transport of amino acids across the tonoplast (Dietz *et al.*, 1990; Martinoia *et al.*, 1991). One mechanism for tonoplast transport of aromatic amino acids is dependent upon the proton motive force generated by the ATPase or V-PPase (Homeyer and Schultz, 1988; Homeyer *et al.*, 1989; Martinoia *et al.*, 1991). There is a second mechanism, specifically for the transport of positively charged amino acids, such as arginine and lysine (Martinoia *et al.*, 1991). Finally, there is a mechanism with broad specificity for the influx and efflux of various amino acids, which is ATP-stimulated but non-energy requiring (Dietz *et al.*, 1989; Dietz *et al.*, 1990; Martinoia *et al.*, 1991; Goerlach and Willmshoff, 1992). It was also suggested by Dietz *et al.* (1990) that the regulation of amino acid accumulation in the vacuole was determined by the utilization/synthesis of proteins in the cytosol. It is possible that there are similar mechanisms for transport of amino acids across the tomato tonoplast.

1.6.2.2 Role of amino acid accumulation in fruit

Amino acids are synthesized for their use in protein synthesis and as a transportable nitrogen source. They are also used as precursors for the synthesis of a wide range of secondary metabolites including hormones and compounds in plant defence (Valle *et al.*, 1998; Buchanan *et al.*, 2000). For these reasons, amino acids are important for growth and development. During the early stages of fruit development there is active cell division and protein synthesis. The main growth phase occurs later (i.e. from the onset of fruit ripening) and is due to cell expansion and uptake of water and assimilates (Ho and Hewitt, 1986). It

seems unlikely therefore that the high accumulation of amino acids in the later stages of developing fruit would be used solely for the purpose of fruit growth.

It has been suggested by Boggio *et al.* (2000) & Gallardo *et al.* (1995) that the increase in glutamate in ripe fruit may be a consequence of the respiratory climacteric and organic acid metabolism during the course of fruit development. Following this reasoning, as respiration and subsequently organic acid levels decline, glutamate production should also cease. However, production does not appear to stop during fruit ripening: glutamate levels continue to increase (Baxter *et al.*, 2005a; Carrari *et al.*, 2006).

Amino acids may accumulate to provide a source of precursors for volatile components. Many volatile components contribute to aroma and therefore play a role in the odour component of flavour (Thimann, 1980; Petro-Turza, 1986; Goff and Klee, 2006). For example, the volatile compound 2-phenylethanol, a major flavour contributor in tomato, cheese, wine and olive oil, is derived from phenylalanine (Goff and Klee, 2006; Tieman *et al.*, 2006a).

Amino acids may accumulate during the process of ripening to make the fruit more palatable to seed dispersers, as discussed previously. They may also contribute by their actual taste themselves (Schiffman *et al.*, 1981) or they may act as 'flavour enhancers'. Although their overall contribution to the total dry weight mass is low (only 2-2.5%) when compared with sugars (50%) and acids (13-15%) (Yilmaz, 2001), they can be detected by receptors on the human tongue at very low concentrations. The human detection threshold for L-glutamate is 0.063 mM and L-aspartate at 0.182 mM (Schiffman *et al.*, 1981). The levels of these amino acids in ripened fruit are 2.77 mM and 1.16 mM respectively (Boggio *et al.*, 2000) i.e. well above the levels of detection. The amino acids themselves have their

own tastes and the levels of asparagine and glutamine have been shown to vary according to variety (Boggio *et al.*, 2000; Roessner-Tunali *et al.*, 2003; Baxter *et al.*, 2005a). In this way, each amino acid may contribute to the flavour differences found between different varieties. A mammalian amino acid taste receptor has been identified that responds to a number of L-amino acids (Nelson *et al.*, 2002). Nelson's research also showed that the amino acid receptor can contribute to sensation as well as taste detection. The receptor was found to be more sensitive to monosodium glutamate, a common flavour enhancer.

1.7 Research Strategy

Introgression lines (ILs) can be an important resource for genetic and molecular studies of the genetic basis of fruit traits (Eshed and Zamir, 1995; Fridman *et al.*, 2000). ILs are produced by crossing an elite crop variety with a species containing desirable germplasm (often a wild species). Successive backcrossing and marker-assisted selection to the elite parent will produce a set of recurrent parent lines with single introgressed segments known as an exotic library. Lines that have overlapping introgressed chromosomal regions can be used to link a phenotypic trait to a smaller chromosomal region, therefore reducing the number of possible genes that may be responsible for the trait to aid candidate gene identification.

ILs in tomato are well characterised and have been used to identify Quantitative Trait Locis (QTLs) and subsequent candidate genes that has facilitated our understanding of fruit metabolism. The QTL *Brix9-2-5* for soluble solids (Brix) was shown to correspond to the fruit-specific apoplastic invertase gene *LIN5*, as described in Section 1.5.1 (Fridman *et al.*, 2000; Fridman *et al.*, 2004). The *fw2.2* QTL for major fruit size in tomato was found to

correspond to the *ORFX* gene and modifies fruit size by controlling carpel cell number before anthesis (Frary *et al.*, 2000). Identification of *malodorous*, a wild species allele affecting tomato aroma, in introgression line 8-2-1 was found to affect the levels of 2-phenylethanol and phenylacetaldehyde (Tadmor *et al.*, 2002). High levels of these volatile compounds gave tomatoes an objectionable aroma but provided a favourable aroma at low levels. Although these compounds were found to alter the aroma in tomato fruits, the biosynthetic pathway for these compounds in plants was largely unknown. Continuation of this research, using introgression line 8-2-1, identified the starting substrate and subsequently the biosynthetic pathway for these compounds (Tieman *et al.*, 2006a).

The aim of this research was to identify the mechanisms regulating organic and amino acid accumulation during tomato fruit ripening. The experimental strategy consisted of exploiting a set of near isogenic tomato introgression lines (Eshed and Zamir, 1994; 1995). In tomato, a population of 76 introgression lines derived from cross between a cultivated processing tomato *Solanum lycopersicum* (M82) and a wild green-fruited tomato *Solanum pennellii* (LA0716) has been produced (Eshed and Zamir, 1995; Liu and Zamir, 1999). Each introgression line in this population contains a single homozygous restriction fragment length polymorphism (RFLP)-defined chromosome segment of the *S. pennellii* wild species in the cultivated *S. lycopersicum* background. The lines contain on average an introgression of approximately 33 cM from a total chromosome size of 1200 cM (Eshed and Zamir, 1994). Within the 75 lines there is complete representation of the entire wild species tomato genome. Each introgression line is nearly isogenic to the *S. lycopersicum* genotype, hence the phenotypic variation found in that line can be associated with the introgressed segment. A further population of sub-introgression lines was produced (Dani Zamir, The

Hebrew University of Jerusalem, Israel). These sub-introgression lines contain smaller introgressed regions from *S. pennellii* in the *S. lycopersicum* background.

These lines showed a range of levels of organic and amino acids in ripe fruit grown in the field and therefore provide a useful resource in which genotype can be linked to altered metabolic phenotypes (Schauer *et al.*, 2006). Lines were selected from this population that had increased organic and amino acids. The lines had minimal changes in sugar content and measures of yield as these could confound interpretation of molecular changes. The lines were grown under greenhouse growth conditions to confirm the metabolic traits reported by Schauer *et al.* (2006) and one line (2-5) was selected that showed increases in organic and amino acid content. This line was exploited experimentally using the following two strategies:

1.7.1 Genetic Strategy

This strategy involved using the genetic differences between the 2-5 introgression line and the recurrent parent to identify the chromosomal region responsible for the metabolite trait. Firstly, methods were developed for quantitatively measuring organic and amino acid content. Metabolite content varies throughout development and in different tissues (Davies and Hobson, 1981; Velterop and Vos, 2001; Baxter *et al.*, 2005a; Mounet *et al.*, 2009). Therefore, metabolite content was analysed in line 2-5 relative to the recurrent parent in specific tissues and at different developmental stages to find which stage and specific tissue the difference was greatest.

Secondly, to link the metabolite traits to specific chromosomal regions, metabolite content was measured in the overlapping introgression lines to line 2-5. To further narrow

the chromosomal region, sub-introgression lines of 2-5 were analysed. Genes in the chromosomal regions linked to the metabolite traits were identified from annotations published by the International Tomato Annotation Group within the International Tomato Genome Sequencing Project (Mueller *et al.*, 2005).

1.7.2 Biochemical Strategy

This strategy involved exploiting the biochemical differences between the 2-5 introgession line and the recurrent parent to probe the molecular factors responsible for these differences. Initially, the TCA cycle was focused on as this is the main source of substrates for organic and amino acids. Differences in expression at the transcript level were assessed by measuring the transcript abundance of TCA cycle enzymes. Then, to identify differences at the protein level, the maximal catalytic activities of TCA cycle enzymes were measured in mitochondria isolated from pericarp tissue. To determine if there were differences in respiratory function, oxygen consumption and respiratory control ratio measurements were made in isolated mitochondria. Next, to assess differences in flux through the TCA cycle, flux was estimated by feeding pericarp discs with positionally-labelled glucose and the rate of labelled-CO_2 release was monitored. This targeted approach was extended to measure the transcript abundance of some of the enzymes in the pathways leading to aspartate and glutamate and in pathways downstream to other amino acids, including the GABA shunt. As it was not possible to measure the transcript abundance in all of the enzymes in these pathways and others, changes in relative expression levels throughout development of genes in the various pathways were extracted from the Tom1 array in the Tomato Functional Genomics database (Cornell University, Ithaca, USA).

Lastly, the focus shifted to the vacuole as organic and amino acids are thought to accumulate in this sub-cellular compartment in tomato fruit. To identify if there were differences in the rate of anion transport across the tonoplast that could have an effect on organic and amino acid accumulation, anion influx transport rates were measured in vacuole vesicles isolated from tomato pericarp tissue.

Chapter 2

Materials and methods

2.1 Reagents

General chemicals were obtained from Sigma-Aldrich Company Ltd. (Poole, UK), VWR International Ltd. (Lutterworth, UK), Melford Laboratories Ltd. (Ipswich, UK) or Merck Chemicals Ltd. (Nottingham, UK). Enzymes were obtained from Sigma-Aldrich Company Ltd. (Poole, UK) or Roche Diagnostics Ltd. (Burgess Hill, UK). Methanol–d_4, sodium 3-(trimethylsilyl) proprionate-d_4 and $^2H_20$ (D_20) were obtained from Goss Scientific Instruments Ltd. (Nantwich, UK).

2.2 Plant material

2.2.1 Tomato lines

Tomato seeds from independent introgression lines (ILs) were kindly provided by C.M. Rick, Tomato Genetics Resource Centre (TGRC, Davis, USA). This resource is composed of a tomato variety, *Solanum lycopersicum* (M82, LA3475) containing single introgressed

genomic regions from the wild green-fruited species *Solanum pennellii* (LA0716). The ILs have been produced through successive introgression backcrossing and marker-assisted selection to generate a set of recurrent parent lines with single introgressed segments (Eshed and Zamir, 1995). Tomato seeds from independent sub-introgression lines (sub-ILs) to IL 2-5 were kindly provided by Dani Zamir (The Hebrew University of Jerusalem, Israel).

2.2.2 Growth conditions

All tomato plants were grown from seed. Seed germination and plant growth was carried out in a greenhouse with a 16 h day length, 22-23°C day temperature, 20-22°C night temperature and supplementary lighting to maintain an irradiance of 250-400 µmol $m^{-2}s^{-1}$.

To germinate the seed, 4 cm^2 propagation trays were filled with Emerald Range soil-based multi-purpose compost (Goundrey's Ltd., Chipping Norton, UK) and well watered. Seeds were depressed through the surface of the soil so that the seed was approximately its own depth under the soil surface. The seed was covered over with the soil and the tray was covered with a clear propagation lid until germination, when the lid was removed. Tomato plants were transplanted approximately four weeks after sowing into individual Number 6 (160 mm diameter) pots using the soil-based multi-purpose compost and placed out in a randomised pattern. Plants were watered daily and supplemented with Osmocote Exact Mini fertiliser granules (Scotts Horticulture Ltd, Newbridge, Ireland). Approximately 3-4 weeks later the plants were transplanted to 7.5 litre pots (270 mm diameter). The plants were supplemented with the same slow release fertiliser granules until flowering when they were fed weekly on alternate weeks with either Levington Tomorite (The Scotts Company Ltd, Godalming, UK) or Phostrogen (Bayer Garden, Cambridge, UK) applied during the daily

watering. A 0.5% (w/v) calcium chloride solution was sprayed directly onto all developing fruit weekly to help control blossom end rot.

2.3 Transcript analysis

2.3.1 RNA isolation

All centrifugation steps were carried out at 4°C. RNA was isolated from 50-60 mg freeze-dried tomato pericarp tissue. The tissue was ground in a mortar and pestle with 1 ml Trizol Reagent (Invitrogen, Paisley, UK), transferred to a 2 ml tube and incubated at room temperature (RT) for 5 min. The sample was centrifuged at 12,000 *g* for 10 min. The supernatant was transferred to a 2 ml tube and 0.2 ml chloroform was added. The sample was mixed vigorously by hand for 15 s then incubated for 2 min at RT. To separate the lower phenol phase from the upper aqueous phase the sample was centrifuged for 15 min at 12,000 *g*. The upper aqueous phase was transferred to a 2 ml tube and the RNA was precipitated by addition of 0.5 ml isopropyl alcohol. The sample was incubated at RT for 10 min and centrifuged at 12,000 *g* for 10 min to pellet the RNA. The supernatant was removed and the pellet was washed with 1 ml 75% (v/v) ethanol and re-centrifuged at 7,500 *g* for 5 min. The pellet was left to air dry for 10 min at RT then resuspended in 200 µl diethyl pyrocarbonate (DEPC) water. To precipitate the RNA, 200 µl 10 M lithium chloride was added to the sample and left overnight on ice. After centrifugation at 12,000 *g* for 10 min the pellet was re-precipitated in isopropanol and washed in 75% (v/v) ethanol as described above. The pellet was resuspended in 100 µl DEPC-water by pipetting.

2.3.2 cDNA synthesis

The extracted RNA was deoxyribonuclease (DNAse) treated with DNAse I to remove possible contamination using an Ambion DNA-free Reagent kit (Applied Biosystems, Warrington, UK) following the manufacturer's instructions. For cDNA synthesis, the following was added to a 0.2 ml tube: 3 µg total RNA, 1 µl Oligo-dT-primers (500 µg/ml) (Invitrogen Ltd, Paisley, UK), 1 µl dNTP mix (10 mM each) and DEPC water to a volume of 12 µl. The RNA was denatured by incubation at 65°C for 5 min then immediately cooled to 4°C. The following reagents were added to the tube: 4 µl 5x First-Strand Buffer (Invitrogen Ltd, Paisley, UK), 2 µl 0.1 M dithiothreitol (DTT) and 1 µl RNaseOUT (40 units/µl) (Invitrogen Ltd, Paisley, UK). The tube was gently mixed by flicking with a finger and incubated at 42°C for 2 min before addition of 1 µl SuperScript II Reverse Transcriptase (Invitrogen Ltd, Paisley, UK). The tube was mixed by gently pipetting up and down then incubated at 42°C for 50 min followed by heat inactivation at 70°C for 15 min to stop the reaction.

2.3.3 Semi-quantitative RT-PCR

Template sequences for primer design were obtained from expressed sequence tag (EST) sequences from the Tomato Gene Index Database (Dana Farber Cancer Institute, Boston, USA). Primers were designed from the EST sequences using Primer3 software (Rozen and Skaletsky, 2000) and are detailed in Appendix I. cDNA was prepared as described in section 2.3.2 and diluted 1:10 (v/v) with milli-Q water. Cycle numbers and annealing temperatures were optimised for each template to ensure that the amplification reaction was tested in the exponential phase. The reaction mix for RT-PCR consisted of 2 µl 1:10 (v/v) diluted cDNA, 15 µl MegaMix-BLUE (Microzone Ltd, Haywards Heath, UK), 0.5 µl forward

primer, 0.5 µl reverse primer. Reactions were carried out in a Mastercycler Gradient (Eppendorf UK Ltd., Cambridge, UK). The reaction conditions used for the RT-PCR were as follows: Step 1, initial denaturation at 95°C for 2 min; Step 2, denaturation at 95°C for 30 s; Step 3, primer annealing at 53-57°C for 45 s; Step 4, extension/elongation at 72°C for 60 s; Steps 2-4 were repeated with a variable number of cycles according to primer optimisation; Step 5, final hold at 4°C. PCR products were visualised using ethidium bromide after separation by agarose gel electrophoresis.

To ensure that the bands seen on the gel were the correctly amplified products, bands were cut from the gels and sequenced. Gel products were stored at -20°C until all products were collected and were thawed on ice before being cleaned up using QIAquick PCR Purification kit (Qiagen Ltd., Crawley, UK). The gene products were quantitated and adjusted for the correct concentration then sent with the associated primers to Geneservice DNA Sequencing Facility (Department of Biochemistry, Oxford, UK) for sequencing. The returned sequences were checked against the National Center for Biotechnology Information (NCBI) (http://www.ncbi.nlm.nih.gov/) and Tomato Gene Index (TGI) (http://compbio.dfci.harvard.edu/tgi/tgipage.html, Dana Farber Cancer Institute, Boston, USA) databases.

To further confirm the subcellular location of EST sequences selected, the template sequences were blasted against the Arabidopsis Information Resource (TAIR) (http://www.arabidopsis.org/) and NCBI databases. The protein sequences of the top hits were input into TargetP version 1.1 (Nielsen *et al.*, 1997; Emanuelsson *et al.*, 2000) and Predotar version 1.03 (Small *et al.*, 2004) prediction software to predict organelle targeting sequences. If protein sequences were not available, the coding sequences were obtained

and translated to protein sequences using the Expert Protein Analysis System (ExPASy) Translate tool (http://www.expasy.ch/) (Gasteiger *et al.*, 2003) then input into the prediction software.

2.3.4 Electrophoresis

Agarose gels were prepared with 0.8% (w/v) or 1% (w/v) agarose in 1x Tris-acetate-EDTA (TAE) buffer. The agarose suspension was heated in a microwave oven until boiling and the agarose dissolved. The solution was removed from the oven and cooled at RT. After addition of 0.01% (v/v) ethidium bromide the gel was poured into a gel tray and left to set at RT. Gels were loaded with 10 µl nucleic acid sample containing 0.1 volume of 10x loading buffer. The loading buffer contained 4% (w/v) glycerol, 0.5 mM EDTA, 0.01% (w/v) SDS and 0.01% (w/v) Orange G. To estimate the sizes of gel products a nucleic acid standard (HyperLadder I, Bioline Ltd, London, UK) was loaded in parallel to the samples. Gels were run at 80-110 V and documented using a UVP Gel Documentation System (Forest Row, UK). Quantification of band intensity was by densiometry using a Molecular Imager FX (Bio-Rad Laboratories Ltd., Hemel Hemstead, UK) with Quantity One software (Version 4.4.1, Bio-Rad Laboratories Ltd., Hemel Hemstead, UK).

2.4 Bioinformatics

Expression data in the Tomato Functional Genomics database (http://ted.bti.cornell.edu/, Cornell University, Ithaca, USA) was extracted from the TOM1 cDNA array wild type tomato fruit development (set 2). Data extracted were in the form of ratios of wild type tomato fruit at 7, 17, 27, 39, 41, 42, 43, 47, 52 and 57 days post anthesis (DAP) relative to a reference tissue sample from wild type tomato. The reference tissue sample consisted of mixed tissues of stem; immature and mature flowers; immature and mature leaves; 1 cm, mature green, breaker, turning and red ripe fruit. Data was transferred to an Excel file format and normalised by transforming to $\log_2$. To view the data and perform cluster analysis the normalised data was imported into the TIGR Multiexperiment Viewer software (MeV in TM4 Microarray Software Suite, version 4.4.0, (Saeed *et al.*, 2006) http://www.tm4.org/mev.html).

2.5 Determination of metabolite content

2.5.1 Amino acids

High Performance Liquid Chomatography (HPLC) was used to measure amino acids. Two methods were used. The first method was developed from Noctor & Foyer (1998). However, because of the problems associated with high back pressure on the column due to salt build up, a second method was developed based on Bruckner *et al.* (1995).

2.5.1.1 Apparatus

Reverse-phase HPLC was performed using a system composed of a Beckman System Gold Solvent Module 126 and Analog Interface Module 406 (Beckman Coulter Ltd., High Wycombe, UK). Separations were performed on a 250 x 4.6 mm column packed with octadecyl silane (C18) and with a precolumn inline filter (Hichrom, Theale, UK). Eluted compounds were detected using a Dionex RF2000 fluorescence detector (Dionex Corporation, Sunnyvale, USA).

Method 1: Excitation wavelength: 280 nm scan 260-350 nm
Emission wavelength: 417 nm scan 415-420 nm

Method 2: Excitation wavelength: 230 nm scan 200-350 nm
Emission wavelength: 445 nm scan 443-447 nm

2.5.1.2 Extraction for HPLC

Method 1: A 4 mg sample of freeze-dried pericarp tissue powder was weighed into a 2 ml tube. The internal standard norvaline (25 µM) was added directly on to the tissue before addition of 600 µl 0.1 M HCl. The sample was vortexed thoroughly and centrifuged at 10,000 *g*, 4°C for 15 min. The supernatant was transferred to a new tube and centrifuged at 10,000 *g*, 4°C for 30 min. The supernatant was filtered with a 0.45 µm Millex-HV filter unit (Millipore Ltd., Watford, UK) and aliquoted into four 0.5 ml tubes, snap frozen and stored at -80°C until analysis.

Method 2: The extraction procedure is as described for Method 1 with the exception that 53 µM ethanolamine was added as internal standard.

2.5.1.3 Pre-column derivatization

The derivatization reagents were made fresh each day and stored on ice in the dark until use.

Method 1: The derivatization reagent mix consisted of 0.9 ml 0.4 N borate buffer pH 10.2 (Agilent Technologies Ltd., West Lothian, UK), 0.1 ml 0.4 M *o*-phthaldialdehyde (OPA) in methanol and 20 µl β-mercaptoethanol. Prior to use the extract (Section 2.5.1.2) was thawed on ice. A 50 µl aliquot was removed to a new tube and 50 µl derivatization reagent was added and mixed. The solution was incubated at RT for 1 min and 80 µl was injected onto the column.

Method 2: The derivatization reagent (OPA-IBDC) mix consisted of 5 µl *N*-isobutyryl-D-cysteine (IBDC) in 0.4 N borate buffer pH 10.2, 5 µl OPA in methanol and 55 µl 0.4 N borate buffer pH 10.2. Prior to use the extract (Section 2.5.1.2) was thawed on ice. A 20 µl aliquot was added to the OPA-IBDC derivatization reagent and mixed. The solution was incubated at RT for 2 min and 80 µl was injected on to the column.

2.5.1.4 Chromatography

All chromatography was carried out at RT. All buffers were sonicated before use for 10 min in an ultrasonic water bath (XB3 model, Grant Instruments Ltd., Cambridge, UK) to remove air bubbles. All solvents used were HPLC grade.

Method 1: OPA derivatives were separated using the following elution buffers: buffer A was 90% (v/v) 20 mM sodium phosphate pH 6.8, 10% (v/v) methanol; buffer B was 40% (v/v) 20 mM sodium phosphate pH 6.8. The elution procedure was: flow-rate at 1 ml/min: 0-5 min, 100% buffer A (isocratic step); 5-45 min, 0-30% buffer B (linear gradient); 45-80 min,

30-100% buffer B (linear gradient); 80-90 min, 100% buffer B (isocratic flush); 90-105 min, 100% buffer A (linear gradient and equilibration).

Method 2: OPA-IBDC derivatives were separated using the following elution buffers: buffer A was 23 mM sodium acetate, 10% (v/v) methanol; buffer B was 60% (v/v) methanol, 5% (v/v) acetonitrile. The elution procedure was used at 1 ml/min: 0-80 min, 0-80% buffer B (linear gradient); 80-90 min, 80-100% buffer B (linear gradient); 90-100 min, 100% buffer A (linear gradient and equilibration).

Amino acid peaks were confirmed by spiking experiments with pure standards. Data were plotted and peak areas calculated using Beckman Gold software (Beckman Coulter Ltd., High Wycombe, UK). Peak areas were compared to standard curves and the metabolite content calculated.

To test the reproducibility of the samples, test mix was added directly onto the tissue at a range of concentrations (0, 0.5, 1, and 2 nmol injected onto the column) before 600 µl 0.1 M HCl. The samples were vortexed and centrifuged at 10,000 *g*, 4°C for 15 min. The supernatant was removed and centrifuged at 10,000 *g*, 4°C for 30 mins. The samples were filtered through a 0.45 µm Millex-HV filter unit (Millipore Ltd, Watford, UK) and aliquoted into three 0.5 ml tubes, snap frozen and stored at -80°C until analysis. Each sample from the range of concentrations was injected three times. The average peak area of the three replicates for each concentration was calculated for each amino acid. The average value of the 0 nmol concentration was subtracted from the average values of 0.5, 1 and 2 nmol concentrations for each amino acid to give a background corrected value.

2.5.2 Organic acids

^{1}H-nuclear magnetic resonance (NMR) was used to measure organic acid content based on the method in Le Gall *et al.* (2003).

2.5.2.1 Extraction for NMR

Approximately 48 mg of freeze-dried pericarp tissue was weighed into a 2 ml tube and 1.2 ml of 70% (v/v) methanol-d_4, 30% (v/v) buffer was added. The buffer consisted of 100 mM K_2HPO_4/KH_2PO_4, 1 mM EDTA and 1 mM sodium 3-(trimethylsilyl) proprionate-d_4 prepared in D_20. The sample was shaken on an orbital shaker for 30 min, 100 rpm and then centrifuged at 9,500 *g* for 10 min. The supernatant was transferred to a new tube and stored at -20°C until analysis. Each NMR sample consisted of 750 µl of the supernatant.

2.5.2.2 NMR spectroscopy

^{1}H-NMR spectra were recorded on a Varian 600MHz spectrometer (Varian Medical Systems Inc., Palo Alto, USA). Methanol-d_4 was used as the internal lock. Each spectrum consisted of 320 scans, with an acquisition time of 4 s, a recycle delay time of 6.02 s per scan, a pulse angle of 90° and with water suppression. Spectra were processed using the NUTS-Pro – NMR Utility Transform software (Acorn NMR Inc., Livermore, USA) where they were Fourier transformed with 1 Hz line broadening, phased, and baseline corrected. Peaks in spectra were manually integrated using NUTS-Pro software where they were outputted to an Excel file format for further data analysis.

2.5.3 Enzymatic determination of metabolites

2.5.3.1 Extraction for enzymatic determination of metabolites

Approximately 10 mg of freeze-dried tomato pericarp tissue was weighed into a 2 ml tube. Pre-heated milli-Q water to near boiling temperature was added to the tissue to a final concentration of 50 mg/ml. The samples were vortexed and heated for 15 min at 95°C. The samples were centrifuged at 10,000 *g*, 4°C for 10 min. The supernatant was removed and stored at -20°C until use (Finkemeier *et al.*, 2003).

2.5.3.2 Glutamate

Glutamate content was determined using an assay kit specific for L-glutamic acid following the manufacturer's instructions (Megazyme International Ltd., Bray, Ireland). Glutamate content was measured using a coupled assay in which the formation of 2-oxoglutarate from L-glutamic acid using glutamate dehydrogenase and NAD^+ as a cofactor was coupled to the reduction of iodonitrotetrazolium chloride (INT) to an INT-formazan product using diaphorase and NADH as a cofactor. The amount of INT-formazan formed in this reaction is stoichiometric with the amount of L-glutamic acid. The reduction of INT was followed spectrophotometrically at 492 nm (ε=19900 M^{-1}).

2.5.3.3 Aspartate

Aspartate content was determined using a coupled assay in which the formation of oxaloacetic acid and L-glutamate from L-aspartate and α-ketoglutarate using glutamate-oxaloacetate transaminase was coupled to L-malate using malate dehydrogenase and NADH

as a cofactor. The reaction mixture contained 200 µl of assay mixture (4 mM α-ketoglutarate, 0.3 mM NADH, 1:476 (v/v) dilution of malate dehydrogenase (5 mg/ml; pig heart) and 20 µl of sample (50 mg/ml extract) in a microtitre plate. The reaction was started by addition of 15 µl start mixture (1:10 (v/v) dilution of glutamate-oxaloacetate transaminase (2 mg/ml; pig heart) in milli-Q water) and incubated at RT for 1 h. The oxidation of NADH was followed spectrophotometrically in a microtitre plate-reader (Anthos htll, Anthos Labtec Instruments GmbH., Wals, Austria) at 340 nm (ε=6.22 mM^{-1}).

2.5.3.4 Citrate

Citrate content was determined using an assay kit for citrate following the manufacturer's instructions (R-Biopharm Rhône Ltd., Glasgow, Scotland). Citrate content was measured using a coupled assay. The formation of oxaloacetic acid and acetate from citrate using citrate lyase was coupled to the formation of L-malate using malate dehydrogenase and NADH as a cofactor. In a second concurrent reaction, L-lactate was formed from pyruvate, the decarboxylation product of oxaloacetic acid, using lactate dehydrogenase and NADH as a cofactor. The amount of NADH oxidized in both reactions is stoichiometric to the amount of citrate. The oxidation of NADH was followed spectrophotometrically at 340 nm (ε=6.3 mM^{-1}).

2.5.3.5 Malate

Malate content was determined as described in an assay kit specific for L-malic acid (Megazyme International Ltd., Bray, Ireland). Malate content was measured using a coupled assay where oxaloacetic acid fomation from L-malic acid using malate dehydrogenase and

NAD^+ as a cofactor was coupled to the formation of 2-oxoglutarate and L-aspartate using glutamate-oxaloacetate transaminase in the presence of excess L-glutamate. The reduction of NAD^+ is followed spectrophotometrically at 340 nm. The reaction mixture contained 42.7 mM glycylglycine, 42.7 mM L-glutamate, 4.1 mM NAD^+, 10.7 mM PVP-40, and 10 µl glutamate-oxaloacetate transaminase (2 mg/ml; pig heart). The reaction was started by addition of 10 µl L-malate dehydrogenase (5 mg/ml; pig heart).

2.6 Protein assay

The protein content of samples was measured using a modified Bradford assay (Pierce Coomassie Plus Protein Reagent kit; Thermo Fisher Scientific Inc., Rockford, USA (Bradford, 1976)). The absorbance of light at 595 nm was measured 5 min after the addition of 195 µl of Coomassie blue dye to 5 µl of a diluted sample. Absorbance was measured using a microtitre plate-reader (Anthos htll, Anthos Labtec Instruments GmbH., Wals, Austria). The absorbance was compared to a bovine serum albumin (BSA) (2 mg/ml; Thermo Fisher Scientific Inc., Rockford, USA) standard curve.

2.7 Extraction from whole pericarp tissue for enzyme assays

Extracts were prepared using 10 mg freeze-dried tomato pericarp tissue. The tissue was weighed into a 2 ml tube and resuspended in 1 ml of extraction buffer (50 mM HEPES-KOH pH 7.4, 5 mM $MgCl_2$, 1 mM EDTA, 1 mM EGTA, 5 mM DTT, 0.5 mM phenymethylsulphonyl fluoride (PMSF), 0.1% (v/v) Triton X-100, 10% (v/v) glycerol, 2 mM benzamidine and 2 mM 6-aminocaproic acid (Geigenberger and Stitt, 1993)). After vortexing

thoroughly the samples were left on ice while Bio-Spin 6 columns (Bio-Rad Laboratories Ltd., Hemel Hemstead, UK) were equilibrated with extraction buffer. The Bio-Spin 6 columns were equilibrated by inversion of columns several times to resuspend the settled gel and to remove any bubbles. The tip was snapped off and the lid removed and the column placed in a cut-off 2 ml tube to allow excess packing buffer to drain by gravity to the top of the gel bed. The column was equilibrated by applying 6 volumes (6x 1 ml volumes) of extraction buffer to the column and allowing it to pass through by gravity. The columns were spun briefly at 230 *g*, RT for approximately 10 s to remove equilibration buffer. The column was placed in a 2 ml tube and the sample was desalted by placing the entire resuspended sample (1 ml) directly on to the centre of the column. The column was centrifuged at 2050 *g*, RT for 5 min. The filtrate collected was used in enzyme assays as described in Section 2.11.

2.8 Isolation of mitochondria

Mitochondria were isolated from freshly harvested tomato pericarp tissue (Holtzapffel *et al.*, 2002). All steps and centrifugations were carried out at 4°C. All equipment used was pre-cooled to 4°C and detergent-free. The tomato fruit were quartered and locular contents and seeds were removed. The pericarp tissue was roughly chopped and 50-100 g was placed in a square polycarbonate container with 200-300 ml grinding medium (0.3 M sucrose, 25 mM tetrasodium pyrophosphate, 25 mM TES pH 7.5, 2 mM EDTA, 10 mM KH_2PO_4, 1% (w/v) polyvinylpyrrolidone (PVP-40), 1% (w/v) BSA, 20 mM ascorbic acid). The sample was homogenised gently in multiple short bursts (less than 1 s) using a Status Polytron blender (Kinematica Inc., Bohemia, USA) on a low setting (4) to minimise heat

generation and frothing. The sample was filtered through one layer of miracloth and two layers of muslin. The filtrate was centrifuged at 1,085 *g* for 5 min. The pellet was discarded and the supernatant centrifuged for 15 min at 23,500 g. The pellet was resuspended in wash buffer (0.3 M sucrose, 10 mM TES pH 7.2, 0.1% (w/v) BSA) to an approximate final volume of 2 ml before being layered onto a 35 ml gradient of 0-4.4% (w/v) PVP-40 in wash buffer containing 18% (v/v) Percoll. The gradient was centrifuged at 40,000 *g* for 40 min and the mitochondria removed from the band near the bottom of the gradient using a 5 ml pipette. The mitochondria were diluted with wash buffer and centrifuged twice at 27,000 g for 15 min. The final pellet was resuspended in a minimal volume of wash buffer.

2.9 Respiration measurements

All measurements of oxygen consumption to follow respiration were carried out using a Clarke type oxygen electrode (Oxygraph model, Hansatech Instruments Ltd., King's Lynn, UK) in a reaction mixture of 1 ml final volume. The respiration buffer consisted of 0.3 M mannitol, 10 mM TES-KOH pH 7.5, 3 mM $MgSO_4$, 10 mM NaCl, 5 mM KH_2PO_4 and 0.1% (w/v) BSA.

Malate and pyruvate respiration was measured by addition of 100 µM ADP to a reaction mixture containing respiration buffer, 5 mM pyruvate, 0.5 mM malate, 0.3 mM NAD^+, 0.1 mM thiamine pyrophosphate (TPP) and known amounts mitochondrial protein.

2.10 Outer mitochondrial membrane integrity

The outer mitochondrial membrane integrity was calculated by measuring the latency of cytochrome c oxidase to cytochrome c. The oxygen consumption of isolated mitochondria (65 µg mitochondrial protein) was measured in the presence of 10 mM ascorbate in respiration buffer, then subsequently after the addition of sequentially added 50 µM cytochrome c and 0.05% (v/v) Triton X-100. The respiration buffer consisted of 0.3 M mannitol, 10 mM Tes-KOH pH 7.5, 3 mM $MgSO_4$, 10 mM NaCl, 5 mM KH_2PO_4, 0.1% (w/v) BSA.

In the presence of cytochrome c, the rate of oxygen consumption in the absence of Triton was divided by the rate in the presence of Triton and multiplied by 100. Both measurements were corrected for non-cytochrome oxygen consumption by subtraction from the rate of oxygen consumption.

2.11 Enzyme assays

Enzyme activity measurements were carried out at 25°C in a final volume of 1 ml using a spectrophotometer (Unicam UV/Vis, UV4 model, Cambridge, UK).

2.11.1 Aconitase (EC 4.2.1.3)

Aconitase activity was assayed spectrophotometrically by coupling the formation of isocitrate to NADPH using isocitrate dehydrogenase (MacDougall and Ap Rees, 1991). The production of NADPH was followed at 340 nm (ε=6.22 mM^{-1}). The reaction mixture contained 80 mM HEPES-NaOH pH 7.5, 0.05% (v/v) Triton X-100, 0.5 mM $MnCl_2$, 0.5 mM

$NADP^+$, 2 units NADP-ICDH (porcine heart) and either isolated mitochondria (30 µg mitochondrial protein) or whole pericarp extract (30-50 µg total protein). The reaction was started by addition of 8 mM aconitate.

2.11.2 Citrate synthase (EC 2.3.3.1)

Citrate synthase activity was assayed using a coupled assay. The formation of oxaloacetic acid from malate using malate dehydrogenase and 3-acetylpyridine adenine dinucleotide (APAD) as a cofactor was coupled to citrate formation (Stitt *et al.*, 1989). The reduction of APAD was followed spectrophotometrically at 365 nm (ε=9.1 mM^{-1}). The reaction mixture contained 90 mM triethanolamine-KOH pH 8.5, 0.5% (v/v) Triton X-100, 10 mM L-malate, 0.2 mM APAD, 20 µl 1/10 (v/v) dilution of malate dehydrogenase (5 mg/ml; pig heart) and isolated mitochondria (45 µg mitochondrial protein). The reaction was started by addition of 0.17 mM acetyl CoA.

2.11.3 Fumarase (EC 4.2.1.2)

Fumarase activity was determined by measuring the formation of fumarate at 240 nm (ε=4.88 mM^{-1}) (MacDougall and Ap Rees, 1991); modified as described by Jenner *et al.* (2001). The reaction medium contained 70 mM KH_2PO_4-NaOH pH 7.7, 0.02% (v/v) Triton X-100 and mitochondria (20 µg mitochondrial protein). The reaction was started by addition of 50 mM malate.

2.11.4 Isocitrate dehydrogenase (NAD^+-dependent) (EC 1.1.1.41)

NAD^+-isocitrate dehydrogenase activity was assayed spectrophotometrically by following the reduction of NAD^+ at 340 nm (ε=6.22 mM^{-1}) (Jenner *et al.*, 2001). The reaction medium contained 50 mM Tris-acetate pH 7.2, 0.05% (v/v) Triton X-100, 20 mM isocitrate, 2 mM NAD^+, 20 mM $MnCl_2$. The reaction was started by addition of isolated mitochondria (45 µg mitochondrial protein).

2.11.5 Isocitrate dehydrogenase ($NADP^+$-dependent) (EC 1.1.1.42)

$NADP^+$-isocitrate dehydrogenase activity was assayed spectrophotometrically by following the reduction of $NADP^+$ at 340 nm (ε=6.22 mM^{-1}) (Jenner *et al.*, 2001). The reaction medium was as for Section 2.13.4 with the exception that 2 mM $NADP^+$ was used in place of 2 mM NAD^+. The reaction was started by addition of whole pericarp extract (30-50 µg total protein).

2.11.6 Malate dehydrogenase (EC 1.1.1.37)

Malate dehydrogenase activity was assayed by following the oxidation of NADH at 340 nm using a spectrophotometer (ε=6.22 mM^{-1}) (Jeffery *et al.*, 1986). The reaction medium contained 90 mM KH_2PO_4-KOH pH 7.4, 0.05% (v/v) Triton X-100, 5 mM $MgCl_2$, 0.2 mM NADH and isolated mitochondria (40 µg mitochondrial protein). The reaction was started by addition of 0.8 mM oxaloacetic acid made in 100 mM KH_2PO_4-KOH pH 7.4.

2.11.7 Malic Enzyme ($NADP^+$-dependent) (EC 1.1.1.40)

$NADP^+$-malic enzyme activity was assayed spectrophotometrically by following the reduction of $NADP^+$ at 340 nm (ε=6.22 mM^{-1}) (Borsani *et al.*, 2009). The reaction medium contained 50 mM Tris-HCl pH 7.5, 0.5 mM $NADP^+$, 20 mM $MgCl_2$ and whole pericarp extract (30-60 µg total protein). The reaction was started by addition of 10 mM malate.

2.11.8 2-Oxoglutarate dehydrogenase (EC 1.2.4.2)

2-Oxoglutarate dehydrogenase activity was assayed spectrophotometrically by following the reduction of NAD^+ at 340nm (ε=6.22 mM^{-1}) (Morgan *et al.*, 2008). The reaction medium contained 70 mM TES-NaOH pH 7.0, 0.05% (v/v) Triton X-100, 0.12 mM coenzyme A (made in 0.1 M cysteine), 2 mM $MgCl_2$, 0.2 mM thiamine pyrophosphate, 2 mM NAD^+, 1.8 units lipoamide dehydrogenase (porcine heart) and isolated mitochondria (15 µg mitochondrial protein). The reaction was started by addition of 1 mM 2-oxoglutarate.

2.11.9 Succinate dehydrogenase (EC 1.3.99.1)

Succinate dehydrogenase activity was assayed spectrophotometrically by following the oxidation of the dye 2,6-dichloroindophenol (Muller *et al.*, 1968). The reaction medium contained 66 mM potassium phosphate-sodium phosphate buffer pH 7.4, 33 µM 2,6-dichloroindophenol, 1 mM phenazine methosulfate, 2 mM KCN (made in potassium phosphate-sodium phosphate buffer pH 7.4), 0.066% (v/v) Triton X-100 and isolated mitochondria (20 µg mitochondrial protein). The reaction was started by addition of 20 mM sodium succinate. The decrease in absorbance was followed at 600 nm (ε=21 mM^{-1}).

2.12 Measurements of respiratory fluxes

Tomato fruit were freshly harvested, halved and the locular cavity and seeds were removed. Discs of pericarp were punched out using a 10 mm diameter cork borer. The skin was discarded and the pericarp was sliced into 3 mm discs using a razor blade. The discs were washed in 10 mM MES-KOH pH 6.5. Eight discs were placed into 100 ml flasks containing 4.5 ml 10 mM MES-KOH pH 6.5. At T=0, 0.5 ml of either [1-^{14}C]-, [2-^{14}C]-, [3:4-^{14}C]-, or [6-^{14}C]-labelled glucose (7.4 kBq/ml) in 10 mM MES-KOH pH 6.5, 10 mM glucose was added to the flasks. As CO_2 is readily dissolved in basic solutions, the released $^{14}CO_2$ was trapped in 0.5 ml of 10% (v/v) KOH. The KOH solution was replaced every hour for 12 hours and at 24 hours. At the end of the experiment 450 µl of the collected KOH was transferred to a scintillation vial. The sample was mixed with 2 ml of scintillation fluid before quantification by liquid scintillation counting.

2.13 Transport measurements

2.13.1 Tonoplast isolation

The method described here is adapted from the methods of Oleski *et al.* (1987), Milner *et al.* (1995) and White & Smith (1989). All steps and centrifugations were carried out at 4°C and all equipment (detergent-free) and buffers used were pre-chilled.

Tomato fruit were freshly harvested prior to isolation. The fruit were sliced in half and the locular cavity and seeds removed. The remaining pericarp tissue was roughly chopped and 80 g was added to 200 ml homogenisation buffer (450 mM mannitol, 3 mM

$MgSO_4$, 5 mM EDTA, 0.5% (w/v) PVP-40, 50 mM Tris-KOH pH 8.0, 0.5 mM butylated hydroxytoluene, 26 mM potassium metabisulphite, 0.5% (w/v) BSA, 1 mM phenymethylsulphonyl fluoride (PMSF) (in ethanol), and 10 mM DTT). The tissue was homogenized in a Moulinex food blender (Groupe SEB, Ecully Cedex, France) for 6 x 3 s bursts and filtered through two layers of muslin avoiding transfer of any froth. The filtrate was centrifuged at 16,000 *g* for 30 min to remove cell debris and intact chloroplasts or mitochondria. The supernatant was transferred to new tubes and centrifuged at 80,000 *g* for 50 min to pellet the tonoplasts (plasmalemma, broken chloroplasts or mitochondria will also pellet at this step). The supernatant was discarded and the pellet resuspended in 1 ml of resuspension buffer (1.1 M glycerol, 1 mM EDTA, 10 mM 1,3-bis[tris(hydroxymethyl)methylamino]propane (BTP)-tricine pH 8.0, 2 mM DTT) with a soft hair 5 mm paintbrush. The tubes were rinsed twice with a small volume of resuspension buffer and all resuspended material was layered onto a 15 ml 28% (w/v) and 10 ml 12% (w/v) stepped sucrose gradient made in resuspension buffer. The gradient was centrifuged at 100,000 *g* for 70 min. The tonoplasts were collected from the 12%/28% interface using a pipette and transferred to a new tube. Approximately 30 ml of resuspension buffer was added to the tube and centrifuged at 100,000 *g* for 45 min to wash the tonoplasts. The supernatant was removed and the pellet (containing the tonoplasts) was resuspended in resuspension buffer to a final volume of 500-700 µl before being aliquoted and snap-frozen in liquid nitrogen and stored at -80°C.

2.13.2 Adenoside triphosphatase (ATPase) assays

Tonoplast ATPase activity was determined by assaying the rate of release of inorganic orthophosphate (P_i) from ATP (Oleski *et al.*, 1987b; White and Smith, 1989). All glassware was acid washed to avoid contamination by phosphates. Each reaction contained 130 µl ATPase reaction medium, 1 µg tonoplast membrane protein in 23 µl volume, 2µM gramicidin in a final reaction volume of 200 µl. The ATPase reaction medium consisted of 50 mM KCl, 3 mM $MgSO_4$, 0.1 mM EDTA, 1 mM molybdate, 500 mM sodium azide, 500 mM sodium orthovanadate, 50 mM tricine-BTP pH 7.0. To quantify the nitrate-sensitive tonoplast membrane ATPase activity two reactions per replicate were set up in parallel and to one reaction 50 mM KNO_3^- (vacuolar ATPase inhibitor) was added to the assay mix (or ATPase reaction medium to the control). The reactions (T=45 min) were started by addition of 3 mM ATP (made up in ATPase reaction medium) and incubated at 37°C for exactly 45 min. The reaction was stopped by addition of 200 µl 12% (w/v) sodium dodecyl sulfate (SDS) incubated for 10 min at RT.

A second set of reactions (T=0 min) were set up in addition as a control set. These reactions were stopped immediately by addition of 200 µl 12% (w/v) SDS to the standard assay mix and incubated for 10 min at RT.

The rate of ATP hydrolysis from P_i release was determined spectrophotometrically (Chifflet *et al.*, 1988) by addition of 300 µl phosphate reaction medium (6% (w/v) ascorbic acid in 1 M HCl and 1% (w/v) NH_4-molybdate in a 1:1 (v/v) ratio mixed just before use) 10 min after the reactions were stopped with SDS. The reactions were incubated at room temperature for 5 min before addition of 300 µl citrate reaction medium (2% (w/v) trisodium citrate, 2% (w/v) sodium metaarsenite, 2% (w/v) acetic acid) and incubated for a

further 10 min at RT before the colour absorbance was determined spectrophotometrically at 850 nm. Phosphate concentration was calculated by reference to a standard curve.

2.13.3 H^+-transport assays

ATP-dependent H^+-transport in tomato tonoplast membranes was monitored by following the fluorescence quenching of the permeant amine dye quinacrine (6-chloro-9-(4-diethylamino-1-methylbutylamino)-2-methoxyacridine dihydrochloride) (Bennett and Spanswick, 1983; White and Smith, 1989). The standard assay was carried out at 25°C and contained 450 µl reaction medium, 30 µg tonoplast protein and 50 µl anion (50 mM final concentration) in a final reaction volume of 500 µl. The reaction medium consisted of 3.6 µM quinacrine, 250 mM mannitol, 10 mM BTP-MES pH 8.0, 6 mM M_gSO_4 and 0.3 mM EDTA. Rates of H^+ transport were determined from the initial maximum linear rates of fluorescence quenching after addition of 3 mM ATP 8 min after the addition of the anion and measured using a LS-50B luminescence spectrometer (Perkin-Elmer, Beaconsfield, UK) The excitation and emission wavelengths were 422 nm and 498 nm respectively, both with a slit width of 5 nm. Each anion was independently added to individual reactions from stock solutions made up in reaction medium and buffered to pH 8.0 with BTP. The anions used were fumarate, citrate, malate, aspartate, glutamate and Cl^- (in the form of HCl). After the fluorescence quench levelled off, 5 mM ammonium sulphate was added to uncouple pH from V-ATPase activity. This was carried out in order to obtain the fluorescence level that takes into account the decay in fluorescence that inherently happens over the duration of the assay. This fluorescence level was arbitrarily set to 100 and was used to normalise the data before the initial maximal rates of all anions was measured.

Chapter 3

Changes in metabolite composition of fruit from a tomato introgression line

3.1 Introduction

A tomato introgression line population containing single introgressed chromosomal segments of *Solanum pennellii* (LA0716) in a *Solanum lycopersicum* (M82) background (Eshed and Zamir, 1995; Liu and Zamir, 1999) was shown to have a range of levels of organic and amino acids in ripe fruit grown in the field therefore providing a useful resource in which genotype can be linked to altered metabolic phenotypes (Schauer *et al.*, 2006). Two lines were selected from the introgression line population that had increased organic and amino acids when grown in field conditions (Schauer *et al.*, 2006). The lines selected had minimal changes in sugar content (e.g. Brix) and measures of yield (e.g. harvest index or total yield) as these changes in these traits could confound interpretation of molecular changes. The two lines that were selected for analysis were lines 5-4 and 2-5. Line 5-4 had increased glutamate, citrate and isocitrate and line 2-5 had increased glutamate, aspartate and isocitrate. These lines were grown under greenhouse growth conditions to confirm the

metabolic traits reported by Schauer *et al.* (2006). Under greenhouse conditions line 5-4 did not show increases in organic acid content and had over a two-fold difference in sucrose content (data not shown). For this reason line 5-4 was not used in any subsequent experiments.

Quantitative traits have been found to alter under different environmental conditions making it difficult to discriminate the effects of genotype from those of the environment (Pooni and Kearsey, 2001). The metabolite data in Schauer *et al.* (2006) is based on data collected from fruit grown in the field from two independent harvests over different years (2001 and 2003) indicating that the changes in metabolites reported are reproducible over different harvests. This data, however, does not take into consideration metabolite changes under differing environmental conditions (i.e. greenhouse conditions).

Metabolites have been shown to change throughout the development of the fruit (Baxter *et al.*, 2005a; Mounet *et al.*, 2009). Organic and amino acid accumulation may, therefore, be restricted to a specific developmental stage. Metabolites have also between shown to change between the different tissue types within the fruit (Davies and Hobson, 1981; Velterop and Vos, 2001). Therefore, organic and amino acid accumulation may be restricted to specific tissues or the difference between the introgression line and the recurrent parent line may be quantitatively greater in certain tissues.

Identifying the metabolite content at different developmental stages requires a method of staging fruit development. The most common method of staging fruit development is to measure days after anthesis (DAA). However, fruit ripening can also be characterised by changes in fruit colour due to breakdown of chlorophyll and synthesis of carotenoids (Gillaspy *et al.*, 1993; Fraser *et al.*, 1994; Carrari *et al.*, 2006).

The aim of this chapter was to quantify changes in a range of metabolites in fruit from introgression line 2-5 grown under greenhouse conditions. Different tissues and developmental stages of the fruit was analysed to assess whether changes in metabolite content are greater in specific tissues and developmental stages. The results of this analysis would then aid in the subsequent research to exploit the metabolite changes in the fruit between the introgression line relative to the recurrent parent, to link the metabolite traits to specific chromosomal regions and to probe the molecular factors responsible for these differences.

3.2 Results

3.2.1 Introgression line IL2-5 has increased amounts of amino acids relative to the recurrent parent (M82) under greenhouse growth conditions

To identify if there were differences in amino acid content between the introgression line 2-5 and the recurrent parent line (M82) in our growth conditions, pericarp tissue was harvested from ripe fruit grown in the greenhouse. Initially, amino acid content was determined by HPLC by Antony Willis (Department of Biochemistry, University of Oxford) while a method was set up and developed (Figure 3.1). Ten of the nineteen amino acids measured showed significant increases in the 2-5 introgression line relative to the recurrent parent. Amino acid content was found to be significantly increased in ripe pericarp tissue from the 2-5 introgression line in the following amino acids: glutamate, serine, glycine, threonine, alanine, valine, methionine, phenylalanine, isoleucine and leucine. No significant differences in amino acid content were found between the 2-5 introgression line

and recurrent parent line for the following amino acids: aspartate, asparagine, glutamine, histidine, arginine, tyrosine, tryptophan, lysine and proline. Line 2-5 showed no significant increases in glucose or fructose content (data not shown).

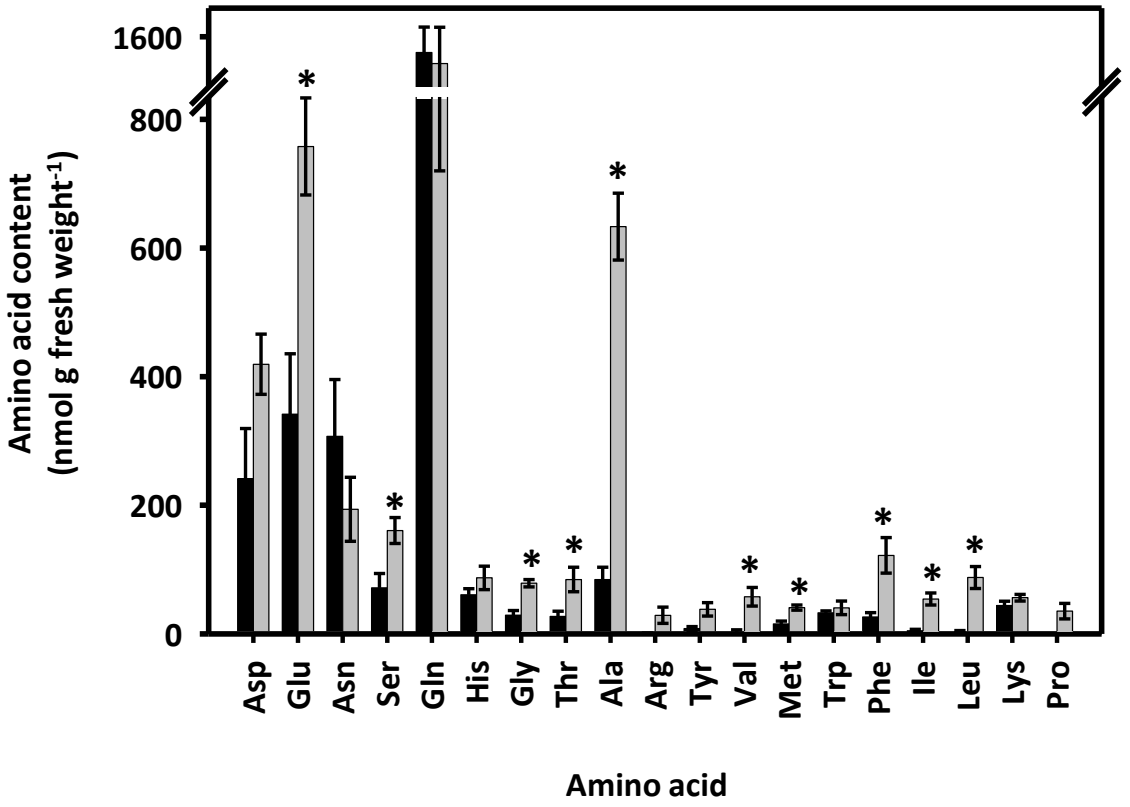

Fig. 3.1. Changes in the amino acid content of introgression line 2-5 relative to the recurrent parent line (M82). Amino acid content was determined by HPLC in ripe pericarp tissue from fruit of the recurrent parent (black) and introgression line 2-5 (grey) grown in greenhouse conditions. Data is the mean ± SEM (n=4). * P≤0.05 (TTest).

3.2.2 Pericarp tissue is suitable tissue to use for analysis

To identify which tissue would be the most appropriate for use for subsequent analysis of metabolites in the introgression line relative to the recurrent parent, amino acid content was determined in different tissue types of the fruit. Three different tissue types (pericarp, columella, locular cavity) were harvested from ripe tomatoes in introgression line 2-5 and the recurrent parent line (M82). The method for amino acid extraction and analysis was as described above in Section 3.2.1. The relative amino acid content for the four main amino acids was determined and compared by calculating the ratio of the amino acid content of line 2-5 to M82 (Figure 3.2). The relative amino acid content of the four amino acids was similar for all three tissue types for glutamate, asparagine and glutamine. For aspartate, the relative amino acid content was similar for the columella and locular cavity but lower in pericarp tissue. Although there was a lower relative aspartate content in the pericarp compared to the other tissues, there was still a 1.7-fold difference between the 2-5 introgression line relative to the recurrent parent. Of the three tissue types used, pericarp tissue is the most abundant tissue found in the tomato fruit, is easy to harvest and is a homogeneous tissue. For these reasons, the pericarp was selected to be the most suitable tissue and will be used for subsequent experiments.

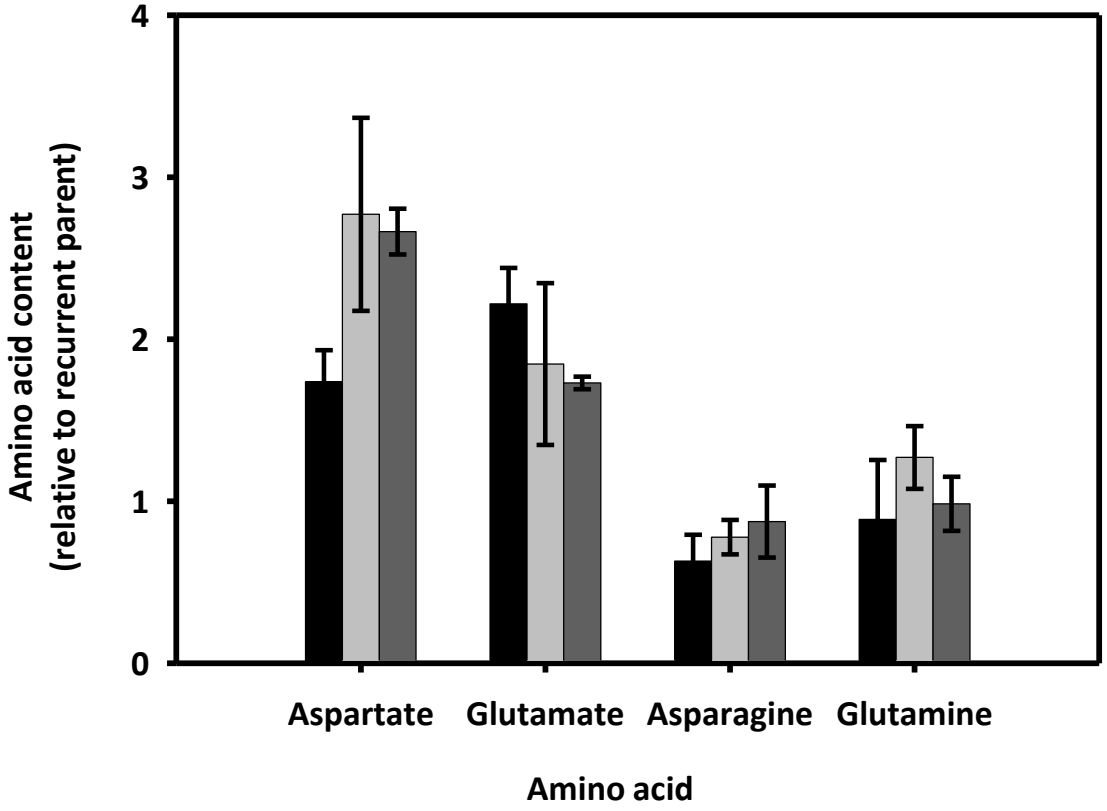

Fig. 3.2. Amino acid content relative to the recurrent parent line (M82) in the four main amino acids in tomato pericarp. Amino acid content was determined by HPLC in pericarp (black), columella (light grey), and locular cavity (dark grey) of ripe tomato fruit (n=4).

3.2.3 Increases in fruit organic and amino acid content are greatest at breaker stage (40 DAA)

Reverse phase-high performance liquid chromotography (RP-HPLC) was used to determine the amino acid content in fruit pericarp tissue at different stages of fruit development. The initial HPLC method to determine amino acid content involved derivatisation with *o*-phthaldehyde (OPA) (Noctor and Foyer, 1998). OPA reacts with the primary amines on amino acids forming a fluorescent indole derivative allowing detection by fluorescence.

Optimisation of the column elution gradient was required to ensure full resolution of all amino acids. The order of amino acid elution was determined by spiking with pure standards and calibration curves were constructed for each amino acid. Recoveries were determined using a test mix of amino acid standards and norvaline as an internal standard. Each amino acid had a concentration of 2.5 mM. A 4 mg aliquot of freeze-dried pericarp tissue was weighed into tubes. To calculate the percentage recovery of each amino acid, the background corrected values were divided by the values obtained for the same nmol concentrations from the standard curve and multiplied by 100. Reproducibility of the injections was tested using four test mix samples, each of which was injected twice on the column in separate runs using the derivatization method described in Section 2.5.1.3, Method 1. Five amino acid peaks were chosen across the chromatogram to analyse. The amino acid peaks were integrated to determine peak areas. The average and standard deviation of the peak areas for the five amino acids was calculated for all injections. The coefficient of variation percentage was calculated by dividing the average peak area by its

standard deviation and multiplying by 100 to give a percentage for each of the five amino acids.

This method was used to determine amino acid content in 30 and 40 DAA pericarp tissue. Nineteen proteinogenic amino acids were detected. The amino acids proline, hydroxyproline and cysteine do not react with OPA and therefore cannot be detected using this method (Roth, 1971). However, because of problems associated with high back pressure on the column due to salt build up (the column is eluted with gradient of sodium phosphate), a second method was developed. In this method samples were derivatised with OPA combined with the chiral thiol *N*-isobutyryl-D-cysteine (IBDC) resulting in a diasteriomeric isoindole derivative that can be separated by RP-HPLC and detected by fluorescence (Bruckner *et al.*, 1995). Spiking and recovery experiments were carried out as described for the Noctor and Foyer method above. The second method was used to determine amino acid content in 55 and 65 DAA pericarp tissue. Seventeen proteinogenic amino acids and GABA could be detected using this method.

The relative amino acid content in 30 DAA pericarp tissue for all amino acids was unchanged (Figure 3.3 A). The relative amino acid content in 40 DAA pericarp tissue for all amino acids was higher than 1.0 (Figure 3.3 B). All amino acids were significantly increased in the IL2-5 line compared to M82 except for glycine, alanine and valine. The relative amino acid content in 55 DAA pericarp tissue for most amino acids was unchanged (Figure 3.3 C). Glutamate, arginine, phenyalanine and GABA showed a significant increase. The relative amino acid content in 65 DAA pericarp tissue was also unchanged for most amino acids (Figure 3.3 D). Only GABA showed a significant increase. Two of the amino acids were significantly lower (glycine/threonine and alanine).

^{1}H-NMR was used to determine the content of abundant organic acids in fruit pericarp tissue as described in Section 2.5.2 (Le Gall *et al.*, 2003) and shown in Figure 3.4. RP-HPLC was used to determine the content of abundant amino acids in fruit pericarp tissue as described in Section 2.5.1 (Bruckner *et al.*, 1995; Noctor and Foyer, 1998) and shown in Figure 3.5. Data for the organic and amino acid content has also been plotted as line graphs and shown together to better visualise the developmental changes and is shown in Figure 3.6.

Citrate content increased throughout development from 30 to 65 DAA in the recurrent parent (Figures 3.4 A and 3.6 A). Citrate content in the introgression line followed a similar increase throughout development except for a slight decrease from 55 to 65 DAA. Citrate content was significantly higher than the recurrent parent line at 30, 40 and 55 DAA. Malate content decreased slightly at 40 DAA before increasing again throughout development in the recurrent parent line (Figures 3.4 B and 3.6 B). Malate content in the introgression line did not increase throughout development as found in the recurrent parent line. Instead, malate content increased slightly (approximately 1.2-fold) from 30 to 40 DAA before decreasing almost 2-fold from 40 to 55 DAA. Then from 55 to 65 DAA malate content increased slightly (approximately 1.2-fold). At 30 and 40 DAA the malate content in the introgression line was significantly higher than the recurrent parent but decreasing to become lower at 55 and 65 DAA, although not significantly than the recurrent parent. Glutamate content in both the introgression and parent line were similar from 30 to 40 DAA but increased over 4-fold from 40 to 55 DAA (Figures 3.5 A and 3.6 C). Glutamate content was unable to be measured in these samples at 65 DAA reliably, even in diluted samples, as the values were not within the linear range of the standard curve. Aspartate content did

decrease slightly from 30 to 40 DAA for the recurrent parent line otherwise aspartate content in both the introgression line and parent line increased similarly throughout development (Figures 3.5 B and 3.6 D). Aspartate content was significantly higher at 40 DAA in the introgression line than the recurrent parent. Data for organic and amino acid content in the recurrent parent line for 30, 40, 55 and 65 DAA can be found in Table 1 in Appendix II.

The relative difference in malate and aspartate content was greatest at 40 DAA. Although the relative citrate and glutamate content was greater at other developmental stages, the relative content was still significantly increased in the introgression line at 40 DAA. Therefore, 40 DAA was selected as the developmental stage at which the organic and amino acid content was consistently increased in the four main organic and amino acids in the introgression line relative to the recurrent parent and this developmental stage was used for all subsequent experiments.

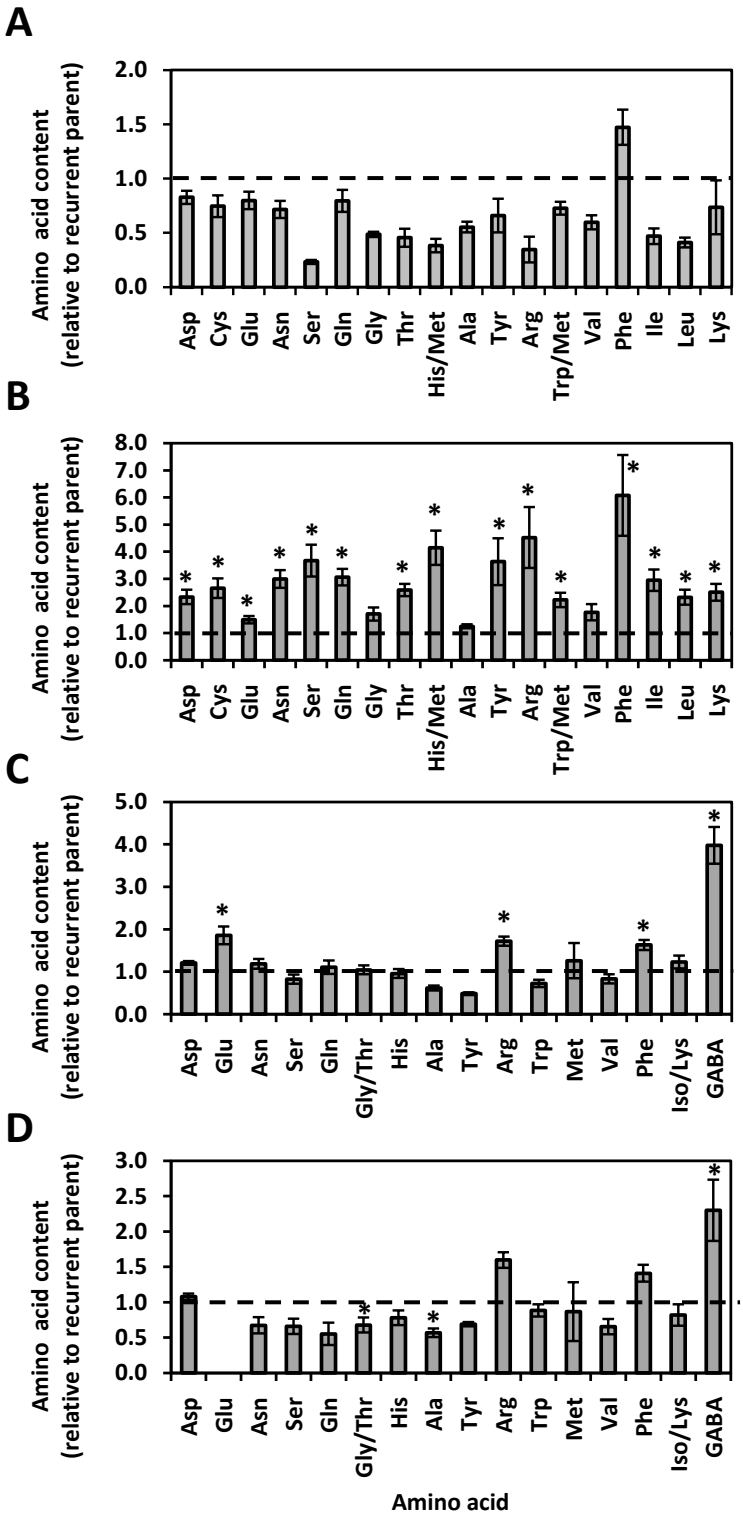

Fig. 3.3. Changes in fruit amino acid content of introgression line 2-5 relative to the recurrent parent line (M82) at different stages of fruit development. Amino acid content was determined by HPLC in pericarp tissue of fruit at 30 DAA (days after anthesis) (A), 40 DAA (B), 55 DAA (C) and 65 DAA (D). Data is presented as the ratio of the means of 2-5 to M82 ± SEM (n=6). Dashed line indicates a ratio of 1. * P≤0.05 (TTest).

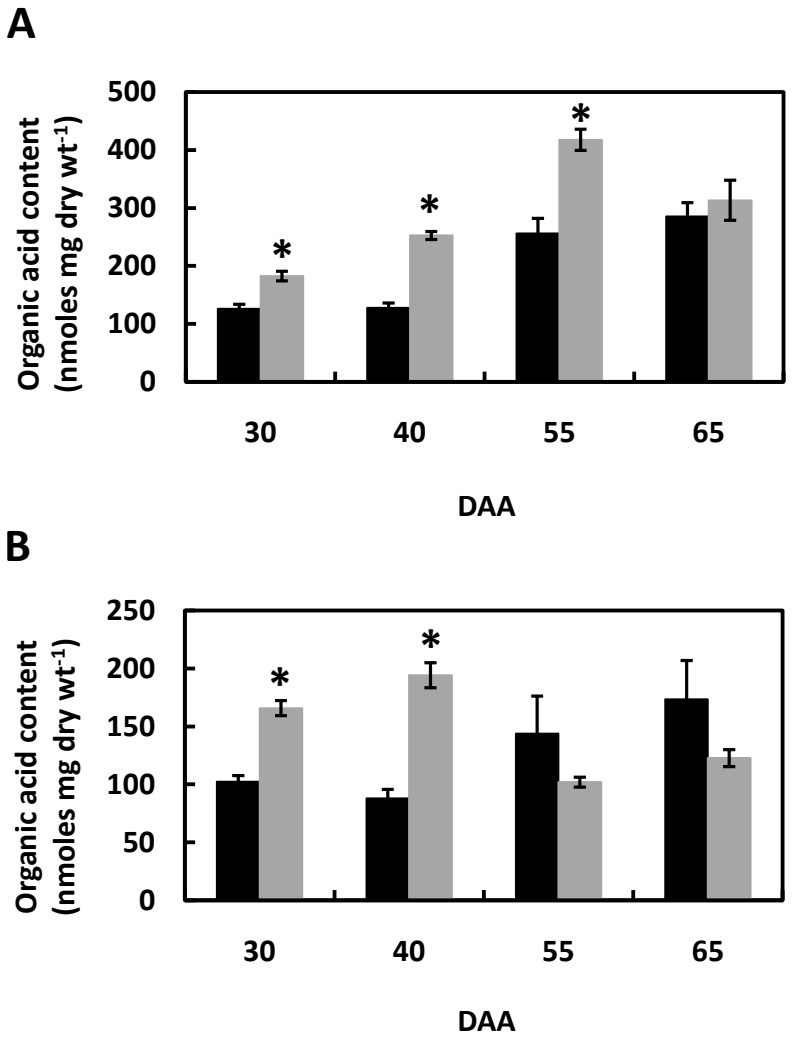

Fig. 3.4. Changes in fruit organic acid content of the recurrent parent line (M82) and introgression line 2-5 at different stages of fruit development. Citrate (A) and malate (B) content was determined in the recurrent parent line (black bars) and introgression line (grey bars) in pericarp tissue of fruit at 30, 40, 55 and 65 DAA (days after anthesis). Organic acid content was determined by ^{1}H NMR. Data is presented as the mean ± SEM (n=6). ***** P≤0.05 (TTest).

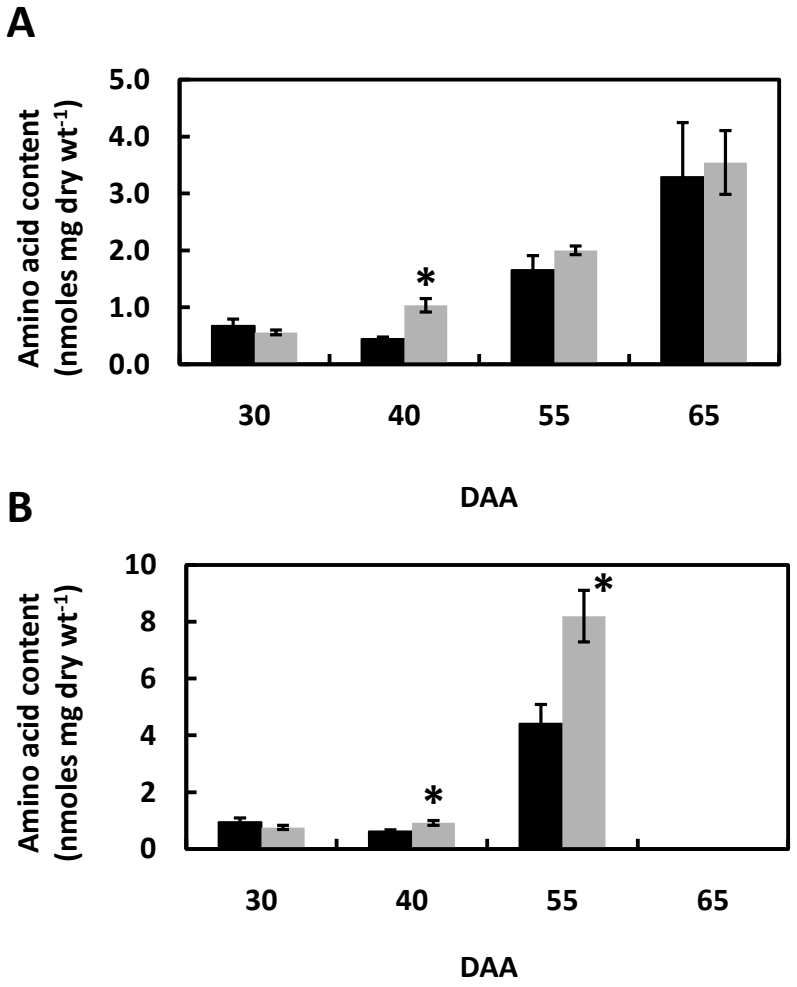

Fig. 3.5. Changes in amino acid content of the recurrent parent line (M82) and introgression line 2-5 at different stages of fruit development. Glutamate (A) and apartate (B) content was determined in the recurrent parent line (black bars) and introgression line (grey bars) in pericarp tissue of fruit at 30, 40, 55 and 65 DAA (days after anthesis). Amino acid content was determined by HPLC. Data is presented as the mean ± SEM (n=6). ***** P≤0.05 (TTest).

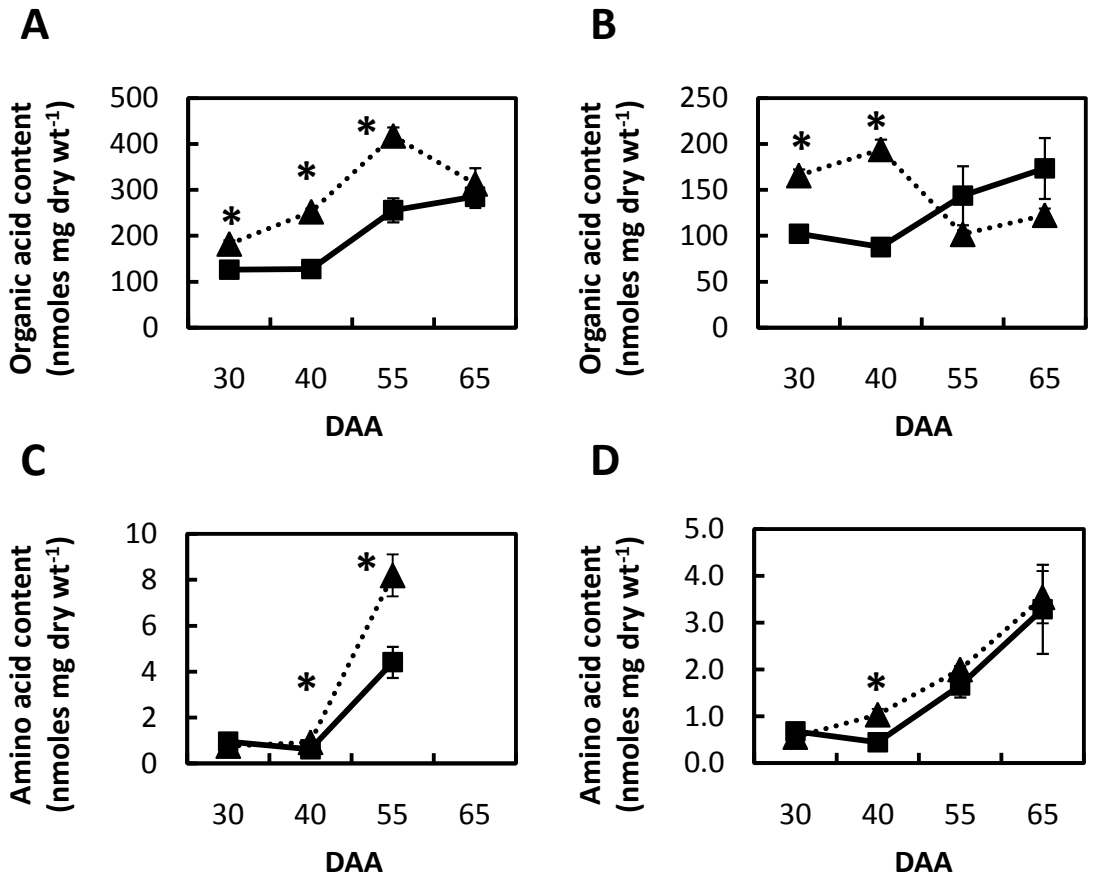

Fig. 3.6. Changes in fruit organic and amino acid content of the recurrent parent line (M82) and introgression line through fruit development. Citrate (A), malate (B), glutamate (C) and apartate (D) content was determined in the recurrent parent line (squares, solid line) and introgression line (triangles, dotted line) in pericarp tissue of fruit at 30, 40, 55 and 65 DAA (days after anthesis). Organic acid content was determined by ^{1}H NMR and amino acid content by HPLC. Data is presented as the mean ± SEM (n=6). * P≤0.05 (TTest).

3.2.4 Fruit development is the same in the introgression line and recurrent parent (M82) as determined by carotenoid content

Development in the fruit tissue was staged using the common method of days after anthesis (DAA). However, this method of staging assumes that the rate of development of fruit in the introgression lines was the same as the M82 parent. To investigate this, pigment content was measured as an independent measure of developmental stage.

Freeze-dried pericarp tissue from 30, 40, 55 and 65 DAA fruit of the introgression line 2-5 and the recurrent parent line were sent to Dr Paul Fraser (Plant Molecular Sciences, Royal Holloway, University of London) for determination of carotenoid content.

The carotenoid content in the introgression line and recurrent parent line for most carotenoids followed a similar developmental pattern (Figure. 3.7 B, C, D and E). Only lutein content in the introgression line was significant lower at 40 DAA and 65 DAA relative to the recurrent parent (Figure 3.7 A) but this is a relatively minor component of the carotenoid content. The three main carotenoids (lycopene, β-carotene and phytoene) followed the same pattern of accumulation in the 2-5 line and M82 parent when plotted on a DAA basis, suggesting that the 2-5 fruit develop at a comparable rate and that DAA is therefore a justifiable basis for developmental staging.

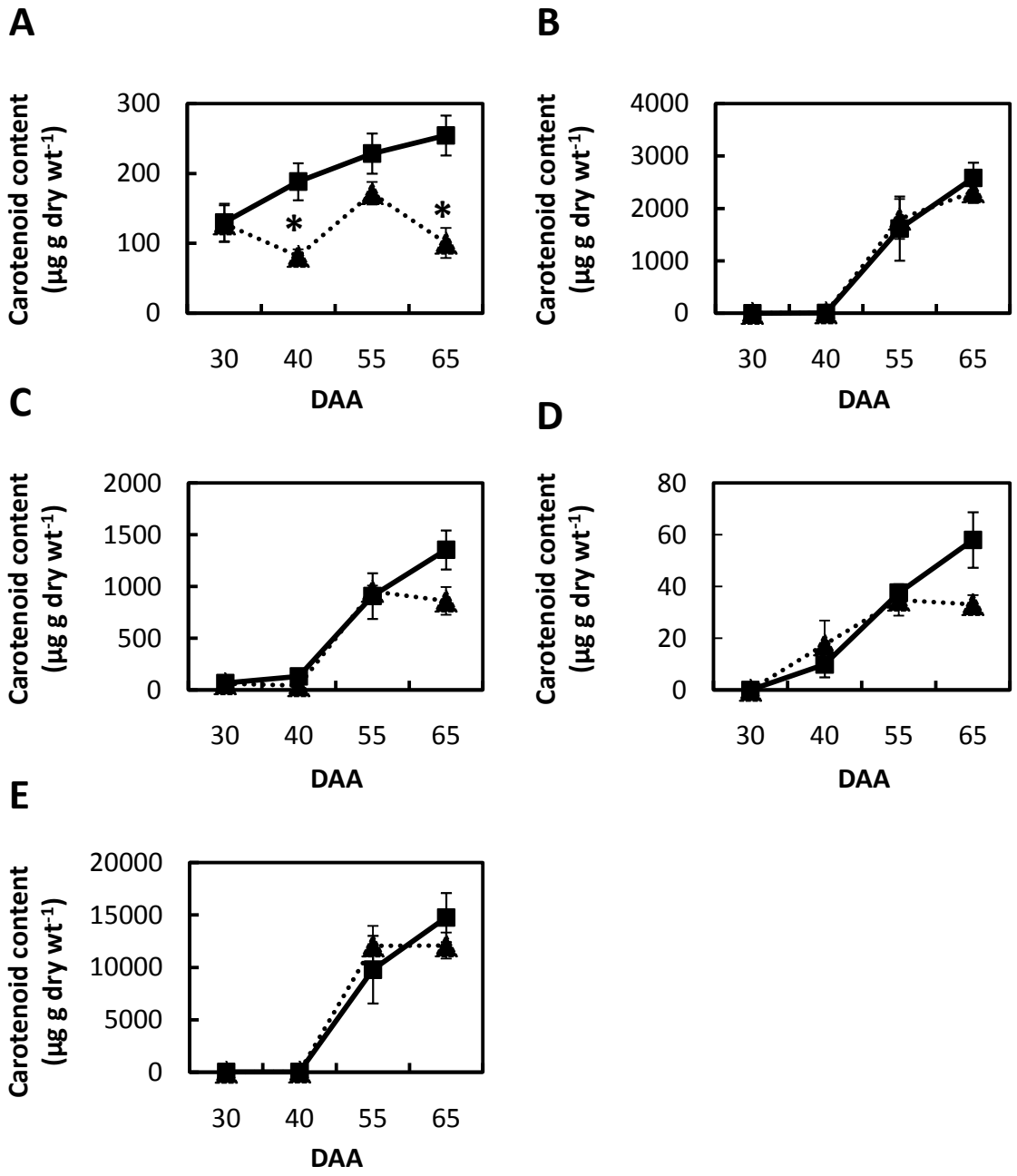

Fig. 3.7. Carotenoid content in the recurrent parent line (M82) and the introgression line 2-5. Developmental staging in the recurrent parent line (squares, solid line) and the introgression line 2-5 (triangles, dotted line) was assessed by determining carotenoid content in tomato fruit pericarp tissue. Carotenoids measured were lutein (A), phytoene (B), β-carotene (C), α-tocopherol (D) and lycopene (E). Data are the mean ± SEM (n=3). * P≤0.05 (TTest).

3.3 Discussion

3.3.1 Metabolite changes in the introgression line are influenced by environmental conditions

The amino acid content (Figure 3.1,Table 1 in Appendix II) is of a similar range to that those reported in Boggio et al (2000). However, the metabolite changes found in the introgression line grown under greenhouse conditions differed to those reported by Schauer *et al.* (2006) in field conditions. In line 5-4, one of the lines initially chosen for analysis, increases were found in the organic acids citrate and isocitrate when grown under field conditions. Under greenhouse conditions, no significant increases were found in any of the organic acids measured. Schauer *et al.* (2006) reported increases in the amino acids aspartate, glutamate and proline in line 2-5 when grown in field conditions. However, significant increases were found in the line 2-5 in ten of the nineteen proteinogenic amino acids that were measured in greenhouse conditions (Figure 3.1) where glutamate did show a significant increase but aspartate and proline did not. Although the data reported by Schauer *et al.* (2006) were significant over two different years, and therefore took into consideration differing environmental conditions from year to year, the conditions of the greenhouse vary considerably to those in the field. This shows that environmental interactions can cause a plants genotype to respond differently therefore altering the phenotypic traits. These results emphasise that differing environmental conditions have an impact on organic and amino acid accumulation. This would also suggest that the environmental influence has a greater effect than phenotype on metabolite levels. This has been shown in research in *Arabidopsis* where a recombinant inbred line compared QTLs

controlling glucosinate content with expression QTLs controlling the transcript levels of biosynthetic genes (Wentzell *et al.*, 2007). The average metabolite traits had a lower heritability than the transcripts. In a later study, with the same lines, the effect of the environment vs genotype on metabolite levels has been quantified (Rowe *et al.*, 2008). The heritability of metabolite traits was found to be lower than global transcript heritability. Thus, suggesting that metabolites would be more susceptible to environmental influences as the extra steps (i.e. transcription and translation) that metabolites require compared to transcripts makes them more susceptible to biological noise.

3.3.2 Metabolite changes in the introgression line are not tissue specific for the four main amino acids in tomato fruit

The content of the four main amino acids (apartate, glutamate, asparagine and glutamine) found in tomato fruit were compared in three different tissue types (pericarp, locular cavity and juice) to identify if metabolite content was greater in specific tissues (Figure 3.2). The results showed that there were no differences in the relative amino acid content between the tissue types for any of the four amino acids apart from slightly lower relative amino acid content for aspartate in pericarp tissue. No comparison of amino acid content in different tissue types has been made in the literature. However, organic acid content has been measured in different tissue types. Research shows that there are differences in the organic acid content of different tissues. Citrate tends to be at least 2-fold higher in the locular cavity compared to the whole fruit or pericarp tissue. Malate content in different tissue tends to vary according to variety and the difference in malate content tends to be lower (1 to 2-fold) (Mahakun *et al.*, 1979; Davies and Hobson, 1981; Grierson

and Kader, 1986; Velterop and Vos, 2001). This suggests that organic acid accumulation is tissue and variety specific. In the introgression line, compared to the recurrent parent, the altered amino acid accumulation does not appear to be tissue specific, therefore, the most suitable tissue for use was not restricted to differences in amino acid accumulation.

3.3.3 Metabolite levels in the introgression line are greater at different stages of fruit development

RP-HPLC and ^{1}H-NMR are suitable methods to use to quantitatively measure organic and amino acid content in fruit grown in greenhouse conditions. Methods were set up and optimised for both RP-HPLC and ^{1}H-NMR. Organic and amino acids were quantitatively measured in the introgression line and recurrent parent line using these methods (Figures 3.3, 3.4, 3.5 and Table 3.1). The amino acid content found in the introgression line relative to the recurrent parent in the pericarp for some amino acids (asparagine, aspartate and glutamate) were of a similar fold difference as those reported in Schauer *et al.* (2006). Differences seen in other amino acids may be due to environmental differences found between the conditions that the lines were grown in as discussed in Section 3.3.1.

Developmental staging in the introgression line and recurrent parent was similar to that reported in (Giovannoni, 2004) where breaker was around 40 DAA. Breaker stage at 40 DAA was earlier than that reported in Carrari et al (2006) where they found breaker to occur between 49 and 63 DAA. This difference could be accounted for by differences in the variety used and/or growing conditions of the tomato plants.

Carotenoid levels in the introgression line and recurrent parent follow a similar trend as reported in the literature (Fraser *et al.*, 1994; Carrari *et al.*, 2006; Fraser *et al.*, 2007;

Radzevicius *et al.*, 2009) where rapid increases in carotenoids were found from breaker stage to ripe (Figure 3.7). However, the levels of carotenoids are much greater in M82 parent that those reported. This again may be due to varietal differences. The levels of carotenoids in the introgression line closely follow the levels found in the recurrent parent line indicating that carotenoid accumulation is occurring at the same rate. This confirms that the rate of development between the lines is similar.

Differences in the rate of accumulation of organic and amino acids were found between the introgression line and recurrent parent (Figures 3.3, 3.4, 3.5 and 3.6) at different stages of development. Almost all amino acids were significantly increased at 40 DAA in the introgression line (Figure 3.3 B) but relatively few were increased at other developmental stages (30, 55 and 65 DAA). This was also seen in Figure 3.5 where glutamate accumulates at a much faster rate in the introgression line relative to the parent line from 40 DAA and aspartate is significantly higher at 40 DAA in the introgression line. A similar trend was also seen in the organic acids (Figure 3.4) where citrate was significantly higher for most developmental stages in the introgression line. Malate accumulation occurs in the introgression line early on in development (Figure 3.4 B) but by 55 DAA is of a similar level to the recurrent parent. This suggests that organic and amino acid accumulation is linked to fruit development and organic acids are not regulated in the same way as amino acids.

3.3.4 Summary

In this chapter methods have been set up to quantitatively determine organic and amino acid content in tomato fruit. This has enabled the quantitative measurement of organic and amino acid content in different tissue types and over different developmental stages in the introgression line and recurrent parent. Organic and amino acid was quantitatively higher in the introgression line at the developmental stage of breaker (40 DAA). Amino acid content was found to be similar in the three different tissue types in the four main amino acids of tomato fruit and therefore, pericarp tissue was chosen as a suitable tissue for use. Accumulation was shown to be different between organic acids and amino acids at different developmental stages. This chapter has provided the foundations to enable further research into linking the metabolite changes seen between the introgression line relative to the recurrent parent. Organic and amino acid content will be determined in pericarp tissue at breaker stage (40 DAA) in subsequent chapters to link the metabolite traits to specific chromosomal regions and to probe the molecular factors responsible for these differences.

Chapter 4

Control of organic and amino acid accumulation in tomato fruit

4.1 Introduction

Introgression line (2-5) has altered levels of fruit organic and amino acids compared to the parent line (M82) (Chapter 3; (Schauer *et al.*, 2006)). Therefore, the 2-5 introgression line must have underlying biochemical changes in comparison to the recurrent parent line (M82) that lead to altered accumulation of organic and amino acids during fruit development. The aim of this chapter was to investigate the molecular factors responsible for these differences and in doing so, to gain an insight into the regulation of organic and amino acid accumulation.

The TCA cycle is the most likely site of biochemical variation that could affect the amounts of organic and amino acids. Not only are organic acids metabolised, they are required to maintain the turnover of the TCA cycle and are also used as a source of carbon skeletons for the synthesis of amino acids. Thus, any metabolic changes to the TCA cycle can have an effect on the levels of organic and amino acids. For example, alterations in the

activity of enzymes in the TCA cycle (through antisense inhibition or mutation) in tomato leaves affected the levels of organic and amino acids and the flux through the TCA cycle (Carrari *et al.*, 2003a; Nunes-Nesi *et al.*, 2005; Nunes-Nesi *et al.*, 2007; Studart-Guimaraes *et al.*, 2007; Sienkiewicz-Porzucek *et al.*, 2008; Sienkiewicz-Porzucek *et al.*, 2010). Therefore, measurement of the flux through the TCA cycle could identify changes to enzymes in the pathway and explain the alterations in metabolite levels found in the 2-5 introgression line.

Flux through a metabolic pathway can be measured using ^{13}C stable isotopes or ^{14}C radiolabelling. Use of ^{13}C stable isotopes allows direct measurement of flux through a pathway, can provide information on positional labelling and is amenable to *in vivo* studies. However, ^{13}C stable isotopes are expensive and the method requires kinetic analysis (due to the complex nature of the isotopomer labelling patterns) and thus, a detailed knowledge of the redistribution of the label. Although this method provides direct measurements of flux through a pathway, it does require a great deal of time, effort and specialised equipment (Mass Spectrometry or Nuclear Magnetic Resonance) (Ratcliffe and Shachar-Hill, 2006). In comparison, ^{14}C radiolabelling is relatively inexpensive method where the isotopes can be detected and analysed using liquid scintillation and thus, not requiring highly specialised equipment. Specific pathways can be measured directly and rates of metabolism can be quantified easily not requiring the complex kinetic analysis. However, only estimates of flux can be achieved. Also, as only single measurements can be made on each sample, parallel incubations are necessary for each measurement that can lead to intersample variability. The quantitative collection of $^{14}CO_2$ is required but extensive TCA cycle activity produces large amounts of $^{14}CO_2$ and therefore, it is not possible to reliably quantify low levels of pentose phosphate pathway activity.

Use of ^{14}C radiolabelling can be used to estimate flux through the TCA cycle by monitoring the relative rates of $^{14}CO_2$ release from specific carbon positions within ^{14}C-labelled substrates, such as glucose. This is performed by incubating the plant tissue in a sealed flask with positionally labelled ^{14}C glucose. Radioactivity released as $^{14}CO_2$ is quantified following capture in a KOH trap. Comparing the relative rates of labelled $^{14}CO_2$ release from specifically labelled glucose allows the flux through different pathways to be estimated (Figure 4.1). For example, the yield of $^{14}CO_2$ release from [1-^{14}C] glucose and [6-^{14}C] glucose from the TCA cycle should give a ratio of one as cleavage of fructose 1,6 bisphosphate and subsequent interconversion of the products yields metabolites that would be equivalently labelled. If the ratio of C1/C6 is greater than one, then this indicates that there was additional release of $^{14}CO_2$ from [1-^{14}C] glucose, most likely due to flux through the oxidative pentose phosphate pathway (Garlick *et al.*, 2002). Yield of $^{14}CO_2$ from [3,4-^{14}C] glucose is derived from ^{14}C glucose metabolised by both the oxidative pentose phosphate pathway and through the TCA cycle and thus, is a measure of the proportion of glucose converted to pyruvate and subsequent decarboxylation via pyruvate dehydrogenase. The ratio of (C1-C6)/C3,4 would therefore, be a measure of the proportion of pyruvate formed from hexose phosphates produced in the oxidative pentose phosphate pathway (Kruger *et al.*, 2007). However, it is important to note that these are just estimates as CO_2 can be released or incorporated from other pathways that interact with glycolysis that can make interpretation of the label less accurate. For example, unlabelled CO_2 can be incorporated into the TCA cycle during the formation of OAA from PEP. Also, $^{14}CO_2$ can be released from [6-^{14}C] glucose during the formation of uridinediphosphate-xylose and uridinediphosphate-arabinose via uridinediphosphate-glucose during cell wall biosynthesis affecting the C6 ratio.

This method also does not take into consideration the subcellular compartmentation of metabolites.

The electron transport chain and the TCA cycle are closely linked (Figure 4.2). NADH and $FADH_2$ produced from glycolysis and the TCA cycle are utilized in the mitochondrial electron transport chain, where a series of complexes catalyse the multi-step transfer of electrons to oxygen, forming water. The transfer of electrons from NADH and $FADH_2$ through Complex I to the other complexes of the electron transport chain is coupled to the translocation of protons across the inner mitochondrial membrane into the intermembrane space generating an electrochemical proton gradient. It is important to note that only complexes I, III and IV of the electron transport chain pump protons across the inner mitochondrial membrane during the transfer of electrons. The electrochemical proton gradient is used to drive the ATP synthase complex to produce ATP. Thus, any change in the functioning of the electron transport chain can impact on the TCA cycle and, therefore, on organic and amino acid accumulation.

The functioning of the electron transport chain can be investigated in isolated mitochondria using an oxygen electrode. Addition of ADP to isolated mitochondria in the presence of substrates (such as pyruvate and malate, succinate, or NADH) causes a rapid consumption of O_2 that can be measured. Mitochondrial respiration in the presence of ADP is known as state 3. On conversion of ADP to ATP the respiration rate decreases again to the rate found before addition of ADP and is known as state 4. In isolated mitochondria the respiratory control ratio (RCR) is the ratio of oxygen uptake in the presence of ADP (state 3) to that in the absence of ADP (state 4) and provides an indication of the tightness of coupling between respiration (i.e. electron transport) and ADP phosphorylation. Therefore,

an alteration in the RCR can indicate use of the AOX complex or the external or internal NADH complexes which are not involved in proton translocation (Figure 4.2).

TCA cycle flux can be affected by activity of enzymes of the TCA cycle. Enzyme activity can vary either due to alteration in the enzyme amount (due to altered expression of the corresponding gene, altered rate of synthesis of the encoded transcript or altered degradation rate of the enzyme) or due to post-translational control of enzyme properties. To assess whether enzyme activity had changed at these levels, transcript abundance and maximal catalytic enzyme activity were measured. It remains possible that other changes in enzyme properties (e.g. changes in kinetic properties such as Km) would not be apparent from these measures, but a full analysis of enzyme properties is not feasible for the relatively large number of enzymes to be considered here.

The aim of this chapter was to identify the molecular factors that may be responsible for the biochemical differences between the 2-5 introgression line and the parent line. The initial focus of the research was on the TCA cycle. To determine if there were differences in respiratory function, oxygen consumption and respiratory control ratio measurements were made in mitochondria isolated from 40 DAA pericarp tissue. Differences in expression at the transcript level were assessed by measuring the transcript abundance of TCA cycle enzymes. Then, to identify differences at the protein level, the maximal catalytic activities of TCA cycle enzymes were measured in mitochondria isolated from pericarp tissue. Flux through the TCA cycle was estimated using pericarp discs fed with positionally-labelled glucose and the rate of labelled-CO_2 release was monitored. This targeted approach was extended to measure the transcript abundance of some of the enzymes in the pathways leading to aspartate and glutamate and in pathways downstream to other amino acids, including the

GABA shunt. In addition to the targeted approach, expression data in the Tomato Functional Genomics database (Cornell University, Ithaca, USA) was extracted to identify any correlation between the expression patterns of TCA cycle enzymes and enzymes in the pathways downstream of aspartate and glutamate and with enzymes in other pathways. Correlations between the expression patterns of enzymes in different pathways throughout development can indicate similarities in the regulation of these pathways.

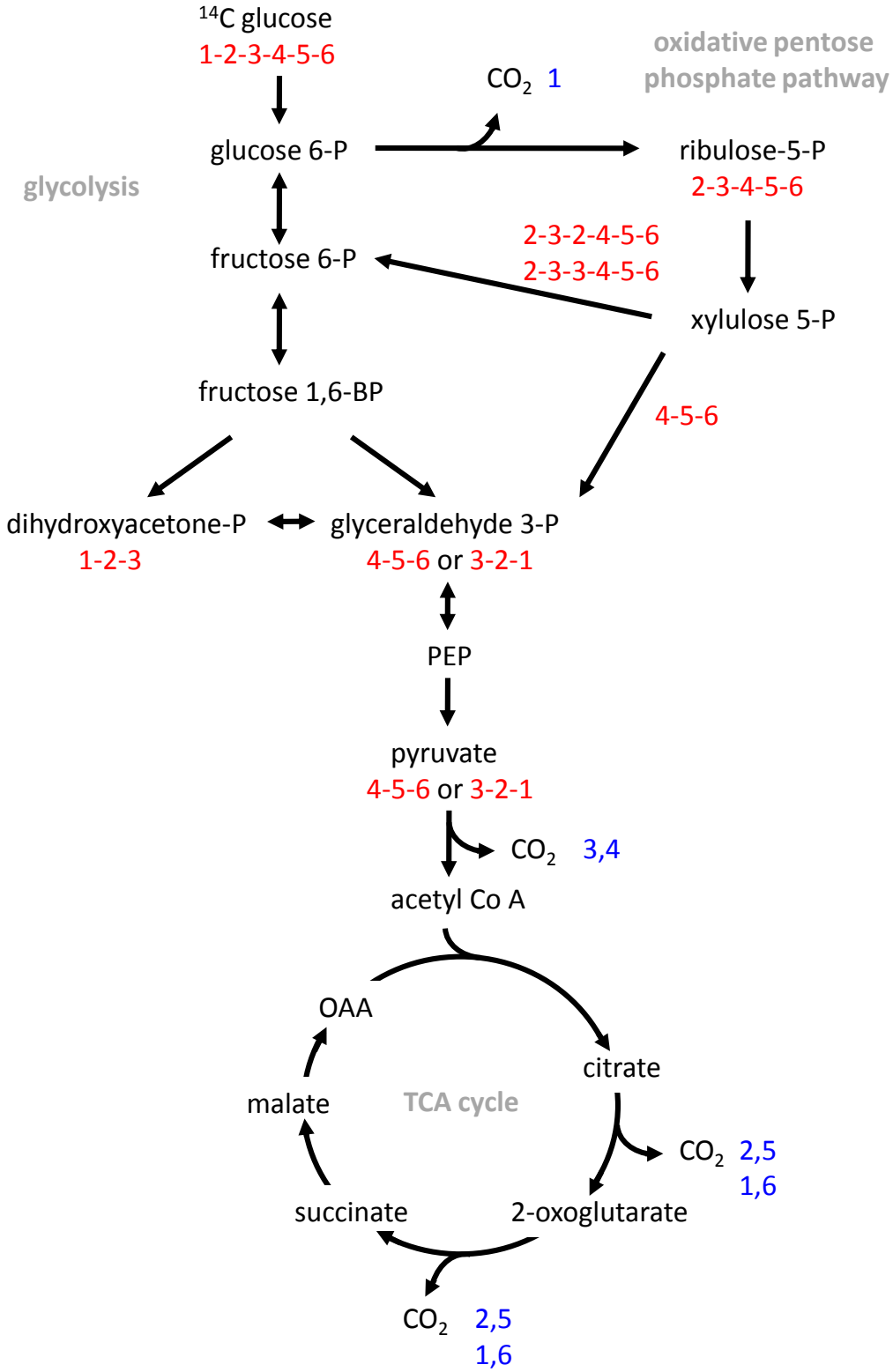

Fig. 4.1. Carbon incorporation and CO_2 release in glycolysis, the pentose phosphate pathway and the TCA cycle. Schematic showing carbon positioning for plant tissue incubated with ^{14}C glucose (red) and locations of isotopic CO_2 release (blue)(Garlick *et al.*, 2002; Kruger and von Schaewen, 2003; Kruger *et al.*, 2007).

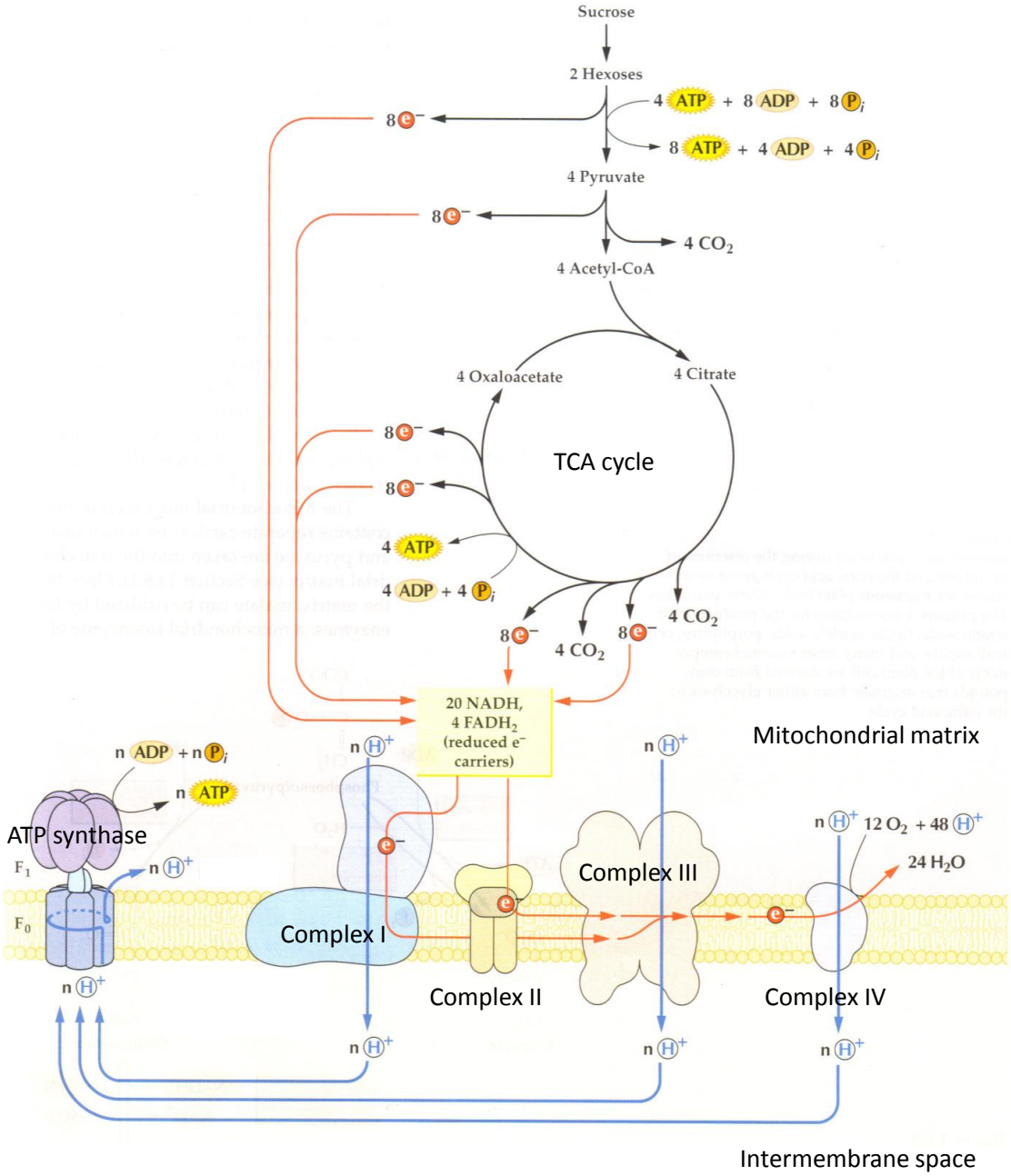

Fig. 4.2. Schematic showing the TCA cycle and the mitochondrial electron transport chain. NADH and $FADH_2$ produced from glycolysis and the TCA cycle transfer electrons to Complexes I and II of the electron transport chain. As electrons are transferred through Complexes I, III and IV protons are pumped from the mitochondrial matrix to the intermembrane space generating an electrochemical proton motive force. The electrochemical proton motive force is used to drive the ATP synthase complex where ADP is converted to ATP. Modified from Buchanan *et al.* (2000).

4.2 Results

4.2.1 There is no correlation between TCA cycle enzyme transcript abundance during tomato fruit development

The aim of the research here was to gain a broad overview of the coordinated regulation of the TCA cycle by exploiting the expression data from the Tomato Functional Genomics database (Cornell University, Ithaca, USA). Investigation into the correlations between the relative abundance of transcripts encoding enzymes of the TCA cycle with those of enzymes in other pathways could suggest similarities in the way the pathways are regulated. Expression data in the Tomato Functional Genomics database was extracted from the TOM1 cDNA array wild type tomato fruit development (set 2). Data extracted were in the form of ratios of wild type tomato fruit at 7, 17, 27, 39, 41, 42, 43, 47, 52 and 57 days post anthesis (DPA) relative to a reference mixed tissue sample from wild type tomato. The data was normalised after transforming to $\log_2$ and cluster analysis performed using the TIGR Multiexperiment Viewer software (MeV in TM4 Microarray Software Suite, version 4.4.0; (Saeed *et al.*, 2006)). Approximately 2,300 unique probe sequences were extracted and cluster analysis grouped the genes into 50 clusters. An overview of the clustering data is shown in Figure 4.3 and the individual clusters in the analysis are shown in Appendix III. Genes encoding TCA cycle enzymes generally did not cluster together and were found to be spread over 12 different clusters. However, several did cluster together showing similar expression patterns to each other and to enzymes in the pathways downstream from aspartate and glutamate.

In cluster 33 (Figure 4.4 A) relative transcript abundance was generally low and increased throughout development which generally follows the trend for the accumulation patterns of glutamate and aspartate content. In this cluster aspartate amino transferase (AAT), glutamine synthetase (GS), phosphoenolpyruvate carboxykinase (PEPCK) and pyrroline-5-carboxylate reductase (P5CR) were found with one V-ATPase as well as genes related to various transcription factors and post-translational modification of proteins.

In cluster 37 (Figure 4.4 B) a stronger, but similar expression pattern to cluster 33 where expression was low and increased throughout development. This expression pattern generally follows the trend for the accumulation patterns of citrate and aspartate content. This cluster showed cytosolic aconitase and two aspartate amino transferases (AAT) with genes related to various transcription factors, protein degradation or synthesis and stress.

In cluster 39 (Figure 4.4 C) there was generally a fairly high and consistent pattern of expression seen throughout development. This expression pattern loosely follows the trend for the accumulation of citrate but not for glutamate. In this cluster cytosolic aconitase and GABA amino transferase (GABA-T) clustered with two V-ATPases as well as genes related to various transcription factors and post-translational modification of proteins. In cluster 41 (Figure 4.4 D) the expression pattern was different to the previous clusters in that the expression was high and decreased though development. Citrate synthase, succinate dehydrogenase and malate dehydrogenase clustered with AAT, glutamate decarboxylase (GDC; GAD) and a V-ATPase as well as genes related to various transcription factors, cell wall proteins, photosynthesis, secondary metabolism and post-translational modification of proteins. This pattern of expression does not follow the trend for the accumulation of citrate, malate, aspartate or glutamate.

Cluster 43 (Figure 4.4 E) had a similar, but stronger, expression pattern to cluster 41 where expression was high and decreased through development. In this cluster 2-oxoglutarate (2OGDH) and isocitrate dehydrogenase (ICDH) clustered with arginase and genes related to post-translational modification of proteins, hormone metabolism and various transcription factors. This pattern of expression does not follow the trend for the accumulation of citrate, malate, aspartate or glutamate.

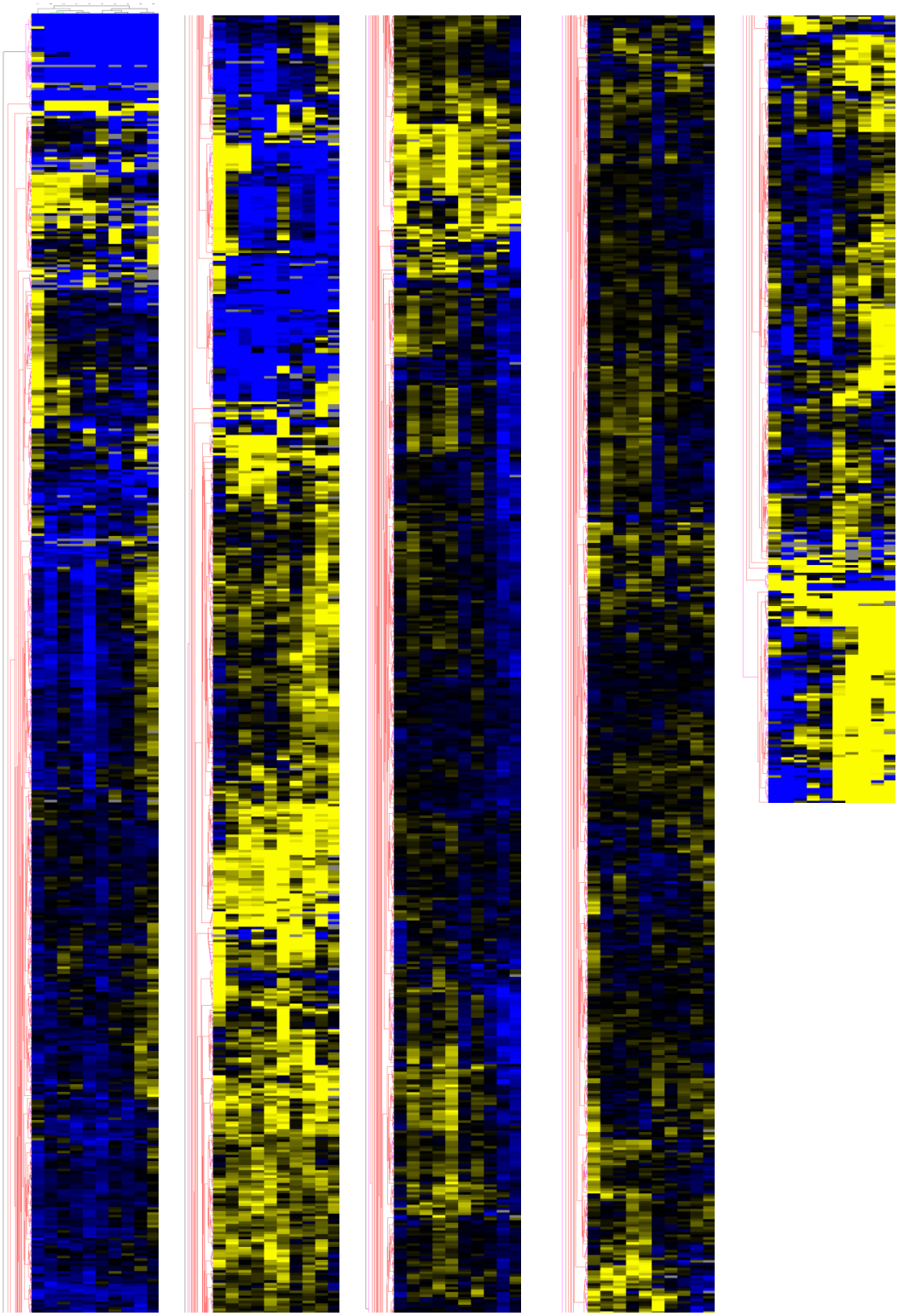

Fig. 4.3. Hierarchical cluster of differentially expressed genes. Genes are grouped by hierarchical clustering based on expression values (log_2 ratios) across all the samples. Samples (7, 17, 27, 39, 41, 42, 43, 47, 52 and 57 days post anthesis) are displayed in columns and genes in rows. Gene expression is represented as a colour, normalized across each row, with yellow for higher values and blue for lower values.

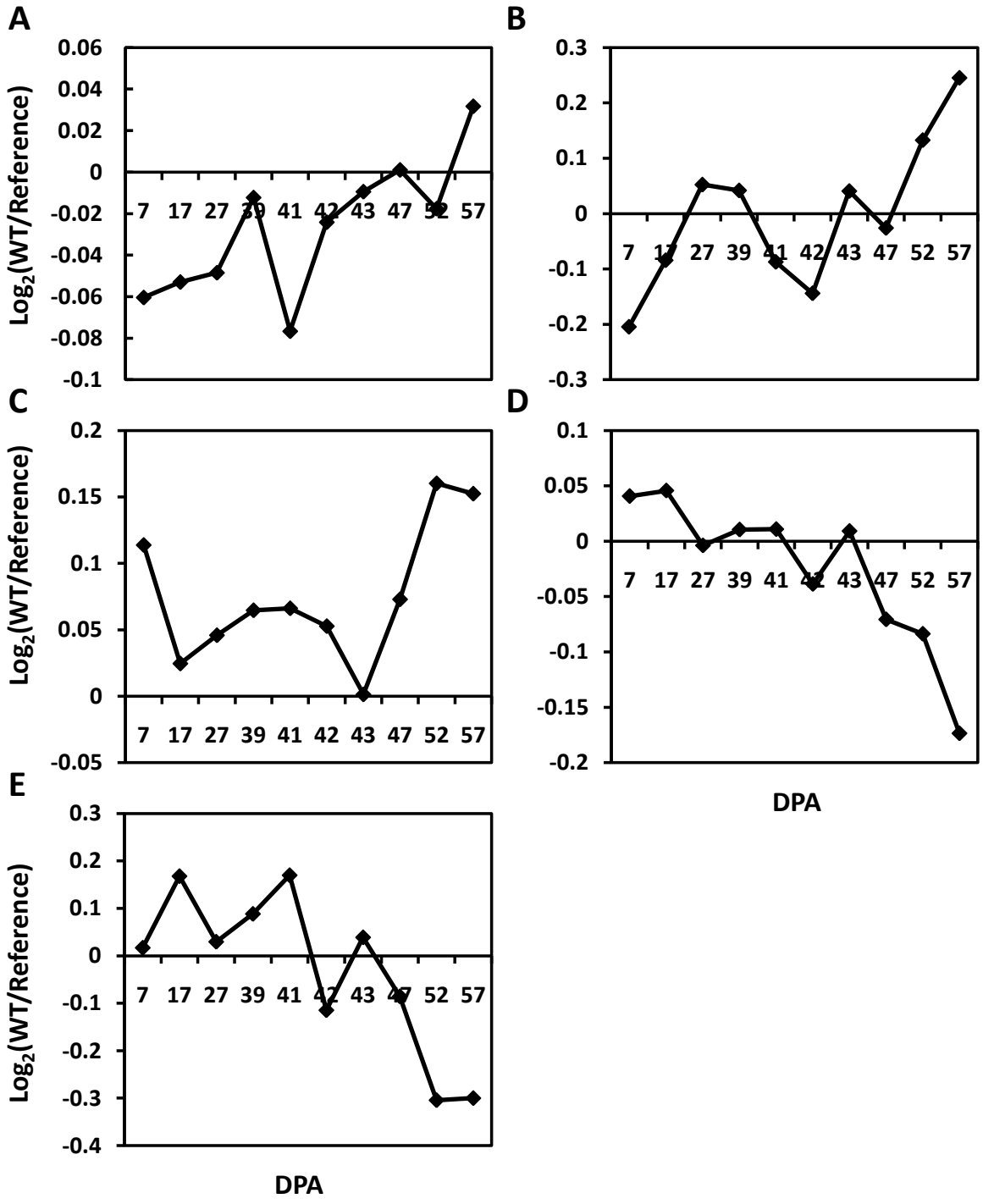

Fig. 4.4. Average expression profiles of five clusters. The expression profile of each gene in a cluster was normalized onto a log2 scale and then averaged. Five clusters, cluster 33 (A), 37 (B), 39 (C), 41 (D), and 43 (E), showing similar expression patterns TCA cycle enzymes, derived from the analysis, are shown.

4.2.2 Semi-quantitative analysis of transcripts encoding TCA cycle enzymes and enzymes in downstream pathways of aspartate and glutamate synthesis in introgression line 2-5 and the M82 parent line

Semi-quantitative RT-PCR was used to analyse transcript abundance in the 2-5 introgression line and M82 parent for the enzymes of the TCA cycle and in the pathway to apartate and glutamate (Figure 4.5), in the pathways downstream of glutamate and aspartate to asparagine, proline, ornithine, arginine, histidine, glutamine (Figure 4.6) and in the PEPCK and GABA shunt pathways (Figure 4.7). RNA was isolated and cDNA synthesised from 40 DAA pericarp tissue. Primers (Appendix I) were designed from EST sequences obtained from the Tomato Gene Index Database (Dana Farber Cancer Institute, Boston, USA) for the TCA cycle enzymes, aspartate amino transferase and glutamate dehydrogenase and for as many of the enzymes in the other pathways as possible in both the forward and reverse reactions. EC and accession numbers provided in Appendix IV. There was no difference in the transcript abundance for all of the TCA cycle enzymes except for one of the aconitase isoforms, *Acon1*, which showed a decrease (of at least 20% in all replicates) in transcript abundance in the 2-5 introgression line (Figure 4.5). No difference in transcript abundance was found in aspartate amino transferase, the enzyme in the pathway from the TCA cycle to aspartate. However, a decrease (of at least 20% in all replicates) was found in both isoforms of glutamate dehydrogenase (*GDH1* and *GDH2*) in the 2-5 introgression line, the enzyme in the pathway from the TCA cycle to glutamate. No difference in transcript abundance was found for enzymes in the asparagine, ornithine, arginine, histidine or glutamine pathways (Figure 4.6). A decrease (of at least 20% in all replicates) in transcript abundance was found in one isoform of proline dehydrogenase, *PDH1*, in the 2-5

introgression line in the proline pathway. No difference in transcript abundance was found in the other enzymes of this pathway. No differences were found in the transcript abundance of enzymes in the PEPCK or GABA shunt pathways (Figure 4.7).

Transcript	M82	2-5	Ratio[a]	Localisation[b]
Cit Syn	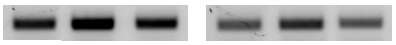		0.94	mitochondrion
Acon1			0.72*	chloroplast/cytosol
Acon2			0.88	chloroplast/cytosol
ICDH1			0.88	mitochondrion
ICDH2			0.86	mitochondrion
ICDH3			1.06	mitochondrion
ICDH4			1.00	plastid
ICDH5	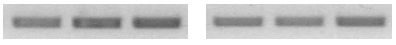		0.95	unknown
2OGDH1			0.94	mitochondrion
2OGDH2	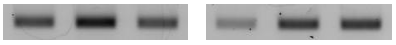		1.03	mitochondrion
SCoA1			0.87	mitochondrion
SCoA2	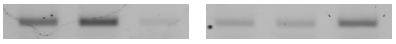		1.02	mitochondrion
SDH1	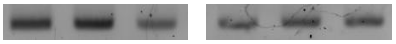		1.05	mitochondrion
SDH2			0.98	mitochondrion
SDH3			0.91	mitochondrion
Fumarase	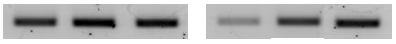		0.98	mitochondrion
MDH1	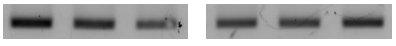		1.09	mitochondrion
MDH2			1.01	mitochondrion
AAT			0.97	mitochondrion
GDH1			0.70*	mitochondrion
GDH2			0.66*	mitochondrion
UBQ				

Fig. 4.5. Semi-quantitative RT-PCR analysis of transcript abundance in the recurrent parent (M82) and 2-5 introgression line at breaker stage for enzymes of the TCA cycle and in the pathway to aspartate and glutamate. PCR products were visualised following electrophoresis and quantified by densitometry. Each transcript was analysed in three independent samples and all three replicates are shown. Quantity values are shown in the column 'ratio' and are expressed as the mean normalised ratio of 2-5 to M82 (a). Sub-cellular localisation by target sequence prediction using Predotar and TargetP (b). *=difference between lines of 2O% or more in all replicates.

Transcript	M82	2-5	Ratio
Asparagine Pathway			
AS1			1.20
AS2			0. 81
Proline Pathway			
PDH1			0. 64*
PDH2			1.03
P5CS			0. 93
P5CR			1.06
P5CDH			0. 94
Ornithine Pathway			
NAGS1			1.04
NAGS2			1.21
NAGK1			1.03
NAGK2			0.96
NAOAT			0. 97
OAT			0.91
Arginine Pathway			
ARG1			1.06
ARG2			1.42
ASS1			0. 85
ASS2			0. 89
Histidine Pathway			
IGPD			1.04
IGPS			1.03
Glutamine Pathway			
GS1		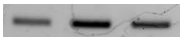	0.99
GS2			1.08
UBQ			

Fig. 4.6. Semi-quantitative RT-PCR analysis of transcript abundance in the recurrent parent (M82) and 2-5 introgression line at breaker stage for enzymes in pathways downstream from aspartate and glutamate. PCR products were visualised following electrophoresis and quantified by densitometry. Each transcript was analysed in three independent samples and all three replicates are shown. Quantity values are shown in the column 'ratio' and are expressed as the mean normalised ratio of 2-5 to M82. *difference between lines of 2O% or more in all replicates.

Transcript	M82	2-5	**Ratio**
PEPCK Pathway			
PEPCK			1.03
GABA Shunt			
GAD1			1.04
GABA1			0.85
GABA2			1.21
GABA3			1.04
SSADH			1.03
UBQ			

Fig. 4.7. Semi-quantitative RT-PCR analysis of transcript abundance in the recurrent parent (M82) and 2-5 introgression line at breaker stage for enzymes in the PEPCK and GABA shunt pathways. PCR products were visualised following electrophoresis and quantified by densitometry. Each transcript was analysed in three independent samples and all three replicates are shown. Quantity values are shown in the column 'ratio' and are expressed as the mean normalised ratio of 2-5 to M82. *difference between lines of 2O% or more in all replicates.

4.2.3 TCA cycle capacity and mitochondrial respiratory capacity in fruit of IL2-5 was not significantly different to the M82 parent line

Mitochondrial electron transport chain activity can affect TCA cycle flux. Therefore, to assess the respiratory function, mitochondria were isolated from fruit pericarp tissue at the breaker stage in the introgresssion line and the parent line (M82). The mean outer mitochondrial integrity was calculated for both lines and was found to be 99.2%±0.3 and 99.2%±0.1 for the M82 parent and 2-5 introgression line respectively based upon five independent isolations. Oxygen consumption by isolated mitochondria was measured using pyruvate and malate as substrates. The respiratory control ratio (RCR) was calculated from the respiration rates of the mitochondria in state 3 (rate of oxygen consumption at substrate saturation in the presence of ADP) and state 4 (after ADP is depleted). No significant difference was found in oxygen consumption using pyruvate and malate as substrates between the parent line and the 2-5 introgression line (Figure 4.8 A). There was also no significant difference found in the respiratory control ratio between the parent line and introgression line (Figure 4.8 B).

The maximal catalytic activities of enzymes in the TCA cycle were measured in mitochondria isolated from fruit pericarp tissue at the breaker stage. The enzymes citrate synthase, aconitase, NAD^+-isocitrate dehydrogenase, 2-oxoglutarate dehydrogenase, succinate dehydrogenase, fumarase and malate dehydrogenase showed no significant differences in their maximal catalytic activities between the 2-5 introgression line and parent line (Figure 4.9 A).

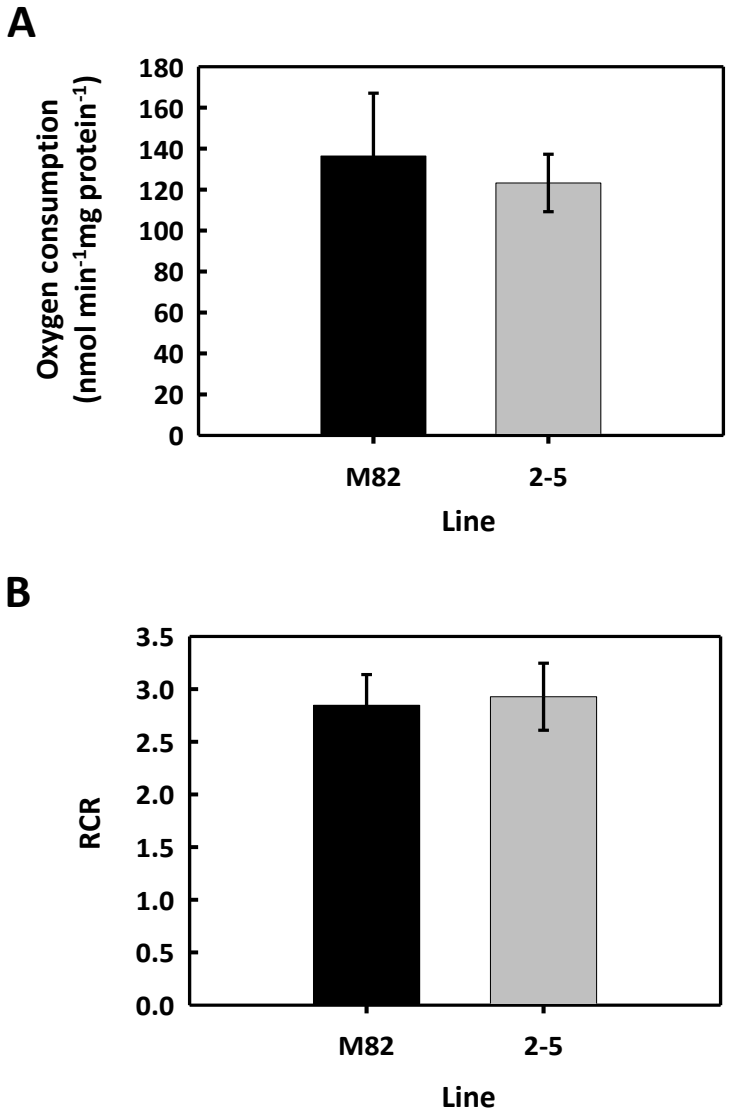

Fig. 4.8. Respiratory function in mitochondria isolated from breaker stage tomato pericarp tissue of 2-5 introgression line and recurrent parent line (M82). O_2 consumption by isolated mitochondria following addition of pyruvate and malate as substrates (A) and respiratory control ratio (RCR) (B). Data presented as mean ± SEM (n=5). * P≤0.05 (TTest).

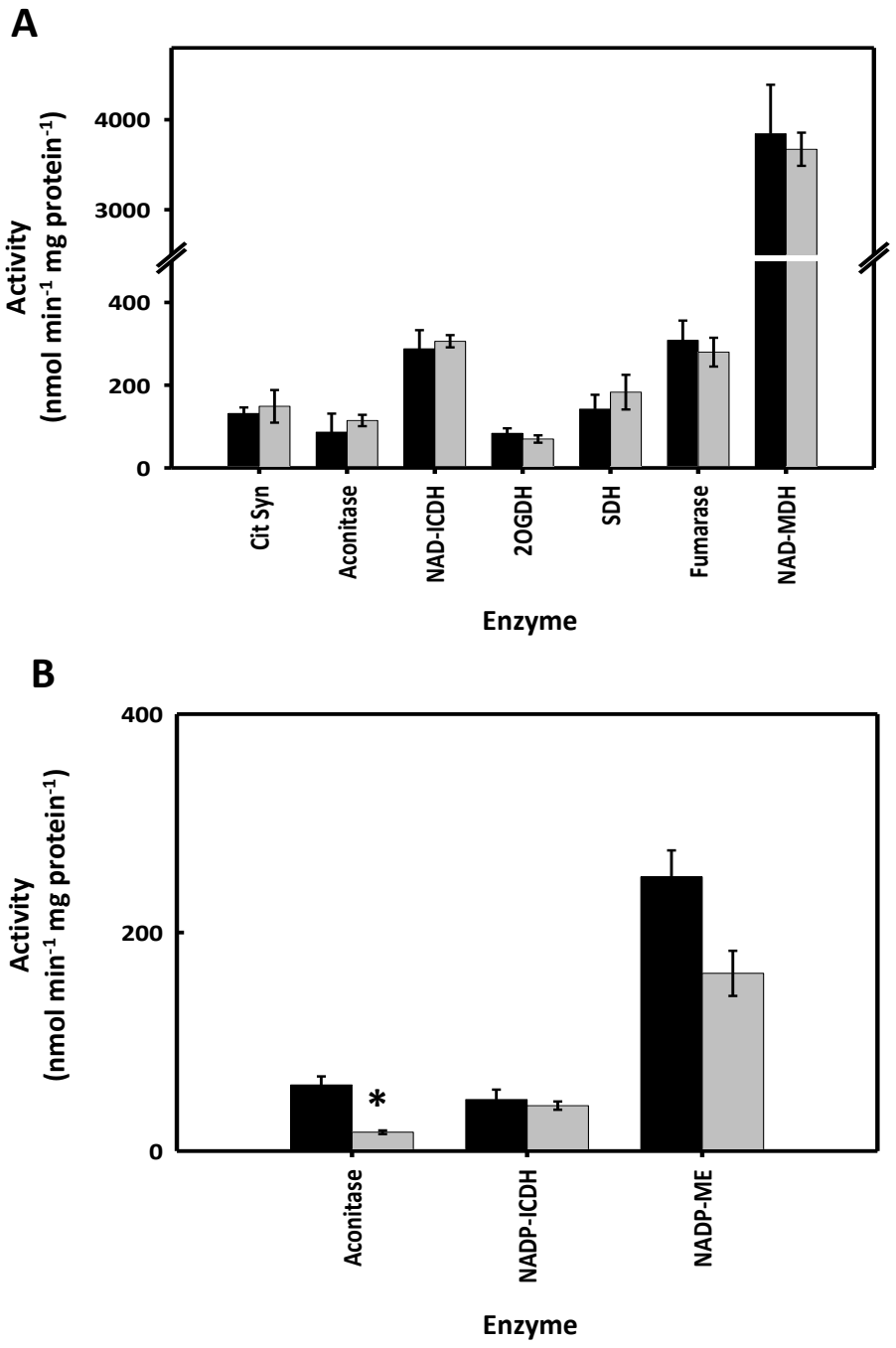

Fig. 4.9. Maximal catalytic activities of enzymes in TCA cycle in introgression line 2-5 and recurrent parent line (M82). Activities of enzymes in recurrent parent (black) and introgression line 2-5 (grey) in isolated mitochondria (A) and whole tissue extracts (B) from breaker stage pericarp tissue. Data presented as mean ± SEM (n=3). * P≤0.05 (TTest). Cit Syn: citrate synthase, NAD-ICDH: NAD^+-isocitrate dehydrogenase, 2OGDH: 2-oxoglutarate dehydrogenase, SDH: succinate dehydrogenase, MDH:malate dehydrogenase, NADP-ICDH: $NADP^+$-isocitrate dehydrogenase, NADP-ME: $NADP^+$-malic enzyme.

4.2.4 Maximal catalytic activity of total cellular aconitase was significantly decreased in IL2-5 at breaker stage

Some enzymes in the TCA cycle have extra-mitochondrial isoforms. Therefore, the maximal catalytic activities of the cytosolic enzymes in whole tissue extracts at the breaker stage were measured for aconitase, $NADP^+$-isocitrate dehydrogenase and $NADP^+$-malic enzyme (Figure 4.9 B). No significant differences were found in NADP-ICDH or NADP-malic enzyme between the 2-5 introgression line and the parent line. A significant decrease (3.5-fold) in aconitase was found in the 2-5 introgression line compared to the M82 parent. The enzymes phospho*enol*pyruvate carboxykinase and phosph*enol*pyruvate carboxylase were not detectable in whole tissue extracts.

4.2.5 TCA cycle flux was not significantly altered in pericarp discs from IL2-5 fruit at breaker stage

TCA cycle flux was estimated by incubating breaker stage fruit pericarp discs in medium supplemented with positionally-labelled [1-^{14}C], [2-^{14}C], [3,4-^{14}C] or [6-^{14}C] glucose. Released $^{14}CO_2$ was quantified over a 24 hour time course. The level of radiolabel in the KOH was determined by liquid scintillation counting. Ratios of cumulative $^{14}CO_2$ release from different combinations of positionally labelled substrates were calculated for the 2-5 introgression line and parent line (Figure 4.10). No significant differences were found in $^{14}CO_2$ release between the 2-5 introgression line and M82 parent for any of the positionally labelled combinations.

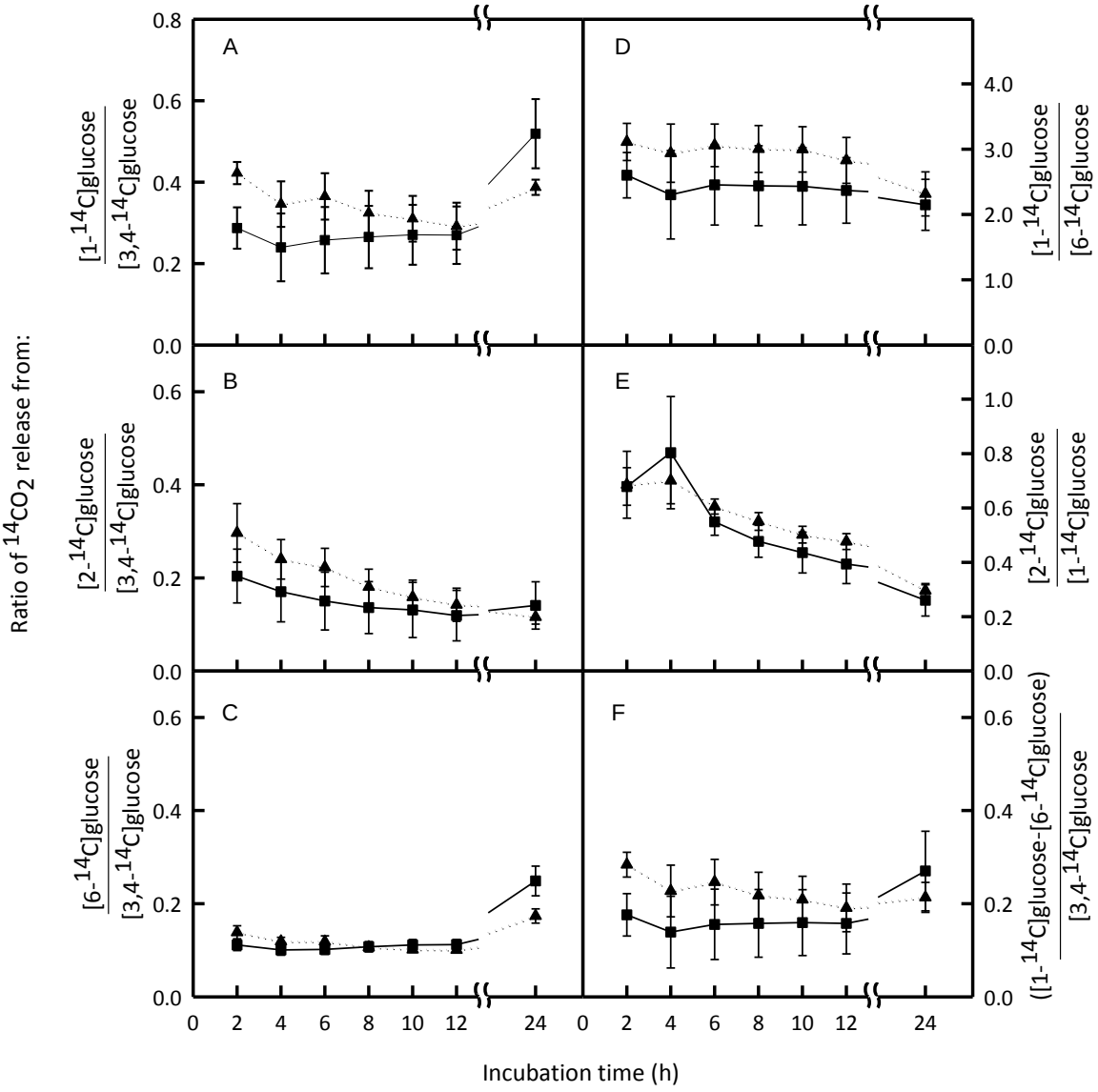

Fig. 4.10. Relative rates of oxidation of specific positions within labelled substrates by pericarp discs of tomato. Pericarp discs were incubated in 10mM Mes-KOH, pH 6.5 supplemented with 50mM [1-^{14}C], [2-^{14}C], [3,4-^{14}C] or [6-^{14}C] glucose (7.4 kBq/ml). $^{14}CO_2$ evolved during each hour of the experiment was trapped in KOH and the level of radiolabel determined by liquid scintillation counting. Ratios of cumulative $^{14}CO_2$ release from different combinations of positionally labelled substrates for the 2-5 introgression line (squares, solid line) and recurrent parent (triangles, dotted line) were calculated. Data presented are ratio of the mean ± SEM (n-=4).

4.3 Discussion

4.3.1 Increased organic and amino acid accumulation in IL2-5 fruit does not require increased TCA cycle capacity

Respiratory function was investigated in the 2-5 introgression line and M82 parent line. The rate of oxygen consumption and respiratory control ratios (Figure 4.8) are of a similar range to those reported in the literature (Holtzapffel *et al.*, 2002; Nunes-Nesi *et al.*, 2005). Respiratory function was not found to be different between the parent line and introgression line suggesting that there is no difference in the coupling between respiration (i.e. electron transport) and ADP phosphorylation. This suggests that mitochondria are capable of maintaining a similar bioenergetic state and that changes in respiratory coupling are unlikely to be responsible for altered TCA cycle poise and altered organic and amino acid accumulation. However, these *in vitro* measurements do not necessarily capture the *in vivo* bioenergetics poise of mitochondria, so some caution must be attached to this statement.

Investigation into the transcript abundance of TCA cycle enzymes revealed no significant differences between the 2-5 introgression line and M82 parent except for decreases in two isoforms of glutamate dehydrogenase (GDH1 and GDH2) (Figure 4.5). The decreases in the two glutamate dehydrogenase isoforms could affect the level of glutamate as this enzyme catalyses the reversible conversion of glutamate to 2-oxoglutarate. However, in tomato, glutamine synthetase and glutamate dehydrogenase activities and protein contents have been shown to have reciprocal induction patterns throughout development (Boggio *et al.*, 2000). Whilst enzyme activities and transcript levels do not always correlate, the interaction shown between these two enzymes suggest that changes would be seen at

the transcript level. Decreases of 30% and 34% in transcript abundance in GDH1 and GDH2, respectively, were found but there were no changes in the transcript abundance of glutamine synthetase (Figure 4.5). Therefore, the decrease seen in glutamate dehydrogenase would be unlikely to cause the 1.5-fold difference seen in glutamate content without affecting the transcript abundance of glutamine synthetase.

At the protein level, no significant differences were found in the maximal catalytic activities of enzymes in the TCA cycle in isolated mitochondria (Figure 4.9 A). However, there was a significant decrease of 72% in cytosolic aconitase activity in the 2-5 line compared to the activity in the recurrent parent in whole tissue extracts (discussed in Section 4.3.3).

Estimation of flux through the TCA cycle revealed no significant differences between the 2-5 introgression line and M82 parent. At first glance, this is difficult to reconcile with the altered accumulation of organic acids and related amino acids. How is it possible for these metabolites to change in amount without concomitant changes in relevant reaction fluxes? Recently *Arabidopsis* cell suspension cultures have been used to investigate metabolic network flux (Williams *et al.*, 2008). TCA cycle flux was measured at two different oxygen concentrations and the levels of organic and amino acids were followed. This research found differences in organic and amino acids levels at the two different oxygen concentrations but no changes to the relative flux distribution. Moreover, it was found that large changes in the levels of organic and amino acids can be produced with relatively small net changes in flux through the TCA cycle. The reason for this being that the fluxes that lead to the accumulation of these metabolites (i.e. their withdrawal from the TCA cycle and storage in the vacuole) is very small relative to the flux through the TCA cycle. For example,

the net flux through the TCA cycle was approximately 0.75 mmol d^{-1} per flask, an order of magnitude higher than found for organic and amino acid synthesis (approximately 0.04 and 0.08 mmol d^{-1} per flask respectively). Thus, withdrawal of small amounts of metabolites from the TCA cycle for organic accumulation and amino acid synthesis would not have a significant effect on the flux through the TCA cycle, but could lead to quite substantial increases in amino acid accumulation over a period of time.

Collectively, these results suggest that organic and amino acid accumulation in the 2-5 introgression line does not require an increase in TCA cycle capacity.

4.3.2 Organic and amino acid accumulation is not regulated at a transcript level by downstream pathways

It could be possible for glutamate and aspartate accumulation to be regulated by changes in the metabolic pathways downstream of these enzymes that also lead to the synthesis of other amino acids. Also, other pathways, such as the PEPCK pathway and the GABA shunt, have been shown to affect organic and amino acid levels (Bahrami *et al.*, 2001; Kisaka and Kida, 2003; Famiani *et al.*, 2005). To identify if there were transcriptional changes in these downstream pathways, transcript abundance was determined for as many enzymes as possible in the both the forward and reverse directions (Figures 4.6 and 4.7). No significant differences were found in any of the transcripts of the enzymes measured except for a 36% reduction in one isoform of proline dehydrogenase (*PDH1*) in the proline degradation pathway (Figure 4.6). A decrease in proline dehydrogenase also could affect the levels of glutamate as proline is oxidised to glutamate in a two step process involving this enzyme and 1-pyrroline-5-carboxylate dehydrogenase. This pathway tends to be regulated

transcriptionally by both proline dehydrogenase and 1-pyrroline-5-carboxylate dehydrogenase as well as enzymes in the proline synthesis pathway (Szabados and Savoure, 2010). Therefore, a change in one isoform of proline dehydrogenase transcript would be unlikely to cause the increase in glutamate.

Although the transcript abundance was measured for a limited number of enzymes, for those that were measured, there is no indication that organic and amino acid accumulation is regulated transcriptionally by enzymes in these downstream pathways.

Correlations between the expression patterns of enzymes in different pathways throughout development can indicate similarities in the regulation of these pathways. Here, expression data in the Tomato Functional Genomics database (Cornell University, Ithaca, USA) was extracted to identify any correlation between the expression patterns of TCA cycle enzymes and enzymes in the pathways downstream of aspartate and glutamate and with enzymes in other pathways. TCA cycle enzymes were spread over 12 clusters from a total of 50 suggesting that they are differentially regulated throughout development. This result is not surprising given that the TCA cycle is a central metabolic pathway and its regulation must be tightly controlled. Having a number of different regulation mechanisms in place would ensure continued functioning under differing physiological conditions. Also, many of the substrates in the TCA cycle take part in other metabolic pathways, and therefore each substrate would be regulated differentially according to the metabolic needs of the pathways concerned. This has been shown in research where alterations in the activity levels of enzymes in the TCA cycle (through antisense inhibition or mutation) did not have severe consequences on the TCA cycle and often resulted in carbon being partitioned from the TCA cycle into alternative pathways (Carrari *et al.*, 2003a; Nunes-Nesi *et al.*, 2005;

Nunes-Nesi *et al.*, 2007; Studart-Guimaraes *et al.*, 2007; Sienkiewicz-Porzucek *et al.*, 2008; Sienkiewicz-Porzucek *et al.*, 2010). The TCA cycle continued to function via alternative pathways by-passing the enzyme with reduced activity (e.g. GABA shunt) or carbon was partitioned to into other pathways completely (e.g. photosynthesis).

All of the five clusters showed similar expression patterns of TCA cycle enzymes and downstream enzymes with various transcription factors. The majority of these are homeobox genes which encode transcription factors involved in the regulation of patterns of development (e.g. morphology, programmed cell death), transcription factors involved in plant defence and bZIP transcription factors involved in abiotic stress which are unlikely to be regulators of TCA cycle enzymes (Janssen *et al.*, 1998; Mayda *et al.*, 1999; Hofmann *et al.*, 2008; Yanez *et al.*, 2009). Three of the five clusters (Cluster 33, 37 and 39) correlated loosely with the pattern of accumulation to the relevant organic or amino acids. However, in some instances, even though the expression pattern of the enzyme concerned correlated with the accumulation pattern of the relevant metabolite, the enzyme expression has been shown in other research to actually be negatively correlated with metabolite accumulation. For example, increases in PEPCK expression in cluster 33 correlated with malate accumulation but was shown to decrease in expression with malate accumulation (Bahrami *et al.*, 2001; Famiani *et al.*, 2005). Also, increases in cytosolic aconitase expression correlated with citrate accumulation in clusters 37 and 39 but has been found to be negatively correlated with citrate accumulation (Section 4.3.3).

Collectively, these results suggest that organic and amino acid accumulation is not regulated at a transcript level by downstream pathways.

4.3.3 Cytosolic aconitase may be involved in regulating citrate accumulation

There was a significant decrease of 72% in total aconitase activity in the 2-5 line compared to the recurrent parent (Figure 4.9 B) whereas the mitochondrial aconitase activity was not significantly altered (Figure 4.9 A). This strongly suggests that an extra-mitochondrial (most likely cytosolic) aconitase is decreased in amount/activity. Notably, transcript abundance of one of the aconitase genes (Acon1) was decreased by 28% in the 2-5 line (Figure 4.5 B). The decreased cytosolic aconitase activity and transcript could result in an increase in cytosolic citrate content (and, thus, an increase in vacuolar citrate content) that could account for the increase of 1.5-2 fold in citrate content previously found in the 2-5 line fruit relative to the recurrent parent (Figures 3.4 A and 3.6 A).

Fruits of *Citrus*, accumulate citrate throughout development to a peak before declining again near maturation, a pattern not dissimilar to tomato (Figures 3.4 A and 3.6 A). There is some evidence from research in *Citrus* fruit that aconitase is a regulatory factor in citrate accumulation, but at the protein level. For example, aconitase was investigated in a low acid (*Citrus limettiodes*) and a high acid (*Citrus limon*) variety (Sadka *et al.*, 2000a). Mitochondrial aconitase activity was found to decline in early development in the high acid variety but remained constant in the low acid variety. Cytosolic aconitase activity was found to increase near maturation in the high acid variety, when acid peaks, but its expression remained constant. The authors proposed that the high mitochondrial aconitase in early fruit development is responsible for the increase in acid accumulation in the vacuole. The cytosolic aconitase, induced towards fruit maturation when acid starts to decline, is involved with acid catabolism from citrate released back into the cytosol. In support of this hypothesis, investigations into aconitase in *Citrus limon* showed that under iron shortage

aconitase activity is reduced and citrate levels increase (Shlizerman *et al.*, 2007). In calli and isolated juice vesicles subjected to iron shortage, mRNA levels were unchanged but cytosolic aconitase showed reduced activity concomitant with increased citrate levels as a result of the slower rate of citrate catabolism. Further supporting research of aconitase in seven acid varieties of *Citrus* differing in their acidity, found two of three aconitase genes expression was induced just prior to or coincident with the acidity peak and high expression at the beginning and during acid reduction (Terol *et al.*, 2010). For two *Citrus* varieties where the expression of aconitase did not follow this pattern, other additional regulatory mechanisms were suggested to account for differences in citrate content, such as the activity of vacuolar membrane transporters. In addition, $NADP^+$-isocitrate dehydrogenase was investigated in *Citrus limon* in relation to citrate accumulation further supporting the hypothesis of aconitase regulating acid in late fruit development (Sadka *et al.*, 2000b). During fruit development isocitrate dehydrogenase activity was predominantly mitochondrial but shifted to become predominantly cytosolic activity as the fruit grew. A similar pattern of expression was seen in aconitase in the same variety (Sadka *et al.*, 2000a). However, the increasing NADP-ICDH cytosolic activity through development correlated with increased gene expression suggesting that regulation was at the transcript level, unlike cytosolic aconitase.

From the results and research in *Citrus*, there is evidence to suggest that cytosolic aconitase may play a part in the regulation of citrate accumulation in tomato. This requires further investigation to identify if, like *Citrus*, the regulation involves accumulation due to a combination of citrate synthesis and catabolism or only citrate synthesis. In addition, there

is suggestion that citrate accumulation could be additionally regulated by vacuolar transport mechanisms (Sadka *et al.*, 2000a; Terol *et al.*, 2010).

4.3.4 Summary

This aim of this chapter was to exploit the metabolic differences between the 2-5 introgression line and M82 parent to identify the molecular factors that could be responsible for these differences and to gain an insight into the regulation of organic and amino acid accumulation. The initial focus of the research on the TCA cycle revealed that organic and amino acid accumulation does not require an increase in TCA cycle capacity. This targeted approach was extended to the enzymes in the pathways downstream of glutamate and aspartate and in the PEPCK and GABA shunt pathways. In addition to this to gain a broader overview, cluster analysis of expression data extracted from the Tomato Functional Genomics database was performed to identify if there were correlations between the expression patterns of enzymes in the TCA cycle and downstream pathways with other metabolic pathways that may indicate similarities in regulation. No major changes were found in the downstream pathways and lack of good correlations in the cluster analysis suggest that organic and amino acid accumulation is not regulated transcriptionally. However, changes in cytosolic aconitase suggest there is some regulation on the metabolic level for the accumulation of citrate but there must also be additional regulatory mechanisms involved such as vacuolar transport. There is no indication that malate, glutamate or apartate are regulated metabolically. Therefore, there must be other mechanisms responsible for their accumulation.

Chapter 5

Tonoplast transport as a determinant of accumulation of organic and amino acids in tomato fruit

5.1 Introduction

The results from Chapter 4 suggest that organic and amino acid accumulation is only partially regulated metabolically and that there must be additional regulatory mechanisms. Organic and amino acids synthesised in the cytosol and mitochondria are stored in the vacuole where they can accumulate to very high levels (Farre *et al.*, 2001; Martinoia *et al.*, 2007). For example, malate and citrate, respectively, can accumulate to concentrations up to 350 mM in the leaves of CAM plants and in the juice cells of *Citrus aurantifolia* (Martinoia and Rentsch, 1994; Brune *et al.*, 1998). This degree of accumulation in the vacuole, relative to the cytosol, requires energy. Plant vacuoles contain two proton pumps, a V-ATPase and a V-PP_iase, which are capable of providing the necessary energy in the form of a chemical and/or electrical potential gradient.

Although tonoplast transport mechanisms have been identified in plants, further research is still needed to identify and fully characterise the proteins that facilitate transport of organic and amino acids across the vacuolar membrane. Much of the research to date has

focused on identifying the transporter protein and on characterising the transport mechanism. There is some consensus from researchers that the vacuolar transporter for malate and citrate influx has been identified as a shared 27-33 kDa tonoplast channel or carrier protein (Oleski *et al.*, 1987a; Oleski *et al.*, 1987b; Rentsch and Martinoia, 1991; Luttge *et al.*, 2000; Martinoia *et al.*, 2000; Ratajczak *et al.*, 2003). There has been an assumption in the literature that there is a single conserved vacuole transporter for malate and citrate influx. However, it is possible that the transporter mechanism may instead be species or tissue dependent. For example, in tomato and barley, an ion channel has been proposed (Hedrich *et al.*, 1986; Oleski *et al.*, 1987a) whereas in *Catharanthus roseus*, a carrier protein has been suggested (Marigo *et al.*, 1988). Malate influx in *Kalanchoe diagremontiana* is via an inward-rectifying anion-selective channel energised by the two vacuolar proton pumps (Smith and Winter, 1996; Hafke *et al.*, 2003). However, in *Arabidopsis thaliana*, the malate transporter (A*tt*DT) was found to be a homolog to the human sodium/dicarboxylic co-transporter (Emmerlich *et al.*, 2003; Hurth *et al.*, 2005). The general conclusion from this work is that there are several potential mechanisms for vacuolar carboxylic acid transport and it may be the case that more than one mechanism operates in the same species. Further research in this area is needed to clarify if there is a single or multiple transport mechanism(s) or if transport is species and/or tissue dependent for citrate and malate influx.

In the plant species that have been studied, including tomato, malate and citrate are transported into the vacuole principally in the forms of malate^{2-} and citrate^{3-} ions (Oleski *et al.*, 1987a; Rentsch and Martinoia, 1991; Martinoia *et al.*, 2000). Although these are the

predominant forms, other forms of influx have been found. For example, in *Catharanus roseus* cells, malate was found to be transported in the $Hmal^-$ form (Marigo *et al.*, 1988).

Malate transport into the vacuole is possibly ATP-dependent. Influx via the malate channel found in vacuoles isolated from barley and *Kalanchoe* leaf mesophyll cells (Martinoia *et al.*, 1985; Martinoia *et al.*, 1991; Pantoja and Smith, 2002; Hafke *et al.*, 2003) is driven by the electrical component of the electrochemical potential generated by the activity of H^+-pumps (Martinoia *et al.*, 2000; Pantoja and Smith, 2002). Also, malate influx in *Catharanus roseus* cells was increased by the activity of the ATPase proton pumps (Marigo *et al.*, 1988). However, in contrast, the CAM plant *Bryophyllum diagremontianum* influx of malate is independent of ATP or the proton gradient in vacuoles isolated from leaf mesophyll protoplasts (Buser-Suter *et al.*, 1982).

Research in tomato shows citrate transport to be ATP-independent (i.e. not dependent upon the activity of the V-ATPase) (Oleski *et al.*, 1987a). However, this is in contrast to other plants. For example, in barley mesophyll vacuoles citrate influx was found to be ATP-dependent (Rentsch and Martinoia, 1991). Also, in *Hevea brasiliensis*, a functional ATPase was identified and thought to drive citrate influx (Marin *et al.*, 1981). In *Citrus* cells, two citrate transport mechanisms (an electrochemical-dependent channel and an electrochemical-independent ATP-dependent transporter) were identified using antibodies raised against the vacuolar malate specific channel of *Kalanchoe diagremontiana* (Ratajczak *et al.*, 2003). Investigations of citrate uptake into *Citrus* tonoplast vesicles, in the presence of malate, indicated that a single transport channel was used for citrate and malate uptake.

Very little is known about the mechanisms of organic acid storage and efflux from the vacuole. Citrate accumulation in tomato is thought to occur via the formation of citrate

complex of impermeant species such as H-citrate^{2-} or Mg-citrate^{-} and possibly in response to membrane potential across the tonoplast or by facilitated diffusion (Oleski *et al.*, 1987a). The mechanism of accumulation of malate in tomato is still largely unknown. In the CAM plant *Kalanchoe diagremontiana*, malate is maintained in the vacuole as Hmalate^{-} or H_2malate complexes (Smith and Winter, 1996; Hafke *et al.*, 2003). Citrate efflux, from the vacuoles in *Citrus* juice cells, is possibly by a tonoplast citrate/H^+-symporter (Shimada *et al.*, 2006). In the well studied CAM plants the mechanisms of malate efflux from the vacuole is also unknown (Winter and Smith, 1996). It is thought that malate efflux occurs in the form of Hmalate^{-} or malate^{2-}possibly via a H^+/malate cotransporter or a slow vacuolar channel, although there is still no evidence to support these hypotheses (Winter and Smith, 1996).

Very little is known about the mechanisms that transport and store amino acids in vacuoles and what is known is limited to research in tonoplasts isolated from barley mesophyll cells. There are indications that at least three different mechanisms exist (Dietz *et al.*, 1990; Martinoia *et al.*, 1991). One mechanism, for the transport of aromatic amino acids, is dependent upon the activities of either the H^+-ATPase or H^+-PPase (Homeyer and Schultz, 1988; Homeyer *et al.*, 1989; Martinoia *et al.*, 1991). There is a second mechanism, specifically for the transport of positively charged amino acids, such as arginine and lysine (Martinoia *et al.*, 1991). Finally, there is an ATP-stimulated but non-energy requiring mechanism with broad specificity for the influx and efflux of various amino acids (Dietz *et al.*, 1989; Dietz *et al.*, 1990; Martinoia *et al.*, 1991; Goerlach and Willmshoff, 1992). However, an amino acid carrier from barley mesophyll cells reconstituted and incorporated into liposomes was shown to be a uniport transporter, and could be a fourth different mechanism (Thume and Dietz, 1991). In this carrier, transport of ^{14}C-glutamine and ^{14}C-

arginine uptake was stimulated by the addition of ATP and transport was thought to be by facilitated diffusion.

The transport properties of isolated tonoplast membranes can be experimentally investigated by virtue of the fact that tonoplast membrane fragments self-seal into transport-competent vesicles. Using isolated tonoplast vesicles has the advantage of allowing membrane transport to be studied in isolation without any interference from metabolic products within the cytosol. Anion uptake into isolated tonoplast vesicles can be measured either directly using ^{14}C-labelled anions or indirectly using fluorescence dyes, such as quinacrine, to measure proton-dependent anion transport (White and Smith, 1989). Although, the method using ^{14}C-labelled anions does measure anion uptake directly, this method is more expensive and has the associated safety concerns. Also, the measurement of uptake is taken as discrete measurements over time. In comparison, the indirect method using fluorescence dyes, is relatively cheaper, safer, and the uptake (by observing fluorescence quenching) can be observed in real time. Therefore, this method was chosen to measure proton-dependent anion transport.

The driving force for solute transport across the tonoplast can be provided by either the ATPase or PP_iase by providing a proton motive force. The ATPase (or PP_iase) pumps protons into the vesicle interior as ATP is hydrolyzed to ADP and inorganic phosphate. By stimulating the proton pumps (by supplying either ATP or PP_i) there is an increase in the transmembrane pH difference (ΔpH) and the electrical potential difference ($\Delta\psi$). ATPase (or PPase) activity would continue until its action is thermodynamically impeded by the interior $\Delta\psi$ (Bennett and Spanswick, 1983). Anion influx across the tonoplast dissipates the $\Delta\psi$ (allowing the ATPase (or PPase) to continue pumping protons) but not the ΔpH, so the

vesicle pH decreases. The pH decrease or rate of ATP- or PPi-dependent vesicle acidification (i.e. the maximum rate of ATPase or PPase activity) can be used to determine the relative permeability of the tonoplast to various anions and therefore, the rate of anion influx. ATP-dependent H^+-transport (tonoplast vesicle acidification) is monitored by following the fluorescence quenching of the monoamine quinacrine (6-chloro-9-(4-diethylamino-1-methylbutylamino)-2-methoxyacridine dihydrochloride) in isolated tonoplast vesicles (Bennett and Spanswick, 1983; White and Smith, 1989). Quinacrine, a weak base, fluoresces when free in solution. Quinacrine is lipid-soluble in its uncharged form and will readily diffuse across the tonoplast membrane and enter the vesicle interior. Further quinacrine is taken up into the vesicle interior as the inside-acid pH gradient decreases due to V-ATPase acitivity. The quinacrine is subsequently ion trapped in the vesicle interior due to protonation of the amino group at low pH (Marceau *et al.*, 2009). The concentration of quinacrine increases within the vesicle interior where it forms dimers resulting in a reduction of the concentration-dependent fluorescence signal due to the molecular stacking (Jennings *et al.*, 1988).

The experimental method monitors ATP-dependent H^+-transport (rate of fluorescence quenching) using a luminescence spectrometer in isolated tomato tonoplast membranes. Addition of ATP to the reaction mix containing tonoplast membrane, quinacrine and the anion of interest (e.g. citrate, malate, aspartate and glutamate) stimulates ATPase activity (Figures 5.1 and 5.2). Ammonium sulphate is added at the end of the experiment to dissipate the pH gradient. Ammonia freely crosses the tonoplast membrane and is rapidly protonated in the vesicle interior. This causes a rapid decrease in vesicle interior pH resulting in release and re-fluorescence of quinacrine. The resulting

fluorescence level takes into account the decay in fluorescence that inherently happens over the duration of the assay and is arbitrarily set to 100 and used to normalise the data. The initial rates of H^+-transport are then determined from the initial linear rates of fluorescence quenching upon the addition of ATP.

The aim of this chapter was to determine if the differences in organic and amino acid accumulation between the introgression line 2-5 and the recurrent parent were related to variations in the rate of anion influx to the vacuole. This was investigated by comparison of the rates of ATP-dependent anion uptake in tonoplast membrane isolated from fruit tissue at two different developmental stages during late fruit development. This was then correlated with fruit metabolite content as the same developmental stages.

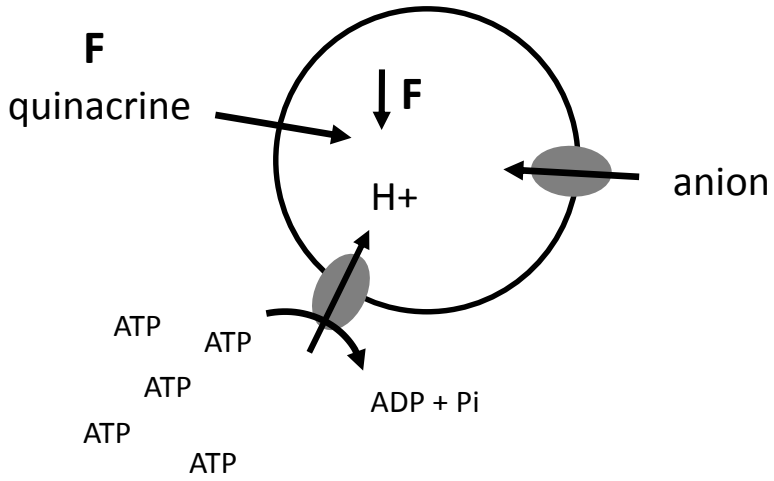

Fig. 5.1. Schematic showing transport in a tonoplast vesicle during quinacrine fluorescence quenching method. ATP is added, in the presence of quinacrine and anion of interest, to stimulate ATPase activity. As ATP is hydrolysed to ADP and inorganic phosphate (Pi), a proton is pumped, acidifying the vesicle interior and allowing anion influx. ATP-dependent acidification of the vesicle results in quinicrine uptake where the concentration increases and fluorescence self-quenching occurs. F=fluorescence intensity.

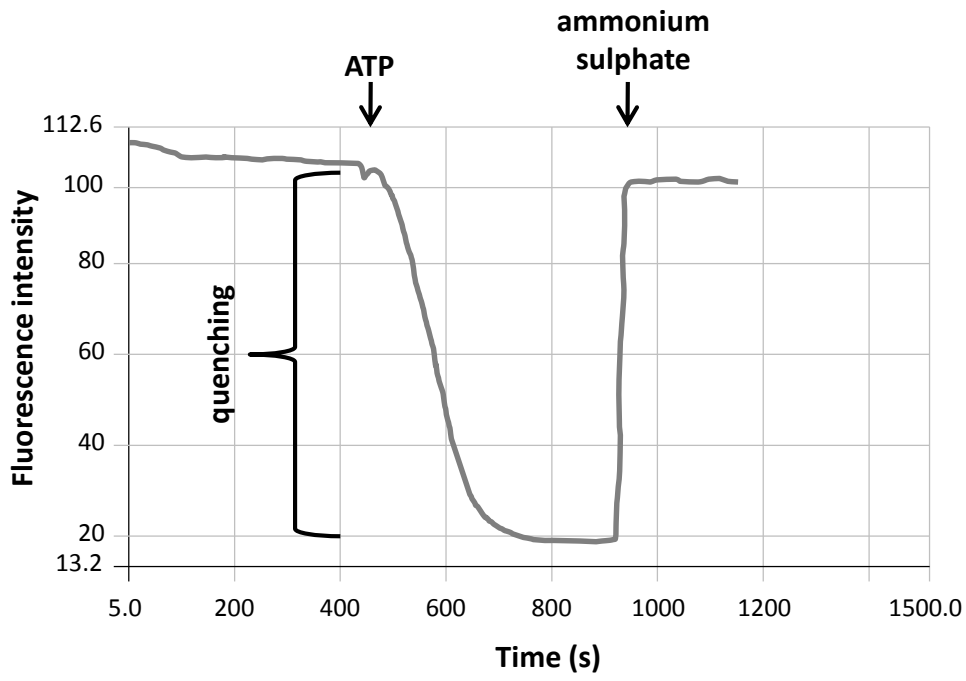

Fig. 5.2. Schematic showing a typical trace of a quinacrine fluorescence quenching experiment. Trace showing fluorescence quenching in reaction medium containing anion, quinacrine and tonoplast membrane. Addition of ATP stimulates the active influx of H^+ leading to vesicle acidification where quinicrine is drawn into the vesicles resulting in fluorescence quenching. Addition of ammonium sulphate dissipates the pH gradient. This causes deprotonation of the quinacrine that is subsequently released from the vesicle interior resulting in rapid re-fluorescence.

5.2 Results

5.2.1 Transport measurement optimisation

Tonoplast membrane, when isolated from homogenised fruit tissue, will invariably contain membranes from other organelles (i.e. plasma membrane and mitochondrial membrane) contaminating the sample. The majority of the contaminating membrane is removed during the process of isolation through filtration, density and sucrose gradient centrifugation. However, there will still be small amounts of extraneous membrane in the enriched tonoplast membrane sample that also contains ATPases, and thus, ATPase activity. To eliminate H^+-ATPase activity produced by ATPases in the extraneous membranes, ATP-dependent H^+-transport rates were measured in the presence of commonly used membrane-specific ATPase inhibitors and normalised to the nitrate-sensitive tonoplast membrane ATPase activity. The inhibitors used were sodium orthovanadate, an inhibitor of the plasma membrane and sodium azide (an inhibitor of the mitochondrial membrane). Nitrate, a specific inhibitor of the tonoplast H^+-ATPase, was used to identify, and exclude, any remaining H^+-transport activity that is not specific to the tonoplast membrane (e.g. H^+-PPase activity). In addition, gramicidin, a channel-forming ionophore, was added to all reaction mixes. Gramicidin induces non-specific pores in the membrane and thus, rapidly reduces both the $\Delta\psi$ and ΔpH across the tonoplast membrane, dissipating the pH gradient. Dissipating the pH gradient allows the H^+-ATPase to function without inhibition by a proton build-up that would otherwise limit the H^+-ATPase activity, thus, allowing the maximum H^+-ATPase activity to be measured. ATPase activity measurements for tonoplast membrane isolated from 40 and 50 DAA fruit for the recurrent parent and line 2-5 is shown in Table 5.1

and 5.2. Average nitrate-sensitive tonoplast membrane ATPase activity (as a % total activity i.e. the gramicidin treatment) for the recurrent parent (M82) were 75.8% and 58.3% for tonoplasts isolated from 40 and 50 DAA tissue. Average nitrate-sensitive tonoplast membrane ATPase activity (as a % of total activity) for the 2-5 line were 74.2% and 56.3% for tonoplasts isolated from 40 and 50 DAA tissue. Although there is a decrease in the nitrate-sensitive tonoplast membrane ATPase activity (as a % of total activity) at 50 DAA compared to 40 DAA, there is no difference between the recurrent parent and the 2-5 line at each developmental stage. This shows that the level of purity in the tonoplast preparation is similar between the lines at both developmental stages.

In other research, azide-sensitive ATPase activity (i.e. mitochondrial ATPase activity) and nitrate-sensitive ATPase activity (i.e. tonoplast ATPase activity) was shown to be pH dependent (Wang and Sze, 1985; Oleski *et al.*, 1987b). Azide-sensitive ATPase activity was shown to be significantly decreased below pH 8.0. Thus, performing the assay below this pH would result in a significant reduction in mitochondrial ATPase activity. In addition, nitrate-sensitive ATPase activity was shown to peak at pH 6.5 but decrease at higher pHs. Therefore, optimization of the pH in the ATPase assay could minimise mitochondrial ATPase activity (i.e. azide-sensitive activity) whilst maximising the nitrate-sensitive ATPase activity. ATPase activities in tomato tonoplast were measured at pH 7.5, 7.0 and 6.5 in the presence of azide, nitrate or gramicidin (Figures 5.3 A and 5.3 B). ATPase activity was shown to decrease in the presence of gramicidin and nitrate as pH decreased. ATPase activity increased in the presence of azide as the pH decreased from 7.5 to 7.0, but was comparable at pH 6.5 to pH 7.0 (Figure 5.3 A). Expressing the treatments as a percentage of gramicidin (i.e. total ATPase activity) showed that the azide-sensitive fraction of ATPase activity (i.e.

total ATPase activity less the ATPase activity in the presence of azide) decreased considerably as the pH decreased (Figure 5.3 B) and the nitrate-sensitive activity increased. However, total activity also decreased, as pH decreased (Figure 5.3 A). Thus, to maximise the total ATPase activity and nitrate-sensitive activity whilst minimizing azide-sensitive ATPase activity, a pH of 7.0 with the addition of azide was chosen.

Rates of ATP-dependent H^+-transport were determined from the initial maximum linear rates of fluorescence quenching after addition of ATP. Kinetic analysis of a proton-translocating ATPase in corn root membrane vesicles determined that upon addition of ATP the initial fluorescence is linear before there is a levelling off (Bennett and Spanswick, 1983). The initial linear rate of fluorescence quench was found to be a measure of the activity of the H^+-ATPase. Therefore, ATP-dependent H^+-transport rates were measured after the addition of ATP in the linear region eight minutes after the addition of the anion as shown in the example trace (Figure 5.4).

The dependence of anion transport on ATPase activity is also illustrated in the example trace (Figure 5.4). An initial quinacrine fluorescence quenching was observed prior to the addition of ATP, which is probably from residual transmembrane pH difference in the vesicle after after re-formation during the membrane isolation. However, this initial quenching levels off, allowing ATP-dependent quenching to be measured without a significant background rate. On addition of ATP, the ATPase is stimulated creating an active influx of protons rapidly increasing the rate of fluorescence quench, thus, demonstrating that ATP (and ATPase activity) is required to generate the inside-acid pH gradient. The rate of fluorescence quench would rapidly plateau without the dependence of anion influx to dissipate the $\Delta\psi$ allowing the ATPase to continue pumping protons. Thus, the rate of

fluorescence quench is dependent on the anion present and its ionic form. This is shown in the trace (Figure 5.4) where the rate of fluorescence quench is much greater for malate than for aspartate or glutamate.

Replicate	Line	Treatment		Nitrate sensitive ATPase activity
		Gramicidin	Gramicidin + nitrate	
1	M82	10.73	3.09	7.64
2	M82	21.41	5.16	16.25
3	M82	22.32	5.42	16.91
4	M82	30.44	6.53	23.90
5	M82	9.42	2.12	7.30
1	IL2-5	7.16	2.74	4.42
2	IL2-5	14.14	3.48	10.66
3	IL2-5	20.65	4.80	15.85
4	IL2-5	19.73	4.61	15.12
5	IL2-5	14.19	2.82	11.37

Table 5.1. ATPase activities in tonoplast membrane isolated from tomato fruit at 40 DAA. Nitrate-sensitive ATPase activity was calculated from the ATPase activity of tonoplast membrane treated with gramicidin subtracted from tonoplast membrane treated with gramicidin and nitrate. Values are expressed as µmol P_i (mg protein)$^{-1}$ hr^{-1}. M82=recurrent parent line.

Replicate	Line	Treatment		Nitrate sensitive ATPase activity
		Gramicidin	Gramicidin + nitrate	
1	M82	4.05	1.67	2.38
2	M82	9.20	3.53	5.66
3	M82	4.40	2.02	2.38
4	M82	15.39	6.45	8.95
1	2-5	2.88	1.31	1.57
2	2-5	4.34	1.99	2.34
3	2-5	5.40	2.50	2.90
4	2-5	9.00	3.45	5.55

Table 5.2. ATPase activities in tonoplast membrane isolated from tomato fruit at 50 DAA. Nitrate-sensitive ATPase activity was calculated from the ATPase activity of tonoplast membrane treated with gramicidin subtracted from tonoplast membrane treated with gramicidin and nitrate. Values are expressed as µmol P_i (mg protein)$^{-1}$ hr^{-1}. M82=recurrent parent line.

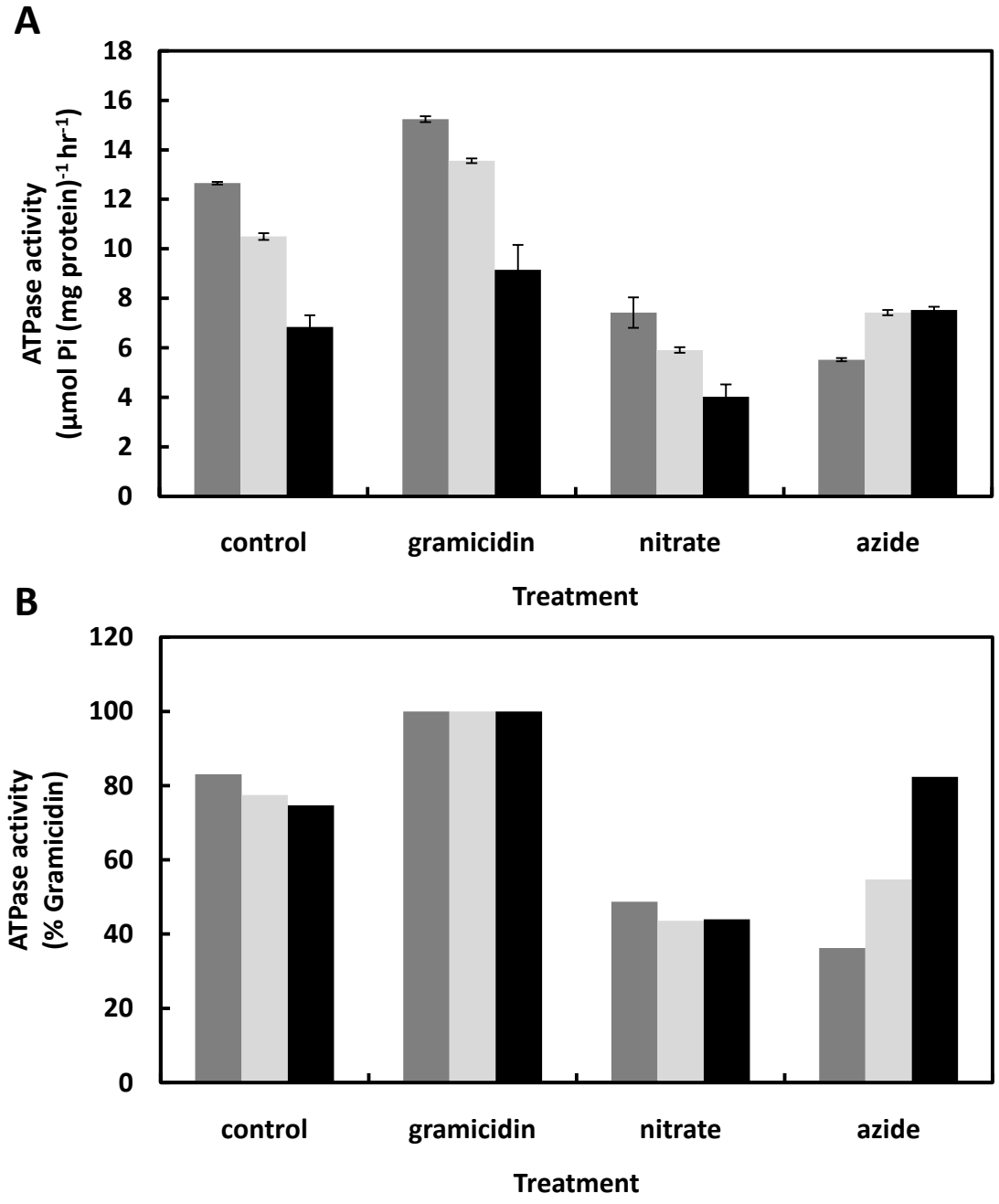

Fig. 5.3. **ATPase activities in isolated tomato tonoplast membrane at different pH values in the presence of gramicidin or inhibitors.** ATPase activity (A) in tomato tonoplasts isolated from 55 DAA fruit tissue in the presence of 2µM gramicidin, 50 mM nitrate or 0.5 mM azide or expressed as a percentage of gramicidin (B) at pH 7.5 (dark grey bars), pH 7.0 (light grey bars) and pH 6.5 (black bars).

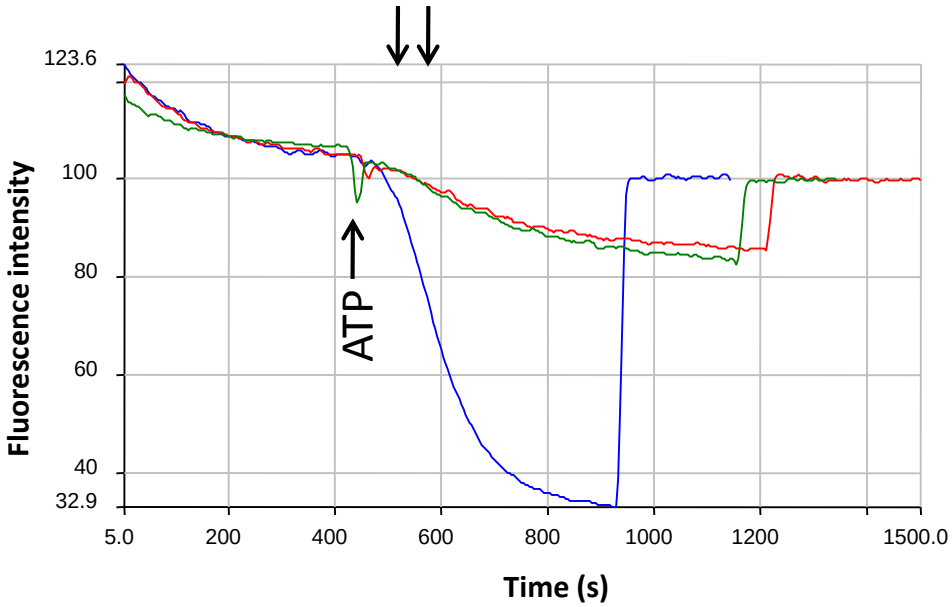

Fig. 5.4. Example trace showing ATP-dependent H^+-transport in tomato tonoplast membrane in the presence of different anions. ATP-dependent H^+-transport was determined from the trace in the linear region as indicated between the arrows for malate (blue), aspartate (red) and glutamate (green). The time at which ATP was added is indicated.

5.2.2 ATP-dependent H^+-transport to investigate secondary anion influx in isolated tonoplast membrane of tomato fruit

To determine the rate of anion influx by monitoring ATP-dependent H^+-transport across the vacuolar membrane, tonoplast membrane was isolated from 40 DAA and 50 DAA tomato pericarp tissues of the 2-5 introgression line and the parent line (M82). Rates of ATP-dependent H^+-transport (i.e. anion influx), normalised to ATPase activity, in tomato tonoplast membranes were determined from the initial maximum linear rates of fluorescence quenching of quinacrine (6-chloro-9-(4-diethylamino-1-methylbutylamino)-2-methoxyacridine dihydrochloride) for each of the anions chloride, citrate, malate, aspartate and glutamate (Figure 5.5 A and B). There were no significant differences in ATP-dependent H^+-transport (i.e. anion influx) between the M82 and 2-5 line in the presence of any of the independently measured anions in tonoplasts isolated from 40 DAA tissue (Figure 5.5 A). However, there was a significant reduction in ATP-dependent H^+-transport in the presence of malate (i.e. malate influx) for the 2-5 line in tonoplasts isolated from 50 DAA tissue compared to the recurrent parent (M82) (Figure 5.5 B). There were no significant differences in ATP-dependent H^+-transport in the presence of the other anions independently measured (i.e. chloride, citrate, aspartate, and glutamate) in tonoplast membrane isolated from 50 DAA tissues.

Metabolite content was determined enzymatically in reserved pericarp tissue used for the tonoplast isolation. Citrate and malate content was significantly increased in the 2-5 introgression line compared to M82 in 40 DAA pericarp tissue (Figure 5.6 A). There was no significant difference in aspartate or glutamate content between the M82 and 2-5 introgression line. There were no significant differences in metabolite content (citrate,

malate, aspartate or glutamate) between the 2-5 introgression line and M82 in 50 DAA pericarp tissue (Figure 5.6 B).

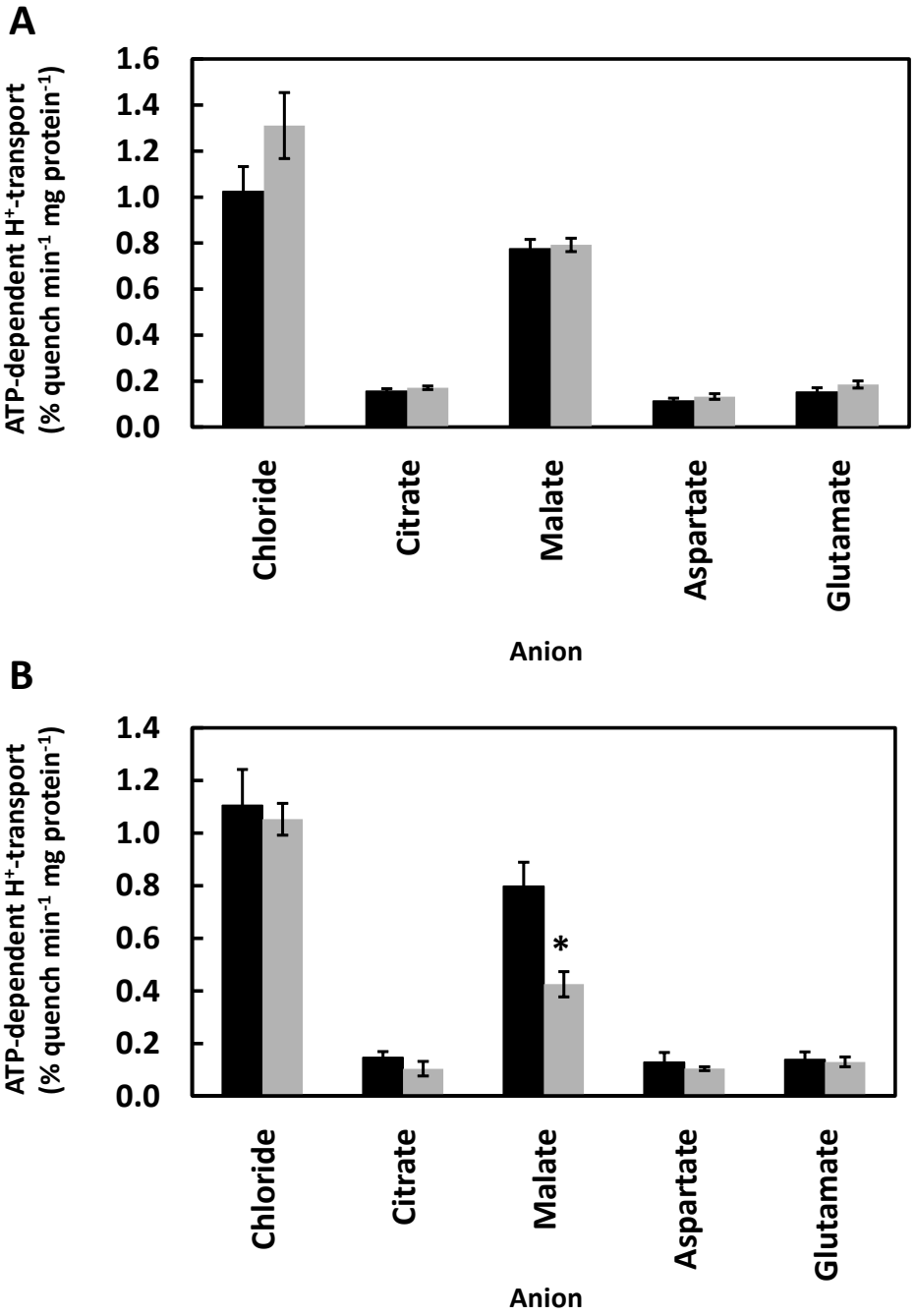

Fig. 5.5. Anion influx determined by ATP-dependent H^+-transport in isolated tonoplasts from the 2-5 introgression line and recurrent parent (M82). Anion influx was determined by ATP-dependent H^+-transport (normalised to ATPase activity) in isolated tonoplasts from 40 DAA (A) and 50 DAA (B) pericarp tissue in the recurrent parent (black) and introgression line 2-5 (grey) using the initial rates of vesicle acidification by monitoring fluorescence quenching of quinacrine. Data is the mean ± SEM where n=5 for 40 DAA and n=4 for 50 DAA. * P≤0.05 (TTest).

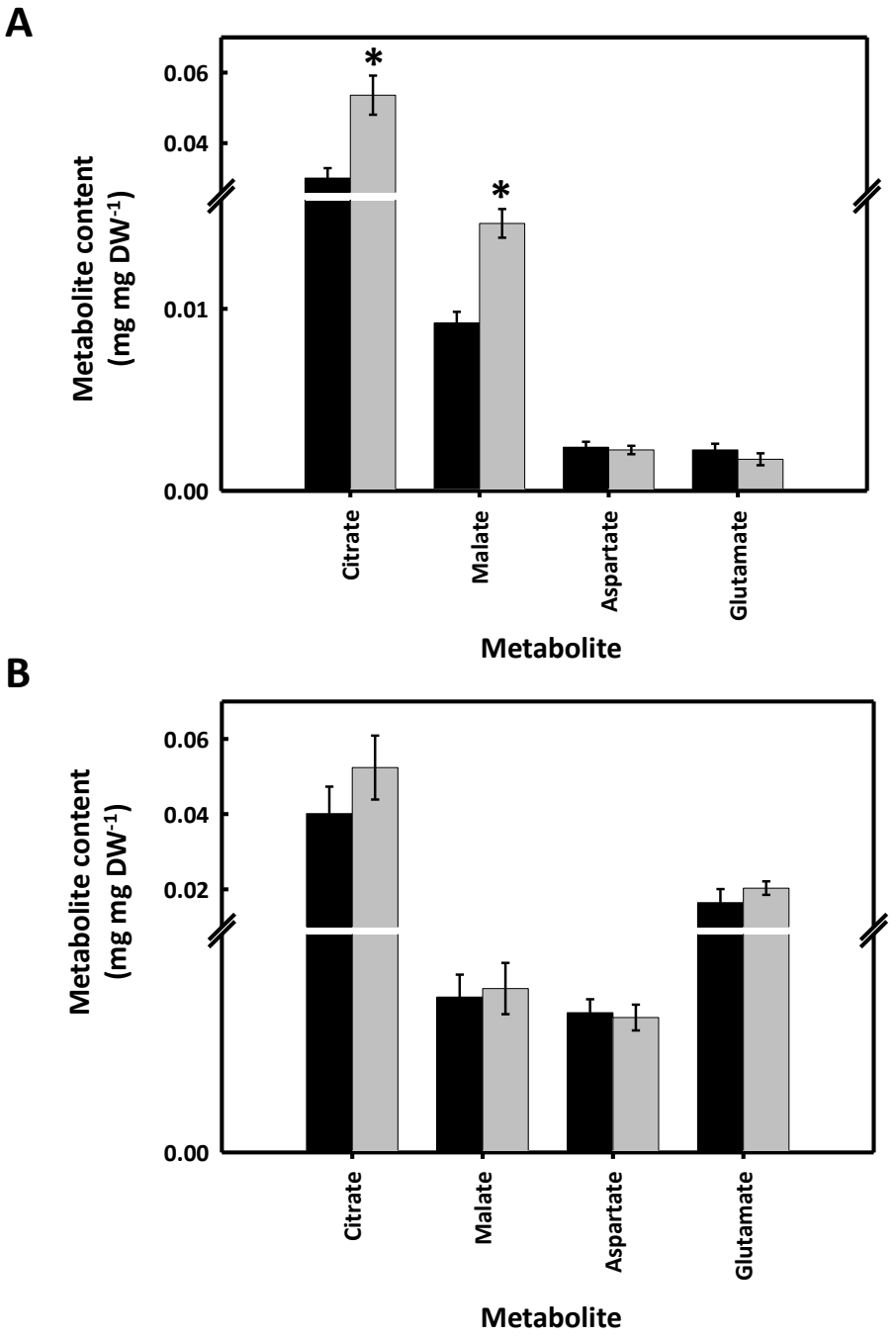

Fig. 5.6. Amino and organic acid content in fruit pericarp tissue of the 2-5 introgression line and M82 parent. Organic and amino acid content was measured enzymatically in pericarp tissue from the M82 parent (black bars) and 2-5 introgression line (grey bars) at 40 DAA (A) and 50 DAA (B). Data presented as mean ± SEM where n=5 for 40 DAA tissue and n=4 for 50 DAA tissue. *=P≤0.05 (TTest).

5.3 Discussion

5.3.1 Malate influx is significantly reduced in the 2-5 line relative to the recurrent parent between 40 DAA and 50 DAA

No conclusion can be made about the relationship between glutamate and aspartate transport across the tonoplast and the accumulation of the respective metabolites (Figure 5.5) because no significant differences were found in glutamate or aspartate content between the recurrent parent and 2-5 introgression line (Figure 5.6). Possible reasons for this are discussed in (Section 6.3.1). It is also worth noting that the H^+-ATPase-dependent transport rates for aspartate and glutamate were very low in comparison to that of citrate and malate which possibly suggests that other transport mechanisms for aspartate and glutamate may be of greater importance.

Citrate content was significantly increased in the 2-5 line at 40 DAA relative to the recurrent parent (Figure 5.6 A), but no significant differences were found at 50 DAA (Figure 5.6 B). However, there was no significant difference between the lines in the rate of ATP-dependent H^+-transport in the presence of citrate (i.e. citrate influx) at 40 DAA or 50 DAA (Figure 5.5). This could suggest an ATPase-independent mechanism of citrate transport, or control of citrate efflux could be more important in controlling the rate of citrate accumulation. This may also explain why the rate of ATPase-dependent citrate influx found in both lines was considerably lower (by approximately 80%) than malate influx even though citrate content in the fruit was greater (between 70-90%) than malate accumulation. Research into citrate influx in tomato tonoplasts identified that citrate influx was ATP-

independent as, although the H^+-ATPase was present and active, it did not affect the rate of citrate influx (Oleski *et al.*, 1987a).

The rate of ATP-dependent H^+-transport in the presence of malate (i.e. malate influx) was not significantly different at 40 DAA between the recurrent parent and 2-5 line (Figure 5.5 A). However, at 50 DAA there was a significant reduction (approximately 50%) in the rate of malate influx in the 2-5 line relative to the recurrent parent (Figure 5.5 B). Malate content at 40 DAA was significantly increased (approximately 60%) in the 2-5 line relative to the recurrent parent (Figure 5.6 A). However, at 50 DAA there were no significant differences between the lines in malate content (Figure 5.6 B). The significant reduction in the rate of malate influx between 40 and 50 DAA could account for the reduced accumulation seen in the 2-5 line from 40 DAA to 50 DAA, resulting in the 2-5 line having comparable malate content as the recurrent parent by 50 DAA. This can be seen more clearly when you observe the accumulation pattern through development (Figure 3.6 B). At 30 and 40 DAA, accumulation of malate is significantly greater than the recurrent parent. Then between 40 and 55 DAA there is a reduction in accumulation in the 2-5 line which then levels by 65 DAA. In the recurrent parent, accumulation of malate at 30 and 40 DAA is significantly less than the 2-5 line. However, between 40 and 55 DAA malate continues to accumulate through to 65 DAA, resulting in comparable malate content as the 2-5 line. The reduction in malate transport can explain the reduced accumulation from 40 DAA in the 2-5 line, however, it does not explain the significantly greater accumulation found at 30 and 40 DAA relative to the recurrent parent. The accumulation at 30 and 40 DAA may still be a due to a transport process (e.g. a metabolite exchanger or efflux transporter) but is not measured in this method. Therefore, further research is required to identify the mechanism

for the significant accumulation found in 2-5 line during early fruit development. However, this does suggest that malate tonoplast transport is involved in the regulation of malate accumulation in the vacuole of tomato fruit during late fruit development.

5.3.2 Summary

The aim of this chapter was to determine if organic and amino acid accumulation in the introgression line 2-5 was due to variations in the rate of anion influx in the vacuole compared to the recurrent parent. No conclusions could be made from data for glutamate, aspartate or citrate. However, the rate of anion influx for malate was significantly reduced in the 2-5 line between 40 and 50 DAA. The reduction in anion influx could account for the concurrent reduction in malate accumulation seen at the same developmental stages. Therefore, malate tonoplast transport could be involved regulating malate accumulation in the vacuole of tomato fruit during late fruit development.

Chapter 6

Use of sub-introgression lines to further define the chromosomal region associated with altered metabolite traits in line IL2-5

6.1 Introduction

Mapping populations formed from introgression lines can be used for the study of quantitative trait loci (QTLs) (Lippman *et al.*, 2007; Fernie and Schauer, 2009). ILs have a number of advantages over other mapping populations such as F_2 populations, backcross mapping populations, double haploids (DHs) and recombinant inbred lines (RILs). For example, ILs are an immortal mapping population unlike F_2 and backcross mapping populations. Once homozygosity is achieved, they can be propagated indefinitely by self-pollination without further segregation and are, therefore, a permanent resource with a characterized genotype. The advantage of an immortal mapping population is that any data obtained from these plants can be replicated and evaluated by several research groups over different locations and years to produce comprehensive phenotype data. This is of value in mapping QTLs as it assists in separating the quantitative trait from environmental variations.

The advantage of ILs over RILs and DHs mapping populations is that these populations must be used in combination with their linkage maps and require statistical analysis of linkage to evaluate a target trait, whereas ILs do not. The other mapping populations tend to segregate simultaneously for multiple QTL that are scattered throughout the genome. Multiple segregating QTLs in a mapping population tend to mask the effects of one another, introduce an epistatic component and generate high variances in statistical analysis. As ILs carry only a single introgressed region containing the QTL they minimise the effects of other QTLs interacting and epistatic effects (Zamir, 2001).

The plants from many other breeding populations, produced from crosses made between divergent genomes, often contain large proportions of wild-germplasm-derived genes that can result in partial sterility (Zamir, 2001). ILs overcome the sterility problems found in other breeding populations as the resulting plants resemble the elite crop variety due to the presence of a single defined introgressed chromosomal segment.

However, a disadvantage of ILs over other mapping populations is that they require approximately ten generations of crossing to develop and therefore take a lot of time and effort to construct (Zamir, 2001; Foolad, 2007). There is also a possibility of linkage drag (when larger than expected fragments are retained during backcross breeding) during construction and are, therefore, not useful for linkage mapping. In addition, the introgressed regions are generally quite large and identification of candidate genes for a trait requires additional sub-introgression lines.

The significant advantages of using introgression lines have led to their construction and use in different species. For example, there are introgression lines available for rice (Li *et al.*, 2005), wheat (Liu *et al.*, 2006), barley (Schmalenbach *et al.*, 2008), pepper (Kargbo

and Wang, 2010) and cucumber (Zhou *et al.*, 2009). However, much of the research using introgression lines in these species are for improvements in crop resistance to diseases or yield-related traits. The use of tomato introgression lines is extensive in the literature and much of which is also related to improvements of yield-related traits. However, tomato ILs have also been used to aid our understanding of metabolism (Fernie and Schauer, 2009). In some cases the use of introgression lines has helped identify the genetics underlying metabolite phenotypes and identify regulatory mechanisms. Examples of this research are detailed below.

The use of metabolic profiling on six ILs containing *S. pennellii* introgressions in *S. lycopersicum* showed that subtle metabolite differences between the ILs could be detected (Overy *et al.*, 2005). Comparison of the fruit metabolite levels in the whole introgression line population (76 lines) containing *S. pennellii* introgressions in a *S. lycopersicum* background to the parent line allowed metabolic differences to be assigned to specific introgressed regions and thus aid characterization of the biochemistry and genetics underlying the phenotypes (Schauer *et al.*, 2006). Many metabolite QTLs were identified including 889 single metabolite QTLs and 326 loci that modify yield-associated traits. Correlation analysis showed that whole-plant phenotypes play a role in the final metabolite composition of the fruit and indicated that this could be a valuable resource for identifying traits that can be used for crop breeding.

Antioxidants present in plants may provide protection against oxidative stresses associated with many human diseases. As such, understanding the genetic factors controlling antioxidant accumulation can aid in improving the nutritional quality in food crops. In this research tomato ILs have been used to identify QTL for nutritional and

antioxidant contents (Rousseaux *et al.*, 2005). Ascorbic acid, lycopene, β-carotene and phenolic content were measured. QTL in two ILs were found to have increased total antioxidant capacity of the water-soluble fraction, one IL with improved phenolic content and one IL with improved ascorbic acid content, although many of these traits were shown to have strong environmental dependency. This suggests that the regulatory control of these compounds is more complex than previously thought. Other research used three mapping populations (ILs containing *S. pennellii* introgressions in *S. lycopersicum*, an advanced backcross population derived from a cross between *S. lycopersicum* and *S. habrochaites*, and a recombinant inbred line derived from a cross between *S. lycopersicum* cv cerasiforme (Cervil) and *S. lycopersicum* cv cerasiforme (Leovil) to identify candidate genes associated with QTLs for ascorbic acid (Stevens *et al.*, 2007). QTLs for ascorbic acid content had been mapped in all three populations previously. A monodehydroascorbate reductase and a GDP-mannose epimerase gene were identified as possible candidate genes that are both known to be involved in ascorbic acid metabolism and therefore could be regulators of ascorbic acid levels.

The research in tomato described here has shown how useful introgression lines are in aiding our understanding of metabolism by linking metabolic phenotypes with specific chromosomal regions. Often the introgressed regions are large containing hundreds of genes (Eshed and Zamir, 1994). Using overlapping ILs, it is possible to narrow the chromosomal region and thus reduce the number of genes in which to identify possible candidates. Narrowing the chromosomal region involves identifying if the trait of interest is associated with two overlapping ILs. If so, then that trait must relate to the chromosomal region where the two lines overlap. For example, if the trait of interest is associated with

both introgression line 2-5 and the overlapping introgression line 2-6, then the trait must relate to the region (or bin) designated as 2-K (Figure 6.1). If however, the trait was only associated with introgression line 2-5 and not the overlapping introgression lines (lines 2-3, 2-4 and 2-6), then that trait would relate to region 2-J. Using this technique, the aim of this chapter was to utilize overlapping and sub-introgression lines to further define the chromosomal region associated with altered metabolite traits found in the tomato introgression line 2-5.

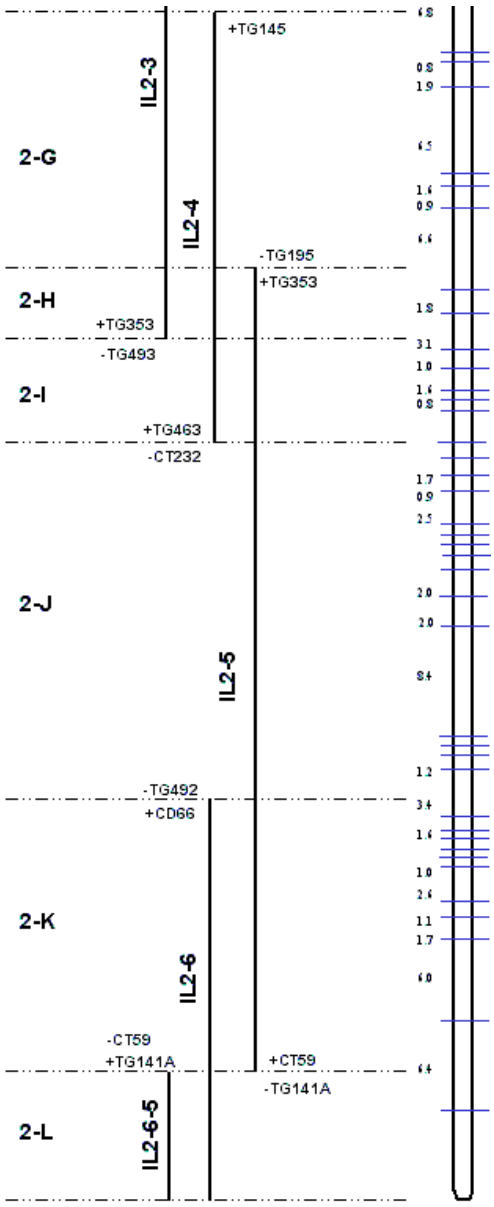

Fig. 6.1. Chromosome 2 Introgression Line Map. Schematic showing regions where introgression lines are mapped to Chromosome 2. Introgressed segments shown as solid bars where the boundary edge of each segment is indicated by inclusive (+) and exclusive (-) RFLP markers. Bins are designated by the chromosome number followed by a capital letter and indicate a unique area of IL overlap (i.e. 2-J). The genetic distances (in cM) are indicated to the left of the chromosome (Tanksley *et al.*, 1992). Adapted from the SOL Genomics Network website http://solgenomics.net/maps/pennellii_il/chr2.pl.

6.2 Results

6.2.1 Increased content of malate, citrate, aspartate and glutamate in tomato map to chromosomal regions 2-K and 2-J

The introgression lines and sub-lines (used in Section 6.2.2) were genotyped by Laurent Grivet's lab, Syngenta (France) (Appendix V and VI) and were shown to be correct based on the mapping information supplied by Dani Zamir's lab with the lines.

The aim of the research was to map the specific traits of increased organic acids (i.e. malate and citrate) and amino acids (i.e. aspartate and glutamate) to chromosomal regions using the introgression line 2-5 and introgression lines that overlap with 2-5 (i.e. lines 2-4 and 2-6) (Figure 6.1). To this end, the content of these metabolites in the introgression line 2-5 and its overlapping introgression lines was quantified relative to the metabolite content of the recurrent parent line M82 using ^{1}H NMR (Figure 6.2 A) and HPLC (Figure 6.2 B). The malate and citrate content were significantly increased in line 2-5 but not increased in lines 2-4 and 2-6 relative to M82 (Figure 6.2 A). The traits were not present in line 2-4 and 2-6, therefore the regions 2-I and 2-K, where these lines overlap with line 2-5, were excluded (Figure 6.2 C). Thus, the traits of increased malate and citrate content were found to map to region 2-J. The aspartate and glutamate content were significantly increased in line 2-5 and the overlapping introgression line 2-6 but there was no significant difference in line 2-4 relative to M82 (Figure 6.2 B). The traits were not present in line 2-4, therefore the region 2-I, that overlaps with line 2-5, was excluded (Figure 6.2 C). The aspartate and glutamate content was increased in both line 2-5 and 2-6, therefore the trait was found to map to region 2-K where the 2-5 and 2-6 introgression lines overlap.

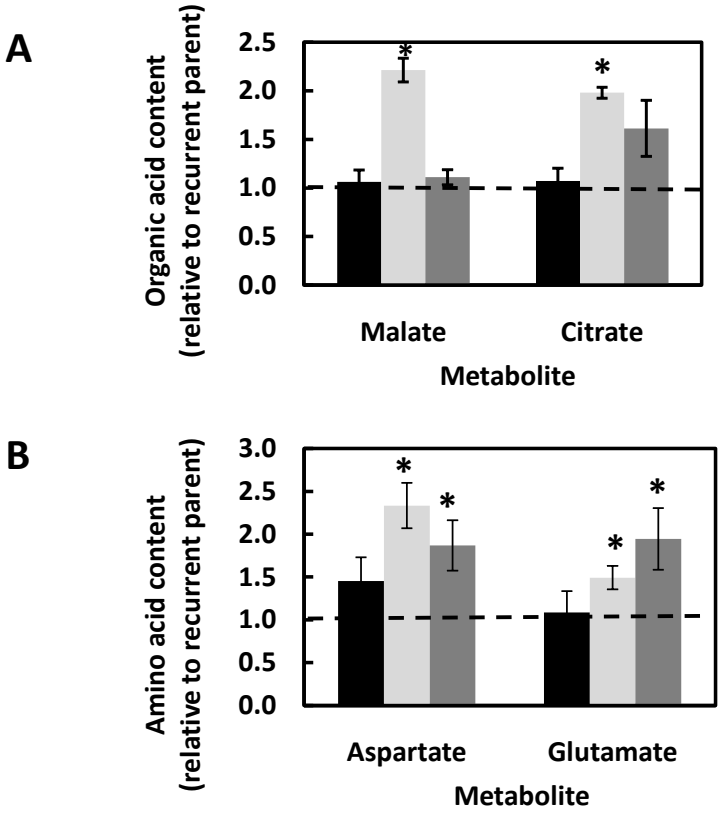

Metabolite	IL2-6	IL2-5	IL2-4	Genetic region
Malate	-	+	-	2-J
Citrate	-	+	-	2-J
Aspartate	+	+	-	2-K
Glutamate	+	+	-	2-K

Fig. 6.2. Mapping of Introgression Lines. Metabolite content was determined in 40 DAA pericarp tissue of introgression lines 2-4 (black bars), 2-5 (light grey bars) and 2-6 (dark grey bars) relative to the recurrent parent line (M82) using ^{1}H NMR (A) and HPLC (B). Data is presented as the ratio of the means of 2-4, 2-5 and 2-6 to M82 ± SEM (n=6). Dashed line indicates a ratio of 1. *P≤0.05 (TTest). (C) Simplified scheme of Figures A and B. Table shows significant differences of relative organic and amino acid content in lines IL2-4, IL2-5 and IL2-6 40DAA pericarp tissue to recurrent parent line (M82). '+' indicates significant difference; '-' indicates no significant difference.

6.2.2 Fine mapping of the increased aspartate and glutamate traits using sub-introgression lines

Lines with sub-introgressions within the 2-5 region were obtained from Dani Zamir (The Hebrew University of Jerusalem, Israel) and grown in two different batches in the glasshouses at the Department of Plant Sciences, Oxford. The lines were grown in two different batches due to space limitations. Batch A consisted of the recurrent parent line, line 2-5 and sub-introgression lines 4603, 4753, 4637 (Figure 6.4). Batch B consisted of the recurrent parent line, line 2-5 and sub-introgression lines 4178, 4176, 4625, 4690 and 4648 (Figure 6.4). Metabolite content in the lines was determined enzymatically and expressed relative to the recurrent parent line.

The glutamate content relative to the recurrent parent of lines in Batch A was significantly increased for line 2-5, significantly decreased for sub-line 4753 but not significantly different for sub-lines 4603 and 4637 (Figure 6.3 A). The relative glutamate content of lines in Batch B was significantly increased for line 2-5 and sub-lines 4176 and 4648 (Figure 6.3 B). No significant difference was found in sub-lines 4178, 4625 and 4690. Based on the overlapping regions of the 2-5 sub-lines, increased relative glutamate content in the sub-line 4176 supports the mapping to the genetic region 2-K in the 2-5 introgression line mapping (Section 6.2.1; Figure 6.2 C and 6.4). The pattern of overlap between 4603 (no change), 4176 (increased) and 4178 (no change) sub-lines suggests that the very small region between 118.0 - 118.5 cM (shown boxed in grey; Figure 6.4) could be responsible for the increased glutamate. However, the mapping is not completely clear cut because 4753 sub-line shows a significant decrease and there is no change in the overlapping (but large) 4637 sub-line. An increase in sub-line 4648 was also found which lies in the region 2-I and

was previously excluded in the 2-5 introgression line mapping (Section 6.2.1; Figure 6.2 C and 6.4).

The aspartate content relative to the recurrent parent in Batch A was not significantly increased for any of the lines, including line 2-5 (as had been previously established), and therefore none of the Batch A lines were included in the analysis (Figure 6.5 A). The relative aspartate content of lines in Batch B was significantly increased for line 2-5 and sub-lines 4176 and 4648 (Figure 6.5 B). No significant difference was found in sub-lines 4178, 4625 and 4690. Based on the overlapping regions of IL2-5 sub-lines, the increased relative aspartate content in the sub-line 4176 supports the mapping to the genetic region 2-K (Section 6.2.1; Figure 6.2 C and 6.6) and may indicate that the same 118.0 - 118.5 cM region linked to increased glutamate is involved. However, for aspartate, the data for 4603 sub-line could not be used (because there was not a reliable change in aspartate in the 2-5 line for this batch) so the region is less well defined (shown boxed in grey). Similar to glutamate, there is an increase in sub-line 4648 found in the region 2-I which has previously been shown to make no contribution to amino acid accumulation (Section 6.2.1; Figure 6.2 C), as found with increased glutamate.

The malate content relative to the recurrent parent was significantly increased in sub-lines 4753 and 4637 in Batch A plants (Figure 6.7 A). However, no significant difference was found in lines 2-5 and 4603. As no significant difference was found in the relative malate content in line 2-5 (as had been previously established) the lines in Batch A were not included in the analysis. The relative malate content was significantly increased in line 2-5, 4176, 4625, and 4690 of Batch B (Figure 6.7 B). No significant difference was found in lines 4178 and 4648. Based on the overlapping regions of IL2-5 sub-lines, the increased relative

malate content in the sub-lines 4690 and 4625 supports the mapping to the genetic region 2-J (Section 6.2.1; Figures 6.2 C and 6.8) and indicating that the candidate region could be in the overlap of these two sub-lines, narrowing the 2-J region further. Combined with the information that line 2-4 shows no increase in malate, one could highlight the region between 87.5 - 111.8 cM (boxed in grey). However, there is also a significant increase in the sub-line 4176 which lies in the 2-K region that had previously been excluded for the trait (Section 6.2.1; Figure 6.2 C).

The citrate content relative to the recurrent parent was significantly increased in line 2-5 and in sub-lines 4603 and 4637 in Batch A plants (Figure 6.9 A). No significant difference was found in sub-line 4753. The relative citrate content was significantly increased in line 2-5, and in all of the sub-lines (4178, 4176, 4625, 4690 and 4648) of Batch B (Figure 6.9 B). Based on the overlapping regions of IL2-5 sub-lines, the increased relative citrate content in the sub-lines 4690, 4625 and 4637 supports the mapping to the genetic region 2-J (Section 6.2.1; Figure 6.2 C) and indicating that the candidate region is in the overlap of these three sub-lines, narrowing the 2-J region further. However, there is a significant increase in sub-line 4648 which would discount this hypothesis and would suggest the trait would be found in the region where sub-lines 4648, 4690, 4625 and 4637 overlap, in region 2-I between 78 cM and 83.10 cM. Again, this is a region that was previously excluded for the increased citrate content (Section 6.2.1; Figure 6.2 C). Also, there are significant increases in the sub-lines 4603, 4176 and 4178, but not in sub-line 4753, in region 2-K which had previously been excluded from the trait (Section 6.2.1; Figure 6.2 C). Therefore, for the purposes of mapping, it is not possible to use the sub-lines to further narrow down the region 2-J for increased citrate content (Figure 6.10).

In summary, data from the sub-line mapping for aspartate and glutamate suggests there may be a key 0.5 cM region (118-118.5 cM) in introgression line 2-5 that is linked to increased glutamate and aspartate. Relative metabolite data for each of the amino acids used for mapping displayed a similar pattern in that sub-line 4648 in the 2-I region and sub-line 4176 in the 2-K region contained increased levels of these metabolites and there are no increases in the other sub-lines for both amino acids. The sub-line 4648 is very interesting, because although it occurs in the 2-4 region that had previously been discounted with respect to glutamate and aspartate, the increases in these amino acids were substantially larger than in 2-5, 2-6 or any of the other sublines. Therefore, the 0.5 cM and 4648 regions will be looked at in further detail by extracting gene annotation data from the SOL Genomics website (Mueller *et al.*, 2005) to identify possible candidate genes responsible for the increased metabolite content seen in these lines.

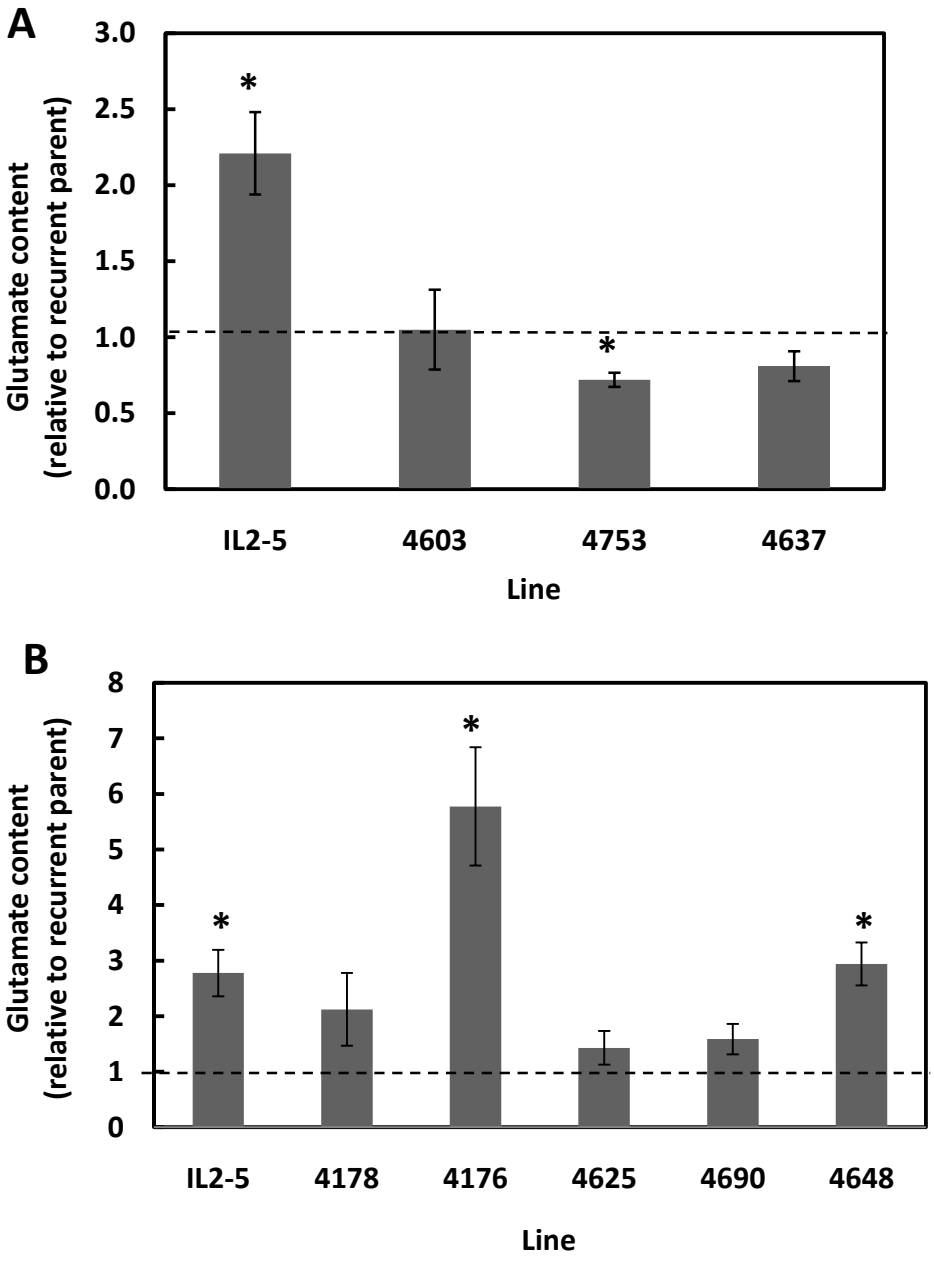

Fig. 6.3. Relative glutamate content in 40DAA pericarp tissue from fruit grown in two batches (A and B) plants to recurrent parent line (M82). Values are mean of six replicates ± SEM except for M82 of Batch A where values are mean of seven replicates ± SEM and for line 4648 of Batch B where values are mean of five replicates ± SEM. *significant (TTest, $P<0.05$).

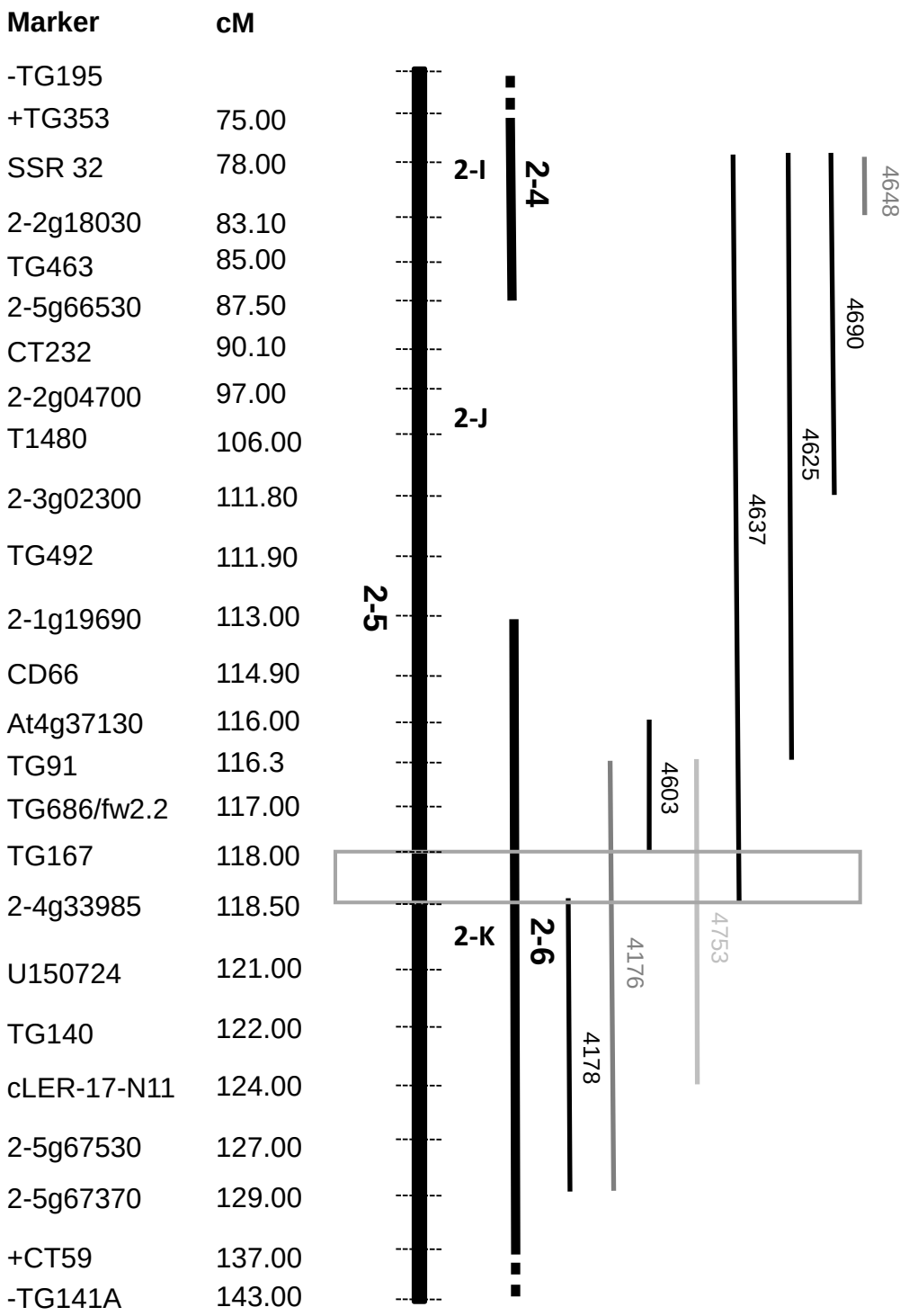

Fig. 6.4. Scheme of sub-line mapping for glutamate. Dark grey=lines significantly increased, light grey=lines significantly decreased, black=no change, grey box=region where 2-5 line was mapped to using IL2-5 overlapping lines.

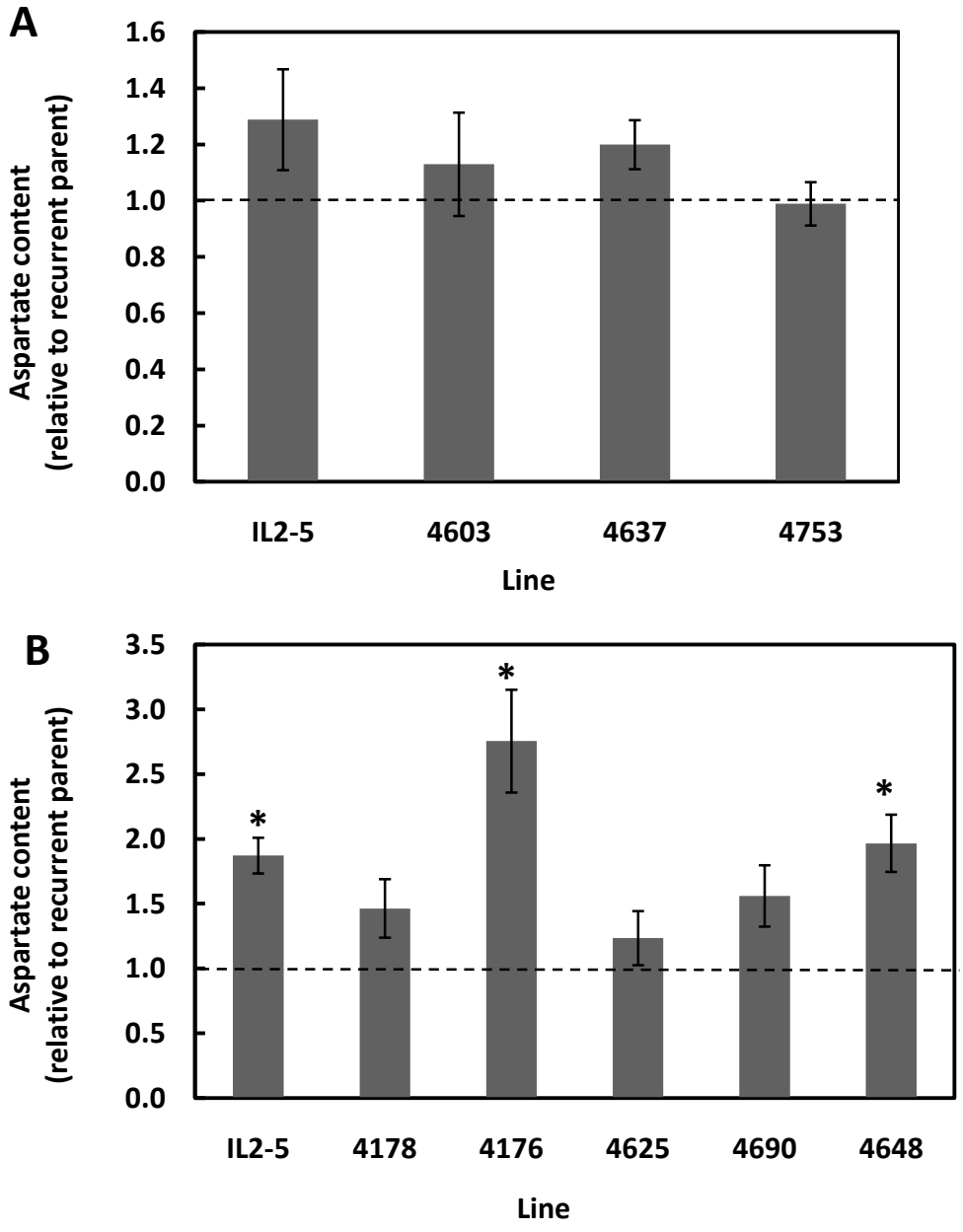

Fig. 6.5. Relative aspartate content in 40DAA pericarp tissue from fruit grown in two batches (A and B) of plants to recurrent parent line (M82). Values are mean of six replicates ± SEM except for M82 where values are mean of seven replicates ± SEM. *significant (TTest, P<0.05).

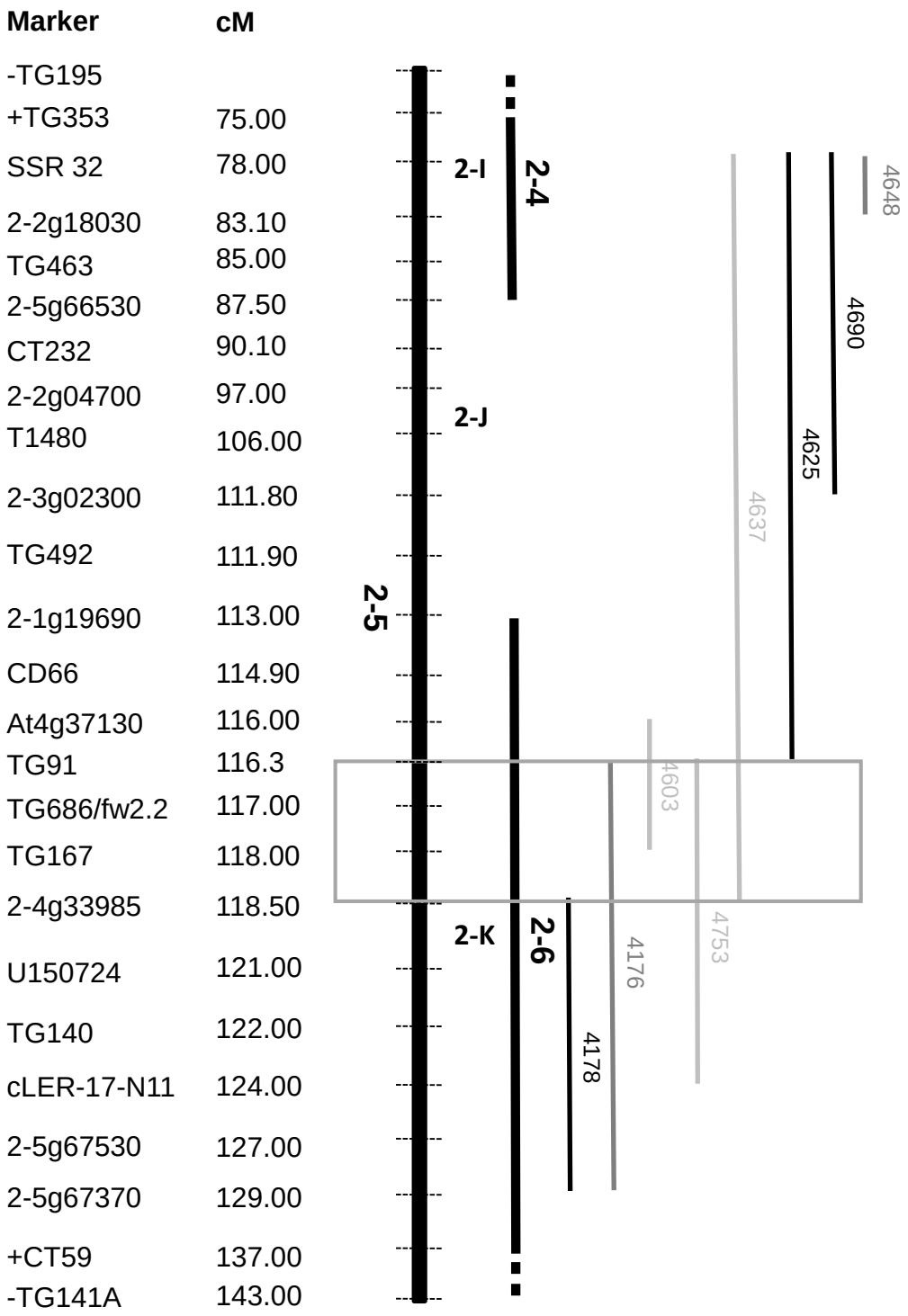

Fig. 6.6. Scheme of sub-line mapping for aspartate. Dark grey=lines significantly increased, light grey=lines where data cannot be used, black=no change, grey box=region where 2-5 line was mapped to using IL2-5 overlapping lines.

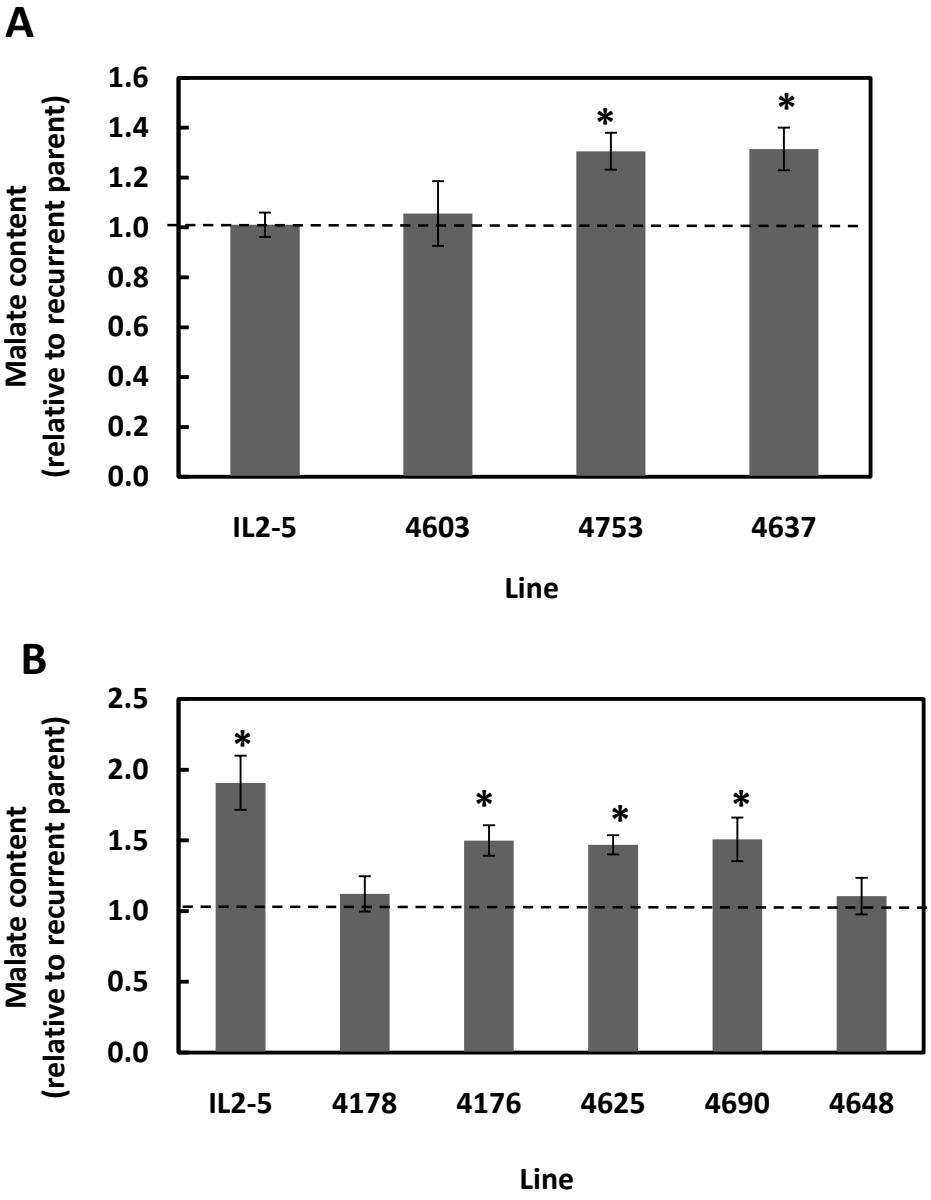

Fig. 6.7. Relative malate content in 40DAA pericarp tissue from fruit grown in two batches (A and B) of plants to recurrent parent line (M82). Values are mean of six replicates ± SEM except for M82 where values are mean of seven replicates ± SEM. *significant (TTest, P<0.05).

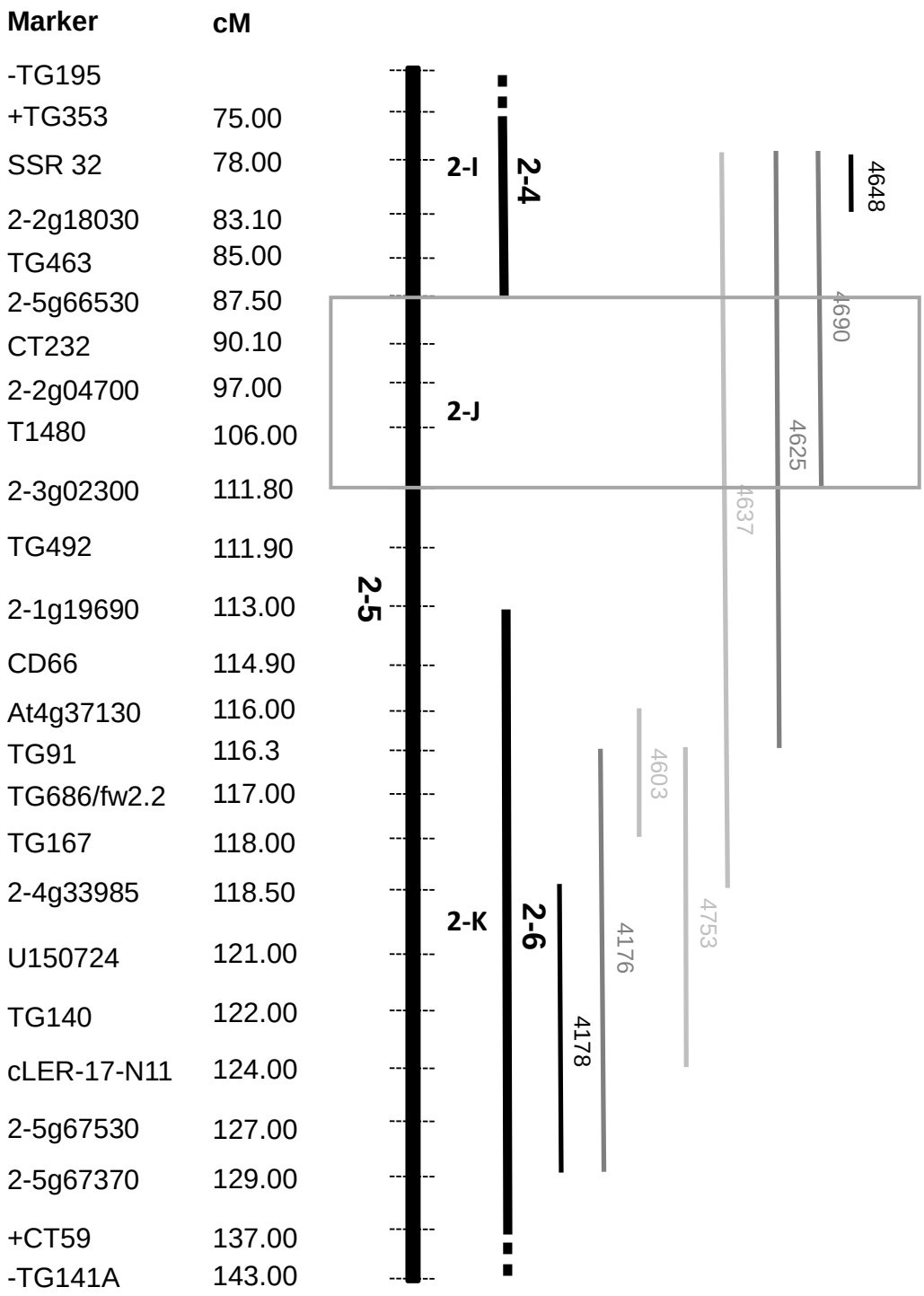

Fig. 6.8. Scheme of sub-line mapping for malate. Dark grey=lines significantly increased, light grey=lines where data cannot be used, black=no change, grey box=region where 2-5 line was mapped to using IL2-5 overlapping lines.

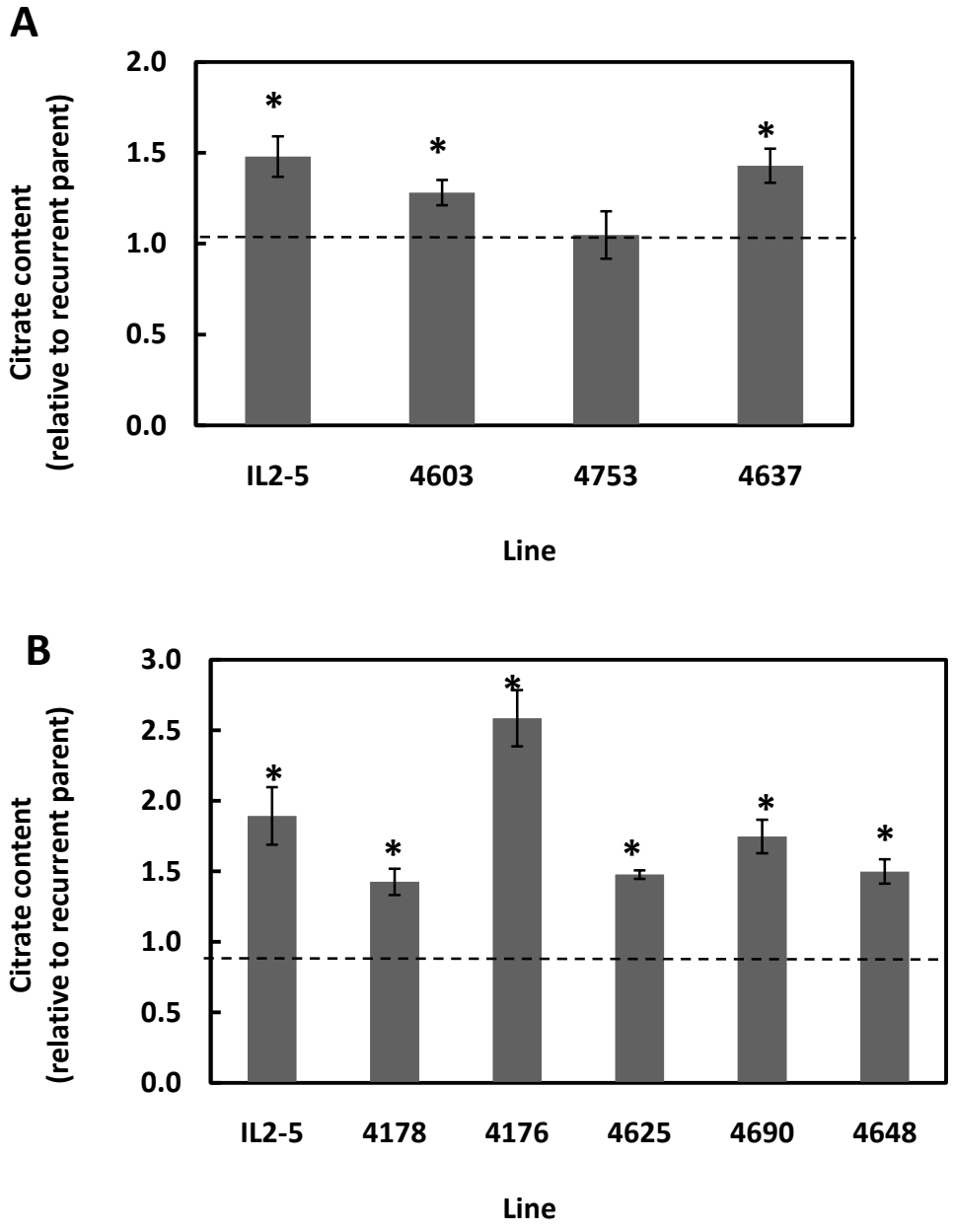

Fig. 6.9. Relative citrate content in 40DAA pericarp tissue from fruit grown in two batches (A and B) of plants to recurrent parent line (M82). Values are mean of six replicates ± SEM except for M82 in Batch A where values are mean of seven replicates ± SEM and 4648 in Batch B where values are mean of five replicates ± SEM. *significant (TTest, P<0.05).

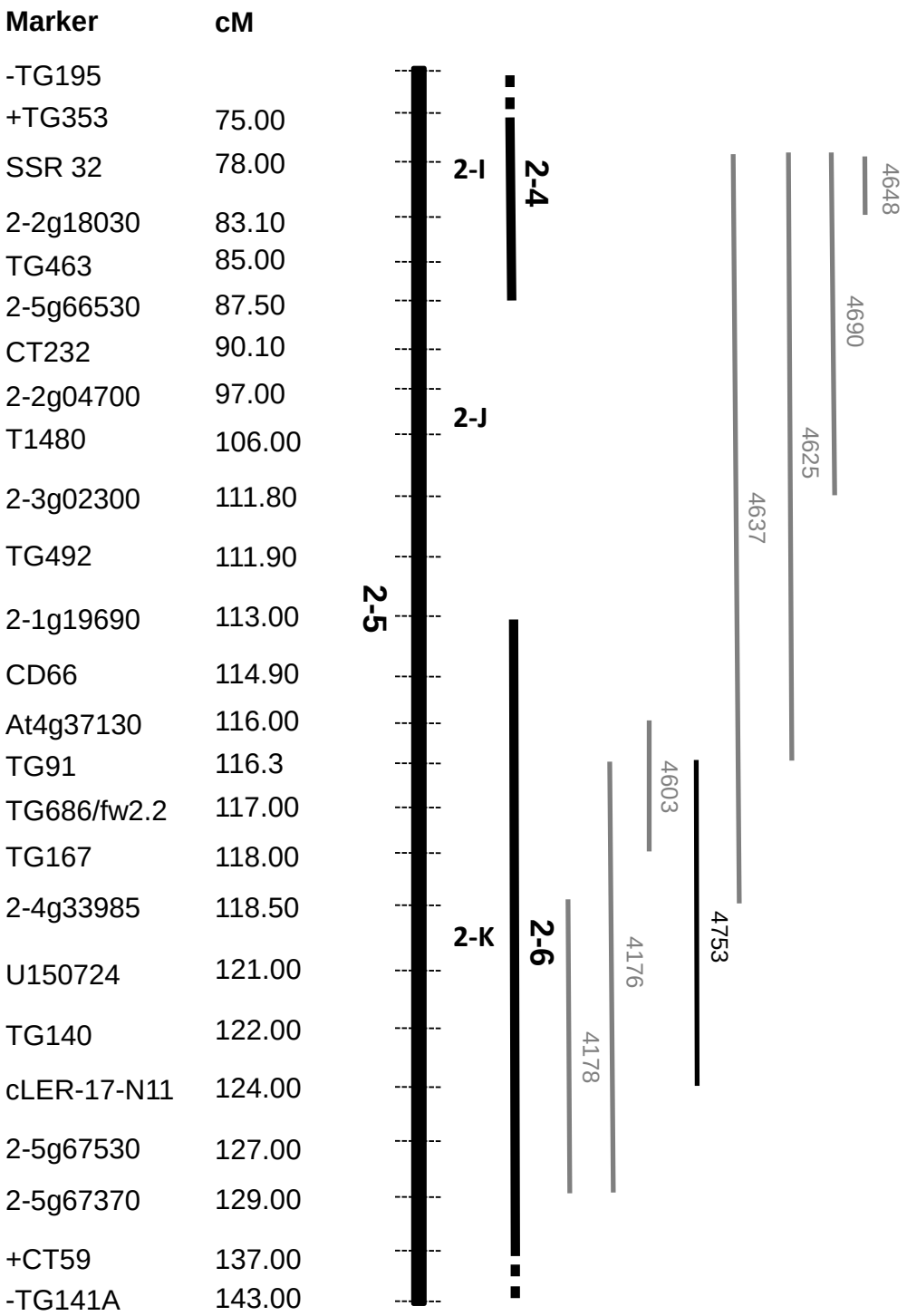

Fig. 6.10. Scheme of sub-line mapping for citrate. Dark grey=lines significantly increased, black=no change.

6.2.3 Candidate genes in the 4648 and 0.5 cM region

Based on the results in Sections 6.2.1 and 6.2.2 gene annotation data was extracted from the SOL Genomics Network website (Mueller *et al.*, 2005) for specific chromosomal regions that appear to be associated with the metabolite traits. Data was extracted for a 1 cM region spanning chromosome 2 from 118.0-119.0 cM between markers TG167 and 2-4g33985 and a 5.1 cM region from 78.0 to 83.1 cM between markers SSR 32 and 2-2g18030. Due to a change in the placement of markers provided in the EXPEN-2000 map for the gene annotation data the 0.5 cM region covered a 1 cM region but will still be referred to here as a 0.5 cM region for consistency.

Although the aim of the research here was to identify candidate genes, both regions, and especially the 4648 region, are still very large containing many genes. Moreover, many of the genes are still not annotated or are of unknown function. Also, the genes extracted for the 0.5 cM region actually spans a 1 cM region and it is not possible to identify which genes lie within the area of interest or outside. Therefore, it is not possible to reliably identify candidate genes for the metabolite changes found in the introgression lines. However, a few genes have been isolated from the list that could potentially affect organic and amino acid accumulation and will be used for further discussion.

In the 0.5 cM region, between markers TG167 and 2-4g33985, a total of 49 genes were found (Table 1, Appendix VII). Of these 49 genes, 8 were not annotated, 12 were unknown or unnamed and 14 were predicted or hypothetical proteins. Of the remaining 15, there were mostly genes involved in stress or stress signalling, ATP synthesis or plant defence. Within these 15 genes, three that could be possible candidates for altered organic

and amino acid levels, were annotated as ATPase beta subunits (SGN-U200563, SGN-U212238 and SGN-U295324) (see Section 6.3 Discussion).

In the 4648 region, that spanned a 5.1 cM between markers SSR 32 and 2-2g18030, a total of 413 genes were found (Table 2, Appendix VII). Of these 413 genes, 76 were not annotated, 137 were unknown or unnamed and 90 were predicted or hypothetical proteins. The remaining 110 genes were generally involved in protein transport, protein degradation, stress and plant defence, RNA degradation and processing, photosynthesis, and flavanoid biosynthesis. Within these 110 genes an NAD^+-dependent isocitrate dehydrogenase (SGN-U567746) and two vacuolar sorting proteins (SGN-U201944 and SGN-U285261) have been identified as possible candidates from this region (see Section 6.3 Discussion).

6.3 Discussion

6.3.1 Introgression lines are subject to environmental interactions

Introgression line 2-5 grown in Batch A (shown in Figures 6.5 A and 6.7 A) with the sub-lines did not show an increase in aspartate or malate relative to the recurrent parent line as had been shown previously (Chapter 3). Material for this experiment was grown under the same conditions as the plants in Batch B (Figures 6.5 B and 6.7 B) and plants used for the mapping of the introgression lines (Section 6.2.1) and fruit from all of these plants did have increased aspartate and malate content. The introgression lines and sub-lines were genotyped by Laurent Grivet's lab (Appendix V and VI) and were shown to be correct based on the mapping information supplied by Dani Zamir's lab with the lines. Six replicates for both the 2-5 line and the recurrent parent were used for the experiments, plants were

grown in a controlled greenhouse environment and in a randomized planting scheme to minimise environmental influences. However, the reasons for lack of increases in aspartate and malate (Figures 6.5 A and 6.7 A) must be due to environmental interactions. As discussed in Section 3.3.1, environmental interactions do affect the metabolite content as seen when lines grown in the field are compared with those grown in the greenhouse. Although the increases in aspartate and malate were consistently around 2-fold relative to the recurrent parent line, this is not a huge increase. Therefore, any environmental influences could easily alter the levels even slightly to make these changes insignificant. A possible explanation of the source of environmental variation may have been from differing feeding and/or watering regimes between different batches of plants. The lighting may have been another source of variation. Although the greenhouse was lit using natural light with supplementary lighting to maintain a fixed irradiance, the ratio between the light sources could be a possible environmental influence as this would change during different months of the year. Also, the temperature fluctuations during the year could affect growing conditions. Again, the temperature conditions within the greenhouse are controlled to set temperatures, but very hot summer days and very cold winter nights would still have a seasonal effect.

6.3.2 Mapping in the sub-lines shows that the levels of the four main organic and amino acids in tomato are under multiple regulatory control

The introgression line mapping in Section 6.2.1 showed that for glutamate and aspartate the region 2-I (the overlap between line 2-4 and 2-5) was excluded. However, for the sub-line 4648, lying in the 2-I region, was shown to contain the traits of increased

glutamate and aspartate. The 4648 region is a 5.1 cM region that overlaps with the much larger sub-lines 4690, 4625 and 4637. During the mapping for increased glutamate and aspartate none of these sub-lines were shown to contain the traits for those lines (where data could be obtained). The candidate regions identified for the traits were instead linked to the 2-K region where the 2-5 and 2-6 introgression lines overlap. A possible explanation for this anomaly could be due to epistatic interactions where epistasis is defined as an interaction between non-allelic genes, especially where one gene suppresses the expression of another (Causse *et al.*, 2007). The introgression lines (but not the sub-lines) have been analysed for epistatic interactions (Eshed *et al.*, 1996; Causse *et al.*, 2007). It was found that epistatic interactions do occur even though introgression lines generally have minimal epistasis compared to other mapping populations (Zamir, 2001). Epistatic interactions may explain why region 4648 shows increased glutamate and aspartate but the larger sub-lines 4690, 4625 and 4637 in the same chromosomal region don't show these traits. The gene(s) responsible for increased glutamate and/or aspartate could be masked within the sub-lines containing larger introgressed segments (i.e. sub-lines 4690, 4625 and 4637) by the expression of other genes contained in those segments. However, in the 4648 sub-line, where the insertion is much smaller, those interacting genes may not be present, and therefore, there is no masking, resulting in the trait being present.

Epistasis also seems to be occurring within the 4176 sub-line for glutamate and aspartate where the interaction tends to be additive. Increased glutamate relative to the recurrent parent in this sub-line is approximately 6-fold compared to the 2.5-fold relative glutamate content in the 2-5 line. For aspartate there is a slight additive interaction in the 4176 line where the content is almost 3-fold in the sub-line but only 2 fold in the 2-5 line.

Citrate and malate mapped to the chromosomal region 2-J using introgression lines that overlapped with the 2-5 line (Figure 6.2). However, it was not possible to narrow down the genetic region further using data generated from the sub-lines for mapping increased citrate and malate at the breaker stage (Figures 6.7 to 6.10) as the majority of the sub-lines showed increases, especially for citrate.

The pattern of widespread increases seen in almost all of the sub-lines for malate and citrate content and the epistatic interactions shown in the sub-lines for glutamate and aspartate is suggestive of multiple genes controlling the regulation of these metabolites within the 2-5 chromosomal region. This is supported by research in *Arabidopsis* where large scale metabolomic analysis was combined with QTL analysis of metabolic traits to investigate QTLs that influence the metabolome (Rowe *et al.*, 2008). In this research, it was found that frequent epistatic interactions controlled a majority of the metabolic variation and it was suggested that the *Arabidopsis* metabolome is organized into epistatically interacting clusters that regulate central metabolism. Although further research is required to verify these findings, what this research does suggest is that central metabolic pathways could be regulated by a number of genetic loci which frequently interact.

6.3.3 Candidate genes in the 4648 and 0.5 cM region

Although the results here showed that it was not possible to reliably identify candidate genes for the metabolite changes found in the introgression lines a few genes have been selected from the two regions for further discussion as likely candidates.

In the 0.5 cM region between markers TG167 and 2-4g33985 there were three genes that could be possible candidates from this region. These were annotated as ATPase beta

subunits (SGN-U200563, SGN-U212238 and SGN-U295324). Plant vacuoles are acidic relative to the cytosol and are generally around pH 5.0-5.5 (Buchanan *et al.*, 2000). Proton pumping across the vacuolar membrane (or tonoplast) helps to regulate the pH of this compartment and energises the membrane enabling carrier-mediated transport of ions. Proton pumping is achieved through the activity of vacuolar ATPases (V-ATPases). V-ATPases consist of a V_1 domain, responsible for ATP hydrolysis, and a V_0 domain, responsible for proton translocation and forms the membrane spanning pore. Linked together, these complexes can couple ATP hydrolysis to proton translocation across the vacuolar membrane. The V_1 complex is organised into multiple subunits including a beta subunit, that contains the regulatory substrate-binding site, and an alpha subunit, that contains the catalytic substrate-binding site. Changes to the activity of the V-ATPase will subsequently affect the acidification and membrane potential of the vacuole and therefore, the ability of the vacuole to transport ions and possibly organic and amino acids stored in the vacuole. For example, in yeast, site-directed mutagenesis of the VMA2 gene encoding the V-ATPase B-subunit (Vma2p) (the catalytic subunit) resulted in loss of proton transport and a reduction in V-ATPase activity in the vacuole (Liu *et al.*, 1996).

In the 4648 region that spanned a 5.1 cM between markers SSR 32 and 2-2g18030 there were three possible candidates from this region. These were annotated as an NAD^+-dependent isocitrate dehydrogenase (SGN-U567746) and two vacuolar sorting proteins (SGN-U201944 and SGN-U285261). NAD^+-dependent isocitrate dehydrogenase (NAD-ICDH) participates in the TCA cycle by catalyzing the oxidative decarboxylation of isocitrate producing 2-oxoglutarate and carbon dioxide while converting NAD^+ to NADH. As such changes in the activity of NAD^+-ICDH can directly affect the levels of the TCA cycle

intermediates citrate and malate. Changes in NAD-ICDH levels can also alter levels of glutamate and aspartate. Glutamate and aspartate are derived from 2-oxoglutarate and oxaloacetate (derived from malate), respectively, and 2-oxoglutarate is also required by the glutamine synthetase/glutamate synthase cycle to assimilate ammonium. This has been shown by research in tomato using transgenic plants with reduced NAD-ICDH activity by antisense inhibition (Sienkiewicz-Porzucek *et al.*, 2010). These transgenic plants showed decreased levels of malate and glutamate compared to control plants. However, there was no change in NAD-ICDH activity in the 2-5 line. This may be because the enzyme might have altered kinetics (like the invertase (Fridman *et al.*, 2004)) which would not be detected in the enzyme activity that only measures maximum catalytic activity (e.g. could have a change in K_m but the same V_{max}).

All proteins contained within the tonoplast membrane, including the transporters involved in the uptake of organic and amino acids, must first be synthesised and then delivered to the tonoplast membrane for integration. Sorting of vacuolar proteins is essential in order for the transportation of these integral membrane proteins to get to the correct vacuole from their site of synthesis. A possible hypothesis is that organic and amino acid uptake is regulated by the numbers of transporters present in the membrane (rather than by tonoplast transporter activity or some other mechanism) therefore, any disruption or changes in the pathway from the site of synthesis to tonoplast membrane integration would therefore be crucial. Most vacuolar membrane proteins are synthesised in the endoplasmic reticulum and travel through the Golgi apparatus where they are sorted away from proteins destined for the cell surface (Marty, 1999). They then exit the Golgi and enter the *trans*-Golgi Network where proteins destined for exocytosis are sorted from vacuolar

proteins. Vacuolar proteins then go to another intermediate compartment referred to as the prevacuolar compartment (PVC) and then via the late biosynthetic vacuolar pathway or via an autophagic vesicle to the vacuole. However, it is not clear if tonoplast transporter proteins follow this route or what regulates the transport of these proteins in the different compartments or the vacuolar sorting proteins involved.

6.3.4 Summary

The aim of this chapter was to utilize overlapping and sub-introgression lines to further define the chromosomal region associated with altered metabolite traits found in the tomato introgression line 2-5. Use of the overlapping introgression lines narrowed the increased citrate and malate trait to the chromosomal region 2-J and the increased glutamate and aspartate trait to the region 2-K. Fine mapping, using the sub-introgression lines, suggested a key 0.5 cM region and the region spanning the sub-line 4648 for glutamate and aspartate traits. However, it was not possible to reliably identify candidate genes for the metabolic changes from gene annotation data although a few likely candidates were identified. In addition, epistatic interactions were shown to occur in the sub-lines for these amino acid traits. For the increased citrate and malate traits it was not possible to narrow down the 2-J region due to widespread increases in the sub-lines. Collectively, the results of the fine mapping suggest that multiple genes control the regulation of these metabolites.

Chapter 7

General discussion

In this thesis, the mechanisms involved in the regulation of organic and amino acid accumulation during tomato fruit development was investigated using an introgression line (2-5) from a tomato population of *S. Lycopersicum* containing genomic introgressions from *S. pennellii*. Line 2-5 had previously been shown to accumulate greater amounts of glutamate, aspartate and isocitrate in ripe fruit relative to the recurrent parent when grown in the field (Schauer *et al.*, 2006). Grown in our greenhouse conditions, this line showed increases in fruit citrate, malate, glutamate and aspartate at the 40 DAA developmental stage. Line 2-5, with altered metabolite levels, enabled investigation of both the underlying genetic and metabolic differences responsible for the accumulation of organic and amino acids.

7.1 Multigenic control of metabolism

The analysis of metabolite traits in overlapping introgression lines to line 2-5 was used to link the phenotypic trait to specific smaller chromosomal regions. Increased citrate and malate was linked to the smaller chromosomal region 2-J and increased glutamate and

aspartate to the smaller 2-K region. Analysis of metabolite traits in the sub-introgression lines revealed a pattern of widespread increases in all of the sub-lines for citrate and malate content and epistatic interactions for aspartate and glutamate suggestive of multiple genes controlling these metabolites. Research in *Arabidopsis*, has demonstrated the multigenic nature of genotype-metabolite associations. Links between genotype and metabolite levels were made using genome-wide association mapping and each metabolite was shown to have a significant association with an average of at least 14 genes and that these genes are normally found as clusters around the same loci (Chan *et al.*, 2010a; Chan *et al.*, 2010b).

The majority of phenotypes found in organisms are controlled by multiple genes (i.e. multigenic) rather than by single genes (i.e. monogenic) (Glazier *et al.*, 2002; Koornneef *et al.*, 2004; Lippman and Zamir, 2007; Chan *et al.*, 2010a). This is partly due to multiple cellular compartments and membrane transport involved in the biochemical steps for the synthesis, transportation and accumulation of these metabolites (Buchanan *et al.*, 2000). The regulation and genetic control would therefore need to encompass these attributes. Also, in addition to the metabolites biosynthetic structural genes there are additional regulatory genes that could alter metabolite levels (e.g. transcription factors, kinases and 14-3-3 proteins). Transcription factors have been shown to control the expression of some of the structural genes in the anthocyanin biosynthetic pathway in maize (Martin, 1996). In addition, these metabolites are not end products of their synthetic pathways but are intermediates or precursors of other pathways. For example, glutamate and aspartate are the precursors for the synthesis of a number of other amino acids. Thus, their regulation needs to be under tighter control and would be shared by the components of the other pathways (Fell, 1997; 1999).

7.2 Altered metabolite levels without alterations in flux or enzyme activity

Investigations of the TCA cycle showed that respiratory function in isolated mitochondria, transcript abundance and activities of enzymes of the TCA cycle were unchanged in the 2-5 line relative to the recurrent parent. In addition, flux through the TCA cycle was also unchanged. This result is counter intuitive as metabolite levels in the 2-5 line were altered but without the expected concomitant changes in TCA cycle flux or enzyme activity (Kinney, 1998). Recent research in *Arabidopsis* investigating metabolic network flux has shown that it is possible to have changes in metabolite levels without changes to TCA cycle flux or enzyme activities (Williams *et al.*, 2008). This research showed that the flux through the TCA cycle is far greater than the individual fluxes that lead to the accumulation of these metabolites. Therefore, any withdrawal of metabolites from the TCA cycle for storage in the vacuole is relatively small, would not have a significant effect on the TCA cycle flux and over a period of time would allow metabolite levels to accumulate to significant levels in the vacuole.

The research by Williams et al. (2008) has interesting implications for plant biotechnology. A number of high value metabolites are derived from the carbon skeletons of the TCA cycle either as primary or secondary metabolic products including amino acids, pigments, flavanoids and fatty acids for the improvement of human and animal food (Galili *et al.*, 2002; Butelli *et al.*, 2008) and alkaloids and isoprenoids for medicines (Carrari *et al.*, 2003b). The TCA cycle would, therefore, be an attractive target to metabolic engineers interested in the commercial production of these metabolites. The focus of metabolic

engineering in plant metabolism has been on altering the expression of enzymes in the biosynthetic pathways of commercially important metabolites to alter flux (Kinney, 1998). The research shown in Williams *et al.* (2008) has shown that targeting the TCA cycle to enhance flux through this pathway to increase primary metabolite concentrations is unlikely to be successful and that targeting the associated biosynthetic pathways would be more fruitful. Also, alterations to flux in the associated pathways to increase desired metabolite levels would be less likely to cause any detrimental side effects to the functioning of central metabolism.

In addition, by providing a better understanding of flux distribution through this central metabolic pathway any future attempts at metabolic engineering will be more likely to be successful.

7.3 Regulation of citrate accumulation

Citrate accumulation in tomato was shown to be partially regulated by cytosolic aconitase as indicated by changes in cytosolic aconitase at the transcript and protein level in the 2-5 line relative to the recurrent parent. Cytosolic aconitase has been shown to be involved in the regulation of citrate accumulation through citrate catabolism in both *Citrus* and *Lupinus albus* (Sadka *et al.*, 2000a; Sadka *et al.*, 2000b; Kihara *et al.*, 2003). However, no changes were found at the transcript level or in activity of $NADP^+$-isocitrate dehydrogenase in the 2-5 line relative to the recurrent parent that would suggest that the catabolic pathway is involved in citrate accumulation in tomato.

In tomato there are two aconitase genes (mapped to chromosome 7 and 12) but neither contains a recognizable sub-cellular targeting sequence (Tanksley and Rick, 1980;

Carrari *et al.*, 2003a). The aconitase enzymes have been localised both to the mitochondria and the cytosol (Carrari *et al.*, 2003a). This is similar to the aconitase enzymes found in *Arabidopsis thaliana* and yeast. In *Arabidopsis* there are three genes encoding aconitase. All have been localized to the mitochondria, do not contain mitochondrial targeting pre-sequences but have cytosolic and mitochondrial isoforms (Peyret *et al.*, 1995; Kruft *et al.*, 2001; Millar *et al.*, 2001). In yeast there is a single gene that encodes aconitase and dual sub-cellular localization of the enzyme (Gangloff *et al.*, 1990). Thus, using transgenic plants to reduce the expression of aconitase to investigate citrate levels would be problematic. This has been attempted in tomato where an acoitase mutant (Aco1) with reduced expression by antisense inhibition did show an increase in citrate accumulation (Carrari *et al.*, 2003a). However, the activity of aconitase was decreased in both the mitochondria and cytosol in these mutants so no specific conclusion can be made concerning the regulation of citrate accumulation by cytosolic aconitase.

In addition, increased cytosolic citrate concentration from decreased cytosolic aconitase activity would be detrimental to the pH homeostasis of the cytosol. Therefore, to reduce local cytosolic accumulation, citrate would need to be transported to and stored in the vacuole, implicating vacuolar transport in citrate regulation. Citrate influx into the vacuole was investigated but a lack of correlation between ATPase-dependent transport and citrate content, in agreement with Oleski et al (1987a), suggested that either citrate efflux or an ATPase-independent mechanism is more important in controlling citrate accumulation.

7.4 Transportation and storage in the vacuole

A decreased rate of malate influx in the 2-5 line correlated with the reduction in malate accumulation in late fruit ripening suggesting malate influx across the tonoplast could be involved in regulating malate accumulation. The regulation of citrate has been shown here as being partially controlled by aconitase, but there are also indications that other mechanisms, such as citrate transport, could be involved in citrate accumulation. The vacuole is a cellular compartment known to accumulate a large variety of molecules including organic and amino acids (Buchanan *et al.*, 2000). The transportation and storage of these metabolites in the vacuole permits their accumulation to high concentrations (up to 350 mM (Martinoia and Rentsch, 1994; Brune *et al.*, 1998)) whilst maintaining optimal metabolic conditions in the sites of synthesis (i.e. cytosol and mitochondria). Thus, the tonoplast proteins involved in the transportation and storage of metabolites in the vacuole should be included as steps in the biochemical pathway when considering the regulation of these metabolites. However, the tonoplast proteins are a neglected source of possible regulatory sites. For example, in the regulation of citrate in *Citrus*, although the storage and accumulation in the vacuole is acknowledged the focus has very much been on the regulation of enzymes in the synthetic and catabolic pathways (Sadka *et al.*, 2000a; Sadka *et al.*, 2000b). The research here has indicated that tonoplast proteins could be regulatory mechanisms in the accumulation of organic acids. Thus, further work with line 2-5 investigating the efflux mechanisms or ATP-independent transport would help to identify if tonoplast transport is indeed a mechanism involved in the accumulation of these metabolites.

The control of metabolite accumulation in plants is multi-level and complex (Carrari *et al.*, 2003b; Sweetlove and Fernie, 2005; Sweetlove *et al.*, 2008). This is partly due to the compartmental nature of metabolism found in plants from possessing sub-cellular membrane-bound organelles and in part due to the highly specialized and tightly regulated developmental programmes associated with metabolite accumulation (Giovannoni, 2007). Plants, being sessile, also require flexibility within their metabolic pathways to maintain optimal metabolic function in order to cope with the ever-changing demands placed on them from biotic and abiotic stresses (Sweetlove and Hill, 2000; Rontein *et al.*, 2002; Sweetlove *et al.*, 2002). Thus, their metabolic pathways often contain multiple routes for a single metabolic product (Plaxton, 1996). Understanding and unravelling the complexity is one of the challenges that must be overcome for plant biotechnologist to successfully manipulation of these commercially important metabolites to improve and exploit crop production.

References

Adams-Phillips, L., Barry, C. and Giovannoni, J. (2004) Signal transduction systems regulating fruit ripening. *Trends in Plant Science*, **9**, 331-338.

Alexander, L. and Grierson, D. (2002) Ethylene biosynthesis and action in tomato: a model for climacteric fruit ripening. *Journal of Experimental Botany*, **53**, 2039-2055.

Bahrami, A.R., Chen, Z., Walker, R.P.*, et al.* (2001) Ripening-related occurrence of phosphoenolpyruvate carboxykinase in tomato fruit. *Plant and Molecular Biology*, **47**, 499-506.

Bai, Y. and Lindhout, P. (2007) Domestication and breeding of tomatoes: what have we gained and what can we gain in the future? *Annals of Botany*, **100**, 1085-1094.

Barry, C.S., McQuinn, R.P., Thompson, A.J.*, et al.* (2005) Ethylene insensitivity conferred by the *green-ripe* and *never-ripe 2* ripening mutants of tomato. *Plant Physiology*, **138**, 267-275.

Baxter, C.J., Carrari, F., Bauke, A.*, et al.* (2005a) Fruit carbohydrate metabolism in an introgression line of tomato with increased fruit soluble solids. *Plant Cell Physiology*, **46**, 425-437.

Baxter, C.J., Sabar, M., Quick, W.P. and Sweetlove, L. (2005b) Comparison of changes in fruit gene expression in tomato introgression lines provides evidence of genome-wide transcriptional changes and reveals links to mapped QTLs and described traits. *Journal of Experimental Botany*, **56**, 1591-1604.

Bennett, A.B. and Spanswick, R.M. (1983) Optical measurements of delta-pH and delta-Psi in corn root membrane-vesicles: kinetic-analysis of Cl^- effects on a proton-translocating ATPase. *Journal of Membrane Biology*, **71**, 95-107.

Boggio, S.B., Palatnik, J.F., Heldt, H.W. and Valle, E.M. (2000) Changes in amino acid composition and nitrogen metabolizing enzymes in ripening fruits of *Lycopersicon esculentum* Mill. *Plant Science*, **159**, 125-133.

Borsani, J., Budde, C.O., Porrini, L.*, et al.* (2009) Carbon metabolism of peach fruit after harvest: changes in enzymes involved in organic acid and sugar level modifications. *Journal of Experimental Botany*, **60**, 1823-1837.

Bradford, M.M. (1976) Rapid and sensitive method for quantitation of microgram quantities of protein utilizing principle of protein-dye binding. *Analytical Biochemistry*, **72**, 248-254.

Brady, C.J. (1987) Fruit ripening. *Annual Review of Plant Physiology and Plant Molecular Biology*, **38**, 155-178.

Bruckner, H., Langer, M., Lupke, M.*, et al.* (1995) Liquid chromatographic determination of amino acid enantiomers by derivatization with *o*-phthaldialdehyde and chiral thiols - applications with reference to food science. *Journal of Chromatography A*, **697**, 229-245.

Brune, A., Gonzalez, P., Goren, R.*, et al.* (1998) Citrate uptake into tonoplast vesicles from acid lime (*Citrus aurantifolia*) juice cells. *Journal of Membrane Biology*, **166**, 197-203.

Buchanan, B.B., Gruissem, W. and Jones, R.L. (2000) *Biochemistry & molecular biology of plants*. Rockville, Maryland: American Society of Plant Physiologists.

Bucheli, P., Voirol, E., de la Torre, R.*, et al.* (1999) Definition of nonvolatile markers for flavor of tomato (*Lycopersicon esculentum* Mill.) as tools in selection and breeding. *Journal of Agricultural and Food Chemistry*, **47**, 659-664.

Buser-Suter, C., Wiemken, A. and Matile, P. (1982) A malic acid permease in isolated vacuoles of a crassulacean acid metabolism plant. *Plant Physiology*, **69**, 456-459.

Bush, D. (1993) Proton-coupled sugar and amino-acid transporters in plants. *Annual Review of Plant Physiology and Plant Molecular Biology*, **44**, 513-542.

Butelli, E., Titta, L., Giorgio, M.*, et al.* (2008) Enrichment of tomato fruit with health-promoting anthocyanins by expression of select transcription factors. *Nature Biotechnology*, **26**, 1301-1308.

Carli, P., Arima, S., Fogliano, V.*, et al.* (2009) Use of network analysis to capture key traits affecting tomato organoleptic quality. *Journal of Experimental Botany*, **60**, 3379-3386.

Carrari, F., Nunes-Nesi, A., Gibon, Y.*, et al.* (2003a) Reduced expression of aconitase results in an enhanced rate of photosynthesis and marked shifts in carbon partitioning in illuminated leaves of wild species tomato. *Plant Physiology*, **133**, 1322-1335.

Carrari, F., Urbanczyk-Wochniak, E., Willmitzer, L. and Fernie, A.R. (2003b) Engineering central metabolism in crop species: learning the system. *Metab Eng*, **5**, 191-200.

Carrari, F., Baxter, C., Usadel, B.*, et al.* (2006) Integrated analysis of metabolite and transcript levels reveals the metabolic shifts that underlie tomato fruit development and highlight regulatory aspects of metabolic network behavior. *Plant Physiology*, **142**, 1380-1396.

Carrari, F. and Fernie, A.R. (2006) Metabolic regulation underlying tomato fruit development. *Journal of Experimental Botany*, **57**, 1883-1897.

Causse, M., Saliba-Colombani, V., Lecomte, L.*, et al.* (2002) QTL analysis of fruit quality in fresh market tomato: a few chromosome regions control the variation of sensory and instrumental traits. *Journal of Experimental Botany*, **53**, 2089-2098.

Causse, M., Chaib, J., Lecomte, L.*, et al.* (2007) Both additivity and epistasis control the genetic variation for fruit quality traits in tomato. *Theoretical and Applied Genetics*, **115**, 429-442.

Chan, E.K.F., Rowe, H.C., Hansen, B.G. and Kliebenstein, D.J. (2010a) The complex genetic architecture of the metabolome. *Public Library of Science Genetics*, **6**, e1001198

Chan, E.K.F., Rowe, H.C. and Kliebenstein, D.J. (2010b) Understanding the evolution of defense metabolites in *Arabidopsis thaliana* using genome-wide association mapping. *Genetics*, **185**, 991-1007.

Chen, G., Wilson, I.D., Kim, S.H. and Grierson, D. (2001) Inhibiting expression of a tomato ripening-associated membrane protein increases organic acids and reduces sugar levels of fruit. *Planta*, **212**, 799-807.

Chifflet, S., Torriglia, A., Chiesa, R. and Tolosa, S. (1988) A method for the determination of inorganic-phosphate in the presence of labile organic phosphate and high-concentrations of protein - application to lens ATPases. *Analytical Biochemistry*, **168**, 1-4.

Coker, J.S., Jones, D. and Davies, E. (2003) Identification, conservation, and relative expression of V-ATPase cDNAs in tomato plants. *Plant Molecular Biology Reporter*, **21**, 145-158.

Coombe, B.G. (1976) Development of fleshy fruits. *Annual Review of Plant Physiology and Plant Molecular Biology*, **27**, 207-228.

Davies, J.N. and Hobson, G.E. (1981) The constituents of tomato fruit - the influence of environment, nutrition, and genotype. *Critical Reviews in Food Science and Nutrition*, **15**, 205-280.

Denny, F.E. (1924) Effect of ethylene upon respiration of lemons. *Botanical Gazette*, **77**, 322-329.

Dibley, S.J., Gear, M.L., Yang, X.*, et al.* (2005) Temporal and spatial expression of hexose transporters in developing tomato (*Lycopersicon esculentum*) fruit. *Functional Plant Biology*, **32**, 777-785.

Dietz, K.J., Martinoia, E. and Heber, U. (1989) Mobilization of vacuolar amino acids in leaf cells as affected by ATP and the level of cytosolic amino acids: ATP regulates but appears not to energize vacuolar amino-acid release. *Biochimica et Biophysica Acta*, **984**, 57-62.

Dietz, K.J., Jager, R., Kaiser, G. and Martinoia, E. (1990) Amino acid transport across the tonoplast of vacuoles isolated from barley mesophyll protoplasts - uptake of alanine, leucine, and glutamine. *Plant Physiology*, **92**, 123-129.

Emanuelsson, O., Nielsen, H., Brunak, S. and von Heijne, G. (2000) Predicting subcellular localization of proteins based on their N-terminal amino acid sequence. *Journal of Molecular Biology*, **300**, 1005-1016.

Emmerlich, V., Linka, N., Reinhold, T.*, et al.* (2003) The plant homolog to the human sodium/dicarboxylic cotransporter is the vacuolar malate carrier. *Proceedings of the National Academy of Sciences, United States of America*, **100**, 11122-11126.

Eshed, Y. and Zamir, D. (1994) A genomic library of *Lycopersicon pennellii* in *L. esculentum*: A tool for fine mapping of genes. *Euphytica*, **79**, 175-179.

Eshed, Y. and Zamir, D. (1995) An introgression line population of *Lycopersicon pennellii* in the cultivated tomato enables the identification and fine mapping of yield-associated QTL. *Genetics*, **141**, 1147-1162.

Eshed, Y., Gera, G. and Zamir, D. (1996) A genome-wide search for wild-species alleles that increase horticultural yield of processing tomatoes. *Theoretical and Applied Genetics*, **93**, 877-886.

Etienne, C., Moing, A., Dirlewanger, E.*, et al.* (2002) Isolation and characterization of six peach cDNAs encoding key proteins in organic acid metabolism and solute accumulation: Involvement in regulating peach fruit acidity. *Physiologia Plantarum*, **114**, 259-270.

Famiani, F., Cultrera, N.G.M., Battistelli, A.*, et al.* (2005) Phosphoenolpyruvate carboxykinase and its potential role in the catabolism of organic acids in the flesh of soft fruit during ripening. *Journal of Experimental Botany*, **56**, 2959-2969.

Farre, E.M., Tiessen, A., Roessner, U.*, et al.* (2001) Analysis of the compartmentation of glycolytic intermediates, nucleotides, sugars, organic acids, amino acids, and sugar alcohols in potato tubers using a nonaqueous fractionation method. *Plant Physiology*, **127**, 685-700.

Faurobert, M., Mihr, C., Bertin, N.*, et al.* (2007) Major proteome variations associated with cherry tomato pericarp development and ripening. *Plant Physiology*, **143**, 1327-1346.

Fell, D.A. (1997) *Understanding the control of metabolism*. London: Portland Press.

Fell, D.A. (1999) Traditional concepts of metabolic control mislead more than enlighten. *The Biochemist*, **21**, 13-16.

Fernie, A.R., Carrari, F. and Sweetlove, L.J. (2004) Respiratory metabolism: glycolysis, the TCA cycle and mitochondrial electron transport. *Current Opinion in Plant Biology*, **7**, 254-261.

Fernie, A.R. and Schauer, N. (2009) Metabolomics-assisted breeding: a viable option for crop improvement? *Trends in Genetics*, **25**, 39-48.

Finkemeier, I., Kluge, C., Metwally, A.*, et al.* (2003) Alterations in Cd-induced gene expression under nitrogen deficiency in *Hordeum vulgare*. *Plant Cell and Environment*, **26**, 821-833.

Foolad, M.R. (2007) Genome mapping and molecular breeding of tomato. *International Journal of Plant Genomics*, **2007**, 64358-64409.

Frary, A., Nesbitt, T.C., Frary, A.*, et al.* (2000) *fw2.2*: a quantitative trait locus key to the evolution of tomato fruit size. *Science*, **289**, 85-88.

Fraser, P.D., Truesdale, M.R., Bird, C.R.*, et al.* (1994) Carotenoid biosynthesis during tomato fruit development. *Plant Physiology*, **105**, 405-413.

Fraser, P.D., Enfissi, E.M.A., Halket, J.M.*, et al.* (2007) Manipulation of phytoene levels in tomato fruit: effects on isoprenoids, plastids, and intermediary metabolism. *Plant Cell*, **19**, 3194-3211.

Fray, R.G. and Grierson, D. (1993) Molecular-genetics of tomato fruit ripening. *Trends in Genetics*, **9**, 438-443.

Fridman, E., Pleban, T. and Zamir, D. (2000) A recombination hotspot delimits a wild-species quantitative trait locus for tomato sugar content to 484 bp within an invertase gene. *Proceedings of the National Academy of Sciences, United States of America*, **97**, 4718-4723.

Fridman, E., Carrari, F., Liu, Y.*, et al.* (2004) Zooming in on a quantitative trait for tomato yield using interspecific introgressions. *Science*, **305**, 1786-1789.

Fuke, S. and Konosu, S. (1991) Taste-active components in some foods: A review of Japanese research. *Physiology and Behavior*, **49**, 863-868.

Fulton, T.M., Bucheli, P., Voirol, E.*, et al.* (2002) Quantitative trait loci (QTL) affecting sugars, organic acids and other biochemical properties possibly contributing to flavor, identified in four advanced backcross populations of tomato. *Euphytica*, **127**, 163-177.

Galili, G., Galili, S., Lewinsohn, E. and Tadmor, Y. (2002) Genetic, molecular, and genomic approaches to improve the value of plant foods and feeds. *Critical Reviews in Plant Sciences*, **21**, 167-204.

Gallardo, F., Galvez, S., Gadal, P. and Canovas, F.M. (1995) Changes in $NADP^+$-linked isocitrate dehydrogenase during tomato fruit ripening - characterization of the predominant cytosolic enzyme from green and ripe pericarp. *Planta*, **196**, 148-154.

Gangloff, S.P., Marguet, D. and Lauquin, G.J.M. (1990) Molecular cloning of the yeast mitochondrial aconitase gene (ACO1) and evidence of a synergistic regulation of expression by glucose plus glutamate. *Molecular and Cellular Biology*, **10**, 3551-3561.

Gao, H.Y., Zhu, B.Z., Zhu, H.L.*, et al.* (2007) Effect of suppression of ethylene biosynthesis on flavor products in tomato fruits. *Russian Journal of Plant Physiology*, **54**, 80-88.

Garlick, A.P., Moore, C. and Kruger, N.J. (2002) Monitoring flux through the oxidative pentose phosphate pathway using [1-^{14}C]gluconate. *Planta*, **216**, 265-272.

Gasteiger, E., Gattiker, A., Hoogland, C.*, et al.* (2003) ExPASy: the proteomics server for in-depth protein knowledge and analysis. *Nucleic Acids Research*, **31**, 3784-3788.

Geigenberger, P. and Stitt, M. (1993) Sucrose synthase catalyzes a readily reversible reaction *in vivo* in developing potato tubers and other plant tissues. *Planta*, **189**, 329-339.

Gillaspy, G., Ben-David, H. and Gruissem, W. (1993) Fruits: a developmental perspective. *Plant Cell*, **5**, 1439-1451.

Giovannoni, J., Yen, H., Shelton, B.*, et al.* (1999) Genetic mapping of ripening and ethylene-related loci in tomato. *Theoretical and Applied Genetics*, **98**, 1005-1013.

Giovannoni, J. (2001) Molecular biology of fruit maturation and ripening. *Annual Review of Plant Physiology and Plant Molecular Biology*, **52**, 725-749.

Giovannoni, J.J., Noensie, E.N., Ruezinsky, D.R.*, et al.* (1995) Molecular genetic analysis of the *ripening-inhibitor* and *non-ripening* loci of tomato: a first step in genetic map-based cloning of fruit ripening genes. *Molecular and General Genetics*, **248**, 195-206.

Giovannoni, J.J. (2004) Genetic regulation of fruit development and ripening. *Plant Cell*. **16**, S170-S180.

Giovannoni, J.J. (2006) Breeding new life into plant metabolism. *Nature Biotechnology*, **24**, 418-419.

Giovannoni, J.J. (2007) Fruit ripening mutants yield insights into ripening control. *Current Opinion in Plant Biology*, **10**, 283-289.

Glazier, A.M., Nadeau, J.H. and Aitman, T.J. (2002) Genetics: finding genes that underline complex traits. *Science*, **298**, 2345-2349.

Goerlach, J. and Willmshoff, I. (1992) Glycine uptake into barley mesophyll vacuoles is regulated but not energized by ATP. *Plant Physiology*, **99**, 134-139.

Goff, S.A. and Klee, H.J. (2006) Plant volatile compounds: sensory cues for health and nutritional value? *Science*, **311**, 815-819.

Gould, W.A. (1978) Quality evaluation of processed tomato juice. *Journal of Agricultural and Food Chemistry*, **26**, 1006-1011.

Gray, J., Picton, S., Shabbeer, J.*, et al.* (1992) Molecular biology of fruit ripening and its manipulation with antisense genes. *Plant Molecular Biology*, **19**, 69-87.

Grierson, D. and Kader, A.A. (1986) Fruit ripening and quality. In *The tomato crop: a scientific basis for improvement.* (J., A. and Rudich, J., eds). London: Chapman and Hall, pp. 241-280.

Guillet, C., Just, D., Benard, N.*, et al.* (2002) A fruit-specific phosphoenolpyruvate carboxylase is related to rapid growth of tomato fruit. *Planta*, **214**, 717-726.

Hafke, J.B., Hafke, Y., Smith, J.A.C.*, et al.* (2003) Vacuolar malate uptake is mediated by an anion-selective inward rectifier. *Plant Journal*, **35**, 116-128.

Hamilton, A.J., Lycett, G.W. and Grierson, D. (1990) Antisense gene that inhibits synthesis of the hormone ethylene in transgenic plants. *Nature*, **346**, 284-287.

Hedrich, R., Flugge, U.I. and Fernandez, J.M. (1986) Patch-clamp studies of ion transport in isolated plant vacuoles. *Febs Letters*, **204**, 228-232.

Herner, R.C. and Sink, K.C. (1973) Ethylene production and respiratory behavior of the *rin* tomato mutant. *Plant Physiology*, **52**, 38-42.

Ho, L.C. (1984) Partitioning of assimilates in fruiting tomato plants. *Plant Growth Regulation*, **2**, 277-285.

Ho, L.C. and Hewitt, J.D. (1986) Fruit development. In *The tomato crop: a scientific basis for improvement.* (Atherton, J. and Rudich, J., eds). London: Chapman and Hall, pp. 202-239.

Ho, L.C. (1988) Metabolism and compartmentation of imported sugars in sink organs in relation to sink strength. *Annual Review of Plant Physiology and Plant Molecular Biology*, **39**, 355-378.

Hofmann, M.G., Sinha, A.K., Proels, R.K. and Roitsch, T. (2008) Cloning and characterization of a novel LpWRKY1 transcription factor in tomato. *Plant Physiology and Biochemistry*, **46**, 533-540.

Holtzapffel, R.C., Finnegan, P.M., Millar, A.H.*, et al.* (2002) Mitochondrial protein expression in tomato fruit during on-vine ripening and cold storage. *Functional Plant Biology*, **29**, 827-834.

Homeyer, U. and Schultz, G. (1988) Transport of phenylalanine into vacuoles isolated from barley mesophyll protoplasts. *Planta*, **176**, 378-382.

Homeyer, U., Litek, K., Huchzermeyer, B. and Schultz, G. (1989) Uptake of phenylalanine into isolated barley vacuoles is driven by both tonoplast adenosine triphosphatase and pyrophosphatase - evidence for a hydrophobic L-amino-acid carrier system. *Plant Physiology*, **89**, 1388-1393.

Hu, L.P., Meng, F.Z., Wang, S.H.*, et al.* (2009) Changes in carbohydrate levels and their metabolic enzymes in leaves, phloem sap and mesocarp during cucumber (*Cucumis sativus L.*) fruit development. *Scientia Horticulturae*, **121**, 131-137.

Hurth, M.A., Suh, S.J., Kretzschmar, T.*, et al.* (2005) Impaired pH homeostasis in *Arabidopsis* lacking the vacuolar dicarboxylate transporter and analysis of carboxylic acid transport across the tonoplast. *Plant Physiology*, **137**, 901-910.

Janssen, B.J., Lund, L. and Sinha, N. (1998) Overexpression of a homeobox gene, LeT6, reveals indeterminate features in the tomato compound leaf. *Plant Physiology*, **117**, 771-786.

Jeffery, D., Goodenough, P.W. and Weitzman, P.D.J. (1986) Enzyme-activities in mitochondria isolated from ripening tomato fruit. *Planta*, **168**, 390-394.

Jenner, H.L., Winning, B.M., Millar, A.H.*, et al.* (2001) NAD malic enzyme and the control of carbohydrate metabolism in potato tubers. *Plant Physiology*, **126**, 1139-1149.

Jennings, I.R., Rea, P.A., Leigh, R.A. and Sanders, D. (1988) Quantitative and rapid estimation of H^+ fluxes in membrane-vesicles - software for analysis of fluorescence quenching and relaxation. *Plant Physiology*, **86**, 1257-1263.

Jones, R.A. and Scott, S.J. (1983) Improvement of tomato flavor by genetically increasing sugar and acid contents. *Euphytica*, **32**, 845-855.

Kameswara Rao, K., Lakshminarasu, M. and Jena, K.K. (2002) DNA markers and marker-assisted breeding for durable resistance to bacterial blight disease in rice. *Biotechnology Advances*, **20**, 33-47.

Kargbo, A. and Wang, C. (2010) Complex traits mapping using introgression lines in pepper (*Capsicum annuum*). *African Journal of Agricultural Research*, **5**, 725-731.

Kihara, T., Wada, T., Suzuki, Y.*, et al.* (2003) Alteration of citrate metabolism in cluster roots of white lupin. *Plant and Cell Physiology*, **44**, 901-908.

Kinney, A. (1998) Manipulating flux through plant metabolic pathways. *Current Opinion in Plant Biology*, **1**, 173-178.

Kisaka, H. and Kida, T. (2003) Transgenic tomato plant carrying a gene for NADP-dependent glutamate dehydrogenase (*gdhA*) from *Aspergillus nidulans*. *Plant Science*, **164**, 35-42.

Kisaka, H., Kida, T. and Miwa, T. (2006) Antisense suppression of glutamate decarboxylase in tomato (*Lycopersicon esculentum* L.) results in accumulation of glutamate in transgenic tomato fruits. *Plant Biotechnology*, **23**, 267-274.

Klann, E.m., Hall, B. and Bennett, A.B. (1996) Antisense acid invertase (*TIV1*) gene alters soluble sugar composition and size in transgenic tomato fruit. *Plant Physiology*, **112**, 1321-1330.

Koornneef, M., Alonso-Blanco, C. and Vreugdenhil, D. (2004) Naturally occurring genetic variation in *Arabidopsis thaliana*. *Annual Review of Plant Biology*, **55**, 141-172.

Kovermann, P., Meyer, S., Hortensteiner, S.*, et al.* (2007) The *Arabidopsis* vacuolar malate channel is a member of the ALMT family. *Plant Journal*, **52**, 1169-1180.

Kruft, V., Eubel, H., Jansch, L.*, et al.* (2001) Proteomic approach to identify novel mitochondrial proteins in *Arabidopsis*. *Plant Physiology*, **127**, 1694-1710.

Kruger, N.J. and von Schaewen, A. (2003) The oxidative pentose phosphate pathway: structure and organisation. *Current Opinion in Plant Biology*, **6**, 236-246.

Kruger, N.J., Huddleston, J.E., Le Lay, P.*, et al.* (2007) Network flux analysis: impact of ^{13}C-substrates on metabolism in *Arabidopsis thaliana* cell suspension cultures. *Phytochemistry*, **68**, 2176-2188.

Le Gall, G., Colquhoun, I.J., Davis, A.L.*, et al.* (2003) Metabolite profiling of tomato (*Lycopersicon esculentum*) using ^{1}H-NMR spectroscopy as a tool to detect potential unintended effects following a genetic modification. *Journal of Agricultural and Food Chemistry*, **51**, 2447-2456.

Lelievre, J.M., Latche, A., Jones, B.*, et al.* (1997) Ethylene and fruit ripening. *Physiologia Plantarum*, **101**, 727-739.

Levin, I., Lalazar, A., Bar, M. and Schaffer, A.A. (2004) Non GMO fruit factories: strategies for modulating metabolic pathways in the tomato fruit. *Industrial Crops and Products*, **20**, 29-36.

Li, Z.K., Fu, B.Y., Gao, Y.M.*, et al.* (2005) Genome-wide introgression lines and their use in genetic and molecular dissection of complex phenotypes in rice (*Oryza sativa* L.). *Plant Molecular Biology*, **59**, 33-52.

Lincoln, J.E. and Fischer, R.L. (1988) Regulation of gene expression by ethylene in wild-type and *rin* tomato (*Lycopersicon esculentum*) fruit. *Plant Physiology*, **88**, 370-374.

Lippman, Z.B., Semel, Y. and Zamir, D. (2007) An integrated view of quantitative trait variation using tomato interspecific introgression lines. *Current Opinion in Genetics and Development*, **17**, 545-552.

Lippman, Z.B. and Zamir, D. (2007) Natural variation as a tool for gene identification in plants. *Electronic Library Service*: Wiley Online Library.

Liu, Q., Kane, P.M., Newman, P.R. and Forgac, M. (1996) Site-directed mutagenesis of the yeast V-ATPase B subunit (Vma2p). *Journal of Biological Chemistry*, **271**, 2018-2022.

Liu, S., Zhou, R., Dong, Y.*, et al.* (2006) Development, utilization of introgression lines using a synthetic wheat as donor. *Theoretical and Applied Genetics*, **112**, 1360-1373.

Liu, Y.S. and Zamir, D. (1999) Second generation *L. pennellii* introgression lines and the concept of bin mapping. *Report of the Tomato Genetics Cooperative*. Fulton, T., Ithaca, NY: Cornell University, 26-30.

Luttge, U., Pfeifer, T., Fischer-Schliebs, E. and Ratajczak, R. (2000) The role of vacuolar malate-transport capacity in crassulacean acid metabolism and nitrate nutrition. Higher malate-transport capacity in ice plant after crassulacean acid metabolism-induction and in tobacco under nitrate nutrition. *Plant Physiology*, **124**, 1335-1347.

MacDougall, A.J. and Ap Rees, T. (1991) Control of the krebs cycle in *Arum spadix*. *Journal of Plant Physiology*, **137**, 683-690.

Mahakun, N., Leeper, P.W. and Burns, E.E. (1979) Acidic constituents of various tomato fruit types. *Journal of Food Science*, **44**, 1241-1244.

Malundo, T.M.M., Shewfelt, R.L. and Scott, J.W. (1995) Flavor quality of fresh tomato (*Lycopersicon esculentum* Mill) as affected by sugar and acid levels. *Postharvest Biology and Technology*, **6**, 103-110.

Manning, K., Tor, M., Poole, M.*, et al.* (2006) A naturally occurring epigenetic mutation in a gene encoding an SBP-box transcription factor inhibits tomato fruit ripening. *Nature Genetics*, **38**, 948-952.

Marceau, F., Bawolak, M.T., Bouthillier, J. and Morissette, G. (2009) Vacuolar ATPase-mediated cellular concentration and retention of quinacrine: a model for the distribution of lipophilic cationic drugs to autophagic vacuoles. *Drug Metabolism and Disposition*, **37**, 2271-2274.

Marigo, G., Bouyssou, H. and Laborie, D. (1988) Evidence for a malate transport into vacuoles isolated from *Catharanthus roseus* cells. *Botanica Acta*, **101**, 187-191.

Marin, B., Smith, J.A.C. and Luttge, U. (1981) The electrochemical proton gradient and its influence on citrate uptake in tonoplast vesicles of *Hevea Brasiliensis*. *Planta*, **153**, 486-493.

Martin, C. (1996) Transcription factors and the manipulation of plant traits. *Current Opinion in Biotechnology*, **7**, 130-138.

Martinoia, E., Flugge, U.I., Kaiser, G.*, et al.* (1985) Energy-dependent uptake of malate into vacuoles isolated from barley mesophyll protoplasts. *Biochimica et Biophysica Acta*, **806**, 311-319.

Martinoia, E., Thume, M., Vogt, E.*, et al.* (1991) Transport of arginine and aspartic-acid into isolated barley mesophyll vacuoles. *Plant Physiology*, **97**, 644-650.

Martinoia, E. and Rentsch, D. (1994) Malate compartmentation - responses to a complex metabolism. *Annual Review of Plant Physiology and Plant Molecular Biology*, **45**, 447-467.

Martinoia, E., Massonneau, A. and Frangne, N. (2000) Transport processes of solutes across the vacuolar membrane of higher plants. *Plant and Cell Physiology*, **41**, 1175-1186.

Martinoia, E., Maeshima, M. and Neuhaus, H.E. (2007) Vacuolar transporters and their essential role in plant metabolism. *Journal of Experimental Botany*, **58**, 83-102.

Marty, F. (1999) Plant vacuoles. *Plant Cell*, **11**, 587-599.

Mathieu, S., Cin, V.D., Fei, Z.*, et al.* (2009) Flavour compounds in tomato fruits: identification of loci and potential pathways affecting volatile composition. *Journal of Experimental Botany*, **60**, 325-337.

Mayda, E., Tornero, P., Conejero, V. and Vera, P. (1999) A tomato homeobox gene (HD-zip) is involved in limiting the spread of programmed cell death. *Plant Journal*, **20**, 591-600.

Millar, A.H., Sweetlove, L.J., Giege, P. and Leaver, C.J. (2001) Analysis of the *Arabidopsis* mitochondrial proteome. *Plant Physiology*, **127**, 1711-1727.

Morgan, M.J., Lehmann, M., Schwarzlander, M.*, et al.* (2008) Decrease in manganese superoxide dismutase leads to reduced root growth and affects tricarboxylic acid cycle flux and mitochondrial redox homeostasis. *Plant Physiology*, **147**, 101-114.

Mounet, F., Moing, A., Garcia, V.*, et al.* (2009) Gene and metabolite regulatory network analysis of early developing fruit tissues highlights new candidate genes for the control of tomato fruit composition and development. *Plant Physiology*, **149**, 1505-1528.

Mueller, L.A., Solow, T.H., Taylor, N.*, et al.* (2005) The SOL genomics network. A comparative resource for *Solanaceae* biology and beyond. *Plant Physiology*, **138**, 1310-1317.

Muller, M., Hogg, J.F. and Deduve, C. (1968) Distribution of tricarboxylic acid cycle enzymes and glyoxylate cycle enzymes between mitochondria and peroxisomes in *Tetrahymena Pyriformis*. *Journal of Biological Chemistry*, **243**, 5385-5395.

Nelson, G., Chandrashekar, J., Hoon, M.A.*, et al.* (2002) An amino-acid taste receptor. *Nature*, **416**, 199-202.

Nielsen, H., Engelbrecht, J., Brunak, S. and vonHeijne, G. (1997) Identification of prokaryotic and eukaryotic signal peptides and prediction of their cleavage sites. *Protein Engineering*, **10**, 1-6.

Noctor, G. and Foyer, C.H. (1998) Simultaneous measurement of foliar glutathione, gamma-glutamylcysteine, and amino acids by high-performance liquid chromatography: comparison with two other assay methods for glutathione. *Analytical Biochemistry*, **264**, 98-110.

Nunes-Nesi, A., Carrari, F., Lytovchenko, A.*, et al.* (2005) Enhanced photosynthetic performance and growth as a consequence of decreasing mitochondrial malate dehydrogenase activity in transgenic tomato plants. *Plant Physiology*, **137**, 611-622.

Nunes-Nesi, A., Carrari, F., Gibon, Y.*, et al.* (2007) Deficiency of mitochondrial fumarase activity in tomato plants impairs photosynthesis via an effect on stomatal function. *Plant Journal*, **50**, 1093-1106.

Oeller, P.W., Wong, L.M., Taylor, L.P.*, et al.* (1991) Reversible inhibition of tomato fruit senescence by antisense RNA. *Science*, **254**, 437-439.

Oleski, N., Mahdavi, P. and Bennett, A.B. (1987a) Transport properties of the tomato fruit tonoplast. II. Citrate transport. *Plant Physiology*, **84**, 997-1000.

Oleski, N., Mahdavi, P., Peiser, G. and Bennett, A.B. (1987b) Transport properties of the tomato fruit tonoplast. I. Identification and characterization of an anion-sensitive H^+-ATPase. *Plant Physiology*, **84**, 993-996.

Overy, S.A., Walker, H.J., Malone, S.*, et al.* (2005) Application of metabolite profiling to the identification of traits in a population of tomato introgression lines. *Journal of Experimental Botany*, **56**, 287-296.

Pantoja, O. and Smith, J.A.C. (2002) Sensitivity of the plant vacuolar malate channel to pH, Ca^{2+} and anion-channel blockers. *Journal of Membrane Biology*, **186**, 31-42.

Paszkowski, J., Shillito, R.D., Saul, M.*, et al.* (1984) Direct gene transfer to plants. *The EMBO Journal*, **3**, 2717-2722.

Peralta, I.E., Knapp, S. and Spooner, D.M. (2006) Nomenclature for wild and cultivated tomatoes. *Tomato Genetics Cooperative Report*. Scott, J., Wimauma: Gulf Coast Research and Education Center, University of Florida, 6-12.

Petro-Turza, M. (1986) Flavor of tomato and tomato products. *Food Reviews International*, **2**, 309-351.

Peyret, P., Perez, P. and Alric, M. (1995) Structure, genomic organization, and expression of the *Arabidopsis thaliana* aconitase gene. Plant aconitase show significant homology with mammalian iron-responsive element-binding protein. *Journal of Biological Chemistry*, **270**, 8131-8137.

Piechulla, B., Glick, R.E., Bahl, H.*, et al.* (1987) Changes in photosynthetic capacity and photosynthetic protein pattern during tomato fruit ripening. *Plant Physiology*, **84**, 911-917.

Plaxton, W.C. (1996) The organization and regulation of plant glycolysis. *Annual Review of Plant Physiology and Plant Molecular Biology*, **47**, 185-214.

Pooni, H.S. and Kearsey, M.J. (2001) *Plant quantitative traits*. Chicester: John Wiley and Sons, Ltd.

Pratta, G., Zorzoli, R., Boggio, S.B.*, et al.* (2004) Glutamine and glutamate levels and related metabolizing enzymes in tomato fruits with different shelf-life. *Scientia Horticulturae*, **100**, 341-347.

Radzevicius, A., Karkleliene, R., Viskelis, P.*, et al.* (2009) Tomato (Lycopersicum esculentum Mill.) fruit quality and physiological parameters at different ripening stages of; Lithuanian cultivars. *Agronomy Research*, **7**, 712-718.

Ratajczak, R., Luttge, U., Gonzalez, P. and Etxeberria, E. (2003) Malate and malate-channel antibodies inhibit electrogenic and ATP-dependent citrate transport across the tonoplast of citrus juice cells. *Journal of Plant Physiology*, **160**, 1313-1317.

Ratanachinakorn, B., Klieber, A. and Simons, D.H. (1997) Effect of short-term controlled atmospheres and maturity on ripening and eating quality of tomatoes. *Postharvest Biology and Technology*, **11**, 149-154.

Ratcliffe, R.G. and Shachar-Hill, Y. (2006) Measuring multiple fluxes through plant metabolic networks. *Plant Journal*, **45**, 490-511.

Rentsch, D. and Martinoia, E. (1991) Citrate transport into barley mesophyll vacuoles - comparison with malate-uptake activity. *Planta*, **184**, 532-537.

Roessner-Tunali, U., Hegemann, B., Lytovchenko, A.*, et al.* (2003) Metabolic profiling of transgenic tomato plants overexpressing hexokinase reveals that the influence of hexose phosphorylation diminishes during fruit development. *Plant Physiology*, **133**, 84-99.

Roitsch, T. (1999) Source-sink regulation by sugar and stress. *Current Opinion in Plant Biology*, **2**, 198-206.

Rontein, D., Dieuaide-Noubhani, M., Dufourc, E.J.*, et al.* (2002) The metabolic architecture of plant cells - stability of central metabolism and flexibility of anabolic pathways during the growth cycle of tomato cells. *Journal of Biological Chemistry*, **277**, 43948-43960.

Roth, M. (1971) Fluorescence reaction for amino acids. *Analytical Chemistry*, **43**, 880-882.

Rousseaux, M.C., Jones, C.M., Adams, D.*, et al.* (2005) QTL analysis of fruit antioxidants in tomato using *Lycopersicon pennellii* introgression lines. *Theoretical and Applied Genetics*, **111**, 1396-1408.

Rowe, H.C., Hansen, B.G., Halkier, B.A. and Kliebenstein, D.J. (2008) Biochemical networks and epistasis shape the *Arabidopsis thaliana* metabolome. *Plant Cell*, **20**, 1199-1216.

Rozen, S. and Skaletsky, H.J. (2000) Primer3 on the WWW for general users and for biologist programmers. In *Bioinformatics methods and protocols: Methods in molecular biology* (Krawetz, S. and Misener, S., eds). Totowa, NJ: Humana Press, pp. 365-386.

Sadka, A., Dahan, E., Cohen, L. and Marsh, K.B. (2000a) Aconitase activity and expression during the development of lemon fruit. *Physiologia Plantarum*, **108**, 255-262.

Sadka, A., Dahan, E., Or, E. and Cohen, L. (2000b) $NADP^+$-isocitrate dehydrogenase gene expression and isozyme activity during citrus fruit development. *Plant Science*, **158**, 173-181.

Saeed, A.I., Bhagabati, N.K., Braisted, J.C.*, et al.* (2006) TM4 microarray software suite. *Methods in Enzymology*, **411**, 134-193.

Saliba-Colombani, V., Causse, M., Langlois, D.*, et al.* (2001) Genetic analysis of organoleptic quality in fresh market tomato. 1. Mapping QTLs for physical and chemical traits. *Theoretical and Applied Genetics*, **102**, 259-272.

Schauer, N., Semel, Y., Roessner, U.*, et al.* (2006) Comprehensive metabolic profiling and phenotyping of interspecific introgression lines for tomato improvement. *Nature Biotechnology*, **24**, 447-454.

Schiffman, S.S., Sennewald, K. and Gagnon, J. (1981) Comparison of taste qualities and thresholds of D-amino and L-amino-acids. *Physiology and Behavior*, **27**, 51-59.

Schmalenbach, I., Korber, N. and Pillen, K. (2008) Selecting a set of wild barley introgression lines and verification of QTL effects for resistance to powdery mildew and leaf rust. *Theoretical and Applied Genetics*, **117**, 1093-1106.

Schuch, W. (1994) Improving tomato fruit quality and the European regulatory framework. *Euphytica*, **79**, 287-291.

Shimada, T., Nakano, R., Shulaev, V.*, et al.* (2006) Vacuolar citrate/H^+ symporter of citrus juice cells. *Planta*, **224**, 472-480.

Shlizerman, L., Marsh, K., Blumwald, E. and Sadka, A. (2007) Iron-shortage-induced increase in citric acid content and reduction of cytosolic aconitase activity in *Citrus* fruit vesicles and calli. *Physiologia Plantarum*, **131**, 72-79.

Sienkiewicz-Porzucek, A., Nunes-Nesi, A., Sulpice, R.*, et al.* (2008) Mild reductions in mitochondrial citrate synthase activity result in a compromised nitrate assimilation and reduced leaf pigmentation but have no effect on photosynthetic performance or growth. *Plant Physiology*, **147**, 115-127.

Sienkiewicz-Porzucek, A., Sulpice, R., Osorio, S.*, et al.* (2010) Mild reductions in mitochondrial NAD-dependent isocitrate dehydrogenase activity result in altered nitrate assimilation and pigmentation but do not impact growth. *Molecular Plant*, **3**, 156-173.

Small, I., Peeters, N., Legeai, F. and Lurin, C. (2004) Predotar: A tool for rapidly screening proteomes for N-terminal targeting sequences. *Proteomics*, **4**, 1581-1590.

Smillie, R.M., Hetherington, S.E. and Davies, W.J. (1999) Photosynthetic activity of the calyx, green shoulder, pericarp, and locular parenchyma of tomato fruit. *Journal of Experimental Botany*, **50**, 707-718.

Smith, J.A.C. and Winter, K. (1996) Transport across the vacuolar membrane in CAM plants. In *Crassulacean acid metabolism: biochemistry, ecophysiology and evolution (ecological studies)* (Winter, K. and Smith, J., eds). Berlin: Springer, pp. 54-67.

Stevens, R., Buret, M., Duffe, P.*, et al.* (2007) Candidate genes and quantitative trait loci affecting fruit ascorbic acid content in three tomato populations. *Plant Physiology*, **143**, 1943-1953.

Stitt, M., Lilley, R.M., Gerhardt, R. and Heldt, H.W. (1989) Metabolite levels in specific cells and subcellular compartments of plant-leaves. *Methods in Enzymology*, **174**, 518-552.

Studart-Guimaraes, C., Fait, A., Nunes-Nesi, A.*, et al.* (2007) Reduced expression of succinyl-coenzyme A ligase can be compensated for by up-regulation of the gamma-aminobutyrate shunt in illuminated tomato leaves. *Plant Physiology*, **145**, 626-639.

Sturm, A. and Chrispeels, M.J. (1990) cDNA cloning of carrot extracellular beta-fructosidase and its expression in response to wounding and bacterial infection. *Plant Cell*, **2**, 1107-1119.

Sturm, A. (1999) Invertases. Primary structures, functions, and roles in plant development and sucrose partitioning. *Plant Physiology*, **121**, 1-7.

Sturm, A. and Tang, G.Q. (1999) The sucrose-cleaving enzymes of plants are crucial for development, growth and carbon partitioning. *Trends in Plant Science*, **4**, 401-407.

Sweetlove, L.J. and Hill, S.A. (2000) Source metabolism dominates the control of source to sink carbon flux in tuberizing potato plants throughout the diurnal cycle and under a range of environmental conditions. *Plant Cell and Environment*, **23**, 523-529.

Sweetlove, L.J., Heazlewood, J.L., Herald, V.*, et al.* (2002) The impact of oxidative stress on *Arabidopsis* mitochondria. *Plant J*, **32**, 891-904.

Sweetlove, L.J. and Fernie, A.R. (2005) Regulation of metabolic networks: Understanding metabolic complexity in the systems biology era. *New Phytologist*, **168**, 9-24.

Sweetlove, L.J., Fell, D. and Fernie, A.R. (2008) Getting to grips with the plant metabolic network. *Biochemical Journal*, **409**, 27-41.

Szabados, L. and Savoure, A. (2010) Proline: a multifunctional amino acid. *Trends in Plant Science*, **15**, 89-97.

Tadmor, Y., Fridman, E., Gur, A.*, et al.* (2002) Identification of malodorous, a wild species allele affecting tomato aroma that was selected against during domestication. *Journal of Agricultural and Food Chemistry*, **50**, 2005-2009.

Tanksley, S.D. and Rick, C.M. (1980) Isozymic gene linkage map of the tomato - applications in genetics and breeding. *Theoretical and Applied Genetics*, **57**, 161-170.

Tanksley, S.D., Young, N.D., Paterson, A.H. and Bonierbale, M.W. (1989) RFLP mapping in plant breeding: new tools for an old science. *Bio-Technology*, **7**, 257-264.

Tanksley, S.D., Ganal, M.W., Prince, J.P.*, et al.* (1992) High density molecular linkage maps of the tomato and potato genomes. *Genetics*, **132**, 1141-1160.

Terol, J., Soler, G., Talon, M. and Cercos, M. (2010) The aconitate hydratase family from *Citrus*. *BMC Plant Biol*, **10**, 222.

Theologis, A. (1992) One rotten apple spoils the whole bushel: the role of ethylene in fruit ripening. *Cell*, **70**, 181-184.

Thimann, K.V. (1980) *Senescence in plants*. Florida: CRC Press Inc.

Thompson, A.J., Tor, M., Barry, C.S.*, et al.* (1999) Molecular and genetic characterization of a novel pleiotropic tomato-ripening mutant. *Plant Physiology*, **120**, 383-389.

Thume, M. and Dietz, K.J. (1991) Reconstitution of the tonoplast amino-acid carrier into liposomes - evidence for an ATP-regulated carrier in different species. *Planta*, **185**, 569-575.

Tieman, D., Taylor, M., Schauer, N.*, et al.* (2006a) Tomato aromatic amino acid decarboxylases participate in synthesis of the flavor volatiles 2-phenylethanol and 2-phenylacetaldehyde. *Proceedings of the National Academy of Sciences, United States of America*, **103**, 8287-8292.

Tieman, D.M., Zeigler, M., Schmelz, E.A.*, et al.* (2006b) Identification of loci affecting flavour volatile emissions in tomato fruits. *Journal of Experimental Botany*, **57**, 887-896.

Valle, E.M., Boggio, S.B. and Heldt, H.W. (1998) Free amino acid composition of phloem sap and growing fruit of *Lycopersicon esculentum*. *Plant and Cell Physiology*, **39**, 458-461.

Velterop, J.S. and Vos, F. (2001) A rapid and inexpensive microplate assay for the enzymatic determination of glucose, fructose, sucrose, L-malate and citrate in tomato (*Lycopersicon esculentum*) extracts and in orange juice. *Phytochemical Analysis*, **12**, 299-304.

Vrebalov, J., Ruezinsky, D., Padmanabhan, V.*, et al.* (2002) A MADS-box gene necessary for fruit ripening at the tomato *ripening-inhibitor* (*rin*) locus. *Science*, **296**, 343-346.

Walker, A.J. and Ho, L.C. (1977) Carbon translocation in the tomato: Carbon import and fruit growth. *Annals of Botany*, **41**, 813-823.

Walz, C., Juenger, M., Schad, M. and Kehr, J. (2002) Evidence for the presence and activity of a complete antioxidant defence system in mature sieve tubes. *Plant Journal*, **31**, 189-197.

Wang, Y. and Sze, H. (1985) Similarities and differences between the tonoplast-type and the mitochondrial H^+-ATPases of oat roots. *Journal of Biological Chemistry*, **260**, 10434-10443.

Wentzell, A.M., Rowe, H.C., Hansen, B.G.*, et al.* (2007) Linking metabolic QTLs with network and cis-eQTLs controlling biosynthetic pathways. *Public Library of Science Genetics*, **3**, 1687-1701.

White, P.J. and Smith, J.A.C. (1989) Proton and anion transport at the tonoplast in crassulacean-acid-metabolism plants: specificity of the malate-influx system in *Kalanchoe daigremontiana*. *Planta*, **179**, 265-274.

Williams, T.C.R., Miguet, L., Masakapalli, S.K.*, et al.* (2008) Metabolic network fluxes in heterotrophic *Arabidopsis* cells: stability of the flux distribution under different oxygenation conditions. *Plant Physiology*, **148**, 704-718.

Winter, H., Lohaus, G. and Heldt, H.W. (1992) Phloem transport of amino-acids in relation to their cytosolic levels in barley leaves. *Plant Physiology*, **99**, 996-1004.

Winter, K. and Smith, J.A.C. (1996) Transport across the vacuolar membrane in CAM plants. In *Crassulacean acid metabolism: biochemistry, ecophysiology and evolution*. Berlin: Springer-Verlag.

Yanez, M., Caceres, S., Orellana, S.*, et al.* (2009) An abiotic stress-responsive bZIP transcription factor from wild and cultivated tomatoes regulates stress-related genes. *Plant Cell Reports*, **28**, 1497-1507.

Yelle, S., Hewitt, J.D., Robinson, N.L.*, et al.* (1988) Sink metabolism in tomato fruit. III. Analysis of carbohydrate assimilation in a wild species. *Plant Physiology*, **87**, 737-740.

Yilmaz, E. (2001) The chemistry of fresh tomato flavor. *Turkish Journal of Agriculture and Forestry*, **25**, 149-155.

Zamir, D. (2001) Improving plant breeding with exotic genetic libraries. *Nature Reviews Genetics*, **2**, 983-989.

Zhou, X.H., Qian, C.T., Lou, Q.F. and Chen, J.F. (2009) Molecular analysis of introgression lines from *Cucumis hystrix* Chakr. to *C. sativus* L. *Scientia Horticulturae*, **119**, 232-235.

Appendix I

Primers

Primer name	Accession number	Primer Orientation	Sequence 5'-3'
aconitase 1	TC171686	fwd	CATGAACAACCTTGGCAGTG
		rev	GCAGCTTCTGCCTCAATACC
aconitase 2	TC185608	fwd	TCCACAAAGATAGCCCTGCT
		rev	TCCCATTCCTACCAAGTTGC
aminobutyrate transaminase 1	TC193582	fwd	GGGGGATATGTGGTGTCATC
		rev	TCATGACCCTTGAACCCTTT
aminobutyrate transaminase 2	TC191531	fwd	GCATGGTATGTTGGTGAGTTTT
		rev	TGACACAATTTATTCAAATGTTGCT
aminobutyrate transaminase 3	TC200790	fwd	GGGAAGCTGAGGCATATGTT
		rev	TCGCTAACGATTTGTTTTTGC
arginase 1	TC191508	fwd	TCAGCGATTGCCTTCTTTTT
		rev	TACTGCCACACCACATAGCC
arginase 2	TC191508	fwd	TCAGCGATTGCCTTCTTTTT
		rev	TACTGCCACACCACATAGCC
argininosuccinate synthase 1	TC191541	fwd	CGTGGATGTTGACTGTTTGG
		rev	CCCTTGCCATAGGAAACTGA
argininosuccinate synthase 2	TC216958	fwd	GGTCCGTTTTGAGCTGACAT
		rev	GTGCATCTTGGGGATCAACT
asparagine synthetase 1	TC212203	fwd	GGAGCAACCGTATCTTCCAA
		rev	GCAACACCGGATAGATGGTT
asparagine synthetase 2	TC215883	fwd	AATTCTCATGCCAAGCGTTC
		rev	CCCGGGTATCAAGAAGAACA
aspartate aminotransferase	TC172935	fwd	ACAATGGAAAACCCGTGGTA
		rev	TCATTGCAGCAAAGTCCAAG
citrate synthase	TC180568	fwd	TGGTCTTGATCTGCGTTCTG
		rev	TCTTTTGATGGCACCTTTCC
fumarase	TC180884	fwd	AACCCACACACAAGATGCAA
		rev	GGAAGCAGCCACGGTATTTA
glutamate decarboxylase 1	TC191731	fwd	TGTCACTGCTGAGGAAGTGC
		rev	TTATGCCCGGATTGATTCAT
glutamate decarboxylase 2	TC207914	fwd	TTCTCTCAAAGTCGTTCCGTCT
		rev	GCTTATCACATTCTGGTTCCAT
glutamate dehydrogenase 1	TC169938	fwd	CAGGGTACAGCACGACAATG
		rev	CCACCGAGATCAACAGGTTT
glutamate dehydrogenase 2	TC171636	fwd	GAGGCTGCTAACCATCCAAC
		rev	TCATTCTTACGCCTCCCATC

glutamate synthase 1	TC171518	fwd	AAGGCAGGCAAGGGATACTT
		rev	AGCATTGCCAAATCATAGGC
glutamate synthase 2	TC171380	fwd	TTCATGGGGAGTTGCTAACC
		rev	TCCCAAATAAGGGAACCTCA
imidazoleglycerol-phosphate dehydratase	TC195065	fwd	GAACTGGTGTTGCGGAGAAT
		rev	CTGTCGAATATGGAGCGTCA
imidazoleglycerol-phosphate synthase	TC192372	fwd	GGCTGGAATGCACTTGAAAT
		rev	CCGCTTTGCAAGTTTAGAGG
isocitrate dehydrogenase 1	TC170372	fwd	ACTGCACCACCCAAGAAATC
		rev	TGCCTCAAGCACAAAAGTTG
isocitrate dehydrogenase 2	TC172709	fwd	CATTGCTACCGCTCTCTCCA
		rev	ATCGCTCAAAGTAAACAGGTG
isocitrate dehydrogenase 3	TC170664	fwd	GAAAGAATTTGGCGAATCCA
		rev	ATAGACGGTACGGTGCAAGG
isocitrate dehydrogenase 4	TC171366	fwd	TGGTCCGACTAGCAAAATCC
		rev	ATAGGCTCCCGGAAAACAGT
isocitrate dehydrogenase 5	TC195343	fwd	GGTACGAACATCGCCTCATT
		rev	TTGTCATTTTCCCGTTCTCC
malate dehydrogenase 1	TC178560	fwd	TTTCTCCGCCGTAGCTTTTA
		rev	GCCCTAGCTGCTCTTCTCCT
malate dehydrogenase 2	TC178790	fwd	GGGAAAAATGGTGTGGAAGA
		rev	CCATCACAAGTCTGCCAATG
N-acetylglutamate kinase 1	TC211604	fwd	TGATCCCCAAGGTGAATTGT
		rev	GGATGGGACCATTATCAAACA
N-acetylglutamate kinase 2	TC197078	fwd	ATGCATTGACCCCCATTAAA
		rev	CTCCCGGGTAAGATTGAACA
N-acetylglutamate synthase 1	TC216183	fwd	TCTTCCAACTCCACCTACCC
		rev	AAGGCCATGCTTCTCTGAAA
N-acetylglutamate synthase 2	TC208234	fwd	TTCAACGAGTTCACCTGCTG
		rev	GCAATAGCAGCAACCTCTCC
N2-acetylornithine aminotransferase	TC195519	fwd	CAAAACGCCTGGTTGCTAAT
		rev	AGGCAGTCCTCAGTGCTTGT
ornithine aminotransferase	TC209829	fwd	GCTAAGGGTTCATCCGTCTG
		rev	TGGAGATTGCAGCCAATGTA
2-oxoglutarate dehydrogenase 1	TC186215	fwd	ACGGAGCATCAAGTGAGGAC
		rev	TGGCACCATCTTAGTGCTTG
2-oxoglutarate dehydrogenase 2	TC171677	fwd	CTGAGAAGGGAACCGACAAA
		rev	AGAGAGGAGAGGGGGAAGAA
phosphoenolpyruvate carboxykinase	TC192889	fwd	GGCTGCAATATGGGAAAAGA
		rev	TTTGGATGAGGACCAACACA
proline dehydrogenase 1	TC209088	fwd	GAGGAAACATCGCCGACTAC
		rev	AGATTTTGGCTCCACTCTGG
proline dehydrogenase 2	TC200139	fwd	TCTGCCTTCGATAGACAACTCA
		rev	AACCAATTACAAAAGTTGGAATAAA

1-pyrroline-5-carboxylate dehydrogenase	TC200529	fwd	GTAGCTCAAGGGTGGCAGAG
		rev	AATTTCTTCGCATGGTCCAG
pyrroline-5-carboxylate reductase	TC193973	fwd	TCATCACTTTGGGGGAAAAG
		rev	GCAGCAACAACTGCATTCAT
1-pyrroline-5-carboxylate synthetase	TC210828	fwd	TTTGAGTCACGACCTGATGC
		rev	GCGCTTAGCCATATCCATGT
succinate dehydrogenase 1	TC181935	fwd	TTTATAGGGTTCAGTCATCTTCG
		rev	AGTCCATTACAGCCGTCGAT
succinate dehydrogenase 2	TC183268	fwd	TCATGGATAGCCGTGATGAATA
		rev	GCACCTTTCATCTCAAATTCAA
succinate dehydrogenase 3	TC187517	fwd	GAGGGTGAGCGATTTATGGA
		rev	GTCCAGGGATCACAGCATCT
succinate-semialdehyde dehydrogenase	TC193174	fwd	AGTTGGTGTTGTTGGTGCAA
		rev	GCATTACCGCCTAGCTCAAG
succinyl Co A 1	TC172461	fwd	GCTGGACTAACTGCTCCTCCT
		rev	TTTGGGACTTCTGAATGATGC
succinyl Co A 2	TC172461	fwd	ATTTTGGGTTGATCCGAATG
		rev	CAGCGAGTGTTGGATTGCTA
ubiquitin	TC170478	fwd	GTGAAGGCCAAAATTCAGGA
		rev	GAACAAGGTGCAGGGTTGAT

Appendix II

Metabolite content

	metabolite content (nmol mg dry weight^{-1})			
	30 DAA	40 DAA	55 DAA	65 DAA
Citrate	126.05±7.88	127.53±8.58	255.76±26.10	285.25±23.93
Malate	102.14±5.45	87.77±7.95	143.83±32.27	173.52±33.32
Fumarate	0.21±0.02	0.37±0.06	0.28±0.06	0.18±0.05
Aspartate	0.68±0.12	0.44±0.03	1.66±0.25	3.29±0.96
Cysteine	0.06±0.02	0.03±0.00	-	-
Glutamate	0.95±0.14	0.62±0.05	4.42±0.68	2.31±1.17
Asparagine	2.19±0..69	0.60±0.20	1.39±0.03	2.20±0.45
Serine	0.70±0.22	0.19±0.03	0.20±0.04	0.25±0.04
Glutamine	9.24±2.41	2.20±0.60	4.80±0.71	8.97±1.90
Glycine	0.12±0.03	0.03±0.01	-	-
Threonine	0.48±0.13	0.11±0.02	-	-
Histidine/Methionine	0.34±0.10	0.06±0.01	-	-
Alanine	0.30±0.10	0.15±0.02	0.25±0.10	0.45±0.08
Tyrosine	0.24±0.08	0.04±0.01	0.07±0.03	0.13±0.04
Arginine	0.12±0.04	0.02±0.01	0.04±0.01	0.05±0.02
Trytophan/Methionine	0.07±0.02	0.02±0.00	-	-
Valine	0.47±0.12	0.12±0.03	0.05±0.01	0.06±0.01
Phenylalanine	0.51±0.14	0.11±0.03	0.14±0.02	0.19±0.04
Isoleucine	0.41±0.11	0.08±0.02	-	-
Leucine	0.21±0.07	0.05±0.01	-	-
Lysine	0.12±0.04	0.04±0.01	-	-
Glycine/Threonine	-	-	0.10±0.02	0.14±0.02
Histidine	-	-	0.14±0.02	0.17±0.02
Tryptophan	-	-	0.05±0.01	0.08±0.01
Methionine	-	-	0.03±0.01	0.06±0.01
Isoleucine/Lysine	-	-	0.03±0.01	0.03±0.01
GABA	-	-	0.29±0.10	0.35±0.08

Table 1. Organic and amino acid content in the recurrent parent line (M82). Data presented is mean ± SEM (n=6) in nmoles mg DW^{-1}. – = not detected. DAA: days after anthesis.

Appendix III

Cluster data

Cluster 1

Days Post Anthesis

Annotation

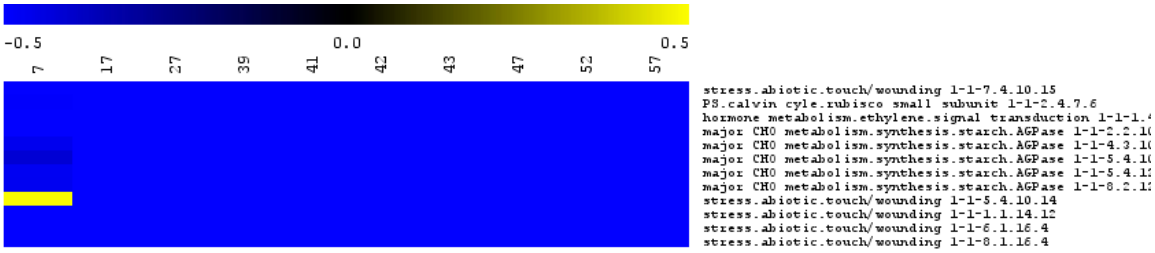

Cluster 2

Days Post Anthesis

Annotation

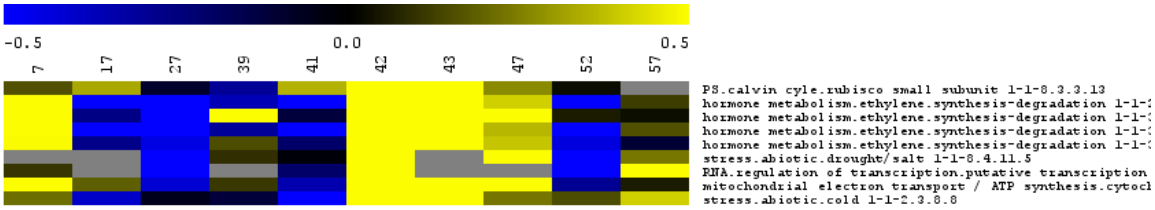

Cluster 3

Days Post Anthesis

Annotation

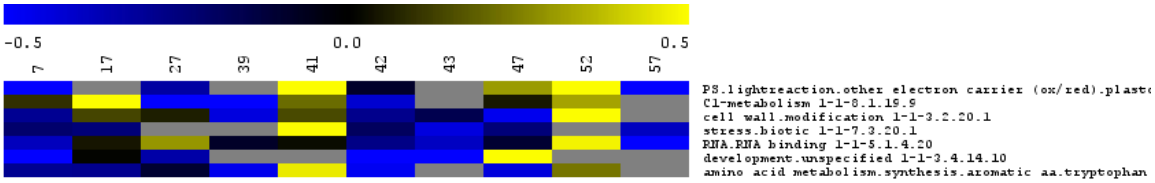

Cluster 4

Days Post Anthesis

Annotation

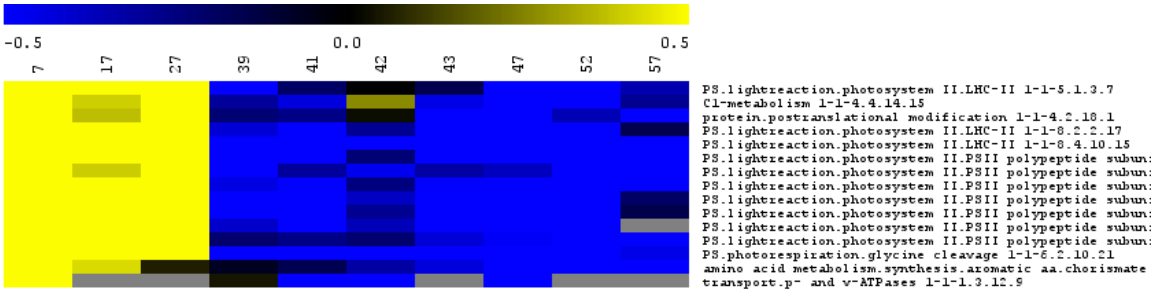

Cluster 5

Days Post Anthesis

Annotation

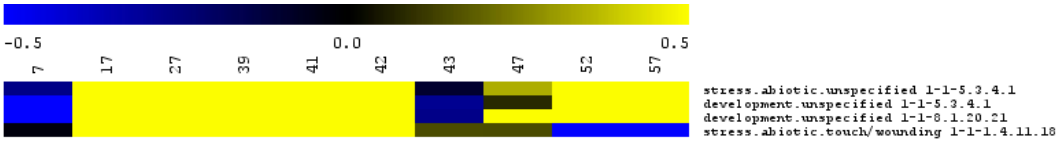

Cluster 6

Days Post Anthesis

Annotation

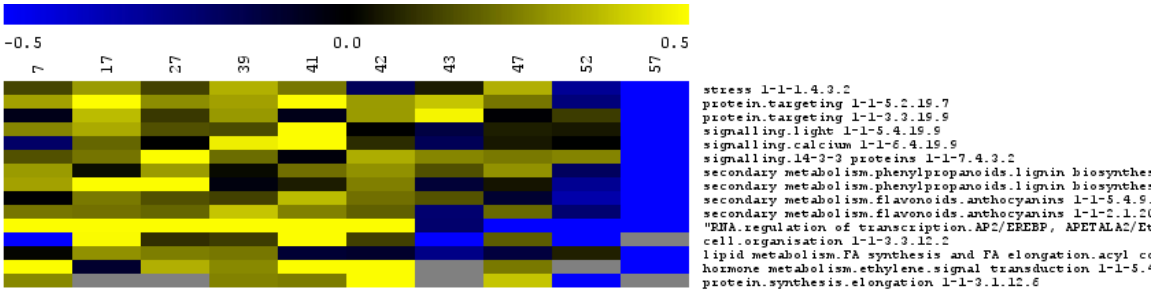

Cluster 7

Days Post Anthesis

Annotation

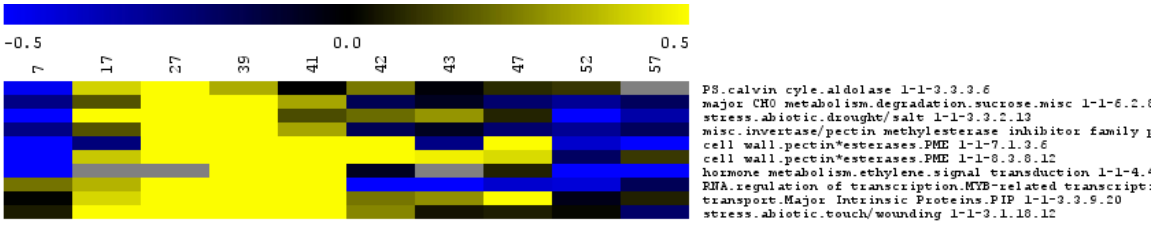

Cluster 8

Days Post Anthesis

Annotation

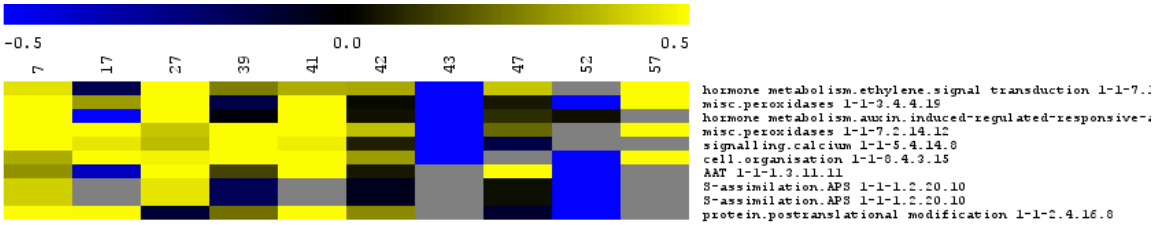

Cluster 9

Days Post Anthesis

Annotation

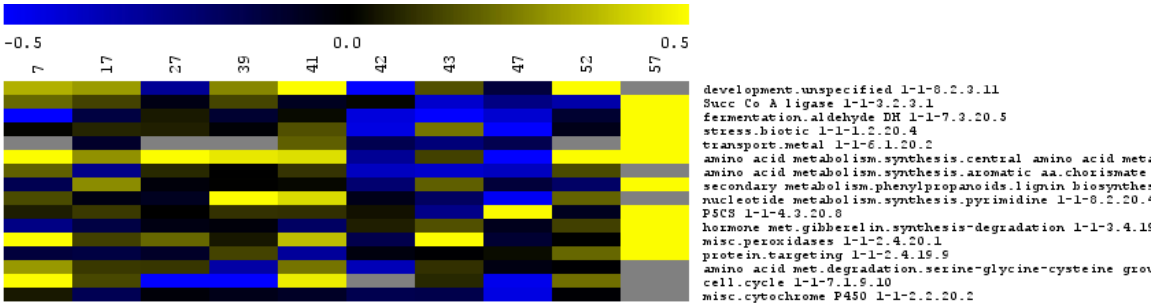

Cluster 10

Days Post Anthesis

Annotation

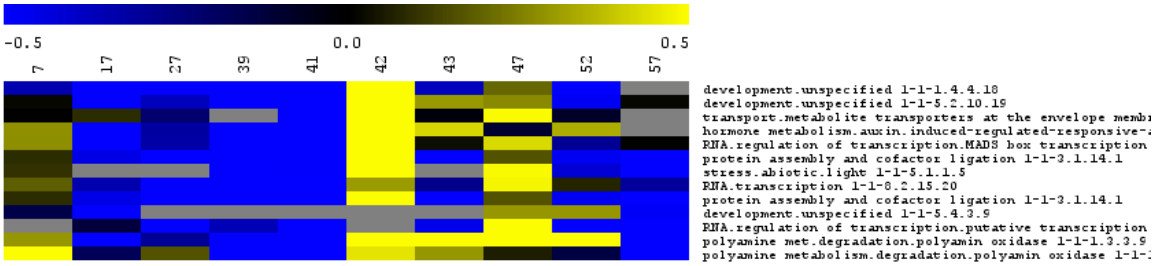

Cluster 11

Days Post Anthesis

Annotation

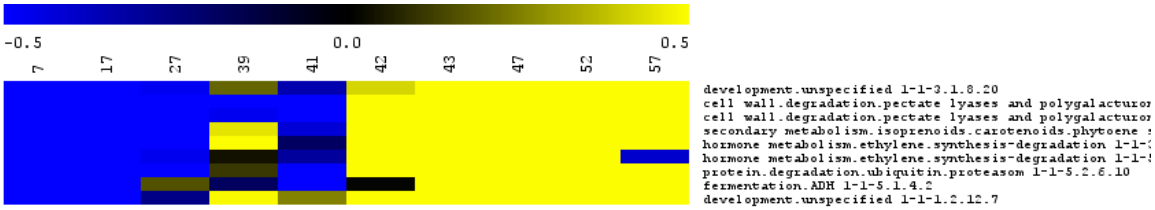

Cluster 12

Days Post Anthesis

Annotation

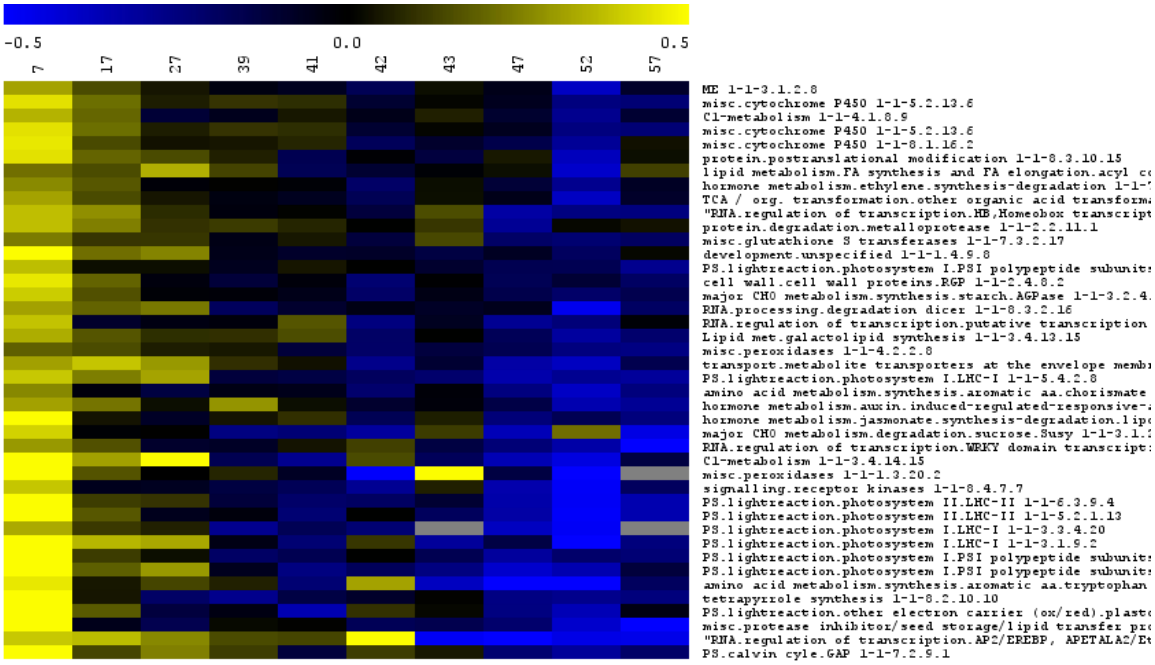

Cluster 13

Days Post Anthesis

Annotation

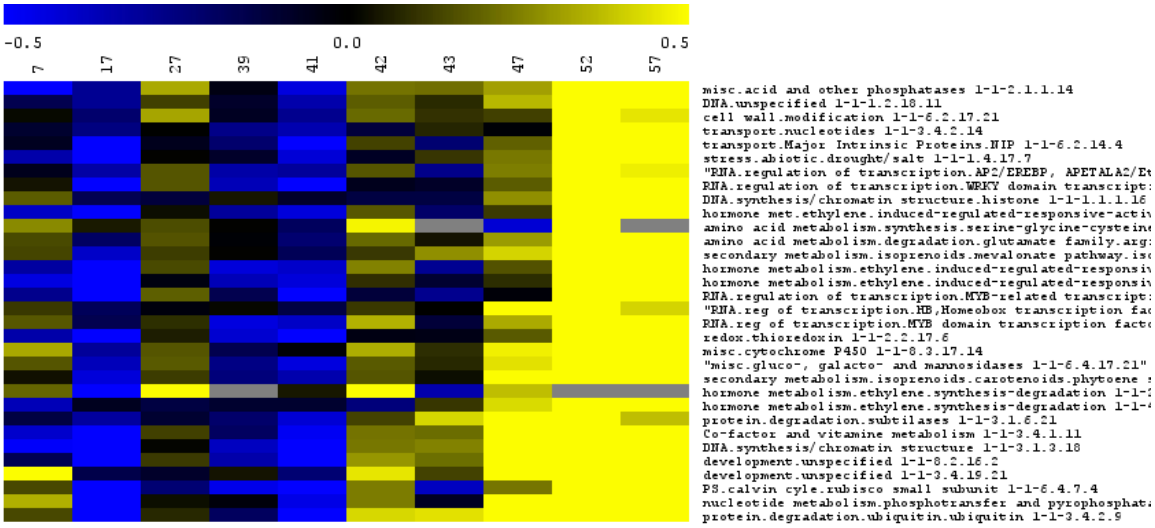

Cluster 14

Days Post Anthesis

Annotation

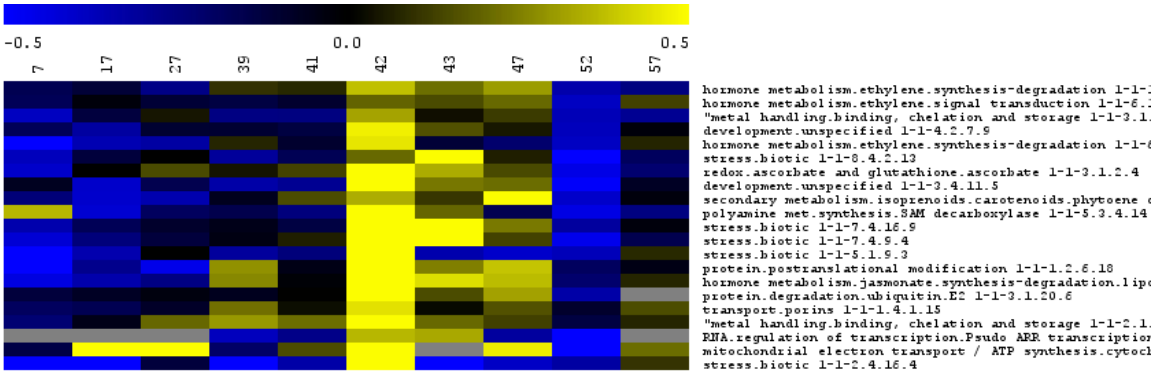

Cluster 15

Days Post Anthesis

Annotation

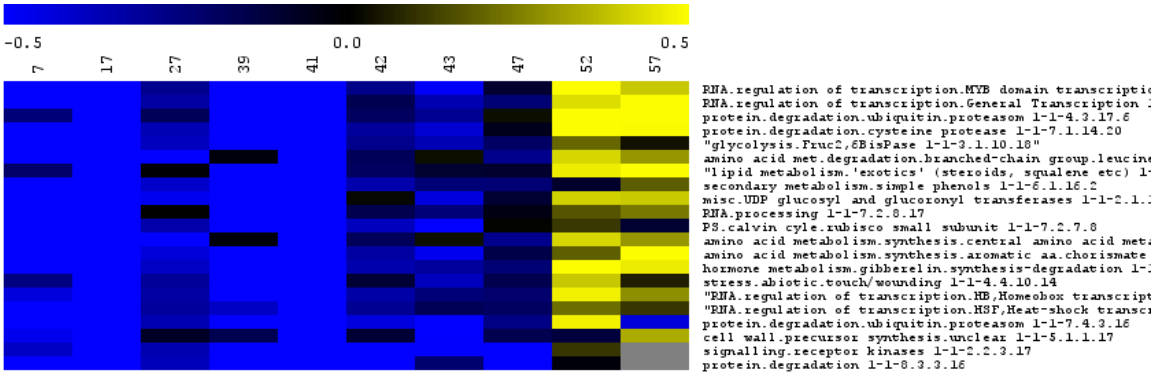

Cluster 16

Days Post Anthesis

Annotation

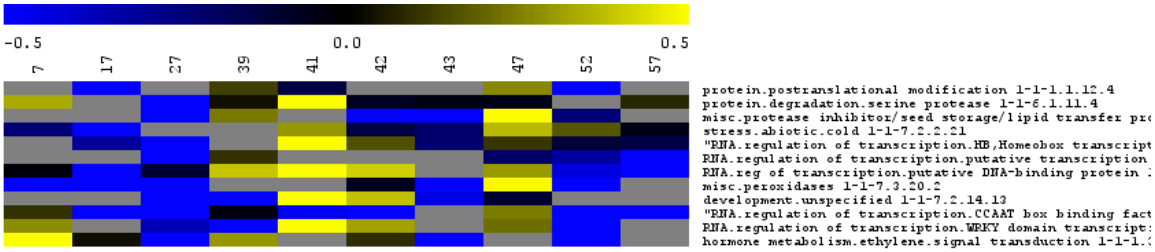

Cluster 17

Days Post Anthesis

Annotation

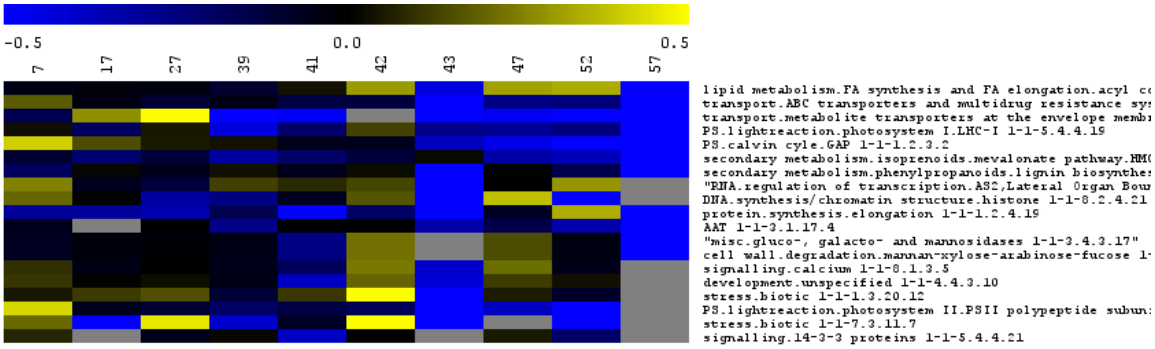

Cluster 18

Days Post Anthesis

Annotation

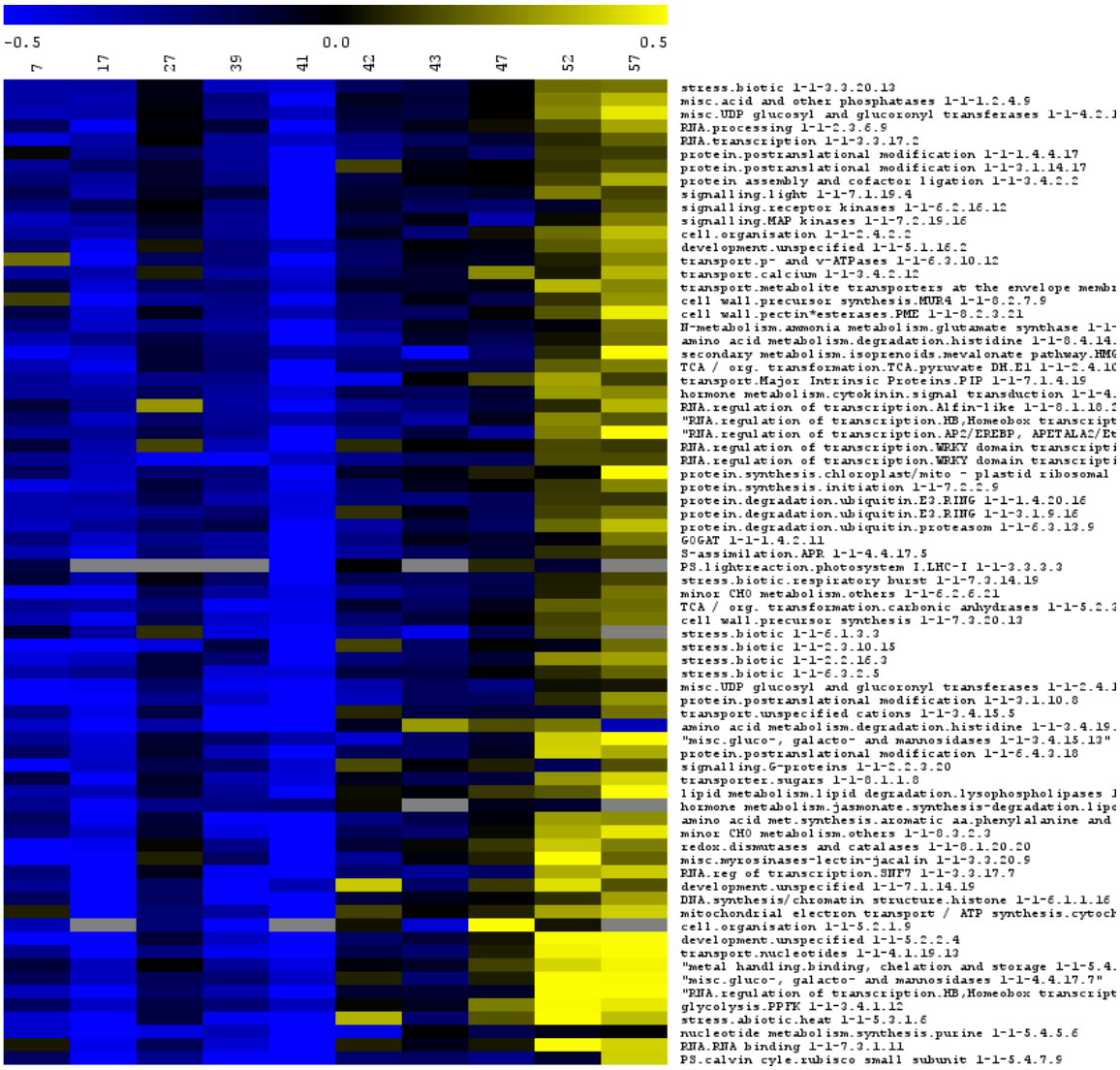

Cluster 19

Days Post Anthesis

Annotation

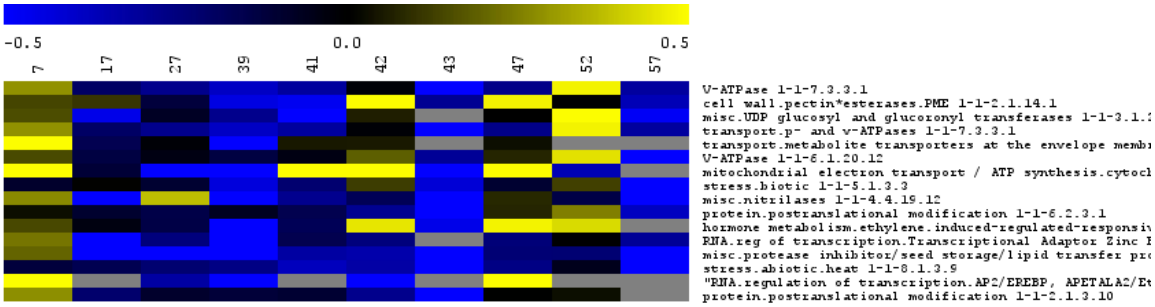

Cluster 20

Days Post Anthesis

Annotation

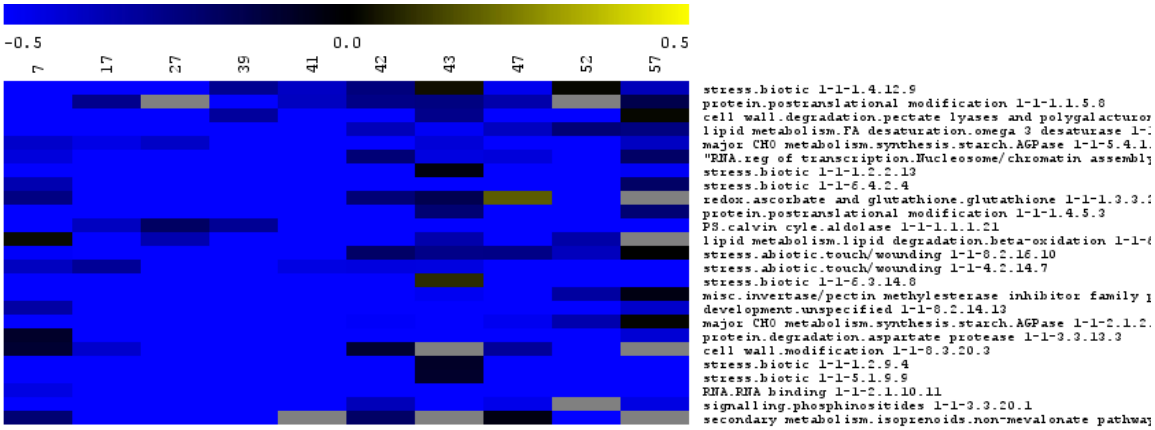

Cluster 21

Days Post Anthesis

Annotation

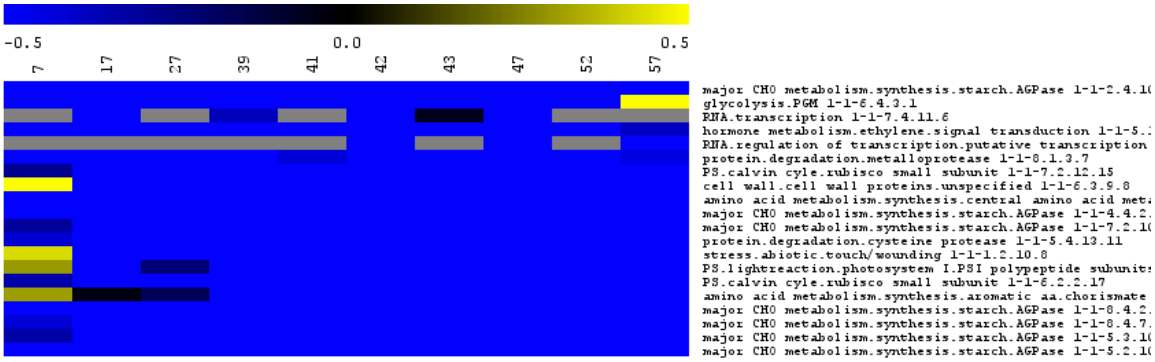

Cluster 22

Days Post Anthesis

Annotation

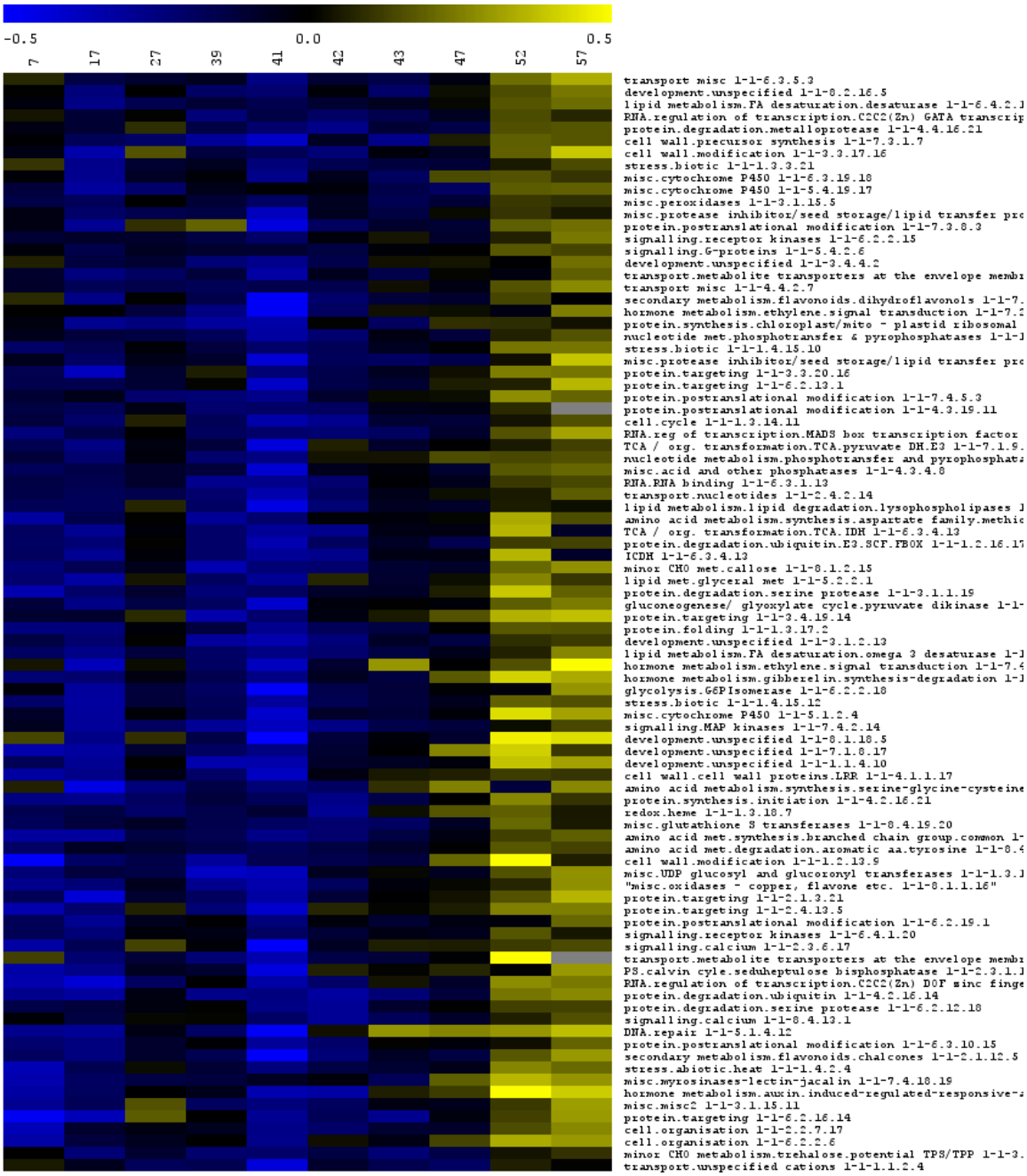

Cluster 23

Days Post Anthesis

Annotation

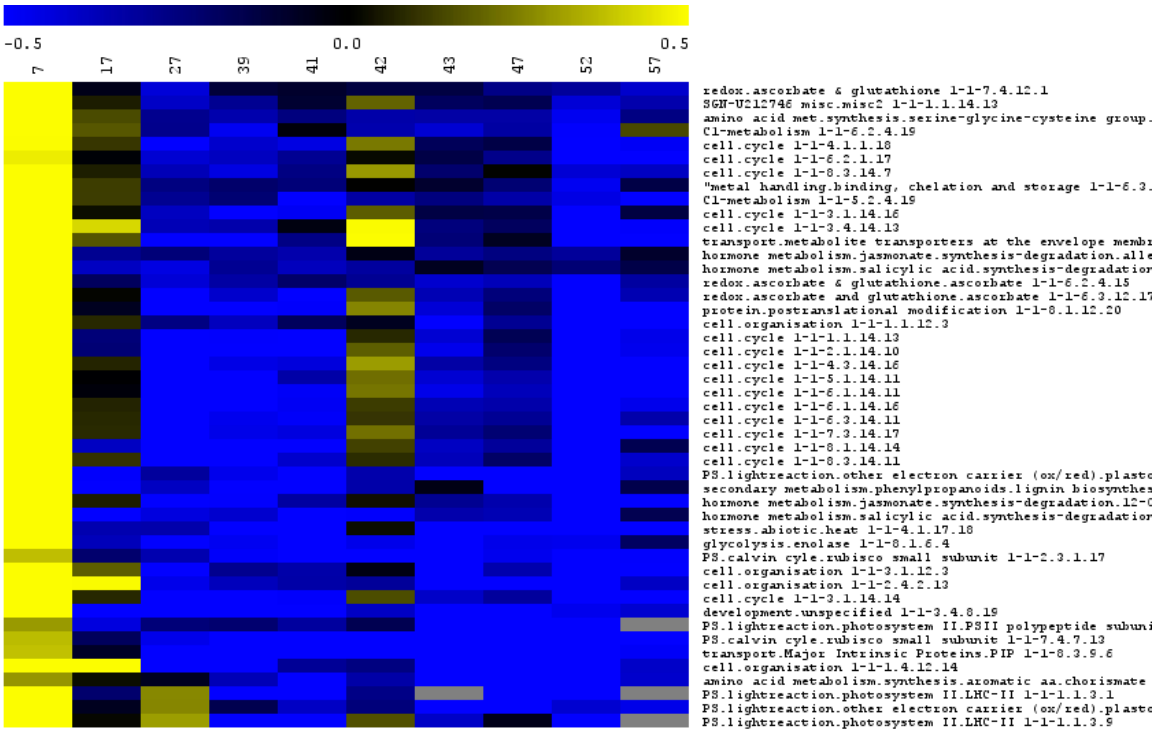

Cluster 24

Days Post Anthesis

Annotation

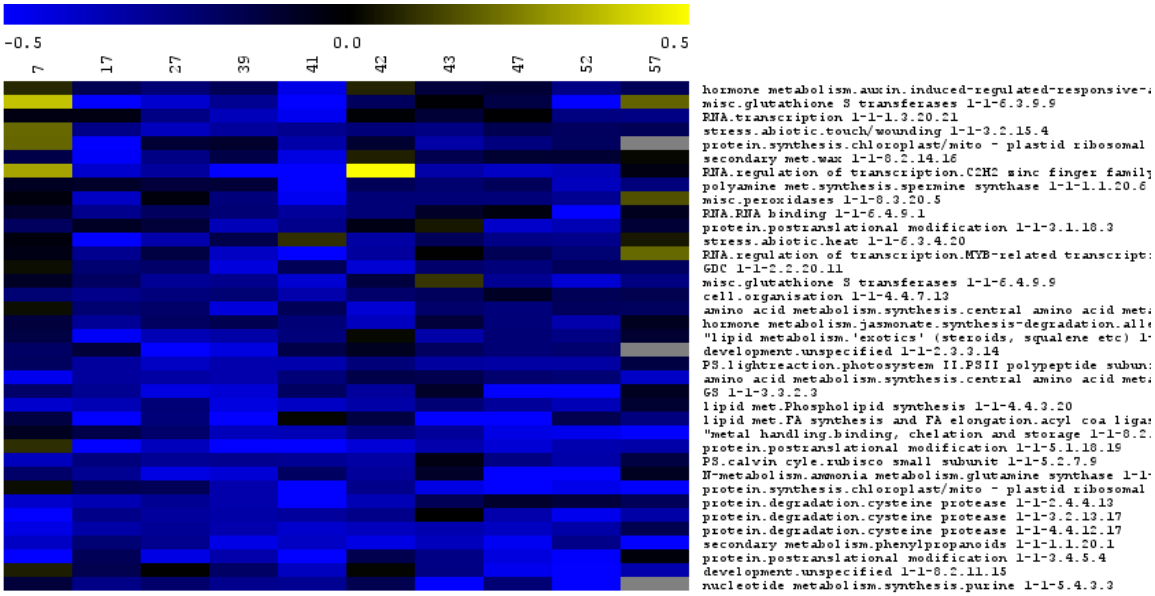

Cluster 25

Days Post Anthesis

Annotation

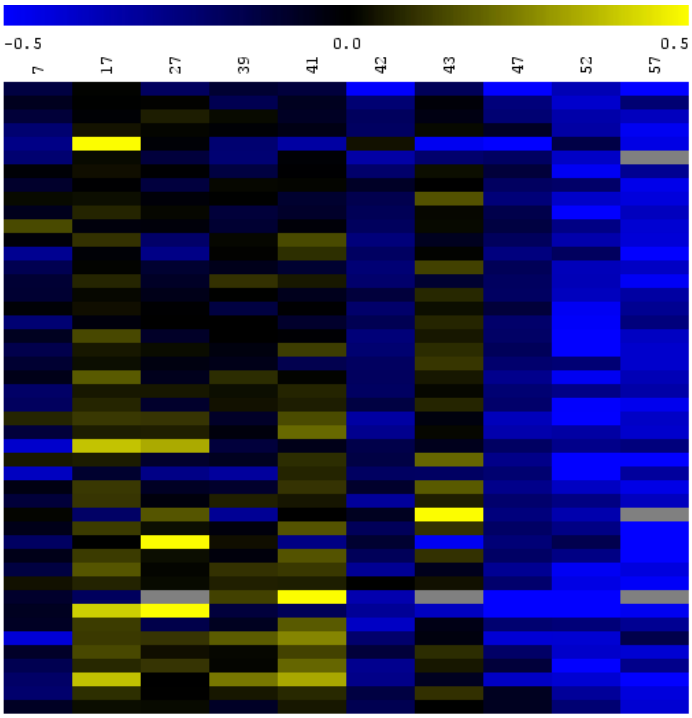

transport.NDP-sugars at the ER 1-1-7.4.20.5
stress.biotic 1-1-3.2.10.20
"misc.oxidases - copper, flavone etc. 1-1-7.3.7.17"
protein.postranslational modification 1-1-8.3.11.18
development.unspecified 1-1-2.3.20.12
transporter.sugars 1-1-6.2.4.20
amino acid metabolism.degradation.aromatic aa.tyrosine
secondary metabolism.phenylpropanoids.lignin biosynthes
hormone metabolism.abscisic acid.synthesis-degradation
hormone metabolism.abscisic acid.synthesis-degradation
transport.Major Intrinsic Proteins.PIP 1-1-2.4.4.16
transport.Major Intrinsic Proteins.PIP 1-1-2.4.7.13
nucleotide metabolism.synthesis.purine 1-1-6.3.11.6
RNA.regulation of transcription.C3H zinc finger family
Co-factor and vitamin met 1-1-8.4.17.8
SGN-U224672 misc.alcohol DHs 1-1-6.4.2.9
secondary met.N misc.alkaloid-like 1-1-3.3.6.4
protein.degradation.aspartate protease 1-1-6.4.13.2
"lipid metabolism.'exotics' (steroids, squalene etc) 1-
secondary metabolism.simple phenols 1-1-8.4.18.17
secondary metabolism.phenylpropanoids 1-1-1.4.18.11
protein.postranslational modification 1-1-3.1.9.20
protein.postranslational modification 1-1-8.4.6.16
signalling.MAP kinases 1-1-6.1.10.6
development.unspecified 1-1-6.2.13.14
transport.ABC transporters and multidrug resistance sys
PS.photorespiration.glycolate oxydase 1-1-8.4.4.13
hormone metabolism.abscisic acid.synthesis-degradation
stress.abiotic.touch/wounding 1-1-8.2.17.4
"RNA.regulation of transcription.HB,Homeobox transcript
RNA.regulation of transcription.AT-rich interaction dom
"RNA.regulation of transcription.bHLH,Basic Helix-Loop-
glycolysis.phosphoglycerate mutase 1-1-5.3.1.17
stress.biotic 1-1-1.2.20.9
glycolysis.phosphoglycerate mutase 1-1-5.3.1.17
misc.cytochrome P450 1-1-8.4.6.3
protein.postranslational modification 1-1-5.1.11.5
"RNA.regulation of transcription.HB,Homeobox transcript
development.unspecified 1-1-1.4.10.2
minor CHO metabolism.others 1-1-5.3.8.5
"misc.oxidases - copper, flavone etc. 1-1-4.3.10.1"
minor CHO metabolism.others 1-1-6.3.9.19
RNA.processing 1-1-4.2.10.6
transport.potassium 1-1-6.2.10.5
hormone metabolism.jasmonate.synthesis-degradation.alle
transport.p- and v-ATPases 1-1-2.3.10.1

Cluster 26

Days Post Anthesis

Annotation

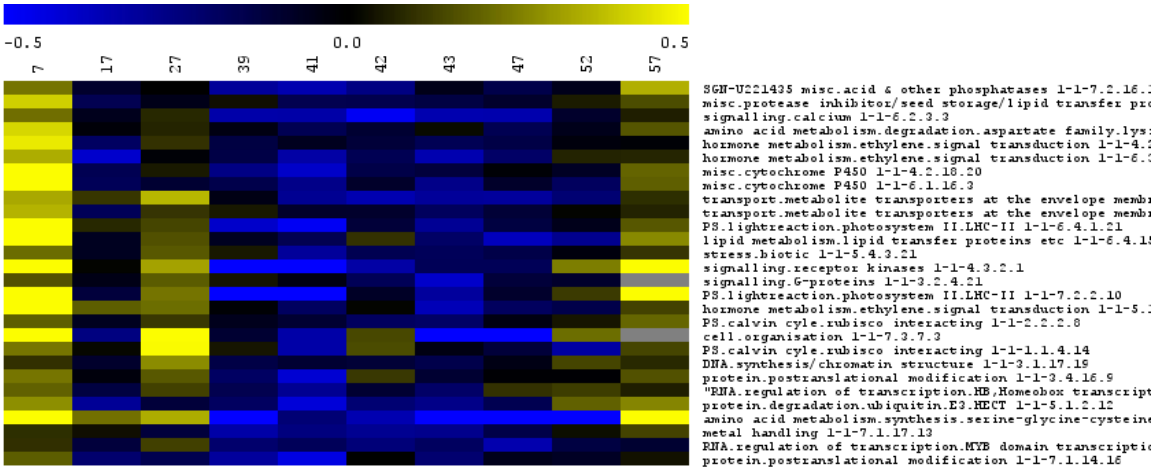

Cluster 27

Days Post Anthesis

Annotation

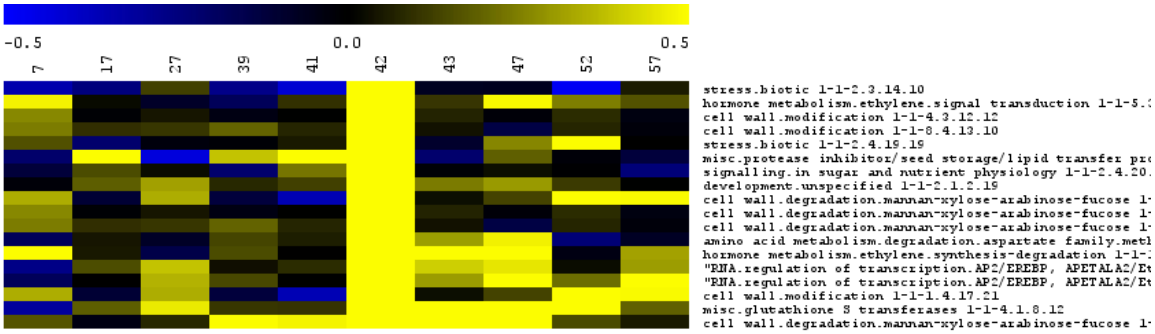

Cluster 28

Days Post Anthesis

Annotation

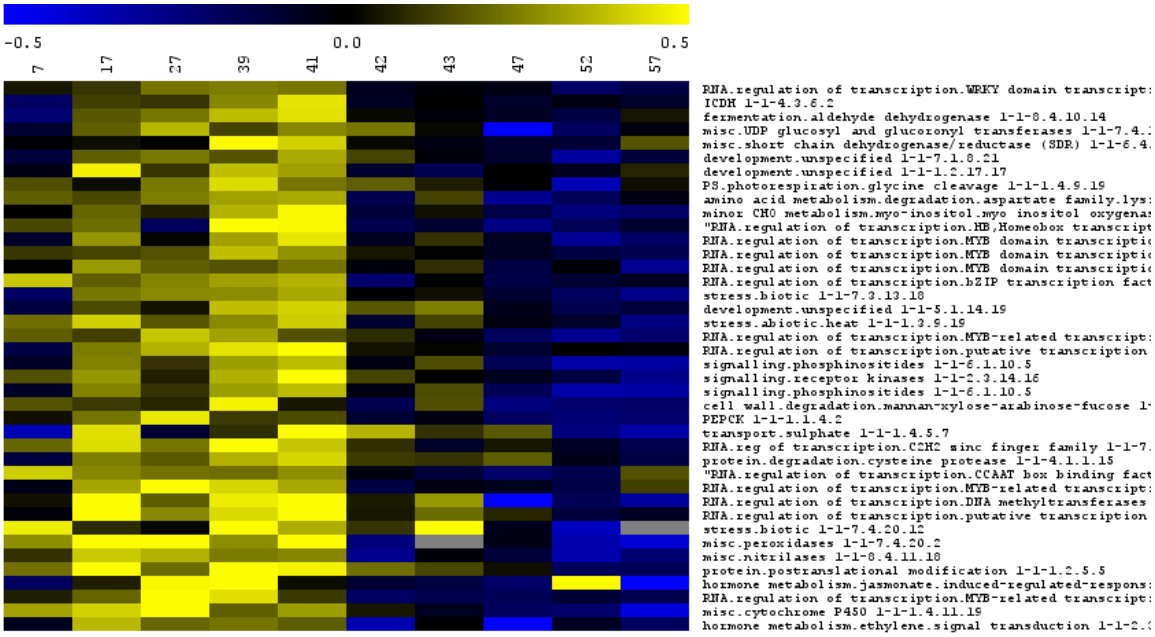

Cluster 29

Days Post Anthesis

Annotation

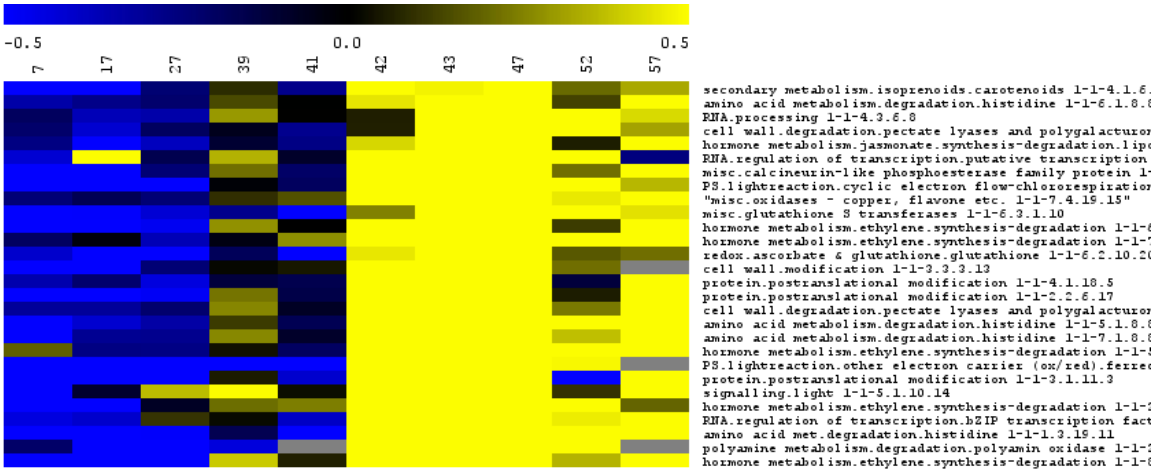

Cluster 30

Days Post Anthesis

Annotation

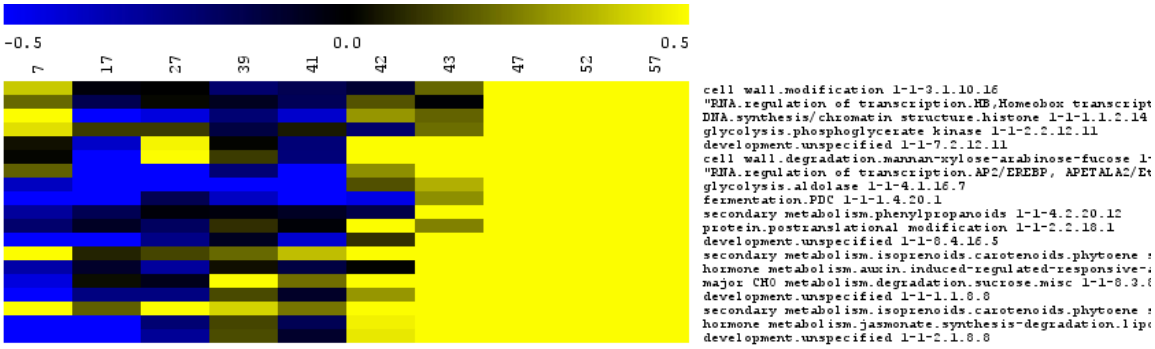

Cluster 31

Days Post Anthesis

Annotation

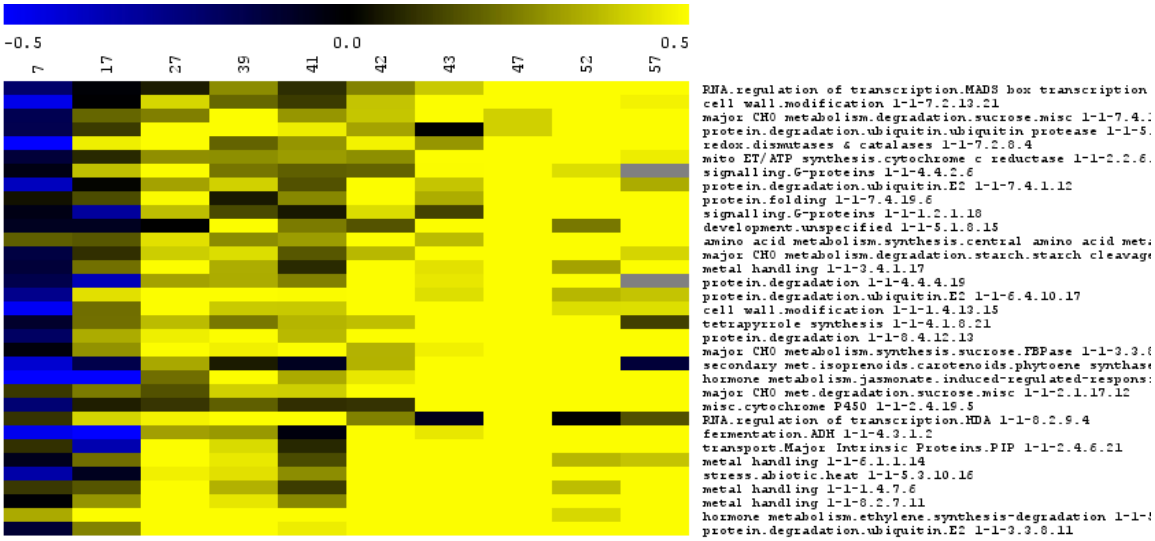

Cluster 32

Days Post Anthesis

Annotation

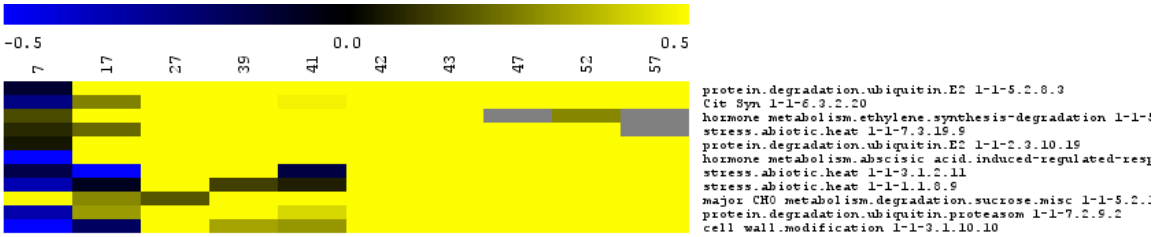

Cluster 33

Days Post Anthesis

Annotation

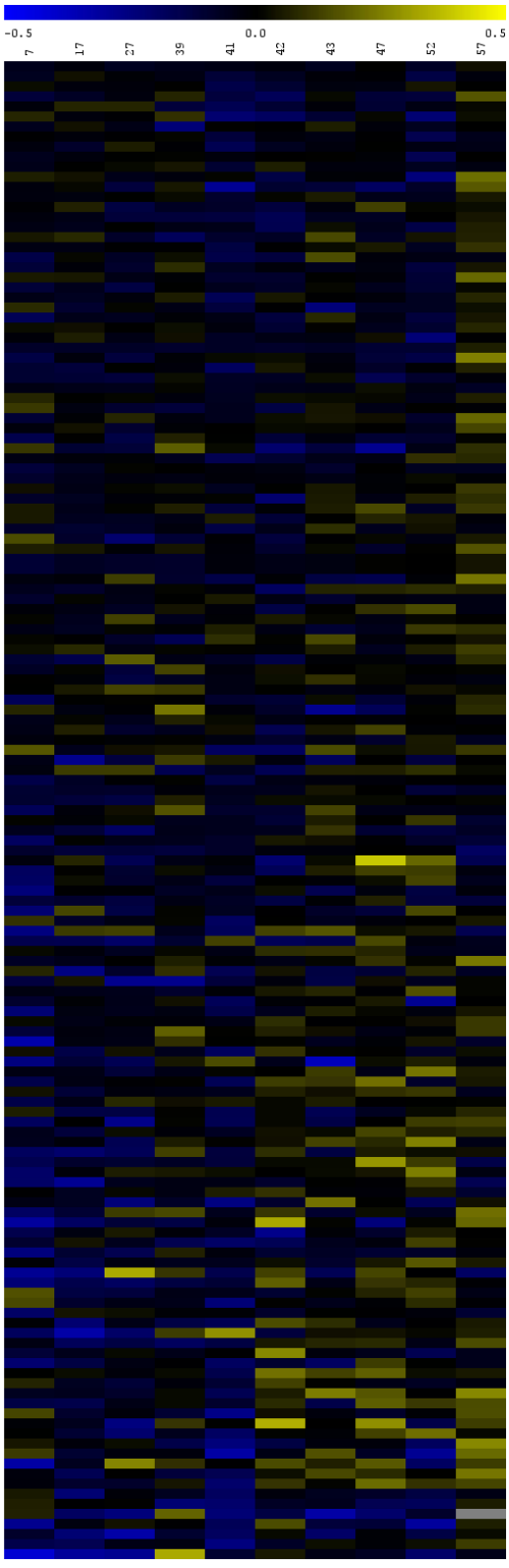

protein.posttranslational modification 1-1-4.4.16.3
protein.posttranslational modification 1-1-6.14.11.8
"RNA.regulation of transcription.G2-like transcription
"RNA.regulation of transcription.HB,Homeobox transcript
protein.synthesis.initiation 1-1-6.4.20.15
protein.degradation.ubiquitin 1-1-7.3.20.20
protein.degradation.ubiquitin.proteasom 1-1-7.4.17.5
protein.degradation.ubiquitin.E3.SCF.SKP 1-1-8.1.11.11
protein.degradation.metalloprotease 1-1-5.2.10.7
AAT 1-1-5.1.6.8
GS 1-1-8.4.4.4
P5CR 1-1-8.1.15.4
M-met.misc 1-1-6.2.7.17
RNA.processing 1-1-3.2.4.17
not assigned.no ontology.C2 domain-containing protein 1
mito electron transport / ATP synthesis.NADH-DH.localis
minor CHO metabolism.others 1-1-6.2.13.9
tetrapyrrole synthesis 1-1-3.2.2.13
redox.ascorbate and glutathione.ascorbate 1-1-6.4.6.14
misc.cytochrome P450 1-1-7.3.20.15
"misc.gluco-, galacto- and mannosidases 1-1-3.3.13.7"
RNA.processing 1-1-8.4.2.4
protein.posttranslational modification 1-1-4.3.20.17
development.unspecified 1-1-2.3.15.3
transport.potassium 1-1-7.3.15.1
transport.protein transport mitochondrial membrane (TIM
transport.phosphate 1-1-2.4.14.10
PS.lightreaction.other electron carriex (ox/red).plastc
TCA / org. transformation.TCA.pyruvate DH.E3 1-1-7.3.11
hormone metabolism.gibberelin.signal transduction 1-1-5
major CHO metabolism.synthesis.starch.AGPase 1-1-4.3.16
RNA.regulation of transcription.C2HC zinc finger family
RNA.regulation of transcription.C2HC zinc finger family
protein.synthesis.initiation 1-1-1.2.2.10
"RNA.reg of transcription.bHLH,Basic Helix-Loop-Helix f
"lipid metabolism.'exotics' (steroids, squalene etc) 1-
tetrapyrrole synthesis 1-1-7.2.13.13
stress.biotic 1-1-5.1.20.18
nucleotide metabolism.phosphotransfer and pyrophosphat
cell.cycle 1-1-5.1.14.16
transport.Major Intrinsic Proteins.PIP 1-1-6.2.14.13
hormone metabolism.gibberelin.synthesis-degradation 1-1
hormone metabolism.jasmonate.synthesis-degradation.lipc
"RNA.regulation of transcription.HB,Homeobox transcript
RNA.regulation of transcription.MADS box transcription
"RNA.regulation of transcription.AP2/EREBP, APETALA2/Et
RNA.regulation of transcription.bZIP transcription fact
protein.synthesis.chloroplast/mito - plastid ribosomal
protein.degradation.cysteine protease 1-1-6.2.13.8
PEPCK 1-1-2.3.11.20
glycolysis.PEPCase 1-1-2.11.20
mitochondrial electron transport / ATP synthesis.cytoch
tetrapyrrole synthesis 1-1-7.3.2.9
stress.biotic 1-1-2.4.2.3
nucleotide metabolism.phosphotransfer and pyrophosphat
misc.cytochrome P450 1-1-5.2.12.10
misc.UDP glucosyl and glucoronyl transferases 1-1-3.2.1
"misc.oxidases - copper, flavone etc. 1-1-1.1.10.16"
RNA.processing 1-1-1.4.2.15
DNA.synthesis/chromatin structure 1-1-7.4.10.11
protein.posttranslational modification 1-1-5.4.13.2
signalling.calcium 1-1-7.3.2.14
development.unspecified 1-1-3.1.15.1
lipid metabolism.lipid degradation.beta-oxidation.enoyl
amino acid metabolism.synthesis.serine-glycine-cysteine
secondary metabolism.phenylpropanoids.lignin biosynthes
RNA.regulation of transcription.C2HC zinc finger family
"RNA.regulation of transcription.HB,Homeobox transcript
"RNA.regulation of transcription.bHLH,Basic Helix-Loop-
protein.synthesis.initiation 1-1-3.1.12.9
protein.degradation.ubiquitin.E2 1-1-6.1.11.2
protein.degradation.ubiquitin.E3.RING 1-1-2.1.15.12
signalling.G-proteins 1-1-2.4.14.21
amino acid met.synthesis.aromatic aa.chorismate 1-1-6.1
glycolysis.phosphoglycerate mutase 1-1-2.3.13.7
glycolysis.glyceraldehyde 3-phosphate dehydrogenase 1-1
stress.biotic 1-1-7.4.12.13
redox.ascorbate and glutathione.glutathione 1-1-6.1.4.6
misc.cytochrome P450 1-1-3.4.16.7
misc.myrosinases-lectin-jacalin 1-1-2.3.20.20
misc.UDP glucosyl and glucoronyl transferases 1-1-2.4.2
DNA.synthesis/chromatin structure 1-1-1.1.2.7
signalling.14-3-3 proteins 1-1-4.1.6.16
cell.organisation 1-1-8.1.6.16
cell.division 1-1-8.2.9.2
development.unspecified 1-1-7.2.16.20
secondary metabolism.isoprenoids.mevalonate pathway.ger
hormone metabolism.ethylene.signal transduction 1-1-3.2
"RNA.regulation of transcription.HB,Homeobox transcript
"RNA.regulation of transcription.HB,Homeobox transcript
"RNA.regulation of transcription.HSF,Heat-shock transcr
RNA.regulation of transcription.WRKY domain transcripti
RNA.regulation of transcription.putative transcription
DNA.synthesis/chromatin structure.histone 1-1-7.4.15.5
protein.degradation.ubiquitin.proteasom 1-1-2.4.4.9
"metal handling.binding, chelation and storage 1-1-2.4.
stress.biotic 1-1-6.2.16.2
misc.cytochrome P450 1-1-7.2.15.12
misc.cytochrome P450 1-1-2.4.12.15
misc.protease inhibitor/seed storage/lipid transfer pro
protein.posttranslational modification 1-1-1.3.6.15
protein.posttranslational modification 1-1-3.4.2.7
protein.posttranslational modification 1-1-6.2.12.19
PS.photorespiration.glycolate oxydase 1-1-6.3.6.15
cell wall.precursor synthesis.UGE 1-1-2.2.13.1
hormone metabolism.gibberelin.synthesis-degradation 1-1
hormone metabolism.gibberelin.synthesis-degradation 1-1
major CHO metabolism.synthesis.starch.AGPase 1-1-3.2.2.
RNA.regulation of transcription.C2HC zinc finger family
V-ATPase 1-1-6.4.10.8
"misc.oxidases - copper, flavone etc. 1-1-8.2.7.15"
mitochondrial electron transport / ATP synthesis.Fl-ATP
tetrapyrrole synthesis 1-1-4.2.10.10
stress.biotic 1-1-4.2.7.16
stress.biotic 1-1-6.2.16.10
stress.biotic 1-1-3.3.4.17
nucleotide metabolism.phosphotransfer and pyrophosphat
misc.cytochrome P450 1-1-4.3.14.13
misc.misc2 1-1-6.1.18.17
signalling.calcium 1-1-1.3.17.6
transporter.sugars 1-1-4.3.1.3
transporter.sugars 1-1-7.4.1.10
hormone metabolism.gibberelin.synthesis-degradation 1-1
"RNA.regulation of transcription.HB,Homeobox transcript
RNA.regulation of transcription.NAC domain transcriptic
"RNA.regulation of transcription.AP2/EREBP, APETALA2/Et
protein.degradation.ubiquitin 1-1-8.4.11.6
3GN-U214783 misc.cytochrome P450 1-1-6.1.9.11
cell wall.modification 1-1-4.2.15.8
misc.UDP glucosyl and glucoronyl transferases 1-1-8.2.2
misc.short chain dehydrogenase/reductase (SDR) 1-1-6.2.
protein.folding 1-1-3.2.2.6
signalling.calcium 1-1-2.4.4.11
cell wall.degradation.mannan-xylose-arabinose-fucose 1-
lipid metabolism.FA synthesis and FA elongation.acyl co
stress.abiotic.drought/salt 1-1-1.3.15.13
mitochondrial electron transport / ATP synthesis.cytoch
protein.posttranslational modification 1-1-4.2.8.2
development.unspecified 1-1-5.4.10.12
development.unspecified 1-1-8.2.8.6
transport.cyclic nucleotide or calcium regulated channe
PS.calvin cyle.rubisco small subunit 1-1-8.4.7.4
signalling.G-proteins 1-1-2.4.10.12
"lipid metabolism.'exotics' (steroids, squalene etc) 1-
"misc.gluco-, galacto- and mannosidases 1-1-8.4.4.20"
protein.posttranslational modification 1-1-5.3.8.12
signalling.MAP kinases 1-1-4.2.18.3
signalling.G-proteins 1-1-7.2.15.5
transport misc 1-1-5.4.8.18

Cluster 34

Days Post Anthesis

Annotation

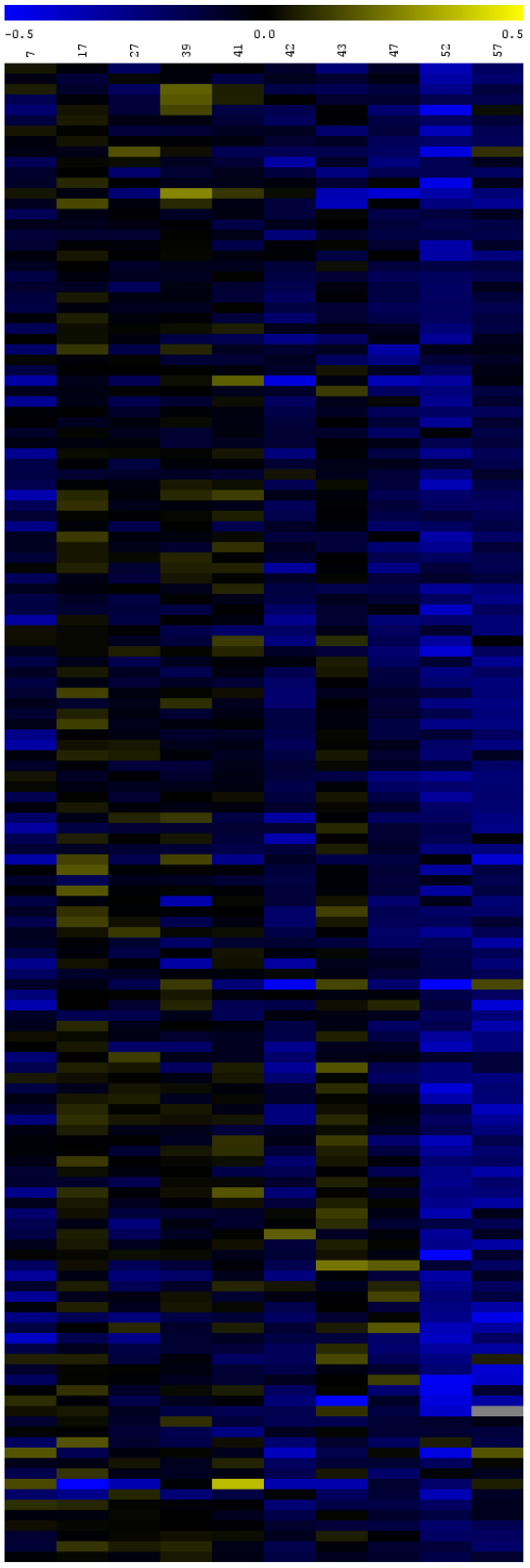

Cluster 35

Days Post Anthesis

Annotation

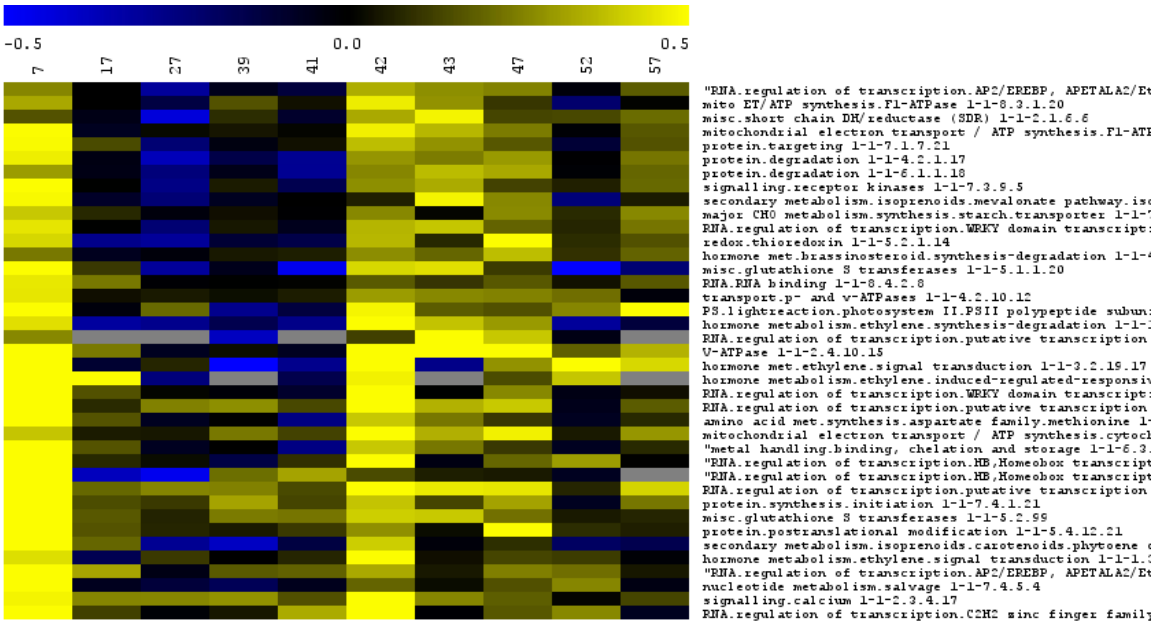

Cluster 36

Days Post Anthesis

Annotation

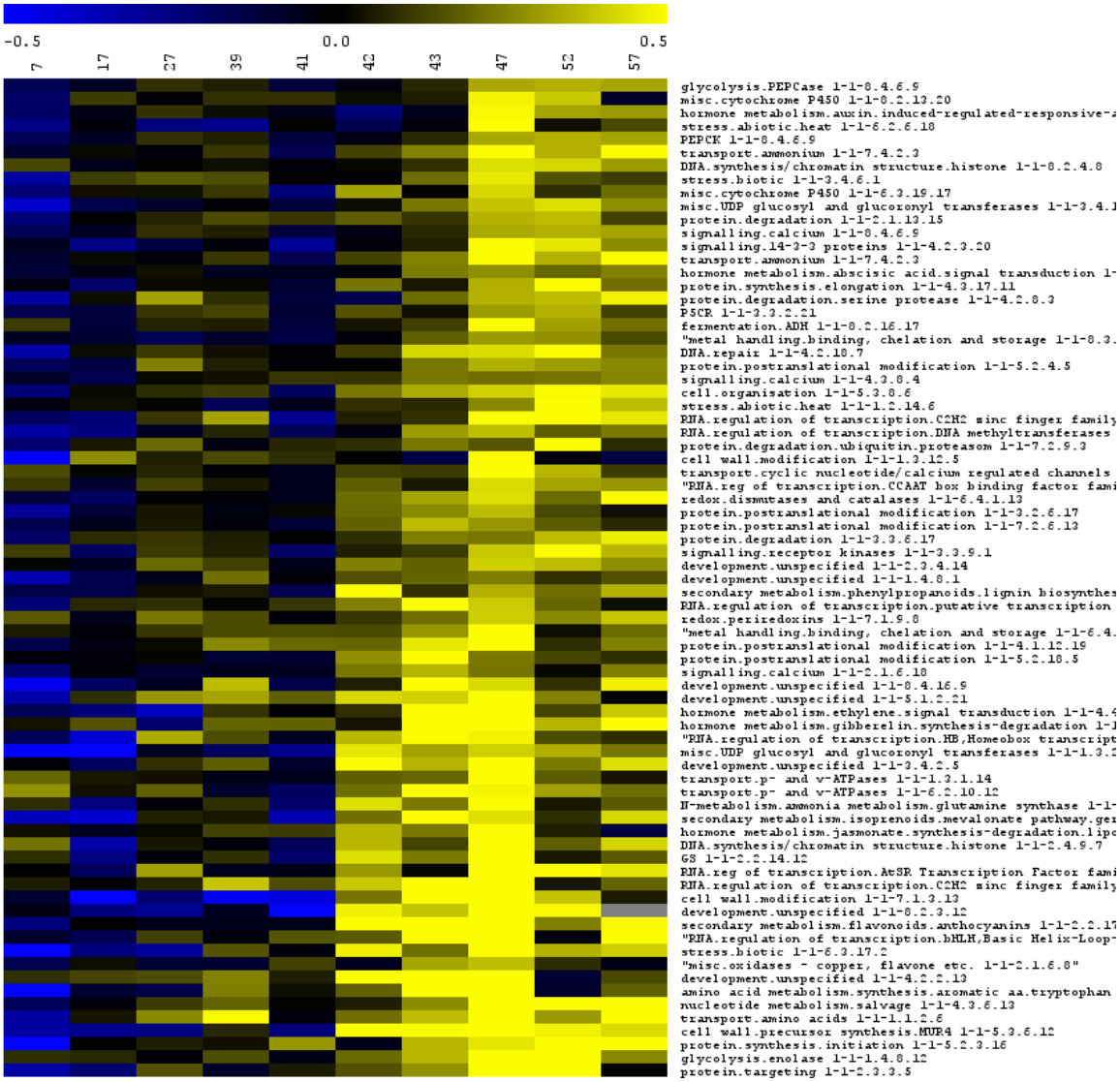

Cluster 37

Days Post Anthesis

Annotation

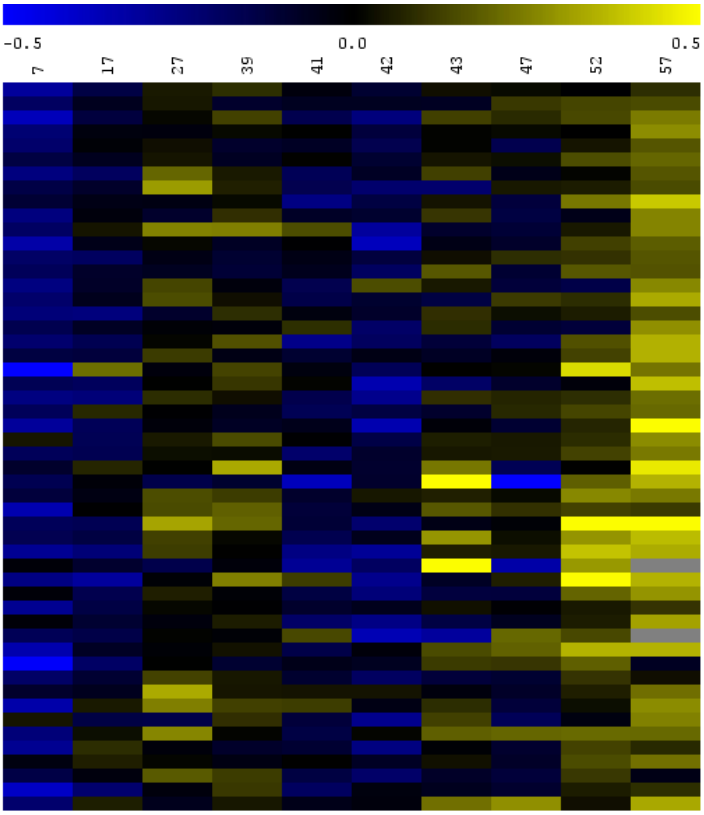

misc.short chain dehydrogenase/reductase (SDR) 1-1-6
amino acid metabolism.degradation.aspartate family.1
RNA.regulation of transcription.Histone acetyltransf
protein.synthesis.initiation 1-1-3.2.15.7
protein.degradation.ubiquitin.E3.SCF.FBOX 1-1-7.2.2.
AAT 1-1-5.1.13.7
SGH-U217541 misc.dynamin 1-1-8.2.6.15
RNA.reg of transcription.WRKY domain transcription f
RNA.reg of transcription.putative transcription regu
RNA.reg of transcription.SET-domain transcriptional
not assigned.no ontology.pentatricopeptide (PPR) rep
lipid metabolism.galactolipid synthesis 1-1-8.2.16.1
redox.thioredoxin 1-1-7.3.4.5
redox.thioredoxin 1-1-3.2.6.4
misc.UDP glucosyl and glucoronyl transferases 1-1-8.
protein.degradation 1-1-5.2.7.16
protein.degradation 1-1-3.1.20.18
signalling.MAP kinases 1-1-1.2.9.2
cell. vesicle transport 1-1-7.1.5.7
development.unspecified 1-1-6.4.15.4
major CHO metabolism.degradation.starch.starch cleav
stress.abiotic.touch/wounding 1-1-8.2.4.20
RNA.regulation of transcription.bZIP transcription f
RNA.regulation of transcription.HDA 1-1-7.1.2.4
Acon 1-1-4.4.3.16
transport.protein transport mito membrane (TIM/TOM)
cell wall.precursor synthesis 1-1-8.3.6.11
stress.biotic 1-1-2.4.10.14
protein.postranslational modification 1-1-4.1.19.11
signalling.receptor kinases 1-1-8.1.4.17
development.unspecified 1-1-3.2.14.21
development.unspecified 1-1-3.3.16.21
hormone metabolism.auxin.induced-regulated-responsiv
cell. vesicle transport 1-1-1.3.4.7
misc.UDP glucosyl and glucoronyl transferases 1-1-5.
stress.abiotic.drought/salt 1-1-5.3.8.3
misc.cytochrome P450 1-1-1.4.15.11
development.unspecified 1-1-2.4.7.4
AAT 1-1-3.1.15.14
"misc.oxidases - copper, flavone etc. 1-1-8.4.3.17"
RNA.regulation of transcription.HDA 1-1-2.1.8.9
misc.GDSL-motif lipase 1-1-8.3.6.10
amino acid metabolism.degradation.aspartate family.1
secondary metabolism.wax 1-1-5.1.2.8
stress.biotic 1-1-1.1.18.12
transport misc 1-1-2.1.6.20
secondary metabolism.isoprenoids.carotenoids 1-1-3.1
major CHO metabolism.degradation.starch.glucan water
stress.abiotic.drought/salt 1-1-7.1.16.11
"RNA.regulation of transcription.bHLH,Basic Helix-Lo
DNA.synthesis/chromatin structure 1-1-8.1.1.11
amino acid metabolism.synthesis.branched chain group

Cluster 38

Days Post Anthesis

Annotation

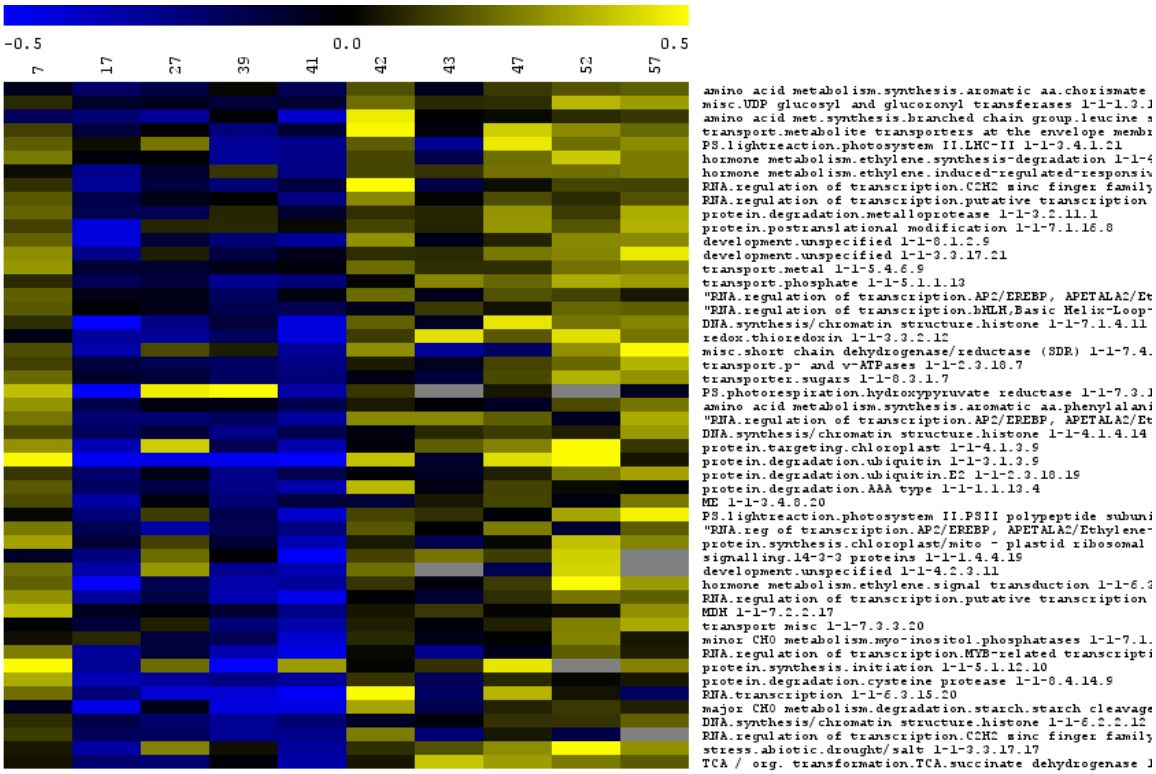

Cluster 39

Days Post Anthesis

Annotation

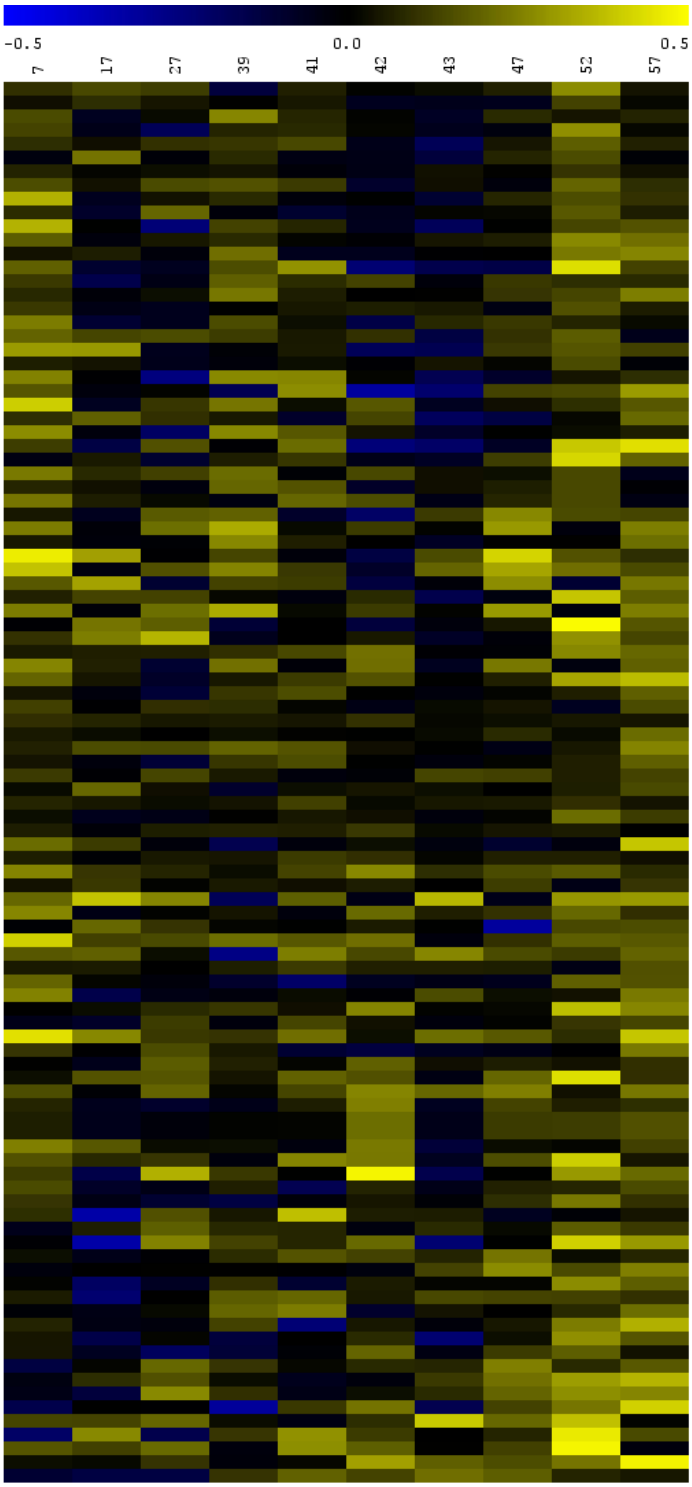

protein.degradation.subtilases 1-1-8.2.17.7
hormone met.auxin.induced-regulated-responsive-activate
stress.biotic 1-1-1.1.2.13
misc.UDP glucosyl and glucoronyl transferases 1-1-8.1.7
protein.postranslational modification 1-1-3.2.18.3
protein.postranslational modification 1-1-2.4.18.3
cell.organisation 1-1-1.1.4.11
cell wall.pectin*esterases.PME 1-1-4.4.1.10
OPP.oxidative PP.G6PD 1-1-1.4.4.3
major CHO metabolism.degradation.starch.D enzyme 1-1-3.
RNA.processing.degradation dicer 1-1-4.4.10.7
RNA.regulation of transcription.bZIP transcription fact
RNA.regulation of transcription.putative transcription
protein.degradation.AAA type 1-1-4.2.3.19
C1-met 1-1-1.3.1.18
signalling.14-3-3 proteins 1-1-4.4.8.3
PS.calvin cyle.GAP 1-1-8.4.10.12
"RNA.reg of transcription.Trihelix, Triple-Helix transc
fermentation.aldehyde dehydrogenase 1-1-4.3.19.6
fermentation.aldehyde dehydrogenase 1-1-5.4.4.8
redox.thioredoxin 1-1-3.2.17.6
redox.ascorbate and glutathione.ascorbate 1-1-6.3.6.9
misc.cytochrome P450 1-1-5.1.19.13
protein.postranslational modification 1-1-2.1.19.20
signalling.receptor kinases 1-1-8.2.19.19
development.unspecified 1-1-1.3.2.8
development.unspecified 1-1-3.2.19.21
hormone metabolism.gibberelin.synthesis-degradation 1-1
"RNA.regulation of transcription.HB,Homeobox transcript
RNA.regulation of transcription.WRKY domain transcripti
"RNA.regulation of transcription.bHLH,Basic Helix-Loop-
protein.degradation.ubiquitin.proteasom 1-1-4.2.8.11
V-ATPase 1-1-6.2.8.1
V-ATPase 1-1-6.2.10.9
tetrapyrrole synthesis 1-1-7.3.5.7
redox.ascorbate and glutathione.ascorbate.GME 1-1-1.1.1
RNA.processing 1-1-8.1.5.2
development.unspecified 1-1-5.1.2.2
transport.p- and v-ATPases 1-1-6.2.8.1
transport.potassium 1-1-6.2.15.17
secondary metabolism.isoprenoids.carotenoids.phytoene s
"RNA.regulation of transcription.HB,Homeobox transcript
"RNA.regulation of transcription.HSF,Heat-shock transcri
protein.targeting 1-1-5.4.17.14
development.unspecified 1-1-5.1.7.16
cell wall.pectin*esterases.PME 1-1-5.4.10.9
stress.abiotic.touch/wounding 1-1-2.1.16.3
Acon 1-1-2.4.16.16
transport.phosphate 1-1-2.3.18.4
RNA.reg of transcription.GRAS transcription factor fami
RNA.transcription 1-1-4.4.7.21
RNA.RNA binding 1-1-1.1.4.3
protein.degradation 1-1-2.3.9.14
transport.sulphate 1-1-5.4.2.10
RNA.regulation of transcription.MYB domain transcriptio
DNA.repair 1-1-6.3.1.17
hormone met.ethylene.synthesis-degradation 1-1-7.3.16.9
"metal handling.binding, chelation and storage 1-1-8.2.
misc.UDP glucosyl and glucoronyl transferases 1-1-3.2.2
"misc.gluco-, galacto- and mannosidases 1-1-2.1.15.19"
protein.postranslational modification 1-1-4.4.12.15
protein.postranslational modification 1-1-2.2.20.8
PS.lightreaction.other electron carrier (ox/red).plasto
secondary metabolism.isoprenoids.carotenoids.phytoene s
hormone metabolism.ethylene.signal transduction 1-1-4.2
hormone metabolism.ethylene.signal transduction 1-1-4.1
RNA.regulation of transcription.MYB domain transcriptio
protein.synthesis.elongation 1-1-6.3.17.15
RNA.reg of transcription.General Transcription 1-1-4.4.
protein.synthesis.misc ribososomal protein 1-1-3.1.8.4
redox.thioredoxin 1-1-3.4.12.14
PS.lightreaction.cyclic electron flow-chlororespiration
hormone metabolism.abscisic acid.synthesis-degradation
hormone metabolism.ethylene.signal transduction 1-1-4.1
hormone metabolism.ethylene.signal transduction 1-1-1.2
minor CHO met.raffinose family 1-1-1.4.14.5
minor CHO metabolism.raffinose family 1-1-1.4.14.5
"lipid metabolism.'exotics' (steroids, squalene etc) 1-
amino acid metabolism.degradation.aspartate family.lysi
RNA.regulation of transcription.WRKY domain transcripti
RNA.regulation of transcription.putative transcription
secondary met.flavonoids.anthocyanins 1-1-7.2.1.21
tetrapyrrole synthesis 1-1-1.17.15
"misc.gluco-, galacto- and mannosidases 1-1-4.1.4.13"
protein.postranslational modification 1-1-6.2.19.20
protein.postranslational modification 1-1-8.1.5.7
signalling.14-3-3 proteins 1-1-7.1.2.1
"RNA.regulation of transcription.HB,Homeobox transcript
"RNA.regulation of transcription.HB,Homeobox transcript
protein.synthesis.chloroplast/mito - plastid ribosomal
cell wall.hemicellulose synthesis 1-1-2.1.7.15
not assigned.no ontology 1-1-3.4.18.4
mitochondrial electron transport / ATP synthesis.cytoch
tetrapyrrole synthesis 1-1-3.3.6.2
development.unspecified 1-1-3.4.13.16
development.unspecified 1-1-5.4.17.21
GABA-T 1-1-5.3.1.4
cell wall.modification 1-1-8.2.17.21
misc.cytochrome P450 1-1-4.4.17.18
misc.myrosinases-lectin-jacalin 1-1-7.2.10.12
S-assimilation.APS 1-1-1.1.16.16
misc.peroxidases 1-1-3.4.13.21

Cluster 40

Days Post Anthesis

Annotation

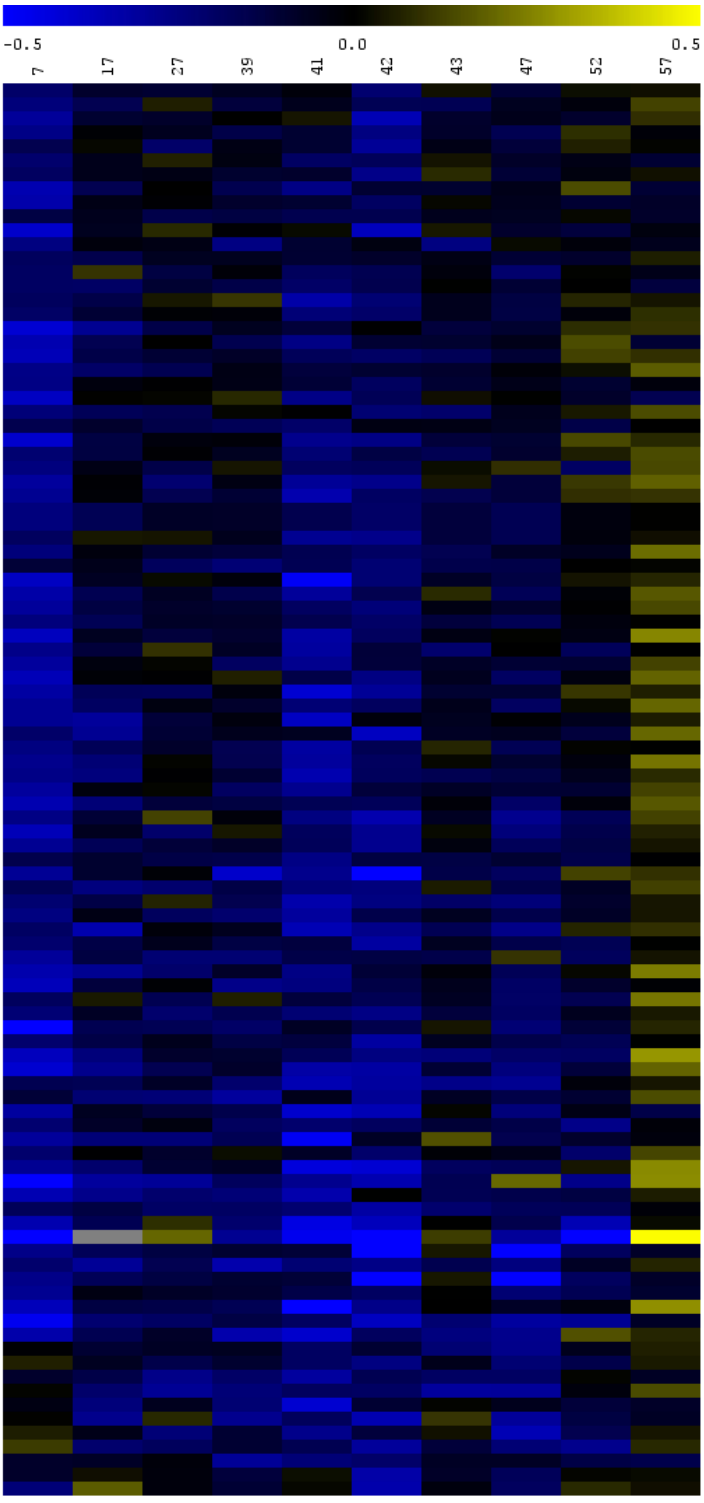

hormone metabolism.auxin.induced-regulated-responsiv
"RNA.regulation of transcription.C2C2(Zn) CO-like, C
mito ET/ATP synthesis.cytochrome c 1-1-7.3.8.7
secondary met.simple phenols 1-1-6.1.20.18
secondary met.flavonoids.flavonols 1-1-5.3.18.17
nucleotide met.synthesis.purine 1-1-7.1.1.15
gluconeogenese/ glyoxylate cycle.citrate synthase 1-
cell wall.modification 1-1-7.4.14.19
C1-metabolism 1-1-3.3.4.5
misc.cytochrome P450 1-1-5.4.17.3
protein.postranslational modification 1-1-5.3.20.12
signalling.MAP kinases 1-1-8.3.18.19
development.unspecified 1-1-7.2.13.19
development.unspecified 1-1-2.1.8.7
transport.calcium 1-1-4.3.10.8
transport.amino acids 1-1-5.4.9.11
transport.metabolite transporters at the envelope me
PS.photorespiration.hydroxypyruvate reductase 1-1-7.
cell wall.degradation.mannan-xylose-arabinose-fucose
lipid metabolism.FA desaturation.omega 3 desaturase
amino acid metabolism.synthesis.branched chain group
amino acid metabolism.degradation.glutamate family.a
major CHO metabolism.synthesis.starch.AGPase 1-1-6.3
RNA.regulation of transcription.MYB domain transcrip
protein.degradation.aspartate protease 1-1-8.4.6.1
misc.peroxidases 1-1-7.1.18.8
misc.acid and other phosphatases 1-1-3.4.17.6
RNA.regulation of transcription.bZIP transcription f
RNA.regulation of transcription.General Transcriptio
redox.glutaredoxins 1-1-3.2.5.8
transport.unspecified cations 1-1-4.3.20.16
transport.unspecified anions 1-1-4.3.20.16
"glycolysis.Fruc2,6BisPase 1-1-7.3.16.17"
cell wall.precursor synthesis 1-1-6.3.20.7
misc.acid and other phosphatases 1-1-7.1.18.9
misc.acid and other phosphatases 1-1-7.4.19.16
protein.postranslational modification 1-1-5.3.7.20
protein.postranslational modification 1-1-5.1.16.8
transport.unspecified cations 1-1-4.3.20.16
transport.ABC transporters and multidrug resistance
lipid metabolism.FA synthesis and FA elongation.acyl
secondary metabolism.isoprenoids.terpenoids 1-1-2.1.
secondary metabolism.isoprenoids.mevalonate pathway.
secondary metabolism.flavonoids.anthocyanins 1-1-1.4
transporter.sugars.sucrose 1-1-3.2.13.9
major CHO metabolism.degradation.sucrose.fructokinas
RNA.regulation of transcription.C3H zinc finger fami
RNA.regulation of transcription.MYB-related transcri
protein.degradation.ubiquitin.E3.SCF.FBOX 1-1-1.6.4.
protein.degradation.serine protease 1-1-7.3.19.3
secondary met.isoprenoids 1-1-2.1.20.10
protein.targeting 1-1-8.3.4.1
not assigned.no ontology.formin homology 2 domain-co
TCA / org. transformation.carbonic anhydrases 1-1-3.
cell wall.modification 1-1-2.3.10.7
stress.biotic 1-1-6.1.17.9
misc.acid and other phosphatases 1-1-7.1.10.18
signalling.calcium 1-1-4.4.18.12
signalling.calcium 1-1-4.4.19.2
signalling.MAP kinases 1-1-3.3.18.21
signalling.MAP kinases 1-1-3.4.16.3
development.unspecified 1-1-8.1.14.19
development.unspecified 1-1-5.3.8.13
lipid metabolism.FA desaturation.omega 3 desaturase
hormone metabolism.auxin.synthesis-degradation 1-1-6
RNA.regulation of transcription.C2H2 zinc finger fam
redox.peroxiredoxins 1-1-8.2.3.19
cell.division 1-1-3.2.8.12
development.unspecified 1-1-8.1.14.19
secondary metabolism.wax 1-1-8.3.9.16
misc.cytochrome P450 1-1-5.4.5.7
cell.organisation 1-1-8.2.2.16
cell. vesicle transport 1-1-7.1.16.21
development.unspecified 1-1-7.2.11.18
development.unspecified 1-1-8.1.15.13
amino acid metabolism.synthesis.aromatic aa.phenylal
hormone metabolism.abscisic acid.synthesis-degradati
RNA.regulation of transcription.GeBP like 1-1-5.2.11
TCA / org. transformation.carbonic anhydrases 1-1-3.
fermentation.aldehyde dehydrogenase 1-1-5.1.19.3
"lipid metabolism.'exotics' (steroids, squalene etc)
misc.cytochrome P450 1-1-4.4.14.13
protein.postranslational modification 1-1-1.4.18.3
transport.amino acids 1-1-8.1.9.19
protein.synthesis.chloroplast/mito - plastid ribosom
transport.peptides and oligopeptides 1-1-8.1.9.19
protein.postranslational modification 1-1-3.1.18.19
transport.ABC transporters and multidrug resistance
RNA.regulation of transcription.MYB domain transcrip
"RNA.regulation of transcription.AS2,Lateral Organ B
secondary metabolism.flavonoids.flavonols 1-1-7.3.20
redox.dismutases and catalases 1-1-1.2.10.21
RNA.regulation of transcription.WRKY domain transcri
"RNA.regulation of transcription.bHLH,Basic Helix-Lo
protein.degradation.ubiquitin.E2 1-1-4.2.11.2
NAOAT 1-1-2.1.11.20
misc.myrosinases-lectin-jacalin 1-1-7.2.10.11
secondary metabolism.isoprenoids.mevalonate pathway.
RNA.regulation of transcription.C2H2 zinc finger fam
redox.thioredoxin 1-1-5.2.20.10
misc.peroxidases 1-1-8.4.13.14

Cluster 41

Days Post Anthesis

Annotation

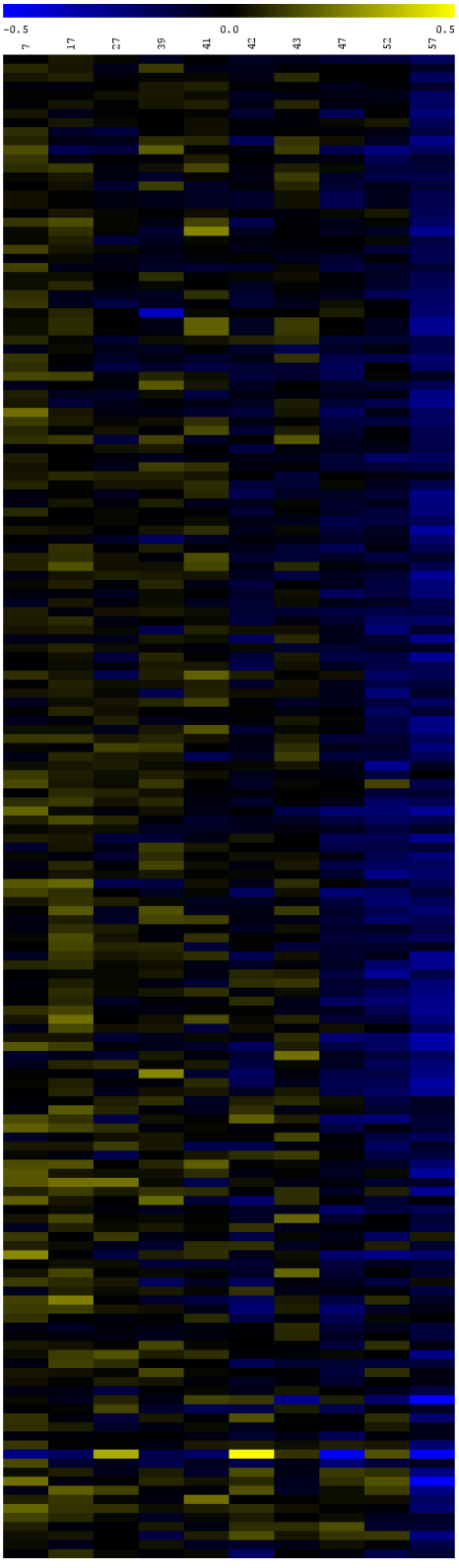

Cluster 42

Days Post Anthesis

Annotation

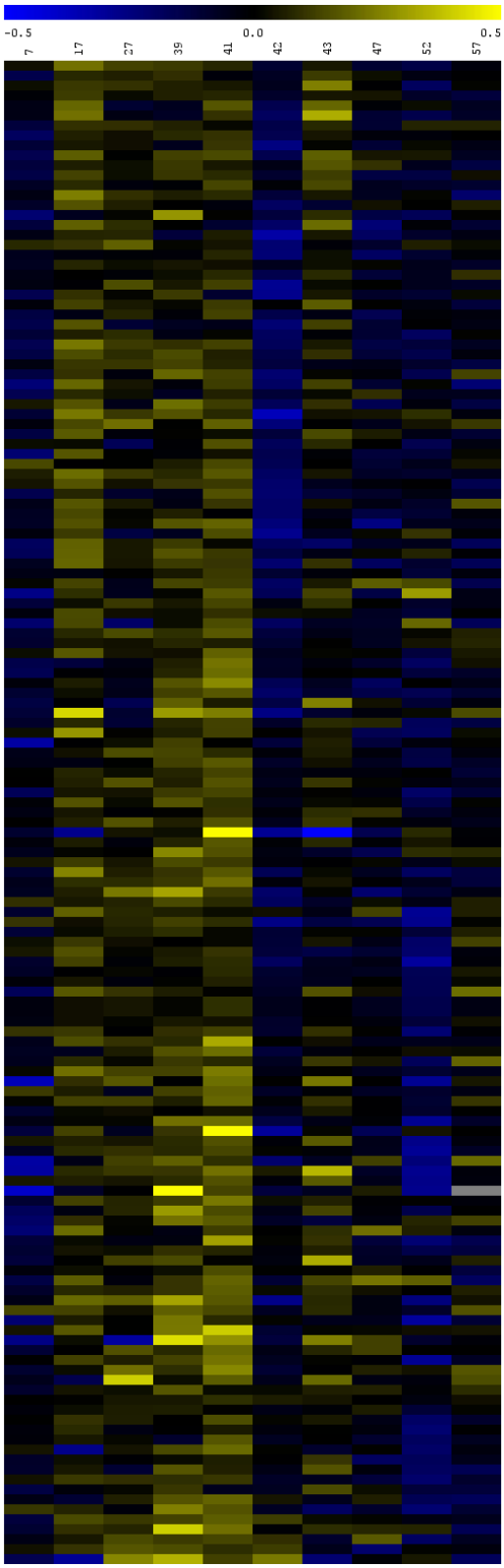

cell wall.pectin*esterases.PME 1-1-6.1.15.7
P5CDH 1-1-3.2.6.9
gluconeogenese/ glyoxylate cycle.citrate synthase 1-
cell wall.hemicellulose synthesis 1-1-2.2.13.15
stress.biotic 1-1-2.3.8.6
polyamine metabolism.synthesis.spermidine synthase 1
misc.cytochrome P450 1-1-2.1.7.17
"misc.gluco-, galacto- and mannosidases 1-1-2.2.13.7
protein.posttranslational modification 1-1-8.3.2.15
signalling.calcium 1-1-3.1.6.5
signalling.MAP kinases 1-1-6.1.14.7
cell.organisation 1-1-6.4.6.8
cell.cycle 1-1-2.1.14.14
cell. vesicle transport 1-1-4.3.8.8
transport.metabolite transporters at the envelope me
PS.lightreaction.photosystem II.PSII polypeptide subu
lipid metabolism.FA desaturation.omega 3 desaturase
"lipid metabolism.'exotics' (steroids, squalene etc)
"lipid metabolism.'exotics' (steroids, squalene etc)
lipid metabolism.lipid degradation.lipases 1-1-5.3.1
lipid metabolism.lipid degradation.lysophospholipase
N-metabolism.nitrate metabolism.nitrite reductase 1-
hormone metabolism.ethylene.signal transduction 1-1-
hormone metabolism.jasmonate.synthesis-degradation.1
stress.abiotic.heat 1-1-5.2.8.7
RNA.regulation of transcription.C2H2 zinc finger fam
RNA.regulation of transcription.C2H2 zinc finger fam
RNA.regulation of transcription.Alfin-like 1-1-7.2.1
RNA.regulation of transcription.Alfin-like 1-1-3.4.7
"RNA.regulation of transcription.HB,Homeobox transcr
RNA.regulation of transcription.MADS box transcripti
RNA.regulation of transcription.Argonaute 1-1-2.4.6.
RNA.regulation of transcription.NIN-like bZIP-relate
RNA.regulation of transcription.putative transcripti
protein.synthesis.chloroplast/mito - plastid ribosom
protein.degradation.ubiquitin.proteasom 1-1-3.4.10.5
protein.degradation.ubiquitin.E2 1-1-7.4.6.18
protein.degradation.serine protease 1-1-2.1.6.9
ICDH 1-1-7.2.13.12
metal handling.acquisition 1-1-4.4.2.2
signalling.MAP kinases 1-1-5.4.10.20
RNA.reg of transcription.C2C2(Zn) DOF zinc finger fa
RNA.reg of transcription.C2C2(Zn) GATA transcription
"metal handling.binding, chelation and storage 1-1-3
stress.abiotic 1-1-4.3.6.4
misc.cytochrome P450 1-1-3.3.7.17
protein.posttranslational modification 1-1-1.4.15.15
signalling.light 1-1-6.2.8.5
lipid metabolism.lipid degradation.lysophospholipase
amino acid metabolism.synthesis.branched chain group
stress.abiotic.heat 1-1-2.4.6.5
"cell wall.degradation.cellulases and beta -1,4-gluc
glycolysis.PK 1-1-3.4.17.4
signalling.MAP kinases 1-1-8.3.4.12
development.unspecified 1-1-4.3.19.18
stress.abiotic.touch/wounding 1-1-5.4.7.13
RNA.regulation of transcription.bZIP transcription f
RNA.regulation of transcription.General Transcriptio
transporter.sugars.sucrose 1-1-2.4.18.13
stress.biotic 1-1-1.4.8.2
misc.peroxidases 1-1-2.4.20.19
"misc.oxidases - copper, flavone etc. 1-1-2.2.7.16"
protein.posttranslational modification 1-1-6.3.5.7
protein.posttranslational modification 1-1-3.4.17.2
development.unspecified 1-1-7.1.8.20
transport.unspecified anions 1-1-6.4.10.14
transport misc 1-1-7.4.6.12
hormone metabolism.cytokinin.synthesis-degradation 1
hormone metabolism.ethylene.signal transduction 1-1-
stress.abiotic.drought/salt 1-1-8.1.4.7
"RNA.regulation of transcription.G2-like transcripti
RNA.regulation of transcription.bZIP transcription f
PEPCK 1-1-4.1.11.18
gluconeogenese/glyoxylate cycle.pyruvate dikinase 1-
misc.nitrilases 1-1-5.4.8.1
PS.calvin cyle.FBPase 1-1-5.3.7.14
glycolysis.PEPCase 1-1-4.1.11.18
signalling.lipids 1-1-1.2.9.17
transport.metabolite transporters at the envelope me
secondary metabolism.flavonoids.anthocyanins 1-1-7.3
major CHO metabolism.degradation.sucrose.misc 1-1-2.
"RNA.regulation of transcription.G2-like transcripti
"RNA.regulation of transcription.HB,Homeobox transcr
RNA.regulation of transcription.MYB-related transcri
V-ATPase 1-1-6.4.4.17
glycolysis.glyceraldehyde 3-phosphate DH 1-1-8.1.13.
glycolysis.PK 1-1-6.4.11.16
secondary metabolism.simple phenols 1-1-1.1.16.21
"misc.gluco-, galacto- and mannosidases 1-1-1.1.7.17
signalling.receptor kinases 1-1-7.3.13.7
hormone metabolism.ethylene.signal transduction 1-1-
hormone metabolism.gibberelin.synthesis-degradation
RNA.regulation of transcription.MYB domain transcrip
RNA.regulation of transcription.putative transcripti
PDH 1-1-1.1.13.15
amino acid met.degradation.glutamate family.proline
hormone met.abscisic acid.induced-regulated-responsi
minor CHO metabolism.others 1-1-4.3.11.5
stress.biotic 1-1-6.2.20.11
RNA.processing 1-1-5.4.4.16
signalling.receptor kinases 1-1-1.2.9.8
signalling.MAP kinases 1-1-7.1.15.6
amino acid metabolism.degradation.aspartate family.1
secondary metabolism.isoprenoids.non-mevalonate path
major CHO metabolism.degradation.sucrose.misc 1-1-1.
stress.biotic.respiratory burst 1-1-5.4.15.6
protein.degradation.aspartate protease 1-1-7.4.11.10
protein.degradation.serine protease 1-1-4.2.7.18
"misc.beta 1,3 glucan hydrolases 1-1-6.3.20.16"
development.storage proteins 1-1-5.2.15.1
tetrapyrrole synthesis 1-1-2.2.6.2
redox.ascorbate and glutathione 1-1-2.2.6.5
"misc.beta 1,3 glucan hydrolases 1-1-6.3.20.16"
"misc.oxidases - copper, flavone etc. 1-1-7.3.3.10"
signalling.calcium 1-1-2.2.18.9
signalling.MAP kinases 1-1-1.2.8.9
development.unspecified 1-1-1.4.18.20
transport.ABC transporters and multidrug resistance
transport misc 1-1-4.4.11.8
protein.synthesis.elongation 1-1-2.2.6.12
redox.ascorbate & glutathione 1-1-2.4.1.10
stress.biotic 1-1-4.3.17.3
misc.cytochrome P450 1-1-2.2.13.20
misc.myrosinases-lectin-jacalin 1-1-8.2.15.1
misc.UDP glucosyl and glucoronyl transferases 1-1-5.
signalling.G-proteins 1-1-4.2.8.10
signalling.MAP kinases 1-1-8.3.8.1
cell.cycle 1-1-5.1.14.10
"RNA.regulation of transcription.HB,Homeobox transcr
"RNA.regulation of transcription.AP2/EREBP, APETALA2
stress.biotic 1-1-7.2.13.3
protein.posttranslational modification 1-1-1.1.9.16
transport.p- and v-ATPases 1-1-1.1.12.9
"RNA.regulation of transcription.HB,Homeobox transcr
protein.posttranslational modification 1-1-2.1.16.12
lipid metabolism.lipid degradation.lysophospholipase
RNA.reg of transcription.Chromatin Remodeling Factor
RNA.regulation of transcription.WRKY domain transcri
"RNA.regulation of transcription.bHLH,Basic Helix-Lo
protein.posttranslational modification 1-1-8.1.14.8
lipid metabolism.galactolipid synthesis 1-1-5.2.20.1
"metal handling.binding, chelation and storage 1-1-1
protein.targeting 1-1-6.3.11.5
transport.unspecified anions 1-1-2.1.1.13
lipid met.lipid transfer proteins etc 1-1-3.4.3.3
transport.phosphate 1-1-8.4.17.2
protein.degradation 1-1-8.2.13.1
stress.biotic 1-1-1.4.7.19
DNA.synthesis/chromatin structure 1-1-8.3.10.15
amino acid met.synthesis.serine-glycine-cysteine gro
protein.degradation.cysteine protease 1-1-1.2.17.12

Cluster 43

Days Post Anthesis

Annotation

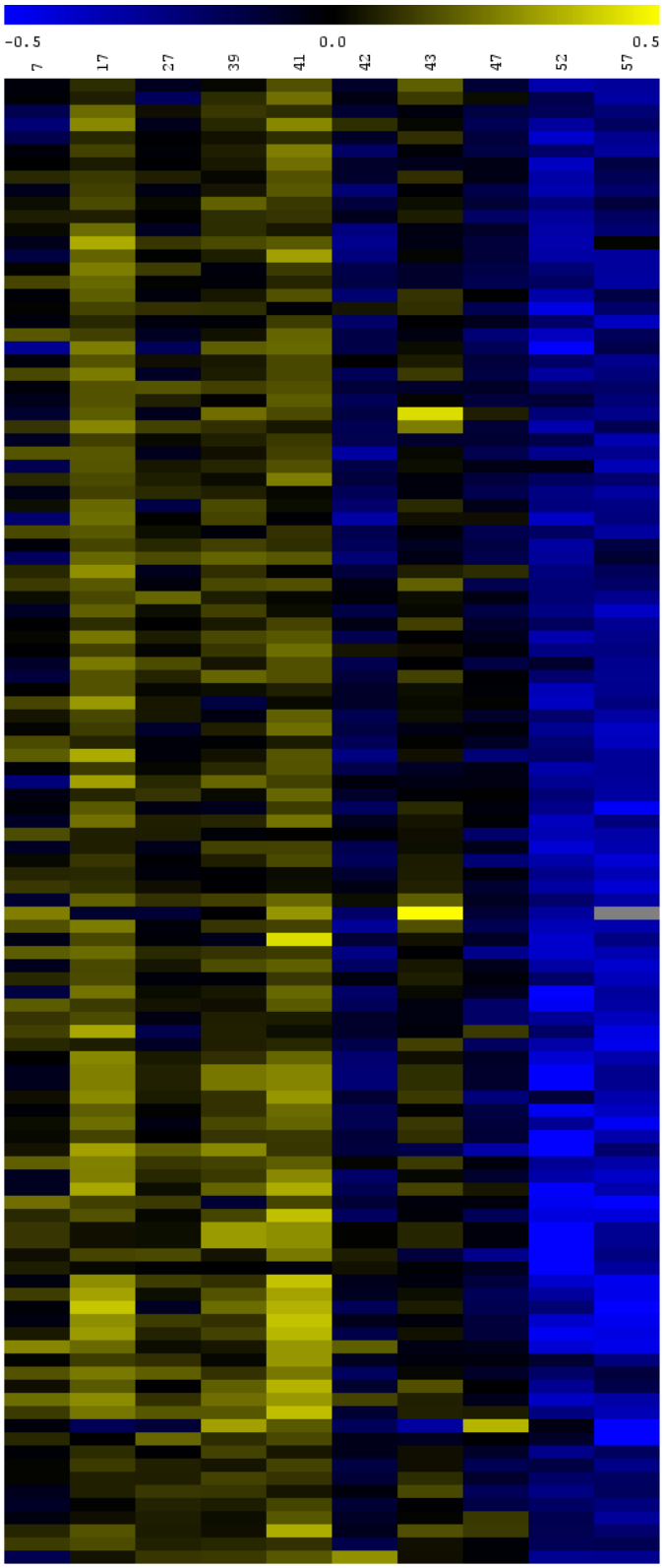

Cluster 44

Days Post Anthesis

Annotation

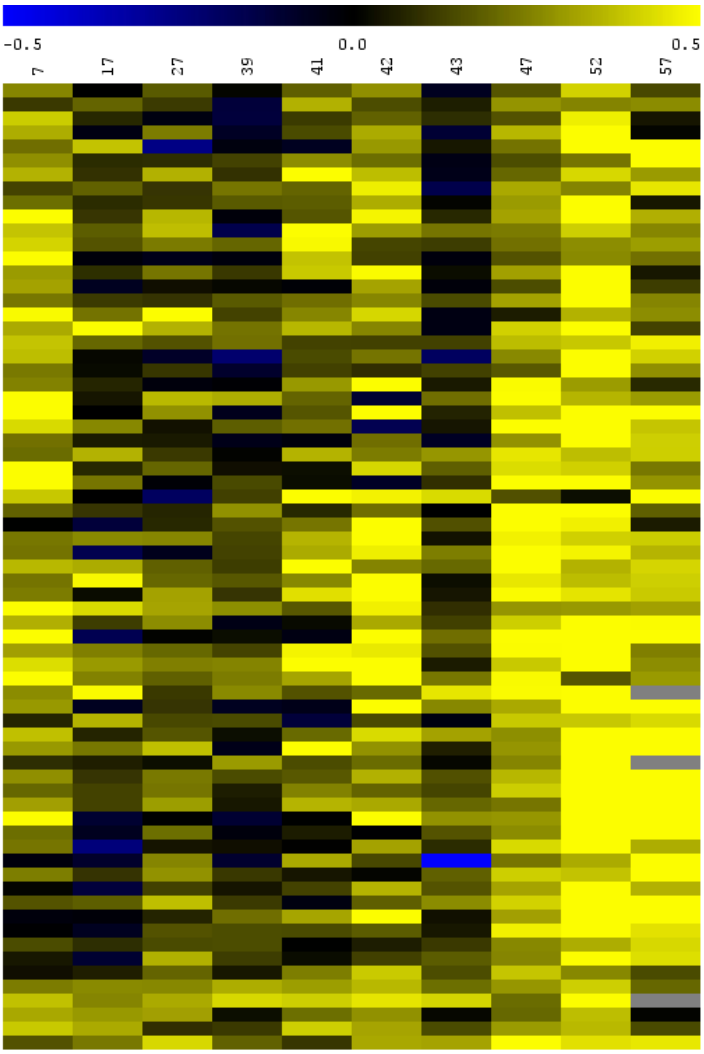

development.unspecified 1-1-5.4.19.21
hormone metabolism.jasmonate.synthesis-degradation.1
transport.p- and v-ATPases 1-1-8.2.10.8
cell wall.precursor synthesis 1-1-7.2.17.20
misc.cytochrome P450 1-1-7.3.19.15
misc.misc2 1-1-1.2.14.5
"misc.oxidases - copper, flavone etc. 1-1-2.3.17.10"
protein.targeting 1-1-6.3.17.14
protein.postranslational modification 1-1-6.4.16.6
protein.postranslational modification 1-1-7.3.16.7
development.unspecified 1-1-5.1.17.12
PS.lightreaction.photosystem II.LHC-II 1-1-1.4.12.21
secondary metabolism.phenylpropanoids.lignin biosynt
"RNA.regulation of transcription.HB,Homeobox transcr
RNA.regulation of transcription.WRKY domain transcri
RNA.regulation of transcription.bZIP transcription f
RNA.regulation of transcription.PH0R1 1-1-5.1.15.17
protein.synthesis.initiation 1-1-6.2.5.2
protein.targeting 1-1-3.2.17.1
development.unspecified 1-1-4.4.19.6
development.unspecified 1-1-5.3.17.21
RNA.regulation of transcription.bZIP transcription f
protein.degradation 1-1-6.2.7.16
signalling.calcium 1-1-6.3.17.11
transport.unspecified cations 1-1-2.1.15.21
amino acid metabolism.synthesis.central amino acid m
secondary metabolism.isoprenoids.carotenoids.phytoen
hormone metabolism.auxin.signal transduction 1-1-8.4
"RNA.regulation of transcription.AS2,Lateral Organ B
protein.synthesis.elongation 1-1-3.3.12.10
protein.degradation.ubiquitin.proteasom 1-1-1.4.12.2
protein.degradation.cysteine protease 1-1-4.3.19.20
V-ATPase 1-1-2.3.17.18
glycolysis.enolase 1-1-2.4.17.21
DNA.unspecified 1-1-6.4.2.14
transport.p- and v-ATPases 1-1-2.3.17.18
transport.p- and v-ATPases 1-1-8.3.17.18
transport.p- and v-ATPases 1-1-4.4.10.17
hormone metabolism.abscisic acid.synthesis-degradati
hormone metabolism.ethylene.signal transduction 1-1-
"RNA.regulation of transcription.AP2/EREBP, APETALA2,
protein.degradation.cysteine protease 1-1-5.3.14.3
transport.metabolite transporters envelope membrane
stress.biotic 1-1-5.1.3.4
misc.UDP glucosyl and glucoronyl transferases 1-1-2.
protein.postranslational modification 1-1-6.1.17.11
signalling.light 1-1-7.3.17.13
cell wall.degradation.pectate lyases and polygalactu
stress.abiotic.drought/salt 1-1-7.1.19.12
GDC 1-1-2.3.17.17
major CHO met.degradation.starch.starch cleavage 1-1
stress.abiotic.heat 1-1-8.2.17.11
stress.biotic 1-1-6.4.20.11
signalling.light 1-1-6.1.17.13
hormone metabolism.ethylene.synthesis-degradation 1-
RNA.regulation of transcription.AtSR Transcription F
protein.synthesis.elongation 1-1-6.1.4.8
protein.postranslational modification 1-1-8.4.1.12
fermentation.aldehyde dehydrogenase 1-1-4.4.8.11
misc.cytochrome P450 1-1-1.4.2.10
"misc.beta 1,3 glucan hydrolases 1-1-4.4.13.20"
signalling.14-3-3 proteins 1-1-5.1.6.10
cell wall.degradation.pectate lyases and polygalactu
"RNA.regulation of transcription.AS2,Lateral Organ B
"RNA.regulation of transcription.HB,Homeobox transcr
protein.targeting 1-1-7.4.19.11
amino acid metabolism.degradation.glutamate family.a
protein.postranslational modification 1-1-1.2.15.16
protein.degradation.ubiquitin.E2 1-1-5.1.11.2

Cluster 45

Days Post Anthesis

Annotation

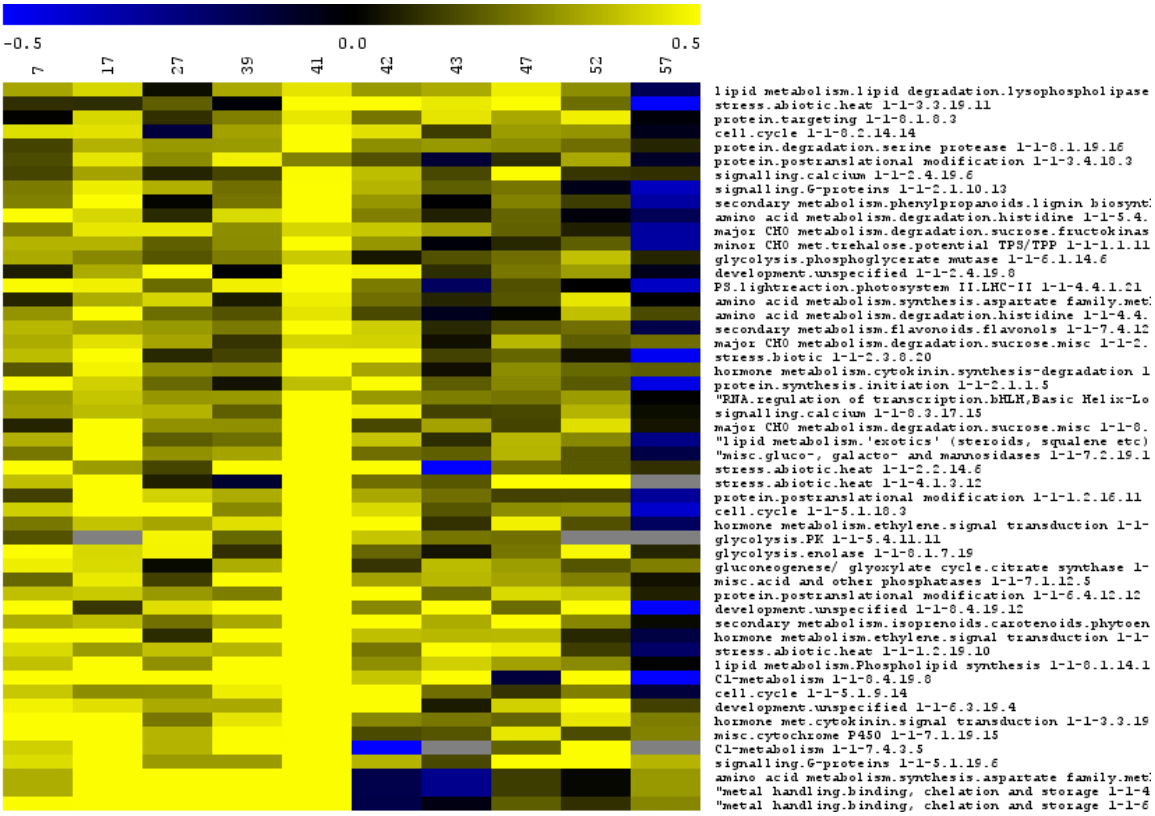

Cluster 46

Days Post Anthesis

Annotation

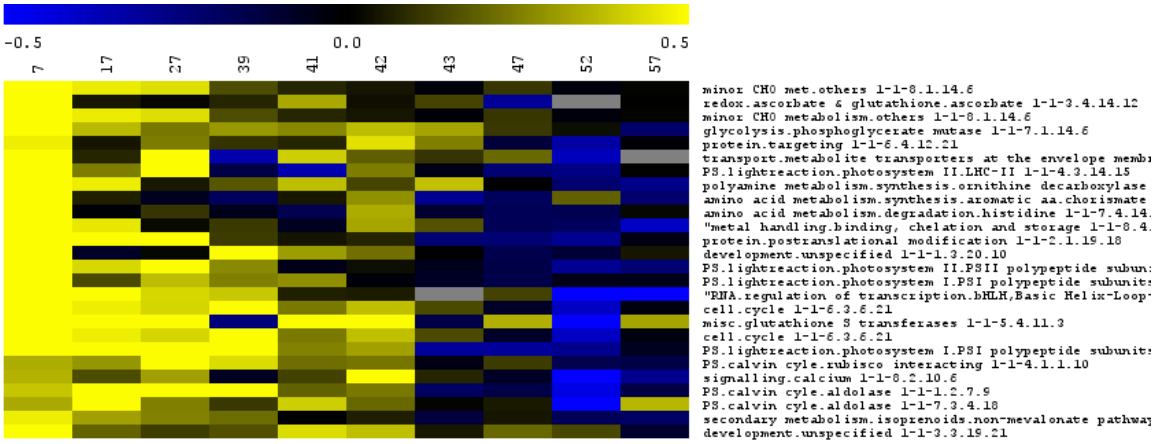

Cluster 47

Days Post Anthesis

Annotation

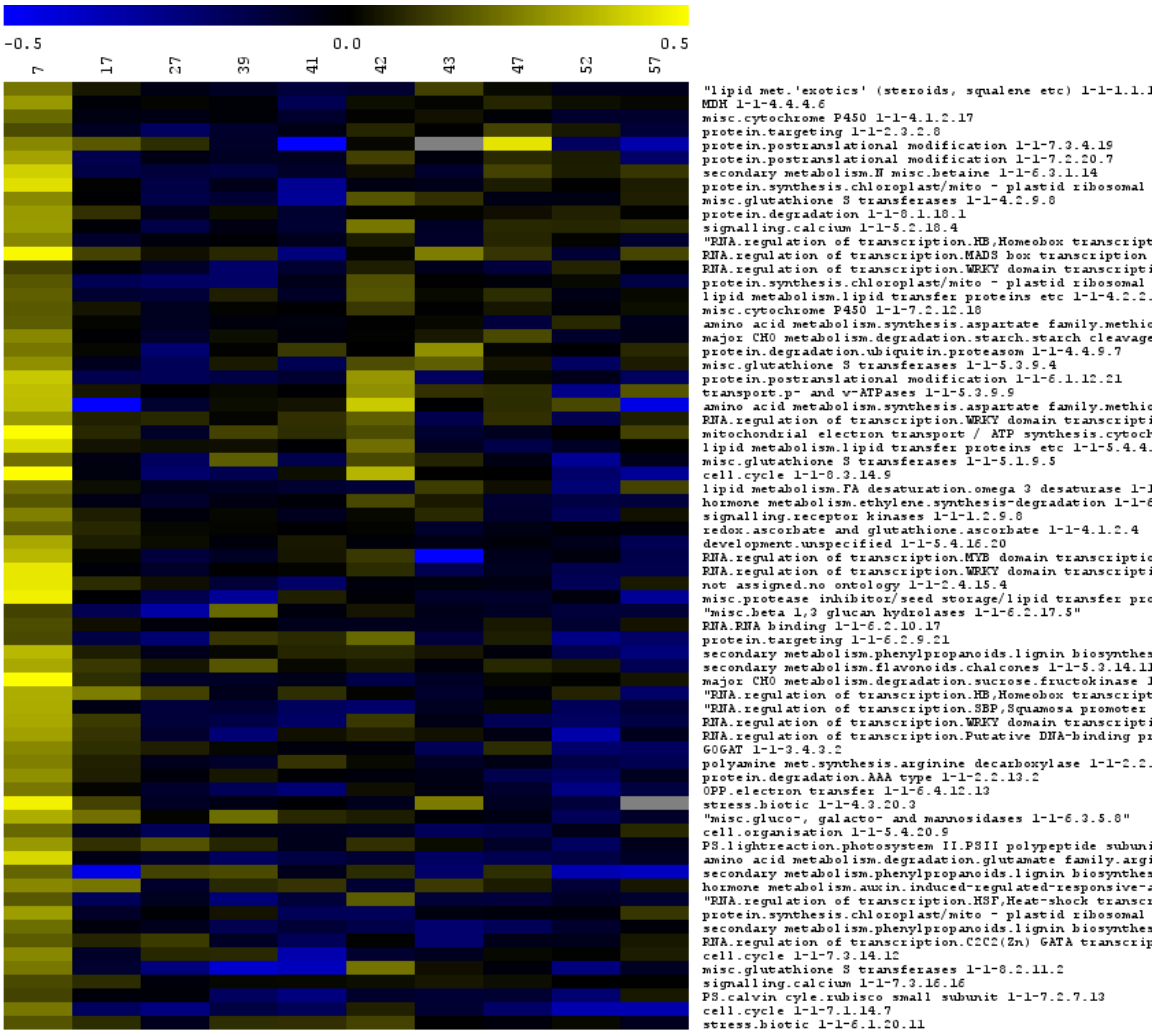

Cluster 48

Days Post Anthesis

Annotation

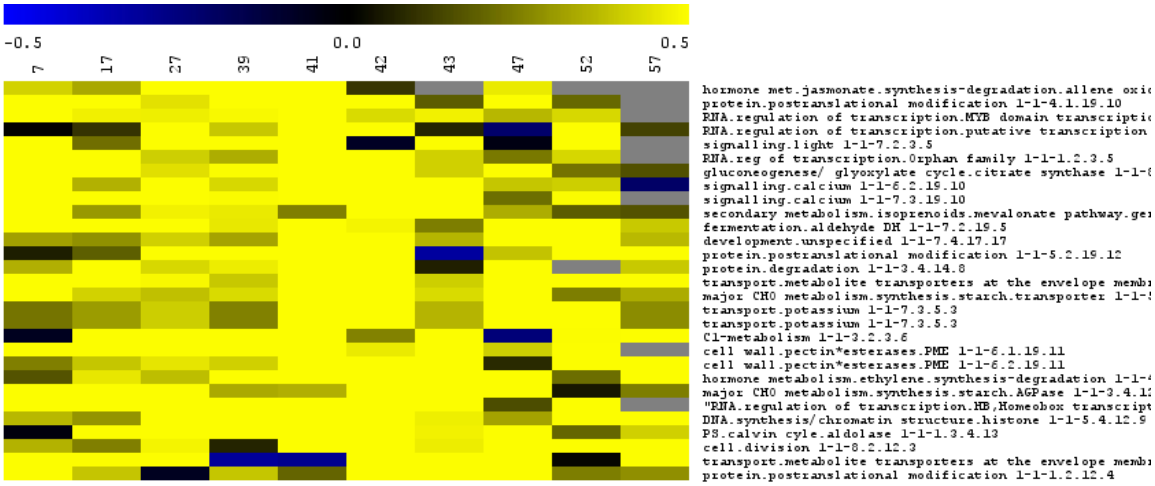

Cluster 49

Days Post Anthesis

Annotation

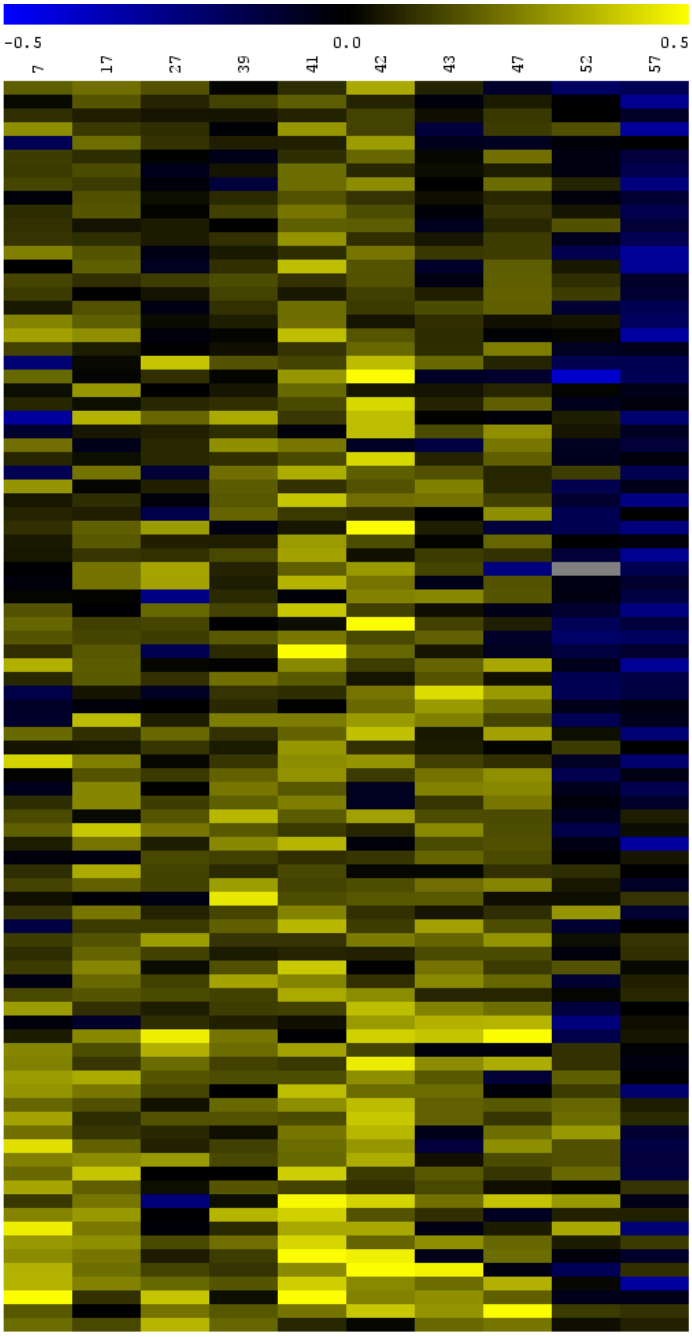

transport.metabolite transporters at the envelope membr
RNA.regulation of transcription.MYB domain transcriptic
hormone metabolism.jasmonate.synthesis-degradation.lipc
stress.abiotic.heat 1-1-3.2.15.21
protein.degradation.serine protease 1-1-4.1.14.5
misc.cytochrome P450 1-1-2.3.18.1
signalling.calcium 1-1-5.1.19.14
amino acid metabolism.degradation.glutamate family.argi
"RNA.regulation of transcription.HB,Homeobox transcript
protein.synthesis.chloroplast/mito - plastid ribosomal
protein.degradation.metalloprotease 1-1-2.1.18.4
glycolysis.PPFK 1-1-7.1.8.9
redox.thioredoxin 1-1-7.3.1.18
"misc.oxidases - copper, flavone etc. 1-1-5.1.17.5"
protein.postranslational modification 1-1-2.2.18.2
development.unspecified 1-1-7.1.7.3
lipid metabolism.FA synthesis and FA elongation.acyl co
amino acid metabolism.synthesis.central amino acid meta
amino acid metabolism.synthesis.histidine 1-1-5.1.5.2
RNA.regulation of transcription.WRKY domain transcripti
secondary met.isoprenoids 1-1-6.2.14.10
stress.biotic 1-1-3.1.9.3
protein.aa activation 1-1-5.2.6.6
transport.metal 1-1-7.1.4.3
tetrapyrrole synthesis 1-1-3.3.8.2
redox.ascorbate and glutathione.ascorbate 1-1-1.1.10.5
protein.postranslational modification 1-1-8.2.14.8
transport.metal 1-1-7.1.4.3
secondary metabolism.isoprenoids.carotenoids.phytoene s
RNA.processing.degradation dicer 1-1-4.4.2.9
RNA.regulation of transcription.Orphan family (Demeter)
protein.synthesis.chloroplast/mito - plastid ribosomal
cell wall.modification 1-1-2.2.12.1
protein.postranslational modification 1-1-2.1.18.2
development.unspecified 1-1-6.4.9.19
amino acid metabolism.synthesis.serine-glycine-cysteine
secondary metabolism.isoprenoids.non-mevalonate pathway
hormone metabolism.auxin.induced-regulated-responsive-
hormone metabolism.ethylene.signal transduction 1-1-3.1
RNA.regulation of transcription.C2H2 zinc finger family
stress.biotic 1-1-5.4.9.7
cell.cycle 1-1-8.4.14.7
secondary metabolism.phenylpropanoids.lignin biosynthes
OPP.oxidative PP.G6PD 1-1-5.1.11.21
RNA.regulation of transcription.C3H zinc finger family
protein.folding 1-1-8.3.4.5
signalling.calcium 1-1-1.2.8.12
cell.cycle 1-1-1.3.14.15
protein.aa activation 1-1-1.1.17.15
PS.lightreaction.ATP synthase 1-1-1.4.17.15
amino acid met.synthesis.histidine 1-1-4.2.8.4
cell wall.modification 1-1-7.2.6.7
protein.targeting 1-1-6.1.7.17
hormone metabolism.ethylene.synthesis-degradation 1-1-
stress.abiotic.drought/salt 1-1-3.1.10.2
"RNA.regulation of transcription.HB,Homeobox transcript
RNA.regulation of transcription.bZIP transcription fact
RNA.reg of transcription.Histone acetyltransferases 1-1
protein.postranslational modification 1-1-2.3.6.6
signalling.14-3-3 proteins 1-1-1.1.2.12
cell.cycle 1-1-1.1.14.17
cell. vesicle transport 1-1-6.3.11.19
RNA.regulation of transcription.WRKY domain transcripti
RNA.regulation of transcription.bZIP transcription fact
RNA.reg of transcription.DNA methyltransferases 1-1-5.1
Co-factor and vitamine metabolism 1-1-1.3.6.3
redox.ascorbate and glutathione.ascorbate 1-1-4.3.15.21
cell. vesicle transport 1-1-5.3.9.15
metal handling.reg 1-1-4.2.9.4
ME 1-1-3.3.20.10
protein.postranslational modification 1-1-3.1.19.17
development.unspecified 1-1-6.3.15.19
secondary metabolism.flavonoids.anthocyanins 1-1-6.2.12
minor CHO metabolism.trehalose.potential TPS/TPP 1-1-6.
"RNA.regulation of transcription.HB,Homeobox transcript
cell wall.precursor synthesis.sugar kinase 1-1-3.4.9.12
stress.abiotic.touch/wounding 1-1-1.2.12.15
misc.cytochrome P450 1-1-1.4.12.19
misc.cytochrome P450 1-1-7.4.19.5
signalling.calcium 1-1-8.2.12.7
signalling.G-proteins 1-1-7.1.8.5
protein.targeting 1-1-7.3.17.14
stress.abiotic.drought/salt 1-1-5.2.6.2
"RNA.regulation of transcription.HB,Homeobox transcript
Cit Syn 1-1-5.3.2.13
"misc.oxidases - copper, flavone etc. 1-1-2.3.17.12"
"RNA.regulation of transcription.AP2/EREBP, APETALA2/Et
major CHO metabolism.degradation.sucrose.misc 1-1-5.1.1
PS.lightreaction.photosystem II.PSII polypeptide subuni
protein.degradation.ubiquitin.E3.SCF.SKP 1-1-4.4.15.17
major CHO metabolism.degradation.sucrose.fructokinase 1

Cluster 50

Days Post Anthesis

Annotation

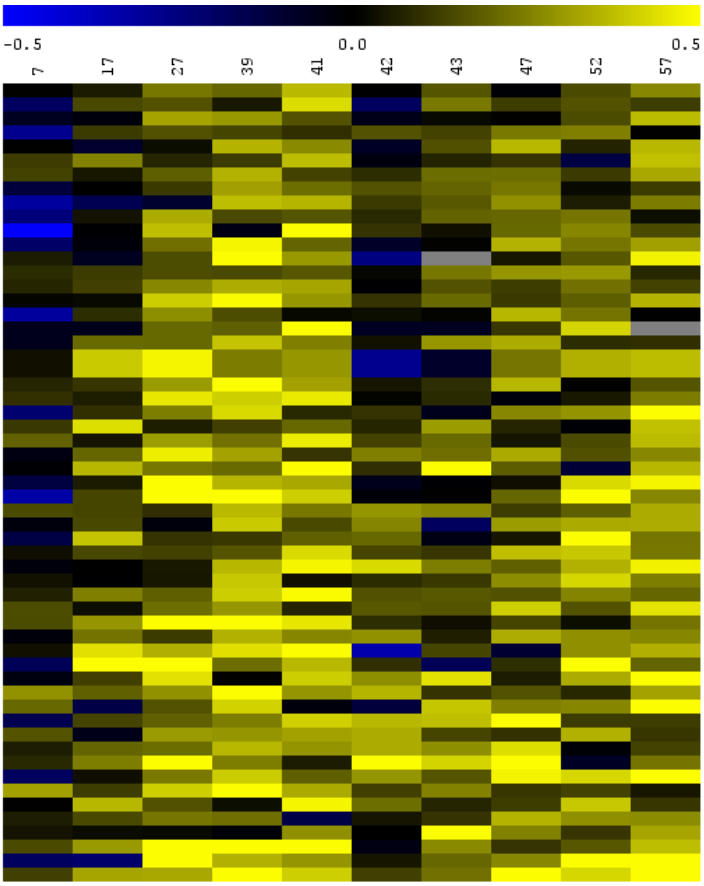

transport.phosphate 1-1-6.3.7.20
"misc.oxidases - copper, flavone etc. 1-1-1.4.20.2"
protein.postranslational modification 1-1-2.3.16.2
protein.degradation 1-1-1.3.11.18
cell wall.precursor synthesis.AXS 1-1-6.1.13.3
RNA.regulation of transcription.MADS box transcripti
P5CDH 1-1-5.3.4.11
"metal handling.binding, chelation and storage 1-1-4
stress.biotic 1-1-6.3.1.19
protein.targeting 1-1-6.3.6.4
RNA.regulation of transcription.WRKY domain transcri
amino acid met.degradation.aspartate family.lysine 1
ICDH 1-1-1.1.2.16
PS.calvin cyle.RPE 1-1-4.4.2.13
fermentation.aldehyde dehydrogenase 1-1-1.3.9.17
misc.glutathione S transferases 1-1-5.3.2.6
cell. vesicle transport 1-1-5.4.18.7
protein.targeting 1-1-6.3.19.11
transport misc 1-1-7.1.8.3
hormone metabolism.auxin.induced-regulated-responsiv
RNA.reg of transcription.Aux/IAA family 1-1-8.4.18.2
redox.thioredoxin 1-1-6.4.14.7
misc.glutathione S transferases 1-1-7.4.9.6
transport.metal 1-1-1.2.4.20
stress.abiotic.heat 1-1-8.1.19.14
RNA.regulation of transcription.C2C2(Zn) DOF zinc fi
protein.degradation.metalloprotease 1-1-5.1.10.7
cell wall.cellulose synthesis 1-1-5.1.20.3
protein.targeting 1-1-5.2.2.16
protein.postranslational modification 1-1-6.2.16.9
signalling.G-proteins 1-1-3.4.2.6
signalling.G-proteins 1-1-1.4.16.10
development.unspecified 1-1-8.1.19.13
development.unspecified 1-1-7.2.17.21
secondary metabolism.isoprenoids.mevalonate pathway.
"RNA.regulation of transcription.Nucleosome/chromati
RNA.regulation of transcription.putative transcripti
protein.synthesis.initiation 1-1-5.1.2.10
RNA.reg of transcription.bZIP transcription factor f
protein.degradation.metalloprotease 1-1-3.1.17.20
"metal handling.binding, chelation and storage 1-1-2
stress.biotic 1-1-2.2.19.16
misc.cytochrome P450 1-1-8.3.19.15
misc.glutathione S transferases 1-1-8.1.11.2
development.unspecified 1-1-1.1.2.18
amino acid metabolism.synthesis.histidine 1-1-5.2.8.
protein.degradation.cysteine protease 1-1-8.3.17.19
protein.targeting 1-1-6.2.13.11
transport.metal 1-1-7.3.2.11
protein.degradation.ubiquitin.E2 1-1-4.1.4.7
stress.biotic 1-1-3.1.3.4
tetrapyrrole synthesis 1-1-7.3.17.19
"misc.oxidases - copper, flavone etc. 1-1-4.2.10.20"
misc.peroxidases 1-1-5.3.3.13
misc.glutathione S transferases 1-1-2.2.9.7
RNA.regulation of transcription.bZIP transcription f
cell.organisation 1-1-5.3.9.18

Appendix IV

EC and accession numbers

Transcript	EC Number	Accession Number
UBQ		TC170478
Cit Syn	4.1.3.7	TC180568
Acon1	4.2.1.3	TC171686
Acon2	4.2.1.3	TC185608
ICDH1	1.1.1.41	TC170372
ICDH2	1.1.1.41	TC172709
ICDH3	1.1.1.41	TC170664
ICDH4	1.1.1.41	TC171366
ICDH5	1.1.1.42	TC195343
2OGDH1	1.2.4.2	TC186215
2OGDH2	1.2.4.2	TC171677
SCoA1	6.2.1.4	TC172461
SCoA2	6.2.1.4	TC170231
SDH1	1.3.5.1	TC181935
SDH2	1.3.5.1	TC183268
SDH3	1.3.5.1	TC187517
Fumarase	4.2.1.2	TC180884
MDH1	1.1.1.37	TC178560
MDH2	1.1.1.37	TC178790
AAT	2.6.1.1	TC172935
GDH1	1.4.1.3	TC169938
GDH2	1.4.1.3	TC171636
AS1	6.3.1.1	TC212203
AS2	6.3.5.4	TC215883
PDH1	1.5.99.8	TC209088

PDH2	1.5.99.8	TC200139
P5CS	1.5.1.12	TC210828
P5CR	1.5.1.2	TC193973
P5CDH	1.5.1.12	TC200529
NAGS1	2.3.1.1	TC216183
NAGS2	2.3.1.1	TC208234
NAGK1	2.7.2.8	TC211604
NAGK2	2.7.2.8	TC197078
NAOAT	2.6.1.11	TC195519
OAT	2.6.1.13	TC209829
ARG1	3.5.3.1	TC191508
ARG2	3.5.3.1	TC191541
ASS1	6.3.4.5	TC209322
ASS2	6.3.4.5	TC216958
IGPD	4.2.1.19	TC195065
IGPS	2.4.2.-	TC192372
GS1	6.3.1.2	TC171518
GS2	6.3.1.2	TC171380
PEPCK	4.1.1.49	TC192889
GAD1	4.1.1.15	TC191731
GABA1	2.6.1.19	TC193582
GABA2	2.6.1.19	TC191531
GABA3	2.6.1.19	TC200790
SSADH	1.2.1.24	TC193174

Appendix V

Introgression line genotyping

Line	1	2	3	4	5	6	7	8	9	10	11	12	13	14	15	16
2-3	O	O	●	●	●	●	●	●	●	●	●	O	O	O	O	O
2-4	O	O	O	O	O	O	O	●	●	●	●	●	●	O	O	O
2-5	O	O	O	O	O	O	O	O	O	O	●	●	●	●	●	●
2-6	O	O	O	O	O	O	O	O	O	O	O	O	O	O	O	●
LA716 A	●	●	●	●	●	●	●	●	●	●	●	●	●	●	●	●
LA716 B	●	●	●	●	●	●	●	●	●	●	●	●	●	●	●	●
LA716 C	●	●	●	●	●	●	●	●	-	●	●	●	●	●	●	-
LA716 D	●	●	●	●	●	●	●	●	●	●	●	●	●	●	●	●
M82 A	O	O	O	O	O	O	O	O	O	O	O	O	O	O	O	O
M82 B	O	O	O	O	O	O	O	O	O	O	O	O	O	O	O	O
M82 C	O	O	O	O	O	O	O	O	O	O	O	O	O	O	O	O
M82 D	O	O	O	O	O	O	O	O	O	O	O	O	O	O	O	O
2-3 A	O	O	●	●	●	●	●	●	●	●	●	O	O	O	O	O
2-3 A	O	O	●	●	●	●	●	●	●	●	●	O	O	O	O	O
2-3 B	O	O	●	●	●	●	●	●	●	●	●	O	O	O	O	O
2-3 B	O	O	●	●	●	●	●	●	●	●	●	O	O	O	O	O
2-3 C	O	O	●	●	●	●	●	●	●	●	●	O	O	O	O	-
2-3 C	O	O	●	●	●	●	●	●	●	●	●	O	O	O	O	O
2-3 D	O	O	●	●	●	●	●	●	●	●	●	O	O	O	O	O
2-3 D	O	O	●	●	●	●	●	●	●	●	●	O	O	O	O	O
2-4 A	O	O	O	O	O	O	O	O	O	●	O	O	O	O	O	O
2-4 A	O	O	O	O	O	O	O	O	O	●	O	O	O	O	O	O
2-4 B	O	O	O	*	O	O	O	*	*	*	*	-	●	O	O	O
2-4 B	O	O	O	*	O	O	O	*	*	*	*	*	*	O	O	O
2-4 C	O	O	O	*	O	O	O	*	*	*	*	*	*	O	O	O
2-4 C	O	O	O	*	O	O	O	*	*	*	*	*	*	O	O	O
2-4 D	O	O	O	O	O	O	O	O	O	O	O	O	O	O	O	O
2-4 D	O	O	O	O	O	O	O	O	O	O	O	O	O	O	O	O
2-5 A	O	O	O	O	O	O	O	O	-	O	●	●	●	●	●	●
2-5 A	O	O	O	O	O	O	O	O	-	O	●	●	●	●	●	●
2-5 B	-	O	O	O	O	O	O	O	-	O	-	O	●	O	O	O
2-5 B	-	-	-	-	-	O	O	-	*	-	-	-	-	-	-	O
2-5 C	-	O	-	-	-	O	O	O	-	O	-	●	●	-	-	●
2-5 C	-	O	O	O	O	O	O	O	O	O	-	●	●	O	-	●
2-5 D	-	-	-	O	O	O	O	-	-	O	-	-	●	-	-	O
2-5 D	-	O	O	O	-	O	O	O	O	-	-	O	-	-	O	O
2-6 A	O	O	O	O	O	O	O	O	O	O	O	O	O	O	O	●
2-6 A	O	O	O	O	O	O	O	O	O	O	O	O	O	O	O	●
2-6 B	O	O	O	O	O	O	O	O	O	O	O	O	O	O	O	●
2-6 B	O	O	O	O	O	O	O	O	O	O	O	O	O	O	O	●

2-6 C	o	o	o	o	o	o	o	o	o	o	o	o	o	o	o	●
2-6 C	o	o	o	o	o	o	o	o	o	o	o	o	o	o	o	●
2-6 D	-	o	o	-	o	o	o	o	-	o	-	-	-	-	-	●
2-6 D	-	o	-	o	o	-	o	-	o	-	-	-	-	-	o	-

Table 1. Sub-introgression line genotyping. *S. pennellii* (black circle), *S. Lycopersicum* (open circle), data inconclusive (*****), data not available (-).

Appendix VI

Sub-introgression line genotyping

Line	Marker																					
	1	2	3	4	5	6	7	8	9	10	11	12	13	14	15	16	17	18	19	20	21	22
2-4 A	o	o	*	*	*	*	●	●	o	o	o	o	o	o	o	o	o	o	o	o	o	o
2-4 A	o	o	*	*	*	*	●	●	o	o	o	o	o	o	o	o	o	o	o	o	o	o
2-4 B	o	o	*	*	*	*	*	o	o	o	o	o	o	o	o	o	o	o	o	o	o	o
2-4 B	o	o	*	*	*	*	*	o	o	o	o	o	o	o	o	o	o	o	o	o	o	o
2-5 A	●	●	●	●	●	●	●	*	●	●	●	●	●	●	●	●	●	●	●	●	●	●
2-5 A	●	●	●	●	●	●	●	●	-	●	●	●	●	●	●	●	●	●	●	●	●	●
2-5 B	●	●	●	●	●	●	●	*	*	●	●	●	●	●	●	●	●	●	●	●	*	●
2-5 B	●	●	●	●	●	●	●	●	●	●	●	●	●	●	●	●	●	●	●	●	*	●
2-5 C	●	●	●	●	●	●	●	●	●	●	●	●	●	●	●	●	●	●	●	●	●	●
2-5 C	●	●	●	●	●	●	●	●	●	●	●	●	●	●	●	●	●	●	●	●	●	●
2-5 D	●	●	●	●	●	●	●	●	●	●	●	●	●	●	●	●	●	●	●	●	●	●
2-5 D	●	●	●	●	●	●	●	●	●	●	●	●	●	●	●	●	●	●	●	●	●	●
2-6 A	o	o	o	o	o	o	o	o	o	o	o	o	o	o	o	●	●	●	●	●	●	●
2-6 A	o	o	o	o	o	o	o	o	o	o	o	o	o	o	o	●	●	●	●	●	*	●
2-6 B	o	o	o	o	o	*	o	o	o	o	o	o	o	o	o	●	●	●	●	●	●	●
2-6 B	o	o	o	o	o	*	o	o	o	o	o	o	o	o	o	●	●	●	●	●	●	●
LA716 A	●	●	●	●	-	●	●	*	-	●	●	●	●	●	●	●	●	●	●	●	-	●
LA716 A	●	●	●	●	●	●	●	●	*	●	●	●	●	●	●	●	●	●	●	●	●	●
LA716 B	●	●	●	●	●	●	●	●	-	●	●	●	●	●	●	●	●	●	●	●	●	●
LA716 B	●	●	●	●	●	●	●	●	●	●	●	●	●	●	●	-	●	●	●	●	*	●
M82 A	o	-	o	o	o	o	o	o	o	-	-	o	o	o	o	o	o	o	-	o	o	o
M82 A	o	o	o	o	o	o	o	o	o	o	o	o	o	o	o	o	o	o	o	o	o	o
M82 B	o	o	o	o	o	o	o	o	o	o	o	o	o	o	o	o	o	o	o	o	o	o
M82 B	o	o	o	o	o	o	o	o	o	o	o	o	o	o	o	o	o	o	o	o	o	o
M82 C	o	o	o	o	o	o	o	o	o	o	o	o	o	o	o	o	o	o	o	o	o	o
M82 C	o	o	o	o	o	o	o	o	o	o	o	o	o	o	o	o	o	o	o	o	o	o
M82 D	o	o	o	o	o	o	o	o	o	o	o	o	o	o	o	o	o	o	o	o	o	o
M82 D	o	o	o	o	o	o	o	o	o	o	o	o	o	o	o	o	o	o	o	o	o	o
4176 A	o	o	o	o	o	o	o	o	o	o	o	o	o	o	o	o	●	●	●	●	●	●
4176 A	o	o	o	o	o	o	o	o	o	o	o	o	o	o	o	o	●	●	●	●	●	●
4176 B	o	o	o	o	o	o	o	o	o	o	o	o	o	o	o	o	●	●	●	●	●	●
4176 B	o	o	o	o	o	o	o	o	o	o	o	o	o	o	o	o	●	●	●	●	●	●
4176 C	o	o	o	o	o	o	o	o	o	o	o	o	o	o	o	o	●	●	●	●	●	●
4176 C	o	o	o	o	o	o	o	o	o	o	o	o	o	o	o	o	●	●	●	●	*	●
4176 D	o	o	o	o	o	o	o	o	o	o	o	o	o	o	o	o	●	●	●	●	●	●
4176 D	o	o	o	o	o	o	o	o	o	o	o	o	o	o	o	o	●	●	●	●	●	●
4178 A	-	o	*	o	o	o	o	o	o	o	o	o	o	o	-	●	-	-	●	●	*	●
4178 A	-	-	-	-	-	-	-	-	-	-	-	-	-	-	-	-	-	-	-	-	-	-
4178 B	o	*	o	o	o	*	o	o	o	o	o	o	o	o	o	o	●	●	●	●	●	●
4178 B	o	o	o	o	o	o	o	o	o	o	o	o	o	o	o	o	●	●	●	●	*	●
4178 C	o	o	o	o	o	o	o	o	o	o	o	o	o	o	*	o	●	●	●	●	*	●
4178 C	o	o	o	o	o	o	o	o	o	o	o	o	o	o	o	o	●	●	●	●	●	●
4603 A	o	o	o	o	o	o	o	o	o	-	o	o	o	o	o	●	●	o	o	o	o	o
4603 A	o	o	o	o	-	-	o	o	-	-	o	o	-	o	o	●	●	o	-	o	o	o
4603 B	-	o	o	o	o	o	o	o	o	o	o	o	o	o	-	-	●	o	o	o	o	o
4603 B	o	o	o	o	o	o	o	o	o	o	o	o	o	o	o	●	●	o	o	o	o	o
4603 C	o	o	o	o	o	o	o	o	o	o	o	o	o	o	o	●	●	o	o	o	o	o
4603 C	o	o	o	o	o	o	o	o	o	o	o	o	o	o	o	●	●	o	o	o	o	o

4603 D	o	o	o	o	o	o	o	o	o	o	o	o	o	o	o	●	●	o	o	o	o	o	
4603 D	o	o	o	o	o	o	o	o	o	o	o	o	o	o	o	●	●	o	o	o	o	o	
4625 A	●	●	●	●	●	●	●	●	●	●	●	●	●	●	●	o	o	o	o	o	o		
4625 A	●	●	●	●	●	●	●	●	-	●	●	●	●	●	●	o	o	o	o	o	o		
4625 B	●	●	●	●	●	●	●	●	●	●	●	●	*	●	●	o	o	o	o	o	o		
4625 B	●	●	●	●	●	●	●	●	●	●	●	●	*	●	●	o	o	o	o	o	o		
4625 C	-	-	-	-	-	-	-	-	-	-	-	-	-	-	-	-	-	-	-	-	-		
4625 C	●	●	●	●	●	●	●	●	●	●	●	●	●	●	●	o	o	o	o	o	o		
4625 D	●	●	●	●	●	●	●	*	●	●	●	*	*	●	●	o	o	o	o	o	o		
4625 D	●	●	●	●	●	●	●	●	●	●	●	●	●	●	●	o	o	o	o	o	o		
4637 A	*	●	●	●	●	●	●	●	*	●	●	*	*	●	●	●	o	o	o	o	*	o	
4637 A	●	●	●	●	●	●	●	●	-	●	●	●	*	●	●	●	o	o	o	o	o	o	
4637 B	*	●	●	●	●	●	●	●	●	●	●	*	●	●	●	●	o	o	o	o	*	o	
4637 B	*	●	●	●	●	●	●	●	-	●	●	*	●	●	●	●	o	o	o	o	*	o	
4637 C	●	●	●	●	●	●	●	●	*	●	●	●	●	●	●	●	o	o	o	o	o	o	
4637 C	●	●	●	●	●	●	●	●	●	●	●	●	*	●	●	●	o	o	o	o	o	o	
4637 D	●	●	●	●	●	●	●	*	*	●	●	●	●	●	●	●	o	o	o	o	o	o	
4637 D	●	●	●	●	●	●	●	●	●	●	●	●	*	●	●	●	o	o	o	o	o	o	
4637 E	●	●	●	●	●	●	●	●	●	●	●	●	●	●	●	●	o	o	o	o	o	o	
4637 E	●	●	●	●	●	●	●	●	●	●	●	●	●	●	●	●	o	o	o	o	o	o	
4648 A	o	o	●	●	●	●	●	●	o	o	o	o	o	o	o	-	o	o	o	o	o	o	
4648 A	o	o	●	●	●	●	●	●	o	o	o	o	o	o	o	o	o	o	o	o	o	o	
4648 B	o	o	●	●	●	●	●	●	o	o	o	o	o	o	*	o	o	o	o	o	o	o	
4648 B	o	o	●	●	●	●	●	●	o	o	o	o	o	o	o	o	o	o	o	o	o	o	
4648 C	o	o	●	●	●	●	●	●	o	o	o	o	o	o	o	o	o	o	o	o	o	o	
4648 C	o	o	●	●	●	●	●	●	o	o	o	o	o	o	o	o	o	o	o	o	o	o	
4648 D	-	o	-	●	●	-	-	●	o	o	o	-	o	o	-	-	-	-	o	o	o	o	
4648 D	o	o	●	●	●	●	●	●	o	o	o	o	o	o	o	o	o	o	o	o	o	o	
4690 A	●	●	●	●	●	●	●	●	●	●	●	●	●	●	●	o	o	o	o	o	o	o	
4690 A	●	●	●	●	●	●	●	●	●	●	●	●	●	●	●	o	o	o	o	o	o	o	
4690 B	●	●	●	●	●	●	●	●	●	●	●	●	●	●	●	o	o	o	o	o	o	o	
4690 B	●	●	●	●	●	●	●	*	*	●	●	●	●	●	●	o	o	o	o	o	o	o	
4690 C	●	●	●	●	●	●	●	●	●	●	●	●	●	●	●	o	o	o	o	o	o	o	
4690 C	●	●	●	●	●	●	●	●	●	●	●	●	●	●	●	o	o	o	o	o	o	o	
4690 D	●	●	●	●	●	●	●	●	●	●	●	●	●	●	●	o	o	o	o	o	o	o	
4690 D	●	●	●	●	●	●	●	●	●	●	●	●	●	●	●	o	o	o	o	o	o	o	
4753 A	o	o	o	o	o	o	o	o	o	o	o	o	o	*	o	o	●	●	o	o	o	o	
4753 A	o	o	o	o	o	o	o	o	o	o	o	o	o	o	o	o	●	●	o	o	o	o	
4753 B	*	o	o	o	o	o	o	o	o	o	o	o	o	o	o	o	●	●	o	o	o	o	
4753 B	o	o	o	o	o	o	o	o	o	o	o	o	o	o	o	o	●	●	o	o	o	o	
4753 C	o	o	o	o	o	o	o	o	o	o	o	o	o	o	o	o	●	●	o	o	o	o	
4753 C	o	o	o	o	o	o	o	o	o	o	o	o	o	o	o	o	●	●	o	o	o	o	
4753 D	o	o	o	o	o	o	o	o	o	o	o	o	o	o	o	o	●	●	o	o	o	o	
4753 D	o	o	o	o	o	o	o	o	o	o	o	o	o	o	o	o	●	●	o	o	o	o	
4753E	*	o	o	o	o	o	o	o	o	o	o	o	o	o	o	o	●	●	o	o	o	o	
4753 E	o	o	o	o	o	o	o	o	o	o	o	o	o	o	o	o	●	●	o	o	o	o	

Table 1. Sub-introgression line genotyping. *S.pennellii* (black circle), *S. Lycopersicum* (open circle), data inconclusive (*****) data not available (-).

Appendix VII

Annotation data

SGN Number	Annotation
SGN-U584807	ATP dependent DNA ligase family protein [Arabidopsis thaliana]
SGN-U200563	ATPase beta subunit [Nicotiana sylvestris]
SGN-U212238	ATPase beta subunit [Nicotiana sylvestris]
SGN-U295324	ATPase beta subunit [Nicotiana sylvestris]
SGN-U562943	hypothetical
SGN-U575468	hypothetical protein [Vitis vinifera]
SGN-U584992	hypothetical protein [Vitis vinifera]
SGN-U295926	MAP3K-like protein kinase [Arabidopsis thaliana]
SGN-U576543	MAPKKK21 ATP binding / protein kinase/ protein serine/threonine kinase [Arabidopsis thaliana]
SGN-U582791	MAPKKK21 ATP binding / protein kinase/ protein serine/threonine kinase [Arabidopsis thaliana]
SGN-U597354	MAPKKK21 ATP binding / protein kinase/ protein serine/threonine kinase [Arabidopsis thaliana]
SGN-U576027	predicted protein [Physcomitrella patens subsp. patens]
SGN-U280266	predicted protein [Populus trichocarpa]
SGN-U295739	predicted protein [Populus trichocarpa]
SGN-U292976	predicted protein [Populus trichocarpa]
SGN-U285476	PREDICTED: hypothetical protein [Vitis vinifera]
SGN-U273820	PREDICTED: hypothetical protein [Vitis vinifera]
SGN-U282893	PREDICTED: hypothetical protein [Vitis vinifera]
SGN-U291352	PREDICTED: hypothetical protein [Vitis vinifera]
SGN-U274694	PREDICTED: hypothetical protein [Vitis vinifera]
SGN-U284774	PREDICTED: hypothetical protein [Vitis vinifera]
SGN-U288252	PREDICTED: hypothetical protein isoform 1 [Vitis vinifera]
SGN-U295062	putative MATE transporter [Nicotiana tabacum]
SGN-U197309	putative oxalyl-CoA decarboxylase [Oryza sativa (japonica cultivar-group)]
SGN-U273712	RNA-binding protein, putative [Ricinus communis]
SGN-U296528	serine-threonine protein kinase, putative [Ricinus communis]
SGN-U202320	SLL2-S9-protein [Brassica rapa]
SGN-U288254	SLL2-S9-protein-like [Solanum tuberosum]
SGN-U288251	SLL2-S9-protein-like [Solanum tuberosum]
SGN-U570151	unknown [Medicago truncatula]
SGN-U600741	unknown [Populus trichocarpa]
SGN-U573782	unknown protein [Arabidopsis thaliana]
SGN-U564510	unknown
SGN-U276366	unnamed protein product [Vitis vinifera]
SGN-U273819	unnamed protein product [Vitis vinifera]
SGN-U575469	unnamed
SGN-U569447	unnamed
SGN-U575840	unnamed
SGN-U578043	unnamed

SGN-U575841	unnamed
SGN-U597806	unnamed
SGN-U106640	none
SGN-U292983	none
SGN-U572142	none
SGN-U589458	none
SGN-U592852	none
SGN-U599569	none
SGN-U603399	none
SGN-U604522	none

Table 1. Annotation of genes in chromosome 2 between marker TG167 at 118.0 cM and marker 2-4g33985 at 119.0 cM. Data was extracted from the SOL Genomics Network http://solgenomics.net/ (Mueller *et al.*, 2005).

SGN Number	Annotation
SGN-U594517	26S proteasome regulatory subunit S5A [Mesembryanthemum crystallinum]
SGN-U275521	3-hydroxy-3-methylglutaryl-coenzyme A reductase 1 [Solanum tuberosum]
SGN-U270642	acidic 27 kDa endochitinase [Solanum lycopersicum]
SGN-U196327	acidic 27 kDa endochitinase precursor chitinase (EC 3.2.1.14) [Lycopersicon esculentum]
SGN-U577871	acidic endochitinase precursor chitinase (EC 3.2.1.14) [Petunia x hybrida]
SGN-U593805	acidic endochitinase Q precursor (Pathogenesis-related protein Q) (PR-Q) - common tobacco
SGN-U592828	acidic endochitinase Q precursor (Pathogenesis-related protein Q) (PR-Q) - common tobacco
SGN-U284413	acyl:coa ligase acetate-coa synthetase-like protein [Populus trichocarpa]
SGN-U581388	antimicrobial peptide snakin [Capsicum annuum]
SGN-U584393	APX3 (ASCORBATE PEROXIDASE 3); L-ascorbate peroxidase [Arabidopsis thaliana]
SGN-U573308	ARO2 (ARMADILLO REPEAT ONLY 2); binding [Arabidopsis thaliana]
SGN-U595179	ARO2 (ARMADILLO REPEAT ONLY 2); binding [Arabidopsis thaliana]
SGN-U595060	ascorbate peroxidase [Zantedeschia aethiopica]
SGN-U584821	ascorbate peroxidase [Zantedeschia aethiopica]
SGN-U274599	aspartic proteinase nepenthesin-1 precursor, putative [Ricinus communis]
SGN-U284732	aspartic proteinase nepenthesin-2 precursor, putative [Ricinus communis]
SGN-U574299	aspartyl protease family protein [Arabidopsis thaliana]
SGN-U574864	aspartyl protease family protein [Arabidopsis thaliana]
SGN-U586456	ATGRIP; protein binding [Arabidopsis thaliana]
SGN-U567247	ATSAC1B (SUPPRESSOR OF ACTIN 1B); phosphatidylinositol-4,5-bisphosphate 5-phosphatase [Arabidopsis thaliana]
SGN-U603131	auxin-induced SAUR-like protein [Capsicum annuum]
SGN-U582757	calcium-binding EF hand family protein [Arabidopsis thaliana]
SGN-U603967	calcium-dependent protein kinase CPK4 [Nicotiana tabacum]
SGN-U582058	calcium-dependent protein kinase CPK4 [Nicotiana tabacum]
SGN-U196648	catalase 1 [Nicotiana tabacum]
SGN-U415793	catalase 1 [Nicotiana tabacum]
SGN-U578479	catalase 1 [Nicotiana tabacum]
SGN-U268890	catalase isozyme 2 [Solanum lycopersicum]
SGN-U273432	chain D, Crystal Structure Of The Plant Rho Protein Rop5
SGN-U593206	chitinase [Solanum lycopersicum]
SGN-U578942	chitinase [Solanum lycopersicum]
SGN-U581507	chitinase [Solanum lycopersicum]
SGN-U584901	chitinase 134 [Nicotiana tabacum]
SGN-U576039	chitinase; endochitinase [Solanum tuberosum]
SGN-U603568	cold inducible histidine kinase 1 [Catharanthus roseus]
SGN-U275197	conserved hypothetical protein [Ricinus communis]
SGN-U285642	conserved hypothetical protein [Ricinus communis]
SGN-U281762	conserved hypothetical protein [Ricinus communis]
SGN-U296051	conserved hypothetical protein [Ricinus communis]
SGN-U279009	conserved hypothetical protein [Ricinus communis]
SGN-U578390	CTP synthase, putative / UTP-ammonia ligase, putative [Arabidopsis thaliana]
SGN-U585713	cyclin B2 [Solanum lycopersicum]
SGN-U588280	cyclin B2 [Solanum lycopersicum]
SGN-U298903	cyclin B2 [Solanum lycopersicum]
SGN-U568781	dehydroquinate synthase [Solanum lycopersicum]

SGN-U269908	dehydroquinate synthase [Solanum lycopersicum]
SGN-U281609	dehydroquinate synthase [Solanum lycopersicum]
SGN-U573837	DnaJ-like protein [Phaseolus vulgaris]
SGN-U573836	DnaJ-like protein [Phaseolus vulgaris]
SGN-U578799	eukaryotic
SGN-U581081	ferredoxin-NADP
SGN-U442674	ferredoxin-NADP
SGN-U591066	ferredoxin-NADP
SGN-U415690	ferredoxin-NADP
SGN-U269372	ferredoxin-NADP reductase, leaf-type isozyme, chloroplastic [Nicotiana tabacum]
SGN-U587471	flavanone 3 beta-hydroxylase [Solanum pinnatisectum]
SGN-U563669	flavanone 3 beta-hydroxylase [Solanum tuberosum]
SGN-U587470	flavanone 3 beta-hydroxylase [Solanum tuberosum]
SGN-U587472	flavanone 3 beta-hydroxylase [Solanum tuberosum]
SGN-U572565	GIL1 (GRAVITROPIC IN THE LIGHT) [Arabidopsis thaliana]
SGN-U597457	glutamate receptor [Malus hupehensis]
SGN-U565454	Grx_S14
SGN-U580763	high mobility group protein [Solanum tuberosum]
SGN-U591786	high mobility group protein [Solanum tuberosum]
SGN-U581082	high mobility group protein [Solanum tuberosum]
SGN-U586523	hypothetical
SGN-U597390	hypothetical
SGN-U565641	hypothetical
SGN-U597107	hypothetical
SGN-U570567	hypothetical
SGN-U568892	hypothetical
SGN-U519195	hypothetical
SGN-U586520	hypothetical
SGN-U565334	hypothetical
SGN-U574889	hypothetical
SGN-U569412	hypothetical protein [Camellia sinensis]
SGN-U587505	hypothetical protein [Camellia sinensis]
SGN-U466818	hypothetical protein [Vitis vinifera
SGN-U576545	hypothetical protein [Vitis vinifera]
SGN-U585584	hypothetical protein [Vitis vinifera]
SGN-U602573	hypothetical protein [Vitis vinifera]
SGN-U490741	hypothetical protein [Vitis vinifera]
SGN-U280509	hypothetical protein [Vitis vinifera]
SGN-U584914	hypothetical protein [Vitis vinifera]
SGN-U595308	hypothetical protein [Vitis vinifera]
SGN-U512924	hypothetical protein [Vitis vinifera]
SGN-U571903	hypothetical protein [Vitis vinifera]
SGN-U582654	hypothetical protein [Vitis vinifera]
SGN-U577396	hypothetical protein [Vitis vinifera]
SGN-U273236	hypothetical protein [Vitis vinifera]
SGN-U295615	hypothetical protein [Vitis vinifera]
SGN-U277562	hypothetical protein [Vitis vinifera]
SGN-U569456	hypothetical protein [Vitis vinifera]
SGN-U280361	hypothetical protein [Vitis vinifera]
SGN-U575470	hypothetical protein [Vitis vinifera]

SGN-U589137	hypothetical protein [Vitis vinifera]
SGN-U200741	hypothetical protein At2g17930 [Arabidopsis thaliana]
SGN-U273661	hypothetical protein OsI_24534 [Oryza sativa Indica Group]
SGN-U582930	hypothetical protein OsI_27866 [Oryza sativa Indica Group]
SGN-U565298	IRE1A; endoribonuclease/ kinase [Arabidopsis thaliana]
SGN-U283113	mitotic control protein dis3, putative [Ricinus communis]
SGN-U203590	MLO10 (MILDEW RESISTANCE LOCUS O 10); calmodulin binding [Arabidopsis thaliana]
SGN-U567746	NAD-dependent isocitrate dehydrogenase [Nicotiana tabacum]
SGN-U567402	Os03g0608800
SGN-U595277	oxidoreductase, 2OG-Fe(II) oxygenase family [Arabidopsis thaliana]
SGN-U597839	pathogenesis-related thaumatin family protein [Arabidopsis thaliana]
SGN-U576588	phospholipase D delta isoform [Gossypium hirsutum]
SGN-U424081	phospholipase D delta isoform [Gossypium hirsutum]
SGN-U204352	phospholipase D delta isoform 1a [Gossypium hirsutum]
SGN-U576591	phospholipase D delta isoform 1a [Gossypium hirsutum]
SGN-U604580	PIP3 (PLASMA MEMBRANE INTRINSIC PROTEIN 3); water channel [Arabidopsis thaliana]
SGN-U275620	plant ubiquilin, putative [Ricinus communis]
SGN-U415685	predicted protein [Physcomitrella patens subsp. patens]
SGN-U284572	predicted protein [Populus trichocarpa]
SGN-U296208	predicted protein [Populus trichocarpa]
SGN-U268947	predicted protein [Populus trichocarpa]
SGN-U297391	predicted protein [Populus trichocarpa]
SGN-U279003	predicted protein [Populus trichocarpa]
SGN-U276038	predicted protein [Populus trichocarpa]
SGN-U273390	predicted protein [Populus trichocarpa]
SGN-U295799	predicted protein [Populus trichocarpa]
SGN-U282140	predicted protein [Populus trichocarpa]
SGN-U293282	predicted protein [Populus trichocarpa]
SGN-U284148	predicted protein [Populus trichocarpa]
SGN-U274447	predicted protein [Populus trichocarpa]
SGN-U274846	PREDICTED: hypothetical protein [Vitis vinifera]
SGN-U270807	PREDICTED: hypothetical protein [Vitis vinifera]
SGN-U278722	PREDICTED: hypothetical protein [Vitis vinifera]
SGN-U285579	PREDICTED: hypothetical protein [Vitis vinifera]
SGN-U286184	PREDICTED: hypothetical protein [Vitis vinifera]
SGN-U277270	PREDICTED: hypothetical protein [Vitis vinifera]
SGN-U278388	PREDICTED: hypothetical protein [Vitis vinifera]
SGN-U292643	PREDICTED: hypothetical protein [Vitis vinifera]
SGN-U279007	PREDICTED: hypothetical protein [Vitis vinifera]
SGN-U280538	PREDICTED: hypothetical protein [Vitis vinifera]
SGN-U291562	PREDICTED: hypothetical protein [Vitis vinifera]
SGN-U284960	PREDICTED: hypothetical protein [Vitis vinifera]
SGN-U292562	PREDICTED: hypothetical protein [Vitis vinifera]
SGN-U277585	PREDICTED: hypothetical protein [Vitis vinifera]
SGN-U285482	PREDICTED: hypothetical protein [Vitis vinifera]
SGN-U274543	PREDICTED: hypothetical protein [Vitis vinifera]
SGN-U293663	PREDICTED: hypothetical protein [Vitis vinifera]
SGN-U284936	PREDICTED: hypothetical protein [Vitis vinifera]

SGN-U280523	PREDICTED: hypothetical protein [Vitis vinifera]
SGN-U275644	PREDICTED: hypothetical protein [Vitis vinifera]
SGN-U271430	PREDICTED: hypothetical protein [Vitis vinifera]
SGN-U275748	PREDICTED: hypothetical protein [Vitis vinifera]
SGN-U271438	PREDICTED: hypothetical protein [Vitis vinifera]
SGN-U273533	PREDICTED: hypothetical protein [Vitis vinifera]
SGN-U280753	PREDICTED: hypothetical protein [Vitis vinifera]
SGN-U280943	PREDICTED: hypothetical protein [Vitis vinifera]
SGN-U295525	PREDICTED: hypothetical protein [Vitis vinifera]
SGN-U288763	PREDICTED: hypothetical protein [Vitis vinifera]
SGN-U292570	PREDICTED: hypothetical protein [Vitis vinifera]
SGN-U272976	PREDICTED: hypothetical protein [Vitis vinifera]
SGN-U270966	PREDICTED: hypothetical protein [Vitis vinifera]
SGN-U287137	PREDICTED: hypothetical protein [Vitis vinifera]
SGN-U268949	PREDICTED: hypothetical protein [Vitis vinifera]
SGN-U277746	PREDICTED: hypothetical protein [Vitis vinifera]
SGN-U274528	PREDICTED: hypothetical protein isoform 2 [Vitis vinifera]
SGN-U283437	PREDICTED: hypothetical protein isoform 2 [Vitis vinifera]
SGN-U278720	PREDICTED: hypothetical protein isoform 2 [Vitis vinifera]
SGN-U280580	PREDICTED: hypothetical protein, partial [Vitis vinifera]
SGN-U279291	prolyl 4-hydroxylase, alpha subunit-like protein [Arabidopsis thaliana]
SGN-U201372	proteasome regulatory subunit S5A [Mesembryanthemum crystallinum]
SGN-U589573	protein
SGN-U586551	protein phosphatase 2C homolog [Mesembryanthemum crystallinum]
SGN-U272158	protein phosphatase 2c, putative [Ricinus communis]
SGN-U415121	protein phosphatase-2c [Mesembryanthemum crystallinum]
SGN-U199752	protein transport protein Sec24, putative [Arabidopsis thaliana]
SGN-U571604	protein transport protein Sec24, putative [Arabidopsis thaliana]
SGN-U576885	PSAT; O-phospho-L-serine:2-oxoglutarate aminotransferase [Arabidopsis thaliana]
SGN-U576886	PSAT; O-phospho-L-serine:2-oxoglutarate aminotransferase [Arabidopsis thaliana]
SGN-U273015	putative anti-PCD protein [Solanum lycopersicum]
SGN-U576696	putative calcium-dependent protein kinase CPK1 adapter protein 2 [Mesembryanthemum crystallinum]
SGN-U472517	putative ferredoxin NADP reductase [Solanum ochranthum]
SGN-U579448	putative ferredoxin-NADP reductase [Solanum peruvianum]
SGN-U202963	putative poly(A) polymerase [Arabidopsis thaliana]
SGN-U200772	Putative protein transport protein Sec24-like At3g07100 [Arabidopsis thaliana]
SGN-U465111	putative Sec24-like COPII protein [Arabidopsis thaliana]
SGN-U200924	putative serine/threonine-protein kinase ctr1 [Oryza sativa (japonica cultivar-group)]
SGN-U199203	putative ubiquitin protein [Oryza sativa (japonica cultivar-group)]
SGN-U201944	putative vacuolar protein sorting-associated protein [Oryza sativa (japonica cultivar-group)]
SGN-U271452	Rac-like GTPase 1 [Nicotiana tabacum]
SGN-U581579	Rac-like GTPase 1 [Nicotiana tabacum]
SGN-U206976	Rho-GTPase-activating protein-related [Arabidopsis thaliana]
SGN-U584800	ribonuclease E [Solanum lycopersicum]
SGN-U284498	ribonuclease E [Solanum lycopersicum]

SGN-U291701	ribonuclease E [Solanum lycopersicum]
SGN-U564495	self-pruning G-box protein [Solanum lycopersicum]
SGN-U566924	senescence-associated protein [Nicotiana tabacum]
SGN-U575688	TPA: TPA_inf: ARO1-like protein 1 [Medicago truncatula]
SGN-U577921	transformer-SR ribonucleoprotein [Nicotiana tabacum]
SGN-U578711	transformer-SR ribonucleoprotein [Nicotiana tabacum]
SGN-U275462	transformer-SR ribonucleoprotein [Nicotiana tabacum]
SGN-U591456	transformer-SR ribonucleoprotein [Nicotiana tabacum]
SGN-U580844	transformer-SR ribonucleoprotein [Nicotiana tabacum]
SGN-U565336	ubiquitin-conjugating enzyme [Plantago major]
SGN-U597108	ubiquitin-conjugating enzyme [Plantago major]
SGN-U285261	vacuolar sorting protein, putative [Ricinus communis]
SGN-U277006	unknown [Glycine max]
SGN-U278792	unknown [Glycine max]
SGN-U280623	unknown [Glycine max]
SGN-U277125	unknown [Glycine max]
SGN-U580388	unknown [Medicago truncatula]
SGN-U595894	unknown [Picea sitchensis]
SGN-U569320	unknown [Populus trichocarpa x Populus deltoides]
SGN-U595914	unknown [Populus trichocarpa]
SGN-U584884	unknown [Populus trichocarpa]
SGN-U578248	unknown [Zea mays]
SGN-U578888	unknown protein [Arabidopsis thaliana]
SGN-U575929	unknown protein [Arabidopsis thaliana]
SGN-U587743	unknown protein [Arabidopsis thaliana]
SGN-U574612	unknown protein [Arabidopsis thaliana]
SGN-U586550	unknown
SGN-U567401	unknown
SGN-U586457	unnamed protein product [Arabidopsis thaliana]
SGN-U582795	unnamed protein product [Arabidopsis thaliana]
SGN-U277641	unnamed protein product [Vitis vinifera]
SGN-U279197	unnamed protein product [Vitis vinifera]
SGN-U291669	unnamed protein product [Vitis vinifera]
SGN-U275614	unnamed protein product [Vitis vinifera]
SGN-U275182	unnamed protein product [Vitis vinifera]
SGN-U273237	unnamed protein product [Vitis vinifera]
SGN-U283884	unnamed protein product [Vitis vinifera]
SGN-U283833	unnamed protein product [Vitis vinifera]
SGN-U437421	unnamed
SGN-U424042	unnamed
SGN-U448026	unnamed
SGN-U578922	unnamed
SGN-U564077	unnamed
SGN-U563079	unnamed
SGN-U566310	unnamed
SGN-U565300	unnamed
SGN-U569602	unnamed
SGN-U565496	unnamed
SGN-U576660	unnamed
SGN-U567704	unnamed

SGN-U424381	unnamed
SGN-U471766	unnamed
SGN-U578511	unnamed
SGN-U576123	unnamed
SGN-U569059	unnamed
SGN-U573884	unnamed
SGN-U566746	unnamed
SGN-U566746	unnamed
SGN-U566245	unnamed
SGN-U566748	unnamed
SGN-U565299	unnamed
SGN-U569712	unnamed
SGN-U588405	unnamed
SGN-U597937	unnamed
SGN-U598631	unnamed
SGN-U584838	unnamed
SGN-U588561	unnamed
SGN-U562622	unnamed
SGN-U466441	unnamed
SGN-U586458	unnamed
SGN-U481992	unnamed
SGN-U563856	unnamed
SGN-U576428	unnamed
SGN-U579495	unnamed
SGN-U566560	unnamed
SGN-U571139	unnamed
SGN-U592324	unnamed
SGN-U604348	unnamed
SGN-U565297	unnamed
SGN-U572451	unnamed
SGN-U565495	unnamed
SGN-U419783	unnamed
SGN-U591328	unnamed
SGN-U567423	unnamed
SGN-U582612	unnamed
SGN-U586312	unnamed
SGN-U604740	unnamed
SGN-U595916	unnamed
SGN-U588649	unnamed
SGN-U581904	unnamed
SGN-U573965	unnamed
SGN-U601102	unnamed
SGN-U601423	unnamed
SGN-U572087	unnamed
SGN-U601166	unnamed
SGN-U603181	unnamed
SGN-U566747	unnamed
SGN-U566747	unnamed
SGN-U577476	unnamed
SGN-U564076	unnamed

SGN-U420521	unnamed
SGN-U602678	unnamed
SGN-U584331	unnamed
SGN-U582756	unnamed
SGN-U588041	unnamed
SGN-U583847	unnamed
SGN-U601809	unnamed
SGN-U574370	unnamed
SGN-U576036	unnamed
SGN-U579369	unnamed
SGN-U586724	unnamed
SGN-U578262	unnamed
SGN-U582265	unnamed
SGN-U565797	unnamed
SGN-U570098	unnamed
SGN-U563682	unnamed
SGN-U598791	unnamed
SGN-U602330	unnamed
SGN-U567174	unnamed
SGN-U590159	unnamed
SGN-U565830	unnamed
SGN-U584932	unnamed
SGN-U571313	unnamed
SGN-U582515	unnamed
SGN-U596671	unnamed
SGN-U475249	unnamed
SGN-U567589	unnamed
SGN-U584361	unnamed
SGN-U576565	unnamed
SGN-U590486	unnamed
SGN-U569058	unnamed
SGN-U519468	unnamed
SGN-U575987	unnamed
SGN-U469314	unnamed
SGN-U584637	unnamed
SGN-U580990	unnamed
SGN-U567175	unnamed
SGN-U565307	unnamed
SGN-U438035	unnamed
SGN-U572091	unnamed
SGN-U455842	unnamed
SGN-U580442	unnamed
SGN-U566222	unnamed
SGN-U563109	unnamed
SGN-U563808	unnamed
SGN-U588040	unnamed
SGN-U478938	unnamed
SGN-U584384	unnamed
SGN-U581603	unnamed
SGN-U106469	none

SGN-U106484	none
SGN-U106485	none
SGN-U106526	none
SGN-U106526	none
SGN-U106526	none
SGN-U106640	none
SGN-U106645	none
SGN-U107521	none
SGN-U107655	none
SGN-U274529	none
SGN-U277223	none
SGN-U287561	none
SGN-U287562	none
SGN-U288704	none
SGN-U288992	none
SGN-U488748	none
SGN-U495994	none
SGN-U563383	none
SGN-U564078	none
SGN-U564293	none
SGN-U564578	none
SGN-U567590	none
SGN-U568277	none
SGN-U568967	none
SGN-U569327	none
SGN-U569410	none
SGN-U569411	none
SGN-U570334	none
SGN-U570391	none
SGN-U570862	none
SGN-U571549	none
SGN-U572452	none
SGN-U573835	none
SGN-U574890	none
SGN-U575047	none
SGN-U575628	none
SGN-U578355	none
SGN-U579852	none
SGN-U580084	none
SGN-U581392	none
SGN-U581806	none
SGN-U582626	none
SGN-U584915	none
SGN-U587248	none
SGN-U589374	none
SGN-U589455	none
SGN-U589460	none
SGN-U589519	none
SGN-U589520	none
SGN-U590598	none

SGN-U590683	none
SGN-U591321	none
SGN-U592251	none
SGN-U592849	none
SGN-U592902	none
SGN-U593333	none
SGN-U593555	none
SGN-U594054	none
SGN-U595460	none
SGN-U595517	none
SGN-U595711	none
SGN-U595892	none
SGN-U595932	none
SGN-U596110	none
SGN-U596111	none
SGN-U596596	none
SGN-U597073	none
SGN-U597306	none
SGN-U597725	none
SGN-U601488	none
SGN-U601761	none
SGN-U601929	none
SGN-U602131	none
SGN-U602780	none
SGN-U603117	none

Table 2. Annotation of genes in chromosome 2 between marker SSR 32 at 78.0 cM and marker 2-2g18030 at 83.1 cM. Data was extracted from the SOL Genomics Network http://solgenomics.net/ (Mueller *et al.*, 2005).